KINETIC MODELLING OF SCRAP TYRE PYROLYSIS AND OXIDATIVE DESULPHURISATION OF TYRE-DERIVED OIL

By

Peter Tumwet Cherop

Thesis submitted in partial fulfilment of the requirements for the Degree

of

DOCTOR OF ENGINEERING: CHEMICAL ENGINEERING

Department of Chemical Engineering

Faculty of Engineering and the Built Environment

Durban University of Technology

Supervisor

Dr. Sammy Lewis Kiambi

Co-Supervisor

Prof. Paul Musonge

NOVEMBER 2018

Declaration

I Peter Tumwet Cherop declare that:

(i) The research reported in this thesis, except where otherwise indicated, is my original work.

(ii) This thesis has not been submitted for any degree or examination at any other university.

(iii) This thesis does not contain other persons' data, pictures, graphs or other information, unless specifically acknowledged as being sourced from other persons.

(iv) This thesis does not contain other persons' writing, unless specifically acknowledged as being sourced from other researchers. Where other written sources have been quoted, then:

a) their words have been re-written but the general information attributed to them has been referenced;

b) where their exact words have been used, their writing has been placed inside quotation marks, and referenced.

(v) Where I have reproduced a publication of which I am an author, co-author or editor, I have indicated in detail which part of the publication was actually written by myself alone and have fully referenced such publications.

(vi) This thesis does not contain text, graphics or tables copied and pasted from the Internet, unless specifically acknowledged, and the source being detailed in the thesis and in the References sections.

Signature: ……. Date…29/11/2018…….

Peter Tumwet Cherop **(Candidate)**

As the candidate's supervisor, I approve this Thesis for submission:

Signature: ……. Date…….

Dr. Sammy Kiambi **(Supervisor)**

As the candidate's Co-supervisor, I approve this Thesis for submission:

Signature: ……. Date…….

Prof. Paul Musonge **(Co-supervisor)**

Journal and Conference papers

Journal Papers published/accepted/under review

1. **P. T. Cherop**, S.L. Kiambi and P. Musonge. *Kinetic study of non-isothermal co-pyrolysis of tyre crumb with eucalyptus sawdust*. International Journal of Environment and Waste Management, Vol. 21, Nos. 2/3, pp.184–200, 2018.

2. **P. T. Cherop**, S.L. Kiambi and P. Musonge. *Non-Isothermal model-free and model-fitting kinetics of tyre crumb pyrolysis.* Journal of Solid Waste Technology and Management. ***Accepted: In press***

3. **P. T. Cherop**, S.L. Kiambi and P. Musonge. *Oxidative desulphurisation of waste tyre pyrolysis oil: A response surface methodology approach.* International Journal of Environmental Technology and Management. ***Under review***

4. **P. T. Cherop**, S.L. Kiambi and P. Musonge. *Modelling and optimisation of oxidative desulphurisation of tyre-derived oil via central composite design approach*. Green Processing and Synthesis (de Gruyter). ***Accepted***

5. **P. T. Cherop**, S. L. Kiambi and P. Musonge. *Kinetics of granulated waste tyre pyrolysis via thermogravimetry and model-free methods*. European Journal of Engineering and Natural Sciences. ***Accepted***

Conference papers

6. **P.T. Cherop**, S. Kiambi and P. Musonge. *Kinetics of granulated scrap tyre pyrolysis via thermogravimetry*. "in Proceedings of Sustainable Research and Innovation Conference", JKUAT, Kenya, 3 - 5 May, 2017, pp. 150-155. ISBN: 2079-6226

Abstract

The amount of tyres generated around the world has been on the rise. This has prompted the need to explore ways in which waste tyres can be disposed. One of the ways of recycling waste tyres is through pyrolysis, a process that has the potential to produce oil products with high calorific value. However, the oil produced from waste tyre pyrolysis has a high sulphur content, resulting in high levels of toxic emissions during combustion.

This research study focuses on two aspects associated with waste tyre pyrolysis. The first aspect deals with the establishment of the kinetics of scrap tyre pyrolysis while the second aspect involves the oxidative desulphurisation (ODS) of tyre-derived oil (TDO). The ODS was carried out with incorporation of the central composite design (CCD) technique of the response surface methodology (RSM) in order to model the desulphurisation process.

In order to study the kinetics of the scrap tyre pyrolysis, three different models were applied to thermogravimetric data. The thermogravimetric (TG) experiments were carried out in a nitrogen environment and a temperature range of 20°C to 600°C at heating rates of 2, 5, 10, and 20 °C min^{-1}. The models used to determine the activation energy (E_a) were Kissinger-Akahira-Sunose (KAS), Flynn-Wall-Ozawa (FWO) and Friedman (FR) whereas the Coats-Redfern (CR) model aided in the determination of the pre-exponential factor. The FWO model had the highest average value (R^2 = 0.9847) of the coefficient of determination, and therefore the E_a values from this model were loaded into the CR model to determine the pre-exponential factors and the order of the reaction model. The thermal decomposition started at a mean temperature of about 285°C and was complete at about 482 °C for the four heating rates. Results indicate that the mass losses become greater with increasing heating rates. The thermogravimetric analysis results revealed that tyre pyrolysis involves three stages i.e. removal of lubricants and oil in the scrap tyre, breakdown of natural rubber and breakdown of butadiene rubber and styrene-butadiene rubber. The average activation energies obtained were 206.01 kJ mol^{-1}, 206.08 kJ mol^{-1} and 204.82 kJ mol^{-1} using KAS, FWO and FR models respectively. A mean pre-exponential factor of 1.27E+10 min^{-1} was obtained. In addition, the results showed that the pyrolysis of the tyre crumb conforms to the second order reaction model (F2).

The second objective of the study involved the use of the CCD methodology to investigate the interaction of parameters during the ODS of tyre-derived oil. The oxidative desulphurisation involved the investigation of the interaction of formic acid and hydrogen peroxide amounts, reaction time and temperature. The liquid-liquid extraction was carried out using two different solvents. In addition, for one of the solvents (acetonitrile), two solvent to oil ratios were used, bringing the total number of solvent extraction scenarios to three. The three extraction scenarios were acetonitrile to oil ratio of 1:1, acetonitrile to oil ratio of 1:2 and dimethylformamide to oil ratio of 1:1. The ODS for each of the

solvent extraction scenarios consisted of 21 experiments. Therefore, the total number of experiments for the three solvent extraction scenarios was 84 i.e. 21 runs for the oxidation stage and 63 runs for the solvent extraction. The maximum sulphur removal achieved was 86.05, 52.77 and 35.00 % respectively for oxidised oils extracted using 1:1 acetonitrile to oil ratio, 1:2 acetonitrile to oil ratio and 1:1 dimethylformamide to oil ratio while the corresponding minimum sulphur removal values were 34.02, 27.91 and 3.8 %. The results of the sulphur removal in which extraction was carried out at 1:1 acetonitrile to oil ratio were further analysed and modelled. From the analysis of variance (ANOVA), the reduced cubic model was found to be the best predictor of sulphur removal during the ODS process. Coefficient of determination ($R^2 = 0.9776$), adjusted $R^2 = 0.9254$, predicted $R^2 = 0.8356$ all showed that the model was significant. Moreover, the p-value for the lack of fit was 0.8926, which is indication of its insignificance relative to pure error.

In summary, the data obtained from the kinetic study of the scrap tyre pyrolysis could play an important role in the design and optimisation of industrial scale scrap tyre pyrolysis units. The findings could provide an insight for improvement of the general operability of scrap tyre thermal conversion processes via pyrolysis. Further research should be carried out to obtain thermogravimetric data at higher heating rates, which can then be used to model the process via the non-isothermal means. On the other hand, the findings from the oxidative desulphurisation of tyre-derived oil obtained from this research can play a key role in minimising the levels of emission during the combustion of oils obtained from the pyrolysis of waste tyres. In addition, the knowledge from the present study could be useful in commercialisation of efficient sulphur removal technology in tyre-derived oils, which can then be blended with other fuels such as diesel for use in real combustion processes. Further work with incorporation of a different organic acid, such as acetic acid and hydrogen peroxide as part of the oxidation system may be carried out to investigate the change in the extent of sulphur removal.

Dedication

This work is dedicated to my late father, Painito Cherop and late cousin brother, Allan Cherop.

Gone, but not forgotten

Acknowledgements

First and foremost, I would like to thank the almighty God for bringing me this far in my academic journey. The results witnessed from this work is a product of hard work over the last few years. I would like to thank my Supervisors, Dr. Sammy Lewis Kiambi and Prof. Paul Musonge for their unwavering support and guidance throughout the research period. Your availability and continuous interest in my work at every stage of my research and your presence at every progress presentation is appreciated. I thank Dr. Suresh Ramsuroop for his involvement and help in obtaining the tyre oil that was used in this research.

Special thanks to my colleagues in the department of Chemical engineering. Your criticism of my work, always made me think more. Nkosi Nkululeko, Martha Chollom, Dennis Asante-Sackey, Emmanuel Tetteh, Kosgey Eric, just to name a few, I thank you. I would also like to thank my colleague and 'brother' in academia, Henry Masinde Barasa who played a pivotal role in encouraging me to pursue my Doctorate.

I would like to thank South Africa's National Research Foundation in collaboration with the World academy of Sciences for the Doctoral financial support that ensured my research was undisturbed at any stage. Special thanks to the Durban University of Technology research office, in particular Prof. Bloodless Dzwairo and Mr Tshabalala for their scrutiny of my documents before submission to NRF, which ensured the funds were always timeously released. I thank Masinde Muliro University of Technology for granting me the study leave to pursue my Doctorate.

I would like to thank Ms Avenal Finlayson of the Library department for her guidance on endnote referencing at the initial stage of my work. I hereby appreciate Avinash Ramsaroop for the TGA analysis and Mufaro Moyo for providing the software. Charney Anderson of Stellenbosch Central analytical facilities unit, I thank you for your flexibility and for always making sure my samples were analysed in time.

Last but not least, I would like to thank my dear mother Jenipher Painito for always supporting my academic endeavours. Your high value for academics is the reason I have made it this far. To my lovely wife Olivia Chebet and daughter Angel Chemtai, your understanding and continuous encouragement has always kept me going. I thank you. To my Brothers Dominic, Lodrick, Victor and my sister Carolyne, thank you for your moral support throughout the journey.

Table of contents

List of Figures

Appendix

List of Tables

Appendix

List of Photographs

Appendix

Nomenclature

List of Abbreviations and Acronyms

Abbreviation	Description
Abbrev.	Abbreviation
AC	Activated carbon
ACN	Acetonitrile
Adj. R^2	Adjusted R^2
AR	Auger reactor
BET	Brunauer–Emmett–Teller
BFBR	Bubbling fluidised bed reactor
BP	Boiling point
BR	Butadiene rubber
BT	Benzothiophene
BTX	Benzene toluene xylene
CB	Carbon black
CBs	Carbon blacks
CCD	Central composite design
CO	Carbon monoxide
CO_2	Carbon dioxide
CR	Coats-Redfern
CSBR	Conical spouted bed reactor
CV	Calorific value (MJ/kg)
DACE	Design and analysis of experiments
DAF	Dry Ash free
DBT	Dibenzothiophene
DF	Degrees of freedom
DFBETAS	Difference in Beta
DFE	Degrees of freedom error
DFFITS	Difference in Fits
DMF	Dimethylformamide
DTG	Derivative thermogravimetry
FBR	Fixed bed reactors
FC	Fixed carbon
FR	Friedman

FWO	Flynn-Wall-Ozawa
GCV	Gross calorific value (MJ kg-1)
GOF	Goodness-of-fit
HC	Hydrocarbons
HDS	Hydrodesulphurisation
ICP-AES	Inductively coupled plasma atomic emission spectroscopy
KAS	Kissinger-Akahira-Sunose
LAR	Least absolute residuals
LOF	Lack of fit
LSD	Least-significant-difference
MC	Moisture content
MS	Mean square
N	Nitrogen
n.r.	Not reported
NaN	Not-a-Number
NOR	Norm of residuals
NO_x	Nitrogen oxides
NPRSM	Non parametric and semiparametric response surface methodology
NR	Natural rubber
ODS	Oxidative desulphurisation
PAHs	Polycyclic aromatic hydrocarbons
PASHs	Polycyclic aromatic sulphur heterocycles
PCB	Pyrolytic carbon black
ppm	Parts per million
Pred. R^2	Predicted R^2
PRESS	Predicted residual error sum of squares
R^2	Coefficient of determination
RCM	Reduced cubic model
Ref.	Reference
RKR	Rotary kiln reactor
RMSE	Root mean square error
RQM	Reduced quadratic model
RSM	Response surface methodology
S	Sulphur
SBR	Styrene-butadiene rubber
SD	Standard deviation

SO_2	Sulphur dioxide
SR	Synthetic rubber
SS	Sum of squares
SSE	Sum of squared errors
TC	Tyre crumb
TDO	Tyre-derived oil
TG	Thermogravimetric
TGA	Thermogravimetric analysis
T_m	Mean temperature
Tr.	Trace
VM	Volatile matter
VOCs	Volatile organic compounds
WTP	Waste tyre pyrolysis

List of symbols

Symbol	**Description**
A	Pre-exponential factor (min^{-1})
dα/dt	Rate of conversion over time
E_a	Activation energy (kJ/mol)
f (α)	Reaction model
g (α)	Conversion integral function
k (T)	Reaction rate constant
R	Universal gas constant (8.314 J mol^{-1} K^{-1})
α	Conversion degree
β	Heating rate (°C min^{-1})

Thesis structure

This thesis is organised in the form of chapters. The details covered in each chapter are presented below.

Chapter 1

This is the introduction chapter, and it provides an overview of the problem of waste tyre generation. Waste tyre pyrolysis as a method of recycling tyres is highlighted here. This chapter also points out the approach of using thermogravimetric analysis to model the tyre pyrolysis process. The existing gap in the understanding of the kinetics of waste tyre pyrolysis is mentioned in this chapter. In addition, in this chapter, various techniques of reducing the sulphur content in tyre-derived oils are briefly discussed. Furthermore, the oxidative desulphurisation method is explained, with particular focus on recent studies that have applied this method for the desulphurisation of both model diesel fuels and tyre-derived oils. The need for the application of response surface methodology on tyre oil oxidative desulphurisation studies is emphasised. This chapter also presents the objectives set for this study.

Chapter 2

In this chapter, a detailed review of literature on waste tyres, waste tyre pyrolysis and desulphurisation of tyre-derived oils is presented. The chapter starts by detailing the tyre components and problems related with the management of waste tyres. What follows is a detailed discussion on waste tyre pyrolysis process where the scheme of the process is presented. Various types of pyrolysis as well as the energy needs of the pyrolysis process are discussed. This chapter further provides a review of the factors that affect waste tyre pyrolysis. The properties and behaviour of waste tyre pyrolysis is also discussed in detail in this chapter. In addition, this chapter presents a review of desulphurisation techniques and narrows down to the recent studies in which the oxidative desulphurisation technique has been used. The chapter then presents recent studies on thermogravimetry and the application of kinetic models to study the waste tyre pyrolysis process. Lastly, a detailed discussion on the techniques of experimental design, with particular focus on response surface methodology is presented.

Chapter 3

This chapter covers the materials and methods used in this research. The methodology presented covers the two broad aspects of the research. The first part describes the thermogravimetric analysis equipment and procedure as well as the steps followed to establish the kinetics of the tyre crumb pyrolysis by non-isothermal means. The software used for thermogravimetric data extraction is mentioned here. The background of kinetic modelling used to study the thermal decomposition of solid materials is also presented in this chapter. In the second part of this chapter, the materials and

experimental set-up used to carry out the oxidative desulphurisation experiments is described. In addition, the procedure for the ODS process as well as the sample analysis methods are presented. The design of experiments criteria, technique and software is also outlined in this chapter.

Chapter 4

In this chapter, the results of the data used in the non-isothermal modelling of waste tyre pyrolysis as well as the results of the modelling process itself are presented. The chapter starts with presentation of the properties of the tyre crumb used during this study and comparison with those obtained from previous studies. Then results from thermogravimetric analysis are described, including presentation of the TG/DTG thermograms for the various heating rates investigated. What follows is the presentation of results and discussion of kinetic modelling of waste tyre pyrolysis. Results of surface fitting are also presented in this chapter.

Chapter 5

This chapter presents the results of the oxidative desulphurisation of the tyre-derived oil. The results for sulphur removal using acetonitrile and NN-dimethylformamide as extraction solvents at two different ratios are presented in this chapter. The modelling of results for 1:1 acetonitrile to oxidised oil ratio during the extraction stage of the ODS are further presented. The presentation of the modelling results includes model fitting and diagnosis, model analysis, model diagnostic plots, influence statistics, perturbation and interaction plots, response surface plots as well as optimisation.

Chapter 6

In this chapter, the conclusions and suggestions for future work are presented. The conclusion section covers the two broad aspects of this research, and each of the aspects is concluded as a subsection of the conclusions and future work section.

References and appendices

The references used in this research are presented after chapter 6. The appendices section then follows, where the figures, tables, photographs and calculations not included in the body of the thesis are presented.

CHAPTER ONE

1. Introduction

1.1. Background and research motivation

With the increasing population size, the global consumption of tyres has increased over the years in order to meet both personal and commercial transport needs. The amount of waste tyres (also commonly called scrap tyres) dumped all over the world is approximately 1.5 billion (Su and Zhao, 2009; Uçar and Karagöz, 2014), of which the percentage taken for reuse is only 15-20 % (Su and Deng, 2010) while the remainder is simply dumped into the earth. As scrap tyres are increasingly dumped, it is necessary that a suitable way of utilising them is explored. Despite the fact that part of these wastes is recycled, the proportion recycled is small given the continuous accumulation of these scraps (Parthasarathy et al., 2016). At the same time, owing to the rising concerns of crude oil prices and environmental impacts governments have been forced to pay particular attention to development of alternative fuels (Lin et al., 2013).

The valorisation of waste plastics and tyres contributes to a reduction in fossil fuel consumption and a deceleration of climate change (Lopez et al., 2009). Appropriate means of treating these wastes should be explored, in the context of recovery of energy. Land filling, because of its simplicity, has always been considered an option to address the problem of the ever increasing amount of waste tyres. However, for this to be achieved, a significant amount of space is required since reduction of the volume of tyres by compaction is not feasible (Islam et al., 2009; Uzun and Yaman, 2014). Different alternative methods such as grinding, incineration, reclaiming, retreading etc. can be used as tyre recycling options, but they have significant drawbacks.

Energy recovery is considered an attractive option for recycling since scrap tyres have high gross calorific value (33-35 MJ kg^{-1}) and volatile compound content (López et al., 2011b). Tyres also have higher heating values in comparison with that of materials such as coal (Leung and Wang, 1999; Miranda et al., 2013). Waste tyre pyrolysis (WTP) can potentially be involved in the recovery of energy from waste tyres. By definition, pyrolysis is simply a thermal degradation process (in an oxygen-free environment), in which the organic volatile matter in the tyres is transformed into products with low molecular weight, while the inorganic constituents, mainly from carbon black and steel are retained as solid residue (de Marco Rodriguez et al., 2001). The main products of waste tyre pyrolysis are waste tyre pyrolysis oil, also called tyre-derived oil (TDO), the non-condensable gases and char.

Tyres contain over 100 different substances such as steel, rubber, silica gel, carbon black, zinc oxide, sulphur among other additives. During the manufacture of tyres, the rubbers commonly used are

butadiene rubber (BR), natural rubber (NR) and styrene-butadiene rubber (SBR) or the blends of these three types. When rubber is subjected to prolonged effort or mild temperatures, plastic deformation occurs due to the sliding of polymer chains (Nieto-Márquez et al., 2016). These components decompose at various temperature ranges. The behaviour of thermal decomposition of waste tyres is dependent upon the kind of rubber as well as its contents (Leung and Wang, 1998; Seidelt et al., 2006; Islam et al., 2009).

The study of waste tyre pyrolysis kinetics has drawn interest from many researchers as understanding the kinetics of pyrolysis is key in the design and optimisation of industrial scale waste tyre recycling and pyrolysis units. To determine the kinetics of mass loss linked to materials' valorisation during the thermal degradation in the absence of oxygen, derivative thermogravimetry (DTG) and thermogravimetric analysis (TGA) are often used (Luyima et al., 2012; López et al., 2013). Kinetic parameters play a vital role in achievement of reactor designs with the best operating conditions (Zhao et al., 2012; Abdelouahed et al., 2017). Model-free and model-fitting methods are commonly used to determine the kinetic parameters associated with the decomposition of solid materials (Vyazovkin and Dollimore, 1996; Anca-Couce et al., 2014; de Godois Baroni et al., 2016). The first motivation for this research, therefore, was to apply model-free and model-fitting methods to thermogravimetric data in order to establish the kinetics associated with the waste tyre pyrolysis process as well as to determine the reaction model that best describes the process.

On the other hand, the major limitation of utilisation of tyre-derived oil in a wider range of application in real combustion processes is its high sulphur content of between 1.0-1.4 wt.% (Laresgoiti et al., 2004). The method commonly used for the removal of organosulphur compounds in the oil refinery industry is hydrodesulphurisation (HDS). This process can remove large sulphur amounts in fuels, but its shortcoming is the need for high temperature for reaction (300-400 °C) and high pressure of hydrogen (30-130 atm) with availability of active catalysts contained in huge reactor in order to facilitate the conversion of sulphur compounds to hydrogen sulphide (Te et al., 2001; Murti et al., 2005). Since TDO is produced mainly on a small scale basis, the application of HDS for sulphur content reduction is limited. Moreover, HDS may not be appropriate for sulphur reduction in TDO owing to high consumption of hydrogen with reduction of the efficiency of the catalyst. Due to the high operating conditions and the need for expensive catalysts in the HDS system, oxidative desulphurisation (ODS) has in the recent past been considered a complementary technology for deep desulphurisation (Al-Lal et al., 2015). The ODS process utilises milder operating conditions.

The ODS process occurs in two stages. First, the organic sulphur compounds are oxidised to their corresponding polar sulphoxides and sulphones using oxidising agents. This is followed by the removal step, in which the sulphoxides and sulphones are extracted using polar solvents (Yu et al., 2005; Chen et al., 2007; Dhir et al., 2009; Fabián-Mijangos and Cedeño-Caero, 2010). Figure 1-1

shows the chemical reaction that takes place during the conversion of sulphur-containing compounds into polar sulphoxides and sulphones . In an ODS process, hydrogen peroxide or its mixture with a strong or organic acid is used to boost the efficiency of sulphur removal (García-Gutiérrez et al., 2008; Haw et al., 2010). As opposed to the cases in conventional liquid fossil fuels, the sulphur compounds present in TDO present themselves in polycyclic aromatic sulphur heterocycles (PASHs) forms, for example DBT and its derivatives (Pakdel and Roy, 1994; Williams and Bottrill, 1995).

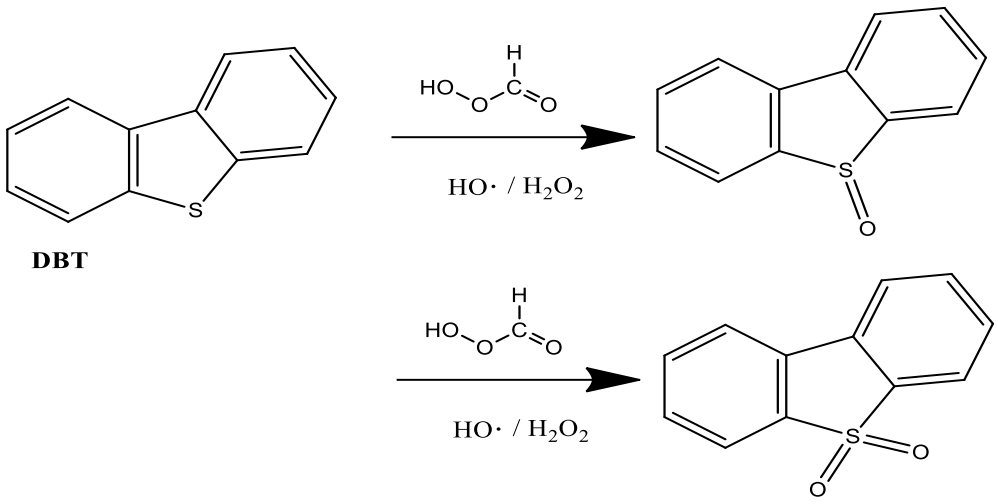

Figure 1-1: Mechanism of oxidation of sulphur-containing compounds (Al-Lal et al., 2015).

Studies on the application of oxidative desulphurisation for sulphur reduction in both model diesel fuels (Yu et al., 2005; Ali et al., 2006; Mokhtar et al., 2015) and tyre-derived oil (Bunthid et al., 2010; Chen et al., 2010; Aydın and İlkılıç, 2012; Al-Lal et al., 2015) have previously been carried out. Most of these studies, however, have been conducted at constant temperatures and reaction time while varying only the oil to acid and/or H_2O_2 ratio during the oxidation stage of the ODS process. Therefore, the second motivation behind this research was to study the oxidative desulphurisation of tyre-derived oil with incorporation of parameter interaction option by applying the central composite design technique of the response surface methodology.

1.2. Objectives

In view of the background provided in the previous section, this research study focused on addressing two aspects associated with the waste tyre pyrolysis process. In order to do so, two main objectives were set for this research study. The first main objective was to study the non-isothermal kinetic modelling of the waste tyre pyrolysis process while the second main objective was to study the oxidative desulphurisation of tyre-derived oil with incorporation of the central composite design methodology. In order to achieve the aforementioned aims, the following specific objectives were set:

- To assess the mass loss kinetics of waste tyre pyrolysis via thermogravimetry.
- To determine the kinetic parameters of waste tyre pyrolysis through non-isothermal model-free and model-fitting methods.
- To apply the oxidative desulphurisation technique for sulphur reduction in tyre-derived oil
- To assess the effect of two different solvents and solvent to oil ratio during the extraction of the oxidised tyre-derived oil
- To explore the interaction of parameters, via response surface methodology, during the oxidative desulphurisation of tyre-derived oil.
- To model and optimise the oxidative desulphurisation process of tyre-derived oil.

CHAPTER TWO

2. Literature review

This chapter presents a detailed review of literature on waste tyres, waste tyre pyrolysis and desulphurisation of tyre-derived oils. The chapter starts by detailing the tyre components and problems related with the management of waste tyres. What follows is a detailed discussion on the waste tyre pyrolysis process where the scheme of the process is presented. Various types of pyrolysis as well as the energy needs of the pyrolysis process are discussed. This chapter further provides a review of the factors that affect waste tyre pyrolysis. The properties and behaviour of waste tyre pyrolysis is also discussed in detail in this chapter. In addition, this chapter presents a review of desulphurisation techniques and narrows down to the recent studies in which the oxidative desulphurisation technique has been used. The chapter then presents recent studies on thermogravimetry and the application of kinetic models to study the waste tyre pyrolysis process. Lastly, a detailed discussion on the techniques of experimental design, with particular focus on response surface methodology is presented.

2.1. The problem of waste tyre generation

Recently, a lot of research is being carried out in in order to address the diverse world-wide view of energy. The overdependence on fossil fuels and consumption has led to energy depletion, and has also negatively impacted on the environment as a result of global warming and emission of harmful pollutants such as SO_2, NOx and volatile organic compounds (VOCs). In addition to this, solid wastes disposal is a major problem all over the world. In the European Union waste generation stands at above 1.43 billion tons per annum and this value has been increasing in rates in tandem with economic growth (World Business Council for Sustainable Development, 2008; Martínez et al., 2013). Despite many of these residues being non-biodegradable materials, they are dumped either because there is lack of specific regulations and/or because of high costs of recycling. Scrap tyres belong to the same category of the residues here aforementioned and they are managed as wastes whether it is going to undergo recycling or re-manufacturing. This is a burden that significantly increases the cost associated with disposal and generally is a hindrance to resource efficiency improvement (European Tyre and Rubber Manufacturers' Association, 2011).

2.1.1. Components of a tyre

A standard tyre could be made up of 30 various synthetic rubber types and 8 distinct natural rubbers. Additionally, it could contain 40 distinct chemicals and an array of various carbon black fillers (Evans and Evans, 2006). Rubber constitutes 60-65 % of the tyre composition while carbon black makes up 25-35 %. The remaining percentage is that of the accelerators and fillers, which are additives used

during the process of tyre manufacture. The rubbery materials in tyres is represented in the form of C_xH_y with a good proportion of fibrous materials (Leung and Wang, 1998) and they are regarded as thermoset polymers. Both passenger and truck vehicle tyres are usually a blend of NR and synthetic rubber (SR) like a co-polymer of SBR and butyl rubber/ isobutylene isoprene rubber. Synthetic rubber is generally obtained from petroleum-based products while NR is obtained from Hevea tree (Shulman, 2004). Natural rubber, which is a key element of the tyre possesses distinctive elastic properties. Rubber consists of elastomeric polymers characterised by the existence a network of structure which when subjected to external forces, can temporarily undergo deformation.

In general, over one hundred compounds can be used as additives in the tyre depending upon the specific trademark as well as the intended use of the tyre (Mastral et al., 1999b; Mastral et al., 2000c). The addition of accelerators is usually toward the final stages of the mixing cycle when the internal mixer or mill temperatures are falling (Mirmiran et al., 1992). During the tyre manufacturing process, vulcanisation takes place whereby an irreversible reaction involving sulphur, elastomer and other chemicals leads to the formation of crosslinks between molecular chains of the elastomer as well as the formation of a chemical network that is three-dimensional in nature. The cross-linked elastomers comprise of insoluble, infusible and solid thermoset materials (Isayev, 2005) which provide high elasticity and strength that makes the tyre degradation difficult. The sulphur content in tyre rubber is usually about 1.5 wt.% (Mastral et al., 2000c). During the vulcanisation process, an organic sulphur compound, an accelerator in presence of ZnO and stearic acid, as a catalyst are added with the primary aim of controlling the process and enhancing the physical characteristics of rubber (Williams and Besler, 1995; Mastral et al., 1999b; Mastral et al., 2000c; Kyari et al., 2005). Clay fillers, silicates, magnesium and calcium carbonates, and a range of inorganic pigments are the other inorganic compounds used as additives during vulcanisation (Dodds et al., 1983).

2.1.2. Challenges in waste tyre management and recycling

Tyres are made in such a way that they can withstand severe mechanical and weather conditions such as ozone, bacteria and light. This complicates the ability to recycle and/or further process them. In addition, they are bulky and do not undergo degradation in landfills (Leung and Wang, 1998). The lifetime of a tyre in a landfill is believed to be in the range of 80-100 years. Melting and separation of tyres into their chemical constituents is impossible since tyres are thermosetting polymers (Clark et al., 1993).

Despite waste tyres not presenting an immediate danger at the onset, their disposal in an inappropriate manner or production in large quantities can lead to environmental pollution or pose problems if improperly treated. Waste tyres storage boosts pests and insects' growth. The storage also presents a potential risk of fire, that in turn can be hard to extinguish, and to the environment as a result of

uncontrolled emissions into the atmosphere, groundwater and soil of compounds that are potentially harmful.

Although combustion can easily be used for recovery of energy from wastes such waste tyres, emissions like particulate matter, VOCs, polycyclic aromatic hydrocarbons (PAHs), dioxins etc., produced during the combustion process, hinders this possibility from a public health and environmental point of view (Levendis et al., 1996; Mastral et al., 1999b; Mastral et al., 1999c; Mastral et al., 2000b; Mastral et al., 2000c; Gieré et al., 2006; Conesa et al., 2008).

It has been reported since the 1970s that rubber combustion leads to emission of sizeable amounts of particles of Zn (Buekens, 1977). Burning of tyres in open air has a mutagenic emission factor of 3-4 orders of magnitude more than the values reported for coal, oil or wood combustion in utility boilers (DeMarini et al., 1994). Polycyclic aromatic hydrocarbons emissions, under controlled conditions, from coal combustion are 1.5-2 times lower than those of tyres at corresponding equivalence ratios (Levendis et al., 1996). The higher PAHs emissions in tyres could be due to the tyre structure and specifically carbon black, whose surface to weight ratio is high, thereby acting as support for deposition of PAHs (Mastral et al., 2000a). Similarly, the low rate of solid-gas reaction during the oxidation of carbon black (CB) present in the tyre could also have an effect on this behaviour (Alvarez et al., 2004).

Scrap tyres have extensively been used in many energy applications such as power plants, cement kilns, tyre manufacturing facilities, and pulp and paper production etc. (Barlaz et al., 1993). The aforementioned uses have proven to be capable of extracting energy from the tyres in a manner that is acceptable from the environmental concern point of view (Clark et al., 1993). Majorly, tyres have been used as a fuel supplement in cement kilns (Buekens, 2006). The tyre transformation, and in particular CB combustion, in cement kilns is highly favoured due to longer residence time and higher temperatures involved. Moreover, the process of cement production can make use of the iron present in the tyre steel belts and beads without affecting the quality of cement (Clark et al., 1993).

Singh et al. (2009) proved the viability of using scrap tyre as a secondary fuel source in power plants with the aim of reducing coal use and NOx emissions. The use of blends of scrap tyre and coke in cement kilns do not necessitate major modifications in the layout and operation of the plant (Giugliano et al., 1999). Tyre recycling also finds its application in the field of civil engineering, in the manufacture of asphalt and concrete or roofing purposes (Siddique and Naik, 2004; Benazzouk et al., 2007; Arabani et al., 2010; Navarro et al., 2010).

2.2. Scrap tyre pyrolysis

2.2.1. Feedstock for scrap tyre pyrolysis

The proximate analysis of any fuel provides the characteristics of fuel in terms of the amount of volatile matter, moisture content (MC), ash and fixed carbon (FC). The volatile matter (VM) in tyres is mainly made up of polymeric compounds that originate from NR and SR, while the fixed carbon ought to correspond to the carbon black used during the manufacturing of the tyre. Therefore, the amount of volatile matter should match with the gas and liquid amount obtained from the pyrolysis process, whereas the non-volatile matter amount should correspond to the solid residue that remains post pyrolysis (de Marco Rodriguez et al., 2001). The calorific value (CV) of vehicle tyres (passenger car tyres and truck tyres) is in the range of 35-40 MJ/kg, a value greater than that of most standard coal used in power plants. The CV of a motorcycle tyre is lower and it is no more than 30 MJ/kg. This is because of lower fraction of volatiles (~ 58 wt.%) and higher ash content (~ 20 wt.%) for this kind of tyre (Islam et al., 2008).

A summary of the results of proximate and ultimate analyses as well as calorific values of tyre rubber as reported by different authors are shown in Tables 2-1 and 2-2 respectively. It can be seen that the VM ranges between 57.50 and 73.74 wt. %, while the ash content varies between 2.40 and 20.10 wt. %. The fixed carbon, on the other hand ranges from about 20.22 to 30.40 wt. % (Table 2-1). The variation in the composition of various tyre brands can have an effect on the product yields of the pyrolysis process. It is worth noting that there is a huge variation in the content of carbon in various tyres, whereas the H, N and S contents, as seen in Table 2-2, appear to be within a narrower range.

Table 2-1: Proximate analyses of different tyres (Martínez et al., 2013)

wt.%				Reference
VM	Ash	MC	FC	
66.50	2.40	0.80	30.30	Williams et al. (1990a)
65.74	4.88	0.40	28.98	López et al. (2011b)
63.40	4.30	1.90	30.40	Scala et al. (2003)
67.50	5.30	2.10	25.20	Leung et al. (2002)
73.74	4.95	1.09	20.22	Xiao et al. (2008)
64.10	5.00	1.20	29.70	Larsen et al. (2006)
62.32	10.21	1.31	26.26	Chang (1996)
64.87	6.07	0.50	28.56	Roy et al. (1990)
62.20	7.10	1.30	29.40	Cunliffe and Williams (1998b)
57.50	20.10	1.53	20.85	Rofiqul Islam et al. (2008)

Table 2-2: Ultimate analyses and calorific values of various tyres (Martínez et al., 2013)

wt.%							Reference
C	N	S	H	O	Ash	CV (MJ/kg)	
75.50	0.81	1.44	6.75	15.50[f]		29.18[b,e]	Rofiqul Islam et al. (2008)
74.30	0.90	1.71	7.20	15.89[f]		30.50[b,d]	Ucar et al. (2005b)
81.72	0.55	1.87	6.54	2.68	6.64	n.r.	Aylón et al. (2010)
86.70	0.40	1.40	8.10	1.30	2.10	36.20[b]	González et al. (2001)
82.36	2.30	1.40	6.92	2.03	5.00	37.06[a]	Xiao et al. (2008)
84.00	0.49	1.42	7.19	3.30	3.60	38.80[b]	Betancur et al. (2009)
85.90	0.40	1.00	8.00	2.30	2.40	40.00[b]	Williams et al. (1990b)
86.09	0.19	1.93	6.74	1.35	3.70	n.r.	Conesa et al. (2004)
84.33	0.49	1.66	7.81	3.32	2.40	40.00[b]	Cunliffe and Williams (1998b)
86.70	0.30	1.90	6.90	0.90	3.30	31.80[a]	Senneca et al. (1999)

[a] Lower; [b] Higher; [c] Passenger car and truck tyres mixture; [d] Passenger car tyre; [e] Motorcycle tyre; [f] Including ash.

2.2.2. The process of pyrolysis

Pyrolysis, also commonly referred to as thermolysis or thermal distillation is a process of thermochemical treatment that leads to chemical bonds breaking apart (Wampler, 2006). Pyrolysis, which is also the first stage in any combustion or gasification process, is accomplished via thermal decomposition in an oxygen free environment. Thermolysis, semantically, is a more appropriate term than pyrolysis in the sense that pyro, Latin for fire, denotes oxygen presence (Buekens, 2006). Pyrolysis has also been termed polymer cracking, reverse polymerisation or thermal depolymerisation. The main advantage of pyrolysis, from the recycling perspective, is that it can address the issue of wastes, which are hard to recycle, and thus can lead to creation of reusable products (Buekens et al., 2006).

Pyrolysis can be applied in feedstock recycling via solid wastes transformation into monomers, chemicals, high calorific value fuels or other valuable materials. During pyrolysis of solid materials, high-energy-density volatile gases (both condensable and non-condensable) are released. In addition, there is also the release of carbonaceous solid (commonly referred to as char) where most of the ash and FC are confined. Pyrolysis, in essence, entails subjecting feedstock to heating, in an oxygen free environment, to temperatures above 400 °C. This process takes place in a self-generating or inert environment and it leads to degradation and volatilisation of the various structures contained in the feedstock. When feedstock is subjected to heat under the aforementioned conditions, a number of reactions occur. They include: cracking, dehydrogenation, dehydration, isomerisation, condensation and aromatisation (Rezaiyan and Cheremisinoff, 2005). Although pyrolysis of wastes seemingly is a straightforward concept, the products are usually low-value hydrocarbon mixtures, comprising of a wide range of composition, at times ranging from coke to light alkane gases (Scheirs, 2006). Owing to the complex nature of the pyrolysis products, it is prudent to identify the optimum conditions for the type of feedstock and process parameters such as reaction time, temperature, heating rate and the size of the particle.

2.2.2.1. Scheme of scrap tyre pyrolysis process

Polymers, in general, comprise of carbon atoms linked by double or single bonds (Zadgaonkar, 2006). Rubbers are designated by $C = C$ double bonds, and thermal degradation leads to production of extremely reactive free radicals, which are commonly the sub-components of the initial molecule of rubber (Dodds et al., 1983). According to Aguado et al. (2006), the process of thermal decomposition is a chain reaction involving radicals which comprise of progressive polymer backbone breaking and hydrogen transfer. It has been reported that the recombination of monomers, probably via Diels-Alder mechanism, contributes greatly to dimer establishment during the pyrolysis of rubber (Groves et al., 1991). There has also been a suggestion of polyisoprene depolymerisation followed by cyclisation as

a possible reaction pathway for tyre rubber conversion (Mastral et al., 2000c). Pakdel et al. (2001) reported that the β-scission mechanism is involved in the thermal decomposition of polyisoprene to an intermediate isoprene radical. This is followed by its transformation to isoprene through depropagation, and these molecules of isoprene undergo dimerisation to form dipentene. Other researchers have suggested that the thermal decomposition process of the waste tyres occurs through bond cleavage on every monomer of the major tyre constituents, after which hydrogenation and reintegration takes place as a result of gas-phase reactions (Kwon and Castaldi, 2009).

From a wider perspective, it can be said that waste tyre pyrolysis encompasses free radical intramolecular reactions that vary with conditions of pyrolysis. The reactions that are a part of tyre pyrolysis, according to Li et al. (2004), can be grouped into three categories;

- Primary pyrolysis process which takes place at temperatures of between 250 and 520 °C.
- Secondary volatiles post-cracking process which occurs at 600 - 800 °C and has a great effect on benzene, toluene, and xylenes (BTX) yields.
- Gasification reaction of CB with the gases (CO_2/H_2O/O_2) that occurs in the temperature range of 750 - 1000 °C.

The significance of each of the reactions depends on the reaction time and temperature in accordance with Arrhenius reaction rates equation.

Although pyrolysis involves complex pathways that cannot be explained by one or more chemical reactions, there exists an empirical formula, based on the law of conservation of mass, which can provide a viable and practical scheme of the pyrolysis reaction (Buekens, 2006). Waste tyre pyrolysis leads to decomposition of the tyre, forming volatiles and a carbonaceous fraction. For example, if a 40 wt. % solid conversion occurs, and that the organic portion in the tyre solely is involved in the interaction during the pyrolysis reaction, then as shown in Figure 2-1, the process can be presented using the ultimate analysis of the CB and the tyre (Martínez et al., 2013). Based on this approach, and also factoring in the tyre reaction enthalpy, an energy balance can be developed to aid in the determination of the volatile portion energy content. Figure 2-1 shows a scenario in which 40 % solid conversion takes place. Assuming 100 % solid conversion, the number of carbon atoms in the volatile fraction would be less than that in the solid fraction.

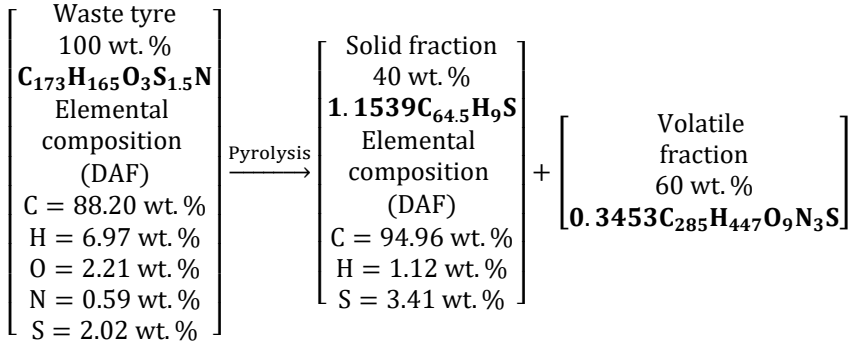

Figure 2-1: Elemental approach of tyre pyrolysis reaction (Martínez et al., 2013)

2.2.3. Types of pyrolysis

Depending on the conditions of operation, such as the residence time of volatiles, heating rate and temperature, pyrolysis can be classified into many types. The two simplest forms of classification are slow and fast pyrolysis. Fast pyrolysis is also termed flash pyrolysis, although the later can also imply shorter residence time of the vapours and higher heating rates than the former. Hydro-pyrolysis, oxidative pyrolysis, catalytic pyrolysis, vacuum pyrolysis and steam pyrolysis are the classifications that exist based on the environment in which the process occurs while plasma or microwave pyrolysis are the classifications on the basis of the heater system. Fixed bed reactors (FBRs) are typically associated with slow pyrolysis while entrained and fluidised bed reactors are commonly used for fast pyrolysis. It is important to note, however, that FBRs can be used for fast pyrolysis processes through the adjustment of the residence time of volatiles and the heating rate. Auger reactor (AR) and the rotating cone may also be used for fast pyrolysis processes.

2.2.3.1. Fast pyrolysis

Fast pyrolysis is a pyrolysis type characterised by quick thermal degradation, and the heating rates involved are higher than those of slow pyrolysis. For this process, small-sized particles of the feedstock are normally required in addition to the need for specially designed equipment to facilitate quick removal of the vapours liberated. The short residence times in the hot region coupled with high heating rates and quick products' quenching are ideal for liquid products' formation, as volatiles produced during pyrolysis undergo condensation prior to further breakdown (by reaction) of the higher molecular mass compounds into gaseous components (Cunliffe and Williams, 1998b). As a result, higher-calorific value liquid fuel is produced. Fast pyrolysis is known as the ideal route for higher yield (50-60 wt. %) of chemicals, liquid fuel and derived products during conversion.

Fluidised bed, free-fall, ablative and entrained reactors are commonly used to carry out fast pyrolysis, where the reaction time can range from milliseconds (ms) to seconds. In general, the acceptable

residence time of the volatiles is anything less than two seconds (Bridgwater and Peacocke, 2000). When thermal cracking is carried out at temperatures above 700 °C, heating rate above 1000 °C/s, reaction time below 500 ms and quick quenching of the products is involved then the pyrolysis processes is termed ultra-rapid or ultra-pyrolysis (Fairburn et al., 1990).

2.2.3.2. Slow pyrolysis

Slow pyrolysis involves low temperatures and is characterised by relatively prolonged vapour and solid residence times in the range of minutes to hours. Owing to extended residence times, primary products undergo secondary conversion, thereby leading to production of more tar, coke and products with thermal stability (Buekens, 2006). Slow pyrolysis is sometimes referred to as carbonisation. As opposed to fast pyrolysis, slow pyrolysis objectively, is meant to produce char despite gases and tar also being produced, but certainly not retrieved.

2.2.3.3. Catalytic pyrolysis

When a catalyst is used in the pyrolysis process with the aim of favouring or upgrading a certain yield, then the pyrolysis process is termed catalytic. The fractional yield of the liquid product as well as its fuel characteristics was enhanced when perlite was used as the catalytic material (Kar, 2011). The liquid fraction was boosted by 8.48 wt. % when a 0.1 catalytic material to tyre ratio was used. Similarly, lower temperatures of the pyrolysis process were favoured by addition of NaOH (Zhang et al., 2008) where 49.7 wt.% liquid yield was achieved at 400 °C in addition to an enhanced H_2 amount in the gas portion. Dũng et al. (2009) found out that there was a substantial rise in the yield of the gaseous product when Ru/MCM-41 was used as the catalytic material. A remarkable decrease in the concentrations of C_2-C_4 and CH_4 and a marked increase in the concentrations of CO and H_2 at 800 and 500 °C respectively was observed when the process of pyrolysis-gasification (in two stages) was used to pyrolyse the waste tyre using Ni-Mg-Al as the catalytic material (Elbaba et al., 2010).

2.2.4. Energy needs and pyrolysis efficiency

The energy needed to develop the process of pyrolysis, also called pyrolysis heat or enthalpy, is the energy (sensible energy) needed for the feedstock to be raised to a reaction temperature up from room temperature. It is also the energy (reaction enthalpy) needed for feedstock conversion into pyrolysis products (Daugaard and Brown, 2003). The following heat sources can be used for a pyrolysis process:

- Burning the solid and/or the gas fraction generated in the process
- Auxiliary fuel burning
- Using molten salts, solvents or hot sand as heat conveyers

- Electric heat

In spite of WTP being a process that is generally endothermic, it encompasses a sequence of exothermic and endothermic reactions (Collins et al., 1974; Yang and Roy, 1996). In a study conducted by Yang and Roy (1996) on the changes of enthalpy (that accompany the pyrolysis of rubber) as a temperature function in the entire range of pyrolysis conversion, it was found that the chemical reactions in the initial process stage contribute to exothermic reactions whereas pyrolysis products vapourisation lead to an endothermic reaction. At the initial stage of the pyrolysis process, in an exothermic process, there is the crackdown of organic matter where small fractions are formed (Cheung et al., 2011). With increase in temperature, the crackdown of primary products to secondary ones occurs before subsequent vapourisation.

The WTP net energy balance, on the basis of tyre combustion heat, shows that around 75-82 % of energy can be recovered (Dodds et al., 1983). The efficient energy use in a pyrolysis process, according to Laird et al. (2009), usually encompasses the main process product in relation to how marketable it is, but can also be distributed across all products. In addition, the energy used to produce the feedstock can also be factored in when determining the energy efficiency. Therefore, for the tyre scenario, this can be looked at as the energy needed to produce the NR, SR and CB, as well as the energy required to meet transport costs. These energy requirements together with the energy needed for pyrolysis equipment fabrication, plant erection and maintenance would form a life-cycle assessment of the processes and products (Laird et al., 2009).

Reaction enthalpy has the greatest representation compared to other energy requirements in a pyrolysis process since it is directly involved in the accomplishment of the process. Secondary reaction processes that take place between char and volatiles, and autocatalytic effects resulting from impurities, are often considered the causes for vast differences in values for the pyrolysis process available in literature (Gomez et al., 2009).

The variations among the various tyre types with regard to composition, also cannot be neglected. From this perspective, Yang and Roy (1996) reported a net (endothermic) change in enthalpy of 870 and 550 kJ/kg for NR and SBR respectively when heated from 30 to 510 °C. Similarly, an enthalpy of reaction of 267.6 KJ/kg was obtained for a sample of tyre rubber in a study carried out by Aguado et al. (2005). Various enthalpies of reaction were also reported by Cheung et al. (2011) when different temperatures and heating rates were used. For example, they reported a reaction enthalpy of 646 KJ/kg for a reaction temperature and heating rate of 510 °C and 20 °C/min respectively. In addition, they pointed out that less energy is required for pyrolysis process completion when lower heating rates are used, albeit with longer time of completion. On the contrary, more energy is required for pyrolysis completion when the heating rates are higher, but the completion time is less in this case.

In conclusion, despite the fact that the energy needed for accomplishment of pyrolysis of tyre is extremely heterogeneous, its value is lower than that of the tyre heat of combustion (which ranges between 35 and 40 MJ/kg) as well as that of the pyrolysis products, 42 MJ/kg for volatiles and 31 MJ/kg for solid fractions (Martínez et al., 2013).

2.3. Factors affecting tyre pyrolysis process

The process of waste tyre pyrolysis is endothermic in nature and it is sustained by temperature. Consequently, temperature plays a major role as far as products and the degree of conversion are concerned during the pyrolysis process. The other factors that influence the pyrolysis process are the heating rate, particle size and feedstock composition, residence time of the volatiles as well as the duration of the pyrolysis process. The type the environment in which the process occurs and flow of the carrier gas also affect pyrolysis.

2.3.1. Tyre brand and composition

In a study carried out by Kyari et al. (2005) using seven various types of the waste tyre and brands from different countries, it was found that the origin and the type of the tyre did not have a significant effect on the oil, char, and gas yields. Nonetheless, the composition of the oils and produced gases were noticeably different. Pyrolysis oil analysis indicated that some aromatic compounds had varied concentrations depending upon the tyre origin and brand. Additionally, the seven tyres were mixed and subjected to pyrolysis, and the results, both composition and yield wise, showed that the obtained values were a mean of separate tyre compositions and yields. In another study, using a two-stage reactor, six waste tyre types were pyrolysed. The first stage involved pyrolysis while the gases underwent post-pyrolysis cracking (at higher temperatures) in the second stage. In this case, the product yield differences (depending on the tyre type) were minimal but significant at the same time.

Despite tyres containing several various SR and NR types, typically, the major types of rubber used are NR, polybutadiene rubber and SBR (Williams and Besler, 1995; Seidelt et al., 2006). Three types of tyre of known composition, in a study conducted by Williams and Besler (1995), were used for thermogravimetric analysis (TGA) investigation of the thermal degradation of the tyres. From this study, the thermograms revealed two noticeable sections of weight loss, where SBR decomposed at higher temperature while NR degraded at lower temperature. The decomposition of polybutadiene, on the other hand, occurred at higher temperature despite showing initial degradation at lower temperature. In another study on thermal degradation of SBR, polybutadiene rubber and NR, the link between the composition of the tyre rubber and thermal degradation temperatures of the three rubber components was confirmed (Seidelt et al., 2006). From this study, isoprene dimer and xylene were

found to be the major products of NR thermal degradation whereas cumene, styrene and ethylbenzene were the products of SBR thermal degradation.

The solid fraction in a pyrolysis process can be influenced by tyre composition. There is a variation in the ash content obtained from a tyre pyrolysis process depending on the type of the tyre used. For instance, as pointed out by Ucar et al. (2005a), the ash content in a pyrolysis process in which the passenger car tyre was used was higher than that obtained with the use of the truck tyre for the same process. In addition, the gross calorific value (GCV) of the CB obtained using the truck tyre was higher ($\approx$ 34 MJ kg^{-1}) compared to that of the CB obtained from the passenger car tyre pyrolysis ($\approx$ 15 MJ kg^{-1}).

Nonetheless, it is important to note that the gases and oil compositions and product yield are mainly dependent on the reactor type used and the operating conditions such as pyrolysis temperature and heating rate, as opposed to the variation in the composition of tyres.

2.3.2. Temperature

Temperature is the major factor that influences the process of tyre pyrolysis (Mastral et al., 2000c; de Marco Rodriguez et al., 2001; González et al., 2001; Díez et al., 2004; Aylón et al., 2005; Murillo et al., 2006b; Aylón et al., 2010). As far as conversion is concerned, and from the point of view of many authors, 500 °C (at atmospheric pressure), seems to be the optimal temperature for achievement of complete conversion of the tyre (Miguel et al., 1998; Laresgoiti et al., 2000; Mastral et al., 2000c; de Marco Rodriguez et al., 2001; Berrueco et al., 2005; Ucar et al., 2005a; Murillo et al., 2006b). The major tyre components i.e. BR, SBR and NR are retained in pyrolytic carbon black (PCB) at lower pyrolysis temperatures, which as pointed out by de Marco Rodriguez et al. (2001), shows a sticky and gummy heterogeneous characteristic. In this regard, TGA provides a window of operation for every tyre brand, including process parameters like carrier gas type and flow, heating rate etc.

Although the temperature is the parameter with the highest effect on tyre pyrolysis, the overall effect incorporates other process parameters such as heating rate, pressure as well as the carrier gas superficial velocity. These parameters, collectively, play a key part as far as secondary reactions occurrence is concerned. In the absence of secondary reactions, an increase in temperature for a precise process of pyrolysis should not greatly affect the product yields. Conducting the process at vacuum pressure or at higher carrier gas flow rates enhances the performance.

The yield of the gas, relative to the liquid yield, in a pyrolysis process could be promoted by temperature increase. This, however, is controlled by whether or not secondary reactions occur. Chang (1996), for instance highlighted that the liquid fraction underwent thermal cracking with increasing

temperature of the process that was carried out in a thermogravimetric (TG) balance in nitrogen environment at a flow rate of 50 ml/min. The author noted that there was a slight reduction in the solid yield with temperature shift from 350 to 550 °C and a gas fraction of 50 wt.% was obtained at a temperature of 550 °C. Kawakami et al. (1980), similarly, in an experiment carried out in a rotary kiln (RKR) reactor found out that the liquid yield decreased whereas that of the gas increased with the change in temperature to 740 from 540 °C. A very small variation was noted for the char, with the yield reducing from 40 to 38 wt.% within the same range of temperature. Table 2-3 shows further examples of the temperature effect on the product yields of pyrolysis as reported by various authors.

The yield of solid can also increase with increasing temperature. This trend is common when either spouted and fluidised bed reactors are used, or when the pyrolysis process is carried out at elevated temperatures, thereby favouring the formation of char and tar. In these reactor types (spouted and fluidised bed), higher rates of heating coupled with robust contact between the gas and solid can boost further secondary reactions encompassing particles of PCB (Conesa et al., 1996; Kaminsky et al., 2009; López et al., 2010). Therefore, absorption of the volatiles produced from the process of pyrolysis can occur on the char surface, providing an avenue for fresh carbonaceous materials. In this regard, there is expectation of less liquid yield relative to that of the gas and CB when the temperature is increased. Conesa et al. (1996), for example, in an experiment carried out in a bubbling fluidised bed reactor (BFBR) reported a solid yield increase from 20.4 to 32.5 wt.% when the temperature was increased from 600 to 900 °C. López et al. (2010), in a pyrolysis process conducted in a conical spouted bed reactor (CSBR), noted that heavy hydrocarbons deposition on the solid surface fraction was enhanced by increasing temperatures, which consequently resulted in mass increase. There was an increase in the solid yield to 35.8 up from 33.9 wt.% with temperature change from 425 to 600 °C. In a study conducted in a FBR by Conesa et al. (2004), no liquid fraction was obtained. However, a higher solid yield comprising of approximately 37 and 25 wt.% CB and carbonaceous solid respectively was obtained.

Table 2-3: Effect of temperature on product yields of tyre pyrolysis

Temperature	Average yield (wt.%)			Reactor	Reference
(°C)	Liquid	Gas	Solid		
600	53.1	8.9	38.0	FBR[a]	Cunliffe and Williams (1998b)
525	56.9	5.2	37.8		
450	58.1	4.5	37.4		
575	41.0	19.0	40.0	FBR	Islam et al. (2008)
475	49.0	10.0	41.0		
425	47.0	9.0	44.0		
700	38.0	22.0	38.0	FBR[b]	Lucchesi and Maschio (1983)
600	43.0	18.0	38.0		
500	46.0	14.0	38.0		
700	36.6	26.7	36.7	FBR	González et al. (2001)
600	52.2	10.8	37.0		
500	55.4	6.0	38.6		
680	31.8	10.7	48.9	RKR	Galvagno et al. (2002)
600	33.0	8.2	47.4		
550	38.1	2.4	49.1		
800	27.5	31.5	41.0	AR	Aylón et al. (2010)
700	31.3	29.7	39.0		
600	41.5	17.9	40.6		

[a] Large-scale: [b] Continuous counter-current

2.3.2.1. Influence of temperature on the liquid fraction

In general, for waste tyre pyrolysis, temperature can have an effect on the liquid fraction. The aliphatic compounds are produced in larger quantities at lower temperatures whereas higher temperatures favour the production of aromatic compounds (Scheirs, 2006). The increase in aromatic compounds, however, is controlled by secondary reactions which result in the modification of the product yields and chemical properties. Cunliffe and Williams (1998b), using a FBR, found out that the content of aromatics increased while that of the aliphatic compounds decreased as a result of an increase in temperature

from 450 to 600 °C. These changes in aromatic and aliphatic compounds were accompanied by a 1.4 MJ/kg decrease in GCV to 41.2 MJ/kg. The same trend was observed by Li et al. (2004) where there was a slight decrease in GCV to a value of 41 down from 41.9 MJ/kg with shift in temperature from 450 to 600 °C. In addition, there was a decrease in H/C ratio from 1.55 to 1.26, which was an indication of additional aromatics. Kaminsky et al. (2009), in a study carried out in a BFBR highlighted that at 600 °C, the liquid fraction obtained mainly consisted of aliphatic compounds whereas at 700 °C, more aromatic compounds were obtained. Aylón et al. (2010), in a pyrolysis experiment conducted in an AR, also noted an increase in aromatic compounds with change in temperature from 600 to 800 °C. Conjugated bonds formation in the tyre liquid is favoured by elevated pyrolysis temperatures, which in turn enhances its characteristics for octane booster production, and as feedstock for refining (Benallal et al., 1995).

2.3.2.2. Influence of temperature on the gas fraction

The sensitivity of the gas yield and composition to secondary reactions (heterogeneous reactions encompassing the tyre inorganic compounds and thermal cracking) is very high. Therefore, there is disparity in the results available in literature on the behaviour of gas fractions in relation to calorific value, composition and yield. Díez et al. (2004), for example, in an experiment conducted in a quartz reactor, revealed that CO, H_2 and CH_4 were the main constituents of the gas stream. The authors also pointed out that as the temperature rose from 350 to 550 °C, a decrease in C_4H_6, C_3H_6, C_4H_6, the rest of C_4 hydrocarbon species, CO_2 as well as C_5 and C_6 hydrocarbons was notable. In addition, the CV decreased to 36 from a value of 50 MJ/m^3 with increase in temperature within the same range as a consequence of heavier hydrocarbons concentration decrease. Due to the occurrence of cracking reactions, there was a simultaneous increase in the yield of gas from 20 wt.% to 29 wt.%.

Napoli et al. (1997) carried out a waste tyre pyrolysis study in a FBR at three temperatures where it was observed that at 380 °C, the gas consisted of small amounts of CH_4 and CO_2 and the overall volume of the gas was no more than 0.5 Nm^3 kg^{-1}. As the temperature increased to 450 °C, the overall volume of the gas rose to 3 N m^3 kg^{-1}, while CO_2 surfaced at the initial pyrolysis stage and was still present in the subsequent fractions. At 550 °C, 4.5 Nm^3 kg^{-1} of the gas was produced, of which half consisted mainly of H_2 and CH_4. Conesa et al. (2004) made similar observations from a study carried out in a FBR where a substantial increase in H_2, CH_4 and C_6H_6 , as a result of cracking reactions, was notable when the temperature was increased from 450 to 1000 °C. In another study conducted in a RKR by Galvagno et al. (2002), an increase in CV from 22 to 39 MJ m^{-3} was observed as a result of temperature increase from 550 to 680 °C. The authors pointed out that the secondary reactions were predominant in hydroaromatic as well as cyclisation reactions, with major increases in C_2, C_3 and CH_4 compared to H_2. In a study by González et al. (2001), the yield of the gas as well as that of CO_X (combination of

CO and CO_2) increased when the temperature was changed from 400 to 700 °C. This tendency was ascribed, by the authors, to decarboxylation and decarbonylation reactions as well as the secondary reactions involving carbon black. The increase in temperature coupled with heating rate increase from 5 to 20 °C min^{-1} led to the increase in the concentration of C_2H_6, C_2H_4 and CH_4. In addition, the CV increased from 12 to 43 MJ m^{-3} as the temperature changed while the increase in the heating rate resulted in CV increase from 20 to 29 MJ m^{-3}.

In a study carried out by Berrueco et al. (2005) in a FBR, the influence of temperature on the composition of the gas was greater than it was on other fractions. The authors noted that the CO_X fraction concentration at 400 °C was 0.55 wt.%, and there was a slight decrease in this value in the temperature range of 400-550 °C before a slight increase in concentration at temperatures above 550 °C was observed. As for H_2, the maximum yield was achieved at 550 °C, indicating that its production was favoured by increasing temperatures. The CV ranged between 5.5 - 9.0 $MJN^{-1}m^{-3}$ and it increased with increasing temperature.

The occurrence of cracking reactions with prevailing secondary reactions in fluidised bed reactors has also been reported in literature. Conesa et al. (1996), for instance, found out that at a pyrolysis temperature of 600 °C, the yield of gas was 6.3 wt.% whereas at a process temperature of 800 °C, the yield increased to 37.1 wt.%, translating to a 30.8 wt.% difference in gas yield. The gas obtained at 800 °C consisted mainly of C_2H_4 and CH_4. In another study carried out in a CSBR by López et al. (2010), it was noted that with the shift in temperature from 425 to 600 °C, the C_1 - C_4 species of the gas increased. Additionally, an increase in the yield of gas (which mainly consisted of C_1 - C_4 olefins and CH_4) from 1.81 to 8.26 wt.% due to intense cracking at elevated temperatures was observed.

The yield of H_2, CH_4 and C_1-C_4 species is enhanced with increase in pyrolysis temperatures. For instance, in a WTP study carried out by Kaminsky et al. (2009) using a fluidised bed reactor, the total yields of gas were 20, 24 and 33 wt.% for pyrolysis temperatures of 598, 600 and 700 °C respectively. Additionally, the yield of H_2, CH_4, C_2 species and C_3 species increased from 0.59 to 1.1, 2.9 to 6.9, 2.8 to 5.8 and 2.96 to 5.03 wt.% respectively with the shift in temperature from 598 to 700 °C. Similarly, the yield of CO, H_2S and CO_2 also increased with increasing temperature. In another study conducted by Williams and Brindle (2003) at a pyrolysis temperature range of 450 to 600 °C in a fluidised bed reactor, the gas yields obtained were 2.5, 6 and 14 wt.% for pyrolysis processes carried out at 450, 525 and 600 °C respectively. It was also noted that there was an increase in H_2 and hydrocarbons yield with increasing temperature, and the gas consisted majorly of methane, butadiene, propene, and ethene.

In a tyre pyrolysis study carried out by Galvagno et al. (2002) in a RKR at temperatures of between 550-680 °C, an increase in H_2, CH_4, CO, C_2H_6, C_2H_4 and C_{3+} species yields was reported. Leung et al. (2002), using a FBR at and pyrolysis temperatures ranging from 500-1000 °C, pointed out that H_2,

CH_4 and C_2H_4 were the major components of the gas produced. In the pyrolysis temperature range of 800-1000 °C, it was observed that the H_2 yield kept increasing whereas the yield of CH_4 and C_2H_4 decreased slightly. In a similar study by Conesa et al. (2004) using a drop tube reactor at a pyrolysis temperature range of 450-1000 °C, it was noted that the yield of CH_4 markedly increased with increasing pyrolysis temperature while C_2H_4 and CO_2 yields decreased at pyrolysis temperatures of between 750-1000 °C.

In summary, the influence of temperature on the yield of gas is mainly dependent on the secondary reactions occurrence. The temperature is an important parameter that is involved in gas yield increase during tyre pyrolysis due to the extreme sensitivity of secondary reactions (particularly thermal cracking) to temperature increase. In general, the expectation is that, with increase in temperature, there is a decrease in longer chain hydrocarbons while H_2 and lighter hydrocarbons generation is favoured.

2.3.2.3. Influence of temperature on the solid fraction

From a precise pyrolysis perspective, there is no expectation of change in the yield of the solid fraction with increase in pyrolysis temperature. In this regard, the summation of the initial CB and the content of ash must correspond to the solid fraction. Several authors have reported that If some amount of oxygen is present in the carrier gas (steam and/or CO_2), lower yield of char than the value expected can be promoted when the temperature is increased due to the existence of gasification reactions (Ogasawara et al., 1987; Lehmann et al., 1998; Betancur et al., 2009). Williams et al. (1990b) pointed out that, in an inert environment, higher temperatures of the pyrolysis process could lead to volatilisation of a portion of the char solid hydrocarbon amount. The authors highlighted that the solid yield reduced while that of the liquid and gas increased when the pyrolysis temperature was changed from 420 to 720 °C. The yield of the solid was roughly 26.4 wt.% while the contents of ash and FC were 2.4 and 30.3 wt.% respectively when the pyrolysis process was carried out at a heating rate of 80 °C min^{-1} and a temperature of 720 °C. Zabaniotou and Stavropoulos (2003) also, in a pyrolysis study carried out in a captive sample reactor, made an observation of solid yield decrease as the temperature increases. At 830 °C, the solid yield from this study was about 20 wt.% while the yield of gas went up to an about 73 wt.%. The variation in the amount of char produced during tyre pyrolysis, according to Cunliffe and Williams (1998b), is not only affected by the heating rate and temperature, but it is also a function of particular specifications of the system like reactor size, heat transfer efficiency between the tyre particles and hot surfaces of the reactor as well as the hot zone residence time of the vapours.

In a study carried out by González et al. (2001), there was a slight decrease in the char CV from 27.9 to 27.0 MJ kg^{-1} when the pyrolysis temperature was increased from 550 to 700 °C. Similarly, Li et al. (2004), in a pyrolysis experiment conducted in a RKR, observed that with increase in temperature from

450 to 650 °C, the char CV decreased slightly from 31.2 to a new value of 30.1 MJ kg^{-1}. The size distribution of the char, as revealed by the authors, was insignificantly affected by temperature. The particles of char with sizes below 5100 µ constituted about 83-84 % of the total char particles. In addition, the authors pointed out that as the temperature increased, there was an increase and decrease in the contents of fixed carbon and VM respectively. In a tyre pyrolysis study conducted by Fernández et al. (2012) in a horizontal oven, the CB generated at process temperatures of between 550 -900 °C fell in the size range of 2-50 nm and the temperature had no significant influence. The BET surface area of the CB obtained at 500 °C was roughly 68 $m^2 g^{-1}$ while that obtained at 900 °C was 61 $m^2 g^{-1}$, which was an insignificant variation. López et al. (2010) in an experiment conducted in a CSBR, on the contrary, noted a tendency of carbon black BET surface area increase with increasing temperature, in which case the value increased from 46.5 to 116.3 $m^2 g^{-1}$ when the temperature was changed from 425 to 600 °C. The trend observed by López et al. (2010) was echoed by Williams et al. (1990b), whose experiment was conducted in a FBR. There was an increase in the surface area with increasing temperature, and the use of higher heating rates resulted in even more significant effects.

2.3.3. Pressure

The increase in pressure during the pyrolysis of plastic materials results in production of liquid oils with higher viscosity. The coking also tends to be high, and the dehydrogenation and secondary reactions are more pronounced (Buekens, 2006). Vapour phase secondary reactions occurrence is lower when pyrolysis is carried out at vacuum pressure compared to when the process is carried out at atmospheric pressure. At pyrolysis processes conducted at vacuum conditions, the volatiles residence time is short-lived, thereby limiting the occurrence of secondary reactions (Li et al., 2004; Scheirs, 2006; Zhang et al., 2008); hence undesirable products formation (e.g. carbonaceous layers) on the surface of the char is dampened, leading to an improvement in its surface area and an increase in the quantity of active sites. Additionally, with the use of vacuum pyrolysis, the yield of the liquid fraction is higher than that obtained from a process carried out at atmospheric pressure. The gas and char yields, however, are lower in the vacuum process (Roy et al., 1990; Li et al., 2004; Zhang et al., 2008; Lopez et al., 2010).

According to Lopez et al. (2010), diffusion (as a result of positive pressure gradient) in the direction of the outer section of the volatiles developed inside the tyre granule porous structure is enhanced by the vacuum. Consequently, swift volatiles diffusion within the tyre particle minimises the residence time, which in turn curtails the secondary reactions materialisation. The main desirability of vacuum pressure, according to Roy et al. (1997), is its role in pyrolysis temperature reduction. Furthermore, the inert gas mass flow rate can be reduced with the use of vacuum pressure, resulting in an improved process feasibility. Vacuum pressure also aides to lower the condensation process requirements by

providing a means through which the liquid fraction can be collected with the use of less energy amount for outlet stream cooling (Lopez et al., 2010).

In a pyrolysis study involving the use of a sample of commercial rubber and pure polyisoprene at vacuum pressure in a batch reactor with pressure variation in the range of 0.8-28 kPa, a minimal change in the yields of liquid, gas and solid was observed (Roy et al., 1997). However, more liquid and less gas were produced at lower pressure. The effect of pressure on the pyrolysis process was more remarkable in CB and liquid composition. The quantity of DL-limonene was enhanced by lower process pressure. The solid fraction consisted mainly of CB whose properties were close to those of commercial CB. Similarly, in a pyrolysis study carried out by Zhang et al. (2008) in vacuum conditions at a pressure range of 3.5-4 kPa, it was shown that despite the higher ash content, the CB obtained portrayed characteristics similar to those of commercial CB. Moreover, the liquid fraction DL-limonene concentration was enhanced with decreasing pyrolysis process pressure. It was also noted by the authors that there was formation of some quantity of carbonaceous materials in the solid fraction, a tendency they linked to secondary occurrence of repolymerisation reactions. Therefore, secondary reactions, which provide a pathway for a higher gas yield or carbonaceous materials generation, can still occur at vacuum pressure conditions.

In conclusion, materialisation of secondary reactions can be reduced by conducting the pyrolysis process at lower pressure. In general, an insignificant role of secondary reactions can be observed when lower pressures are used for the pyrolysis process. Furthermore, the pyrolysis temperature could be reduced by decreasing the pyrolysis pressure; hence lowering the process thermal energy requirement.

2.3.4. Heating rate

Pyrolysis heating rate is an important parameter that has an effect on the rate of reaction, and it dictates the profile of temperature in the particles. In general, a shift to higher temperatures in the TGA mass loss profile is a consequence of heating rate increase (Williams et al., 1990b; Williams and Besler, 1995; Leung and Wang, 1998; Senneca et al., 1999; Aguado et al., 2005). This implies that the rate of decomposition is increased with increasing heating rate, and the heating rate also has an effect on initial and final temperatures of maximum devolatilisation. Williams and Besler (1995) attributed this trend to a combination of the effects of changes in degradation kinetics and heat transfer, thereby delaying the degradation. Therefore, apart from promoting an increase in cumulative volatiles amount, fast pyrolysis higher heating rates also contribute to pyrolysis temperature increase as compared to slow pyrolysis (Senneca et al., 1999). Nevertheless, as this could boost secondary reactions materialisation and possibly give way for higher gas yield, the volatiles residence time in a fast pyrolysis process should be reduced to curtail secondary reactions and boost the liquid yield generation from condensable gases. Senneca et al. (1999) and Williams et al. (1990b), thus deduced that the

balance between the products of secondary and primary devolatilisation as well as the heating rate mainly influenced the properties of the pyrolysis vapours. Cheung et al. (2011) pointed out that, despite pronged pyrolysis time, less energy was needed for pyrolysis process completion at lower heating rates. Contrastingly, more energy was required at higher heating rates, but the pyrolysis process completion time was reduced.

There is normally a generalised adoption for explaining how pyrolysis is influenced by the heating rate. Resistance to heat or mass transfer within the particle can occur at low heating rates. At higher heating rates, in fast pyrolysis, mass and heat transfer curtailment is reduced, leading to a decrease in the solid fraction amount and an increase in the liquid yield. According to Senneca et al. (1999), an increase in feedstock particle size and heating rate increase contribute to a steadier process devoid of internal pressure and temperature gradients. Heating rates of 5, 20, 100 and 900 °C min^{-1} and particle size ranging from 1000-3000 µ were used for the study via TGA. An approximate CB yield of 37 wt.%, independent of the heating rate, was obtained using the 1000 µ particle size at a pyrolysis temperature of 600 °C. The char produced using 3000 µ size particles was somewhat more distributed, but the yield was within the same range as that obtained using 1000 µ when the process was conducted at rates above 20 °C min^{-1}. There was, however, an increase in the yield to 40 wt.% when the process heating rate was lowered to 5 °C min^{-1}, a trend the authors attributed to crosslinking and cyclisation mechanism that was favourable for pyrolytic CB generation.

The direction of the internal heating of the particle originates from the exterior side of the surface (where thermal degradation happens) to the central section. Therefore, with progression in pyrolysis spell, the reaction advances towards the centre. The produced vapours from the pyrolysis process can undergo diffusion across the pore and on the outer particle side to the bulk of gaseous phase. Secondary heterogeneous and homogeneous reactions can concurrently take place within the porous particle as well as in the bulk of the gas. Therefore, with variation in heating rate, the occurrence of secondary reactions becomes highly sensitive, which is why there is a wide range of explanations in literature. For example, in a pyrolysis study by Williams et al. (1990b) using heating rates of 5, 20, 40 and 80 °C min^{-1} and temperatures of 300, 420, 600 and 720 °C, gas fraction CV of between 36.5 and 64.7 MJ m^{-3} were obtained when pyrolysis was conducted at the rates of 5 and 80 °C min^{-1} respectively. There was more yield of aliphatic compounds than aromatic ones in the liquid fraction with increasing heating rate in the range 5-40 °C min^{-1}, a tendency that indicates pyrolysis reaction devoid of influence of secondary reactions. In the same way, in a study carried out by Murillo et al. (2006b), the characteristics and yield of the liquid fraction as well as the overall tyre conversion were insignificantly affected by the heating rate. González et al. (2001) noted that the results obtained by heating rate increase from 5 to 20 °C min^{-1} were similar to those obtained with temperature increase, in the sense

that the increase in the heating rates led to an increase in gas yield. It was also observed that the contents of CO, H_2, CO_2, CH_4 C_2H_6 and C_2H_4 increased.

In conclusion, tyre pyrolysis can differently be affected by the heating rate. Despite the varied effects, association with secondary reactions occurrence is common among them. The occurrence of secondary reactions is notably boosted by other parameters, predominantly the residence time of the volatiles.

2.3.5. Pyrolysis time

Pyrolysis time, which is also termed tyre dwell or reaction or residence time within the reactor is an important parameter in industrial systems scale-up (Aylón et al., 2010). The shorter the residence time, the lower the system cost since smaller reactor volumes are involved. There is a link between pyrolysis time and the size of the particles involved. In general, smaller particles require shorter reaction times compared to larger ones if an equal pyrolysis degree of conversion is to be achieved.

Aylón et al. (2008), using an AR and a FBR, with 2000 μ mean particle size, observed that the rubber was fully converted in the two systems. However, the pyrolysis time (3.7 min) using the AR was shorter than in FBR, where it took 30 minutes for the process to be completed. The pyrolysis time in AR is dependent on the residence time of the volatiles. This variation is associated with reactor free volume increase when the duration of pyrolysis is reduced (Aylón et al., 2010), leading to a higher residence time of the volatiles. The conditions under which the apparatus (TG balance) commonly employed to study the kinetics of pyrolysis, according to Olazar et al. (2008b), differs from those used at industrial or pilot plant set-up, where the heating of the particle occurs almost instantaneously with a lot more turbulence in the contact of the gas and the particle. The authors revealed that with increase in temperature, the time for the pyrolysis process is shortened due to higher internal heating of the particle. Similarly, Cheung et al. (2011) reported on pyrolysis time reduction with increase in temperature. It is worth noting that extended pyrolysis time as well as elevated temperatures negatively impact on the amount of heat needed for pyrolysis process completion, which as a consequence reduces the efficiency of the process.

In conclusion, therefore, it can be said that for bigger-sized tyre particles, there is need to employ extended reaction times, even though heating rate or temperature increase could facilitate reduced reaction times. Different pyrolysis reactors have different inherent features, which is why the variation in pyrolysis time can change crucial parameters like the residence time of the volatiles. The reactor technology as well as the size of the particle play a part in pyrolysis time influence on pyrolysis.

2.4. Tyre pyrolysis products

2.4.1. Tyre pyrolysis liquid product

The oil obtained from pyrolysis has a dark brown colour, is moderately viscous, is similar to petroleum fractions and contains an aromatic/sulphurous odour (de Marco Rodriguez et al., 2001; Martínez et al., 2013; Williams, 2013). With over 100 known compounds, tyre-derived oil possesses high chemical complexity (Williams, 2013). The pyrolysis oil fraction is regarded as the plentiful fraction of all the WTP products. Table 2-4 shows the ultimate analysis and CV of tyre-derived oil as reported in literature. As seen in Table 2-4, the energy content of TDO can be as high as 44 MJ/kg, it and depends on the tyre composition as well as the pyrolysis conditions. It is worth noting that the CV of the tyre oil is higher than that of the waste tyre used for its production. Moreover, the TDO possesses characteristics close to those of light liquid fuels that have corresponding sulphur content and calorific value (Cunliffe and Williams, 1998b; de Marco Rodriguez et al., 2001). This is a motivation enough to consider tyre oil as an alternative for conventional fuel liquids.

Studies previously conducted by Williams et al. (1998) showed promising results as far as TDO combustion for long hours is concerned. The only shortcoming was the fact that SO_2 and NO_X emissions (at 2.1 % O_2) were higher (530 and 374 ppm respectively) compared to the corresponding values (110 and 131 ppm) obtained in diesel combustion under the same conditions. The contents of nitrogen in the tyre oil and diesel were 1.45 and 0.05 wt. % respectively while the corresponding sulphur contents were 0.45 and 0.2 wt. %.

The sulphur compounds found in tyre pyrolysis oils originate from the thermal decomposition of the accelerators and vulcanisation additives used during the process of tyre manufacture (Pakdel et al., 2001). This research study focused on reducing the sulphur content in tyre-derived oils via oxidative desulphurisation. Chlorine and fluorine are some of the inorganic compounds present in the TDO. In a study carried out by Benallal et al. (1995), it was found out that in the naphtha fraction, the compounds of sulphur in the tyre oil were centred around the light chunk. This is different from the case in petroleum, in which case the sulphur compounds are centred on the heavy portion (boiling point above 160 °C). The sulphur compounds predominantly present in the naphtha fraction of the tyre oil as reported in by the authors in this study included: benzothiazol, 3-methylthiophene, 2-tert-butylthiophene, 2-methylthiophene, 2.4-dimethylthiophene, 2-isopropylthiophene, 2-ethylthiophene, 2.3-dimethylthiophene, 2.5-dimethylthiophene and 3-ethylthiophene. In the process of primary distillation, it is possible to remove about 60-80 % of the compounds that contain sulphur in the TDO (Pakdel et al., 2001). Sulphur concentration of about 11000 ppm (equivalent to 60 % of the waste tyre sulphur content) in the TDO was reported in a study by Williams et al. (1990b) conducted using a FBR. In another study carried out by Kawakami et al. (1980), the sulphur concentrations in the heavy

and light oil fractions were 16500 and 10100 ppm respectively. Sulphur concentrations of 14000 ppm and 13000 ppm were reported by Cunliffe and Williams (1998b) when pyrolysis was conducted at temperature ranges of 450-475 °C and 500-600 °C respectively. Table 2-4 shows further results on sulphur contents in the tyre oils.

Generally, as seen in Table 2-4, TDO has a high H/C ratio of about 1.5 while its oxygen content is very low. These values represent the aromatic and aliphatic compounds. There is generally an increase in the relative amounts of aromatics with increasing pyrolysis process temperature. The increase in aromatic compounds proportion in the tyre oil is due to aliphatic chains cyclisation as well as free-radical reactions involving aromatic and aliphatic compounds (de Marco Rodriguez et al., 2001). Mastral et al. (2000c) also suggested that primary volatiles aromatisation reactions coupled with cyclisation could affect the aromatic proportion and its composition in the tyre oil. Other authors pointed out that the aromatic composition in the tyre oils is dependent on the rubber aromatic kind, olefins cyclisation as well as on Diels-Alder and dehydrogenation reactions (Ucar et al., 2005a; Lopez et al., 2010; López et al., 2011a). According to Unapumnuk et al. (2006), aromatic hydrocarbons are formed as a result of a mechanism involving Diels-Alder reactions, displacement of methyl and polymer decomposition. In summary, we can say that many authors (Williams et al., 1990b; Williams and Taylor, 1993; Cunliffe and Williams, 1998b; Pakdel et al., 2001; Chen and Qian, 2003; López et al., 2010) have attributed the Diels-Alder reaction to aromatic content rise with increasing pyrolysis temperature.

Tyre-derived oil, in general, consists of a mixture of C_5-C_{20} or higher organic compounds with various ratios of aliphatic and aromatic compounds (de Marco Rodriguez et al., 2001; González et al., 2001; Murillo et al., 2006b), and this depends both on the process environment and the composition of the tyre. The concentrations of alkenes, alkylated benzenes, alkanes and alkylated naphtha-lenes in the tyre oil, as reported in literature, are significant (Kyari et al., 2005). Sulphur-containing compounds and nitrogenated compounds, which are linked to accelerators applied during the manufacture of tyres (Laresgoiti et al., 2004), have also been reported as being present in the tyre oil (de Marco Rodriguez et al., 2001). According to Lopez et al. (2010), tyre oil presents itself as a mixture, complex in nature, containing hydrocarbons with generally low individual composition. In addition, it contains large amounts of styrene, limonene and isoprene, a statement echoed by Conesa et al. (2004).

Tyre oil can find its application as a source of purified chemicals like limonene and BTX or as an addition to the feedstock in the petroleum refinery (Williams and Besler, 1995; González et al., 2001). These chemicals are applied as the major feedstock in the production of resins, plastics, pharmaceuticals, surfactants etc. Correspondingly, it may be hydrocracked in refinery processing units to reduce the content of olefins and aromatics (López et al., 2010) . It has been found that TDO heavy portion, with boiling point above 350 °C, exhibits the technical feasibility for coke production (Chaala

and Roy, 1996). Additionally, subjecting this oil to coking yielded a combustible gas with a high calorific value and a new highly-valuable oil fraction (Chaala and Roy, 1996). The authors classified the new oil fraction into three categories: (i) gasoil heavy fraction (boiling point (BP) of more than 350 °C) with high asphaltene concentration (ii) middle distillate with a BP ranging between 205 and 350 °C and (iii) Naphtha fraction (starting BP of 205 °C) with high aromatic compounds content.

Table 2-4: Ultimate analysis and calorific values of pyrolysis oil as reported in literature

Ultimate analysis (wt. %)						CV (MJ kg^{-1})	Liquid yield (wt.%)	Ref.
C	N	H	S	O	H/C			
86.47	<1	11.73	0.83	n.r.	1.63	42.40[b]	56.00[c]	(Ucar et al., 2005a)
87.57	<1	10.35	1.35	n.r.	1.42	41.60[b]	48.40[d]	
84.90	0.40	9.60	1.60	3.50	1.36	40.77[b]	38.00	(Díez et al., 2004)
85.40	0.40	11.40	0.60	n.r.	1.60	43.27[b]	46.10[e]	(López et al., 2011a)
84.55	0.64	9.59	1.26	3.96[f]	1.36	41.00[a]	44.60	(Li et al., 2004)
87.90	0.50	10.10	1.30	0.1	n.r.	41.20[b]	53.10	(Cunliffe and Williams, 1998b)
85.60	0.40	10.10	1.40	2.10[f]	1.42	42.10[b]	38.00[d]	(de Marco Rodriguez et al., 2001)
87.90	0.70	11.20	1.00	0.2	1.53	44.80[b]	43.00[c]	(Roy et al., 1999)
86.50	0.50	10.80	0.80	2.20	1.50	43.70[b]	45.00[d]	
83.45	1.05	10.31	0.99	n.r.	1.48	n.r.	54.60	(Aylón et al., 2008)

[a] Lower; [b] Higher; [c] Truck tyre; [d] Passenger car tyre; [e] Passenger car and Truck tyres mixture; [f] oxygen and others

Table 2-5 shows a list of compounds contained in the tyre pyrolysis oil. The main chemical fraction classifications of the oil, as seen in Table 2-5, are aromatic, hetero-atom, aliphatic and polar fractions. The tyre oil obtained in a pyrolysis study by Dai et al. (2001) in a circulating fluidised bed consisted of 42.09, 26.77, 26.64 and 4.05 wt.% aromatics, alkanes, non-hydrocarbons and asphalt respectively. In another study conducted by Conesa et al. (1996) in a fluidised bed reactor, the TDO contained 19.1, 39.5, 20.1 and 21.3 wt.% aromatic, aliphatic, polar and hetero-atom fractions respectively, while Aylón et al. (2008) in an experiment carried out in a screw kiln reactor reported TDO with 27.8, 65.6 and 6.7 wt.% polar, aromatic and alkane fractions respectively. The aromatic fraction rose from 53.4 to 74.8 wt. % with a shift in temperature to 700 up from 300 °C in a fixed bed pyrolysis experiment carried out by Laresgoiti et al. (2004).

Table 2-5: Compounds in waste tyre pyrolysis oil (Williams and Bottrill, 1995; Cunliffe and Williams, 1998b; Dai et al., 2001; Conesa et al., 2004; Laresgoiti et al., 2004; Li et al., 2004; Olazar et al., 2008a; Kaminsky et al., 2009; Banar et al., 2012; Williams, 2013)

Aliphatic compounds and HC	Single ring aromatic and N compounds	PAH and S compounds
Aliphatic	*Single ring aromatic*	*PAH*
$C_{10}H_{22}$	Benzene, butenyl-	Acenaphthene
$C_{11}H_{24}$	Benzene, butyl-	Anthracene
$C_{12}H_{26}$	Benzene, cyclohexyl-	Benz[a]anthracene
$C_{13}H_{28}$	Benzene, cyclopentyl-	Benzo[a]pyrene
$C_{14}H_{30}$	Benzene, dimethyl-	Benzo[e]pyrene
$C_{15}H_{32}$	Benzene, dimethylpropyl-	Biphenyl
$C_{16}H_{34}$	Benzene, ethyl–methyl-	Chrysene
$C_{17}H_{36}$	Benzene, hexenyl-	Dihydromethylnaphthalene
$C_{18}H_{38}$	Benzene, hexyl-	Dimethlyphenanthrene
$C_{19}H_{40}$	Benzene, methyl– Benzene, butenyl-	Dimethylbiphenyl
$C_{20}H_{42}$	Benzene, pentyl-	Dimethylfluorene
$C_{21}H_{44}$	Benzene, propyl-	Dimethylnaphthalene
$C_{22}H_{46}$	Dimethylindene	Ethylnaphthalene
$C_{23}H_{48}$	Dimethylindene	Fluoranthene
$C_{24}H_{50}$	Ethylbenzene	Fluorene
$C_{25}H_{52}$	Ethylindene	Methylanthracene
$C_{26}H_{54}$-$C_{35}H_{72}$	Indene	Methylfluorene
C_6H_{12}	Methylindene	Methylnaphthalene
C_7H_{14}	Methylstyrene	Methylphenanthrene
C_8H_{16}	Styrene	Naphthalene
C_9H_{18}	Terphenyl	Phenanthrene
Hydrocarbons	Toluene	Pyrene
Cyclohexane, ethenyl–methyl-	Toluene, ethyl	Tetrahydronaphthalene
Cyclohexene	Trimethylindene	Tetramethylphenanthrene
Cyclohexene, propenyl-	Xylene (1,2-dimethylbenzene)	Trimethylnaphthalene
Cyclopentane, ethylidene-	Xylene (1,3-dimethylbenzene)	Trimethylphenanthrene
Cyclopentene, pentyl-	Xylene (1,4-dimethylbenzene)	*sulphur compounds*
Dimethylphenol	*Nitrogen compounds*	Benzonaphthothiophene
Heptadecanoic acid	Quinoline	Benzothiophene
Hexadecanoic acid	PCDD/PCDF	Dibenzothiophene
Isopropylphenol	Octachlorodibenzodioxin	Dimethylbenzothiophene
Limonene	Hexachlorodibenzofuran	Dimethyldibenzothiophene
Methylbenzaldehyde	Heptadecanenitrile	Methylbenzothiophene
Methylphenol	Heptachlorodibenzofuran	Methyldibenzothiophene
Octadecanoic acid	Diphenylamine	Methylnaphthothiophene
Pentadecanoic acid	Dimethylquinoline	Naphthothiophene
Phenol	Benzothiazole	Tetramethyldihydrobenzothiophene
Pinene	Benzonitrile	Thiophene
Tetradecanoic acid	Aniline	Trimethyldibenzothiophene
		Trimethyldihydrobenzothiophene

2.4.1.1. Aliphatic and aromatic compounds

Straight-chain alkanes ranging from C_6-C_{37} and lower alkenes are the major aliphatic compounds found in the tyre-derived oil. Benzene, xylenes, limonene, toluene, indene and styrene, on the other hand, are the primary aromatic compounds present in the oil. Additionally, PAHs are also contained in the tyre liquids, and they include five-ring benzopyrenes and two-ring naphthalenes.

Studies have shown that the aromatic and aliphatic fractions in the tyre oils increase and decrease respectively with increase in temperature. In a study by Cunliffe and Williams (1998b), the percentage of aromatic and aliphatic fractions were 36.7 and 51.3 wt.% respectively when a 450 °C pyrolysis temperature was used while the corresponding percentages for the same process carried out at 600 °C were 45.6 and 36.1 wt.%. At a prolonged hot zone residence time in the reactor, pyrolysis gases' secondary reactions lead to an increase in the content of aromatic compounds in the oil (Cypres and Bettens, 1989; Williams and Taylor, 1993). The variations in the relative content of fractions, as reported by various author,s could be attributed to reactor configuration differences, temperature, heating rate, secondary reactions duration as well as the fractionation analytical technique.

Toluene and benzene contents of 3.8 and 4.2 wt.% respectively were obtained in a pyrolysis study carried out in a laboratory scale fluidised bed reactor at 740 °C by Kaminsky et al. (2009). In a study by Cunliffe and Williams (1998b), the maximal concentrations reported for total xylenes, toluene, limonene, indene and styrene were 1.68, 1.77, 3.13, 0.32 and 0.36 wt.% respectively. In a similar study carried out by Li et al. (2004) at 550 °C in a RKR, xylene, benzene, toluene, limonene and styrene concentrations of 2.05, 1.49, 5.16, 0.42 and 1.42 wt.% were obtained. The temperature greatly influenced the contents of aromatic fractions, with benzene increasing to 2.09 wt. % up from 0.40 wt. % when the temperature was shifted from 450 to 650 °C. The case was the same for toluene concentration where there was an increase to 7.06 wt. % up from 2.27 wt. % in the corresponding range of temperature. The limonene percentage concentration correspondingly decreased as the temperature was increased (Li et al., 2004). Studies have suggested that at pyrolysis temperatures beyond 500 °C and/or at extended residence times in the hot zone, limonene undergoes decomposition forming products such as xylene, benzene, toluene, styrene, methylstyrene and trimethylbenzene (Pakdel et al., 1991; Williams and Besler, 1995; Li et al., 2004).

2.4.1.2. Polycyclic aromatic hydrocarbons

Polycyclic aromatic hydrocarbons exist in in a wide range in the TDO. Fluorenes, alkylated naphthalenes and phenanthrenes constitute the highest PAHs concentration in the oil. A number of identified PAHs in the tyre-derived oil are shown in Table 2-5. Cunliffe and Williams (1998b) reported total PAHs concentrations of 1.72 wt. % in oil obtained from a pyrolysis process carried out at 500 °C

in a FBR. The total concentrations of PAHs reported for another pyrolysis process conducted by Li et al. (2004) at the same temperature, but using a RKR was higher (16 wt.%). Laresgoiti et al. (2004) reported PAHs comprising mainly of fluorene, naphthalene, phenanthrene and their alkyl derivatives in pyrolysis oil obtained using a fixed bed reactor.

Studies have shown that prolonged residence times coupled with higher pyrolysis temperatures result in production of high PAHs concentrations (Williams and Taylor, 1993; Cunliffe and Williams, 1998b). For instance, in a WTP experiment conducted by Cunliffe and Williams (1998b) using a fixed bed reactor, there was an increase in the total PAHs concentration from 1.53 to 3.43 wt.% with a temperature shift from 450 to 600 °C, as individual concentrations of alkylated fluorene, naphthalene and phenanthrene also increased with temperature. The total alkylated fluorenes increased to 0.26 wt. % up from 0.08 wt. %, naphthalenes to 1.43 from 0.54 wt. %, while phenanthrenes increased to 0.81 up from 0.54 wt. %. Significant concentrations of compounds possessing biological activity such as tri-methylphenanthrenes, tetra-methylphenanthrenes, methylfluorenes and chrysene were also pinpointed. Similar pyrolysis temperature effect (with temperature shift from 450 to 650 °C) on PAHs concentration was reported by Li et al. (2004), where fluorene homologues increased to 2.57 wt.% up from 1.17, naphthalene homologues to 10.1 wt.% up from 8.6 while homologues of phenanthrene increased to 6.51 wt.% up from 2.15 wt.%. A similar trend was also reported by Laresgoiti et al. (2004).

With prolonged residence times and high temperatures in secondary reactors, the gases produced during WTP can be cracked to yield PAHs. In a study (with post-pyrolysis preceded by pyrolysis in a batch reactor) by Williams and Taylor (1993), for example, an increase in tyre oil PAHs total concentration from 1.4 wt.% to above 10 wt.% with change in post-pyrolysis temperatures from 500 to 720 °C was observed. A similar tendency of tyre-derived oil PAHs concentration increase with involvement of secondary gases reactions in post-pyrolysis reactors was reported by Cypres and Bettens (1989), where it was found that with increase in post-pyrolysis temperature (from 600 to 800 °C), naphthalene and phenanthrene concentrations increased. Arabiourrutia et al. (2007), using a CSBR at 500 °C reported low PAHs yield, and attributed this to volatiles' short residence time in addition to the fact that this reactor type performs efficiently with regard to mass and heat transfer. In this regard, as pointed out by Callén et al. (2000), there is discrepancy in literature, which could be ascribed to differences in the technique of analysis and the inherent reactor type and configuration used.

The aromatic content increase with temperature has been attributed to Diels-Alder mechanism by a number of authors (Cypres and Bettens, 1989; Williams and Taylor, 1993). In a pyrolysis experiment carried out in a FBR by Banar et al. (2012), it was observed that an increase in the heating rate resulted in tyre oil PAHs concentration increase, while Kyari et al. (2005), also using a FBR, reported that the use of different tyre brands and types for pyrolysis yielded various oil PAHs and single ring aromatic

compounds concentrations. The composition of the tyre also affects the formation of PAHs in the sense that a butadiene backbone that supports an aromatic ligand is contained in SBR and this speeds up the formation of PAHs. Therefore, pyrolysis of tyres with higher contents of SBR yield significant PAHs concentrations (Kwon and Castaldi, 2008). Kwon and Castaldi (2008) additionally pointed out that during SBR thermal degradation, cyclisation via Diels-Alder mechanism is not a domineering reaction.

Polycyclic aromatic sulphur-containing hydrocarbons and nitrogen-containing PAHs (PANHs) are present in tyre oil. The presence of PASHs, for example, in form of thiophene and its derivatives such as dimethylbenzothiophene, dimethylthiophene, methylthiophene at concentrations ranging from 0.1 to 0.3 wt.% has been reported in literature (Kaminsky et al., 2009). Similarly, aniline, dimethylquinoline and benzothiazol at concentrations of around 0.1 wt.% have been reported as the representative forms of PANHs in tyre oil (Kaminsky et al., 2009). In a study conducted by Williams and Bottrill (1995), it was found that benzothiophene (BT) and dibenzothiophene (DBT), including their derivatives (in addition to naphthothiophenes and their methyl derivatives) were the representative forms of PASHs in the tyre-derived oil. It was observed from this study by Williams and Bottrill (1995), carried out in a fluidised bed reactor, that with increasing pyrolysis temperature, the oil PASHs concentration also increased.

Scanty information is available on concentration determination in TDO of dioxins, in particular polychlorinated dibenzodioxins (PCDDs), and furans, in particular polychlorinated dibenzofurans (PCDFs). In one of the tyre pyrolysis studies carried out in a fixed bed reactor by Banar et al. (2012), concentrations of 1234678-HpCDF, 1234789-HpCDF, 123478-HxCDD and OCDD at 0.021 pg g^{-1}, 0.015 pg g^{-1}, 0.008 pg g^{-1} and 0.021 pg g^{-1} respectively were reported. Additionally, in this study, low metals concentration in the tyre oil was reported for cadmium, arsenic, lead and chromium to be in the order of parts per billion (ppb). The presence of chloride in the oil was also in the ppb level.

2.4.1.3. Fuel characteristics of tyre pyrolysis oil

Table 2-6 presents the fuel properties of oil obtained from waste tyre pyrolysis as reported by various authors while Table 2-7 shows the corresponding properties, for comparison purpose, of fuels derived from petroleum. Literature reports show that the sulphur content in tyre oils can be affected by pyrolysis temperature. For instance, Aydın and İlkılıç (2012) found out that the sulphur content in oil produced at 550 °C was lower by about 0.3 wt.% than that of oil obtained at a pyrolysis temperature of 400 °C. Similar observation was made in a study carried out earlier by Cunliffe and Williams (1998b), where oil produced at 450 and 475 °C pyrolysis temperature contained more sulphur (1.4 wt.%) than oil obtained at elevated temperatures.

The characteristics of liquid fuel provide information on fuels' properties in regard to its ability to perform in systems of combustion, probable emissions, transport and storage matters, range of distillation, among others. Liquid fuel flash point depicts the temperature at which flammable gases are generated and will ignite. This fuel property is an indicator of the fire hazards related with transport, storage and fuel use. Tyre pyrolysis oils, in general, have a lower flash point in comparison with petroleum-derived fuels, and this difference in flash points is occasioned by the fact that TDO is unrefined and has an array of boiling point fractions, volatile hydrocarbons included. The standard method of measuring the likelihood of carbon formation when oil is poorly combusted is by considering its carbon residue. As a result, the spray combustion burners or fuel injector nozzles in the diesel engine may undergo carbon coking. As seen in Tables 2-6 and 2-7, the carbon residue of the tyre oil is relatively high (1.78-2.2 %) in comparison with that (< 0.35) of gas oil. This implies that the blockage of the spray burner or nozzle may occur with prolonged duration of use.

In a study carried out by Aydın and İlkılıç (2012) on sulphur removal in TDO, the oil was found to have properties similar to those of diesel fuel derived from petroleum. In addition, the blends of diesel fuel and TDO yielded a fuel mixture with characteristics close to those of diesel. The range of distillation and boiling point of the tyre-derived oils was an indicator that owing to the unrefined nature of the TDO, the boiling point array, as expected, would consequently be wide. The calorific value of tyre oils (38-42.66 MJ kg^{-1}) is slightly lower than those of the fuels derived from petroleum (Tables 2-6 and 2-7). Tyre-derived oil CV range of 38-49.5 MJ kg^{-1} has been reported by other authors (Williams et al., 1998; Li et al., 2004; Murugan et al., 2008c; Banar et al., 2012; Rada et al., 2012). The burning rate coefficient is an important parameter related to fuel characteristics. Williams et al. (1998) reported a tyre oil burning rate coefficient value of 0.75 mm s^{-1}, a coefficient value comparable with that of gas oil and light fuel oil with respective values of 0.88 mm s^{-1} and 0.82 mm s^{-1}.

Table 2-6: Fuel characteristics of waste tyre pyrolysis oil as reported by different authors

Property	Reference			
	Li et al. (2004)[a]	Williams et al. (1998)	Murugan et al. (2008c)	Banar et al. (2012) [b]
Flash point (°C)	17	20	43	65
10 % BP (°C)	-	140	114.5	58.2
50 % BP (°C)	-	264	296.1	174.8
90 % BP (°C)	-	355	386.4	-
Ash (wt.%)	Tr.	0.002	0.31	-
CV (MJ kg^{-1})	41.7	42	38	42.66
Carbon (wt.%)	84.26	88	-	79.61
Carbon residue (%)	1.78	2.2	-	-
Density (kg l^{-1})	0.962	0.91	0.924	0.833
Hydrogen (wt.%)	10.39	9.4	-	10.04
Initial BP (°C)	-	100	70	38.5
Moisture	0.88 wt.%	4.6 vol.%	-	-
Nitrogen (wt.%)	0.42	0.45	-	0.94
Oxygen (wt.%)	3.39	0.5	-	9.3[c]
Sulphur (wt.%)	1.54	1.5	0.72	0.11
Viscosity, cSt (at 40 °C)	-	6.3	3.77	-
Viscosity, cSt (at 50 °C)	2.44	-	0.924	1.01
Viscosity, cSt (at 60 °C)	-	2.38	-	-

[a] Pyrolysis oil obtained at 500 °C; [b] Pyrolysis oil obtained at 35 °C/min.

Table 2-7: Properties of petroleum fuels (Harker and Backhurst, 1981; Williams, 2013)

Property	Gas oil	Kerosene	Light fuel oil
Flash point (°C)	75	40	79
50 % B.Pt. (°C)	300	200	347
90 % B.Pt. (°C)	-	315	-
Ash (wt.%)	0.01	-	0.02
CV ($MJkg^{-1}$)	46	46.6	44.8
Carbon (wt.%)	87.1	-	85.5
Carbon residue (%)	< 0.35	-	-
Density ($kg\ l^{-1}$)	0.78	0.84	0.89
Hydrogen (wt.%)	12.8	13.6	12.4
Initial B.Pt. (°C)	180	140	200
Moisture (vol.%)	0.05	-	0.1
Nitrogen (wt.%)	0.05	-	0.15
Sulphur (wt.%)	0.9	0.1	1.4
Viscosity, cSt (at 40 °C)	3.3	1.2	21

2.4.1.4. Limonene in tyre-derived oil

Limonene ($C_{10}H_{16}$), a cyclic terpene, consists of two isoprene units (Fernández et al., 2012), and is a value-added product found in the TDO and its applied as pigments' dispersing agent during resins, industrial solvents, cosmetics and adhesives formulation. In addition, it also serves as feedstock in flavourings and fragrances manufacture (Pakdel et al., 1991; Cunliffe and Williams, 1998b). The forms in which limonene exists are two isomeric forms (D- and L-limonene), DL-limonene (a mixture of D- and L- forms) and racemic limonene, also commonly referred to as dipentene (Pakdel et al., 1991; Cunliffe and Williams, 1998b; Pakdel et al., 2001).

DL-limonene formation from a tyre pyrolysis process is dependent upon the temperature, residence of the vapours, composition, sample size as well as the pressure. Owing to secondary reactions, an increase in temperature leads to a decrease in the yield of DL-limonene. The secondary reactions lead to transformation of DL-limonene into aromatics like m-cymene, indane, trimethylbenzene etc. (Pakdel et al., 2001). DL-limonene yield can be enhanced by observing short residence times of the

volatiles and using low pressure during pyrolysis, which in turn minimise secondary reactions occurrence. In this regard, the concentration of limonene under atmospheric pyrolysis conditions is lower than that obtained at vacuum pressure (Pakdel et al., 1991; Benallal et al., 1995; Roy et al., 1997; Pakdel et al., 2001). A similar observation of limonene sensitivity to pyrolysis pressure and temperature was made by Zhang et al. (2008) whereby limonene concentration in the oil fraction (obtained at pyrolysis pressure range of 3.5 and 4.0 kPa) reduced to 4.72 down from 11.97 wt.% with temperature increase from 450 to 550 °C. In addition, it was noted that at a fixed temperature of 500 °C, the concentrations of limonene oils obtained at pyrolysis pressures of 3.5 and 10 kPa were 11.73 and 7.8 wt.% respectively, which indicated limonene concentration drop with increasing pressure (Zhang et al., 2008). Cunliffe and Williams (1998b) also noted that the limonene concentration in TDO obtained in a fixed bed reactor at a pyrolysis temperature of 450 °C was higher (3.1 wt.%) than that (2.5 wt.%) in oil obtained at 600 °C. In another study carried out by Arabiourrutia et al. (2007) in conical spouted bed reactor batch operations, it was observed that there was a reduction in the liquid portion with increasing temperature. The C_{10} chunk, associated with D-limonene, in the fraction reduced from 28 to 17.99 wt.% when the temperature was increased from 425 to 610 °C. The yield of D-limonene, in this case, was 23.39 wt.% at 425 °C and 5.66 wt.% at 610 °C. Tyre oil limonene concentration decrease from 5.4 to 0.07 wt.% with pyrolysis temperature shift from 450 to 650 °C was observed by Li et al. (2004) in an experiment conducted in a rotary kiln reactor.

With pure polyisoprene pyrolysis taking place in a batch reactor under vacuum conditions, a 16.6 wt.% limonene concentration was reported by Roy et al. (1997). There was a decrease to 5 wt.% limonene concentration when a rubber sample with polyisoprene, carbon black and SBR contents of 52.2, 31.0 and 5.4 wt.% respectively was pyrolysed under the same conditions of 0.8 kPa and 500 °C. Several authors have reported various pathways of reactions involved in limonene generation from pyrolysis of tyres (Groves et al., 1991; Mastral et al., 2000c; Pakdel et al., 2001; Zhang et al., 2008; Kwon and Castaldi, 2009), majority of whom, in addition to other authors (Pakdel et al., 1991), are in agreement that the major source of limonene in the TDO is polyisoprene, the primary chemical constituent of natural rubber (Mastral et al., 2000c; Zhang et al., 2008; Kwon and Castaldi, 2009). Kwon and Castaldi (2009), additionally, linked the content of styrene to SBR, and they noted that chemical species like 4-ethenylcyclohexene and styrene were observed only during the pyrolysis of SBR whereas during the pyrolysis of polyisoprene, 1-methyl-4-(1-methyl-lethyl)-benzene and limonene were observed.

2.4.1.5. Fractionation of tyre-derived oil

The tyre-derived oil contains aromatic, aliphatic and polar compounds with a 70 - 400 °C boiling point range. The TDO, therefore, has to be subjected to separation or purification before being commercialised (Murillo et al., 2006a). In general, a distillation curve typically indicates diesel and

gasoline fuels mixture with a broad BP range, which points to the unrefined nature of the tyre oil. Tyre pyrolysis oil distillation cuts can be categorised into light, medium and heavy fractions, which are obtained at average temperatures of less than 200 °C, between 200-350 °C and above 350 °C respectively (Martínez et al., 2013). Kyari et al. (2005), using a simulated distillation method at distillation temperatures of between 105-375 °C obtained light, medium and heavy fraction cuts of 58, 26 and 6 vol. % respectively, which was an indication that the TDO was unrefined as evidenced by the broad boiling point ranges. de Marco Rodriguez et al. (2001) obtained light, medium and heavy fraction cuts of 30, 30 and 34 vol.% respectively using automatic distillation test and distillation temperatures in the range of 78-388.7 °C. The oil was not near, in properties, to diesel oil due to the high percentage of low-boiling products. In another TDO distillation process carried out by Li et al. (2004) using true-boiling-point distillation system, light, medium and heavy fractions of about 39, 32 and 28 wt.% respectively were obtained. The oil was a lot lighter compared to crude oil since its heavy fraction content was only about 28 wt.% vis-à-vis ≈ 59-68 for crude oil (Li et al., 2004). İlkılıç and Aydın (2011), using distillation temperatures above 400 °C, obtained light, medium and heavy fraction cuts of 30, 55 and 15 vol.% respectively. The final distillation temperature in this case was higher than that of diesel, and therefore slower combustion was expected.

Fractionation of TDO aides in identifying its similarity with standard fuels such as diesel and gasoline as well as the possibility of its application in processes different from combusting it directly. The variation in results available in literature is linked to tyre composition, pyrolysis conditions as well as the distillation technique used i.e. simulated or real. Laresgoiti et al. (2004), for example, in a distillation process carried out (at atmospheric pressure) on oil obtained at 500 °C using an autoclave, observed that 20 and 10 wt.% of the TDO fell in the category of light (< 160 °C) and heavy naphtha (between 160 and 204 °C) respectively. In another study by Benallal et al. (1995), the TDO obtained at 510 °C and a pressure of between 2 and 20 kPa was subjected to distillation and it yielded about 20, 6.8, 30.7 and 42.5 wt.% light naphtha (BP < 160 °C), heavy naphtha (BP between 160 and 204 °C), middle distillate (BP between 204 and 350 °C) and bottom residue (BP > 350 °C) respectively. Murillo et al. (2006a) used HYSYS to simulate the separation process and obtained five streams whose properties were compared with those of conventional fuels using BP ranges. The first stream, with a BP range of 61.5- 107.5 °C, was characteristically close to light naphtha and it constituted 7.4 wt.%. Stream two, with a BP range of 146.4-199.5 °C, showed characteristics similar to commercial naphtha and constituted 22.37 wt.%. Stream three corresponded to No. 1 fuel oil based on the sulphur concentration, flash point and BP ranges, and it constituted 15.18 wt.%. Streams four and five, based on their BP ranges of 305.1 to 363.3 and 335.3 to 374.4 °C fell in the category of heavy gas oil.

Many authors (Pakdel et al., 1991; Benallal et al., 1995; Napoli et al., 1997; Cunliffe and Williams, 1998b; Mastral et al., 2000c; Pakdel et al., 2001; Laresgoiti et al., 2004) have reported that there is

high limonene content (up to 25 wt.%) in the naphtha fraction. The naphtha fraction obtained and analysed by Benallal et al. (1995) revealed that its octane number was higher than that of petroleum. Testing of the light fraction as an additive to gasoline, middle fraction as rubber plasticiser and heavy fraction for use in road pavements and production of coke was reported by Roy et al. (1999). The middle fraction was reported to have a played a part in cure time reduction, which subsequently sped up the process of vulcanisation.

2.4.1.6. Combustion of tyre-derived oil

Tyre-derived oil, owing to its flexibility storage and transportation-wise, is a promising alternative fuel for use in internal combustion engines. However, the use of TDO directly in internal combustion engines is limited by its broad distillation spectrum consisting of large concentrations of aromatic and olefenic compounds. In addition to viscosity and sulphur content issues, these characteristics contribute to lower cetane number and flash point than those of conventional diesel fuels. Some studies on TDO-diesel fuel blending effect on the performance of diesel engines and emissions have been carried out by a number of researchers (Murugan et al., 2008b, 2008c; Rofiqul et al., 2008; Murugan et al., 2009; İlkılıç and Aydın, 2011; Doğan et al., 2012). The results from these studies varied owing to different TDO characteristics, and probably due to the differences in the engines used for testing.

The cetane number of standard diesel fuels is in the range of 40-55 (Heywood, 1988) whereas values of 40 and 44 have been reported for TDO (Rofiqul et al., 2008; İlkılıç and Aydın, 2011). The implication of a cetane number below 40 is that the fuel ignition is delayed, which means that excess fuel ends up getting injected into the cylinder prior to ignition of the first particles of the fuel. This leads to rapid and huge increase in pressure at the initial stage of combustion, a situation that is responsible for reduced thermal efficiency, high emissions and exhaust smoke levels as well as rough running of the engine (Pulkrabek, 1997). In a study by İlkılıç and Aydın (2011), it was observed that the TDO, directly injected in a diesel engine, emits higher amounts of smoke, HC, CO and SO_2 compared to standard diesel fuel. This behaviour, according to the authors, is ascribed, mainly, to low cetane number and poor atomisation. In addition, excess fuel injection mass base-wise was due to the high density and this in turn led to rich condition of combustion; hence to higher opacity of the smoke. The authors revealed that TDO blends with up to 75 % by weight diesel were fit for efficient use in diesel engines without the need to modify the engine. In another study carried out by Murugan et al. (2009), increase in emissions of HC, NO_X and CO was observed when TDO and diesel fuel blends of different proportions were injected into the diesel engine. This behaviour was attributed to aromatics concentration, lower fuel volatility and higher viscosity. The aromatics poorly ignite, and together with cycloalkanes generally lead to the reduction in cetane number, save for when there is an attachment to the ring of a long chain of n-alkane (Heywood, 1988).

Due to the high TDO viscosity, issues such as oil ring sticking and carbon deposition are likely to arise (Murugan et al., 2008b), and this has an effect on the flow of fuel inside the pipes, atomisation of the fuel as well as fuel pump operation and wear (Taylor and Bottrill, 1995; Li et al., 2004). The TDO is highly viscous due to the huge chemical structure and molecular weight of compounds contained in it. In addition to having higher concentration of sulphur, some amount of char solid particles, alkali metals or sand may be present in the tyre oil (Zabaniotou and Stavropoulos, 2003), and this can contribute to engine wear issues as well as health and environmental problems. According to Murugan et al. (2008b), tar compounds and some polymers are also present in the tyre oil, which could possibly lead to the formation of carbonaceous material within the combustion section, grooves of the piston ring as well as in the exhaust valves and ports. Owing to this, in order to better the combustion properties, it is appropriate to refine the TDO before direct feeding in the engine (Roy et al., 1999; Murugan et al., 2008b; Rofiqul et al., 2008). In this regard, a study on modification of TDO was carried out by Murugan et al. (2008b). The modification encompassed three processes. Firstly, the moisture was removed followed by desulphurisation and then finally vacuum distillation was performed. From this TDO refining process, the CV increased by around 7 %. The use of refined tyre oil for engine testing presented higher CO and HC emissions compared to standard diesel fuel. However, the TDO produced less (by around 18%) NO_X emissions than diesel fuel. The engine could not run with 100 % tyre oil. In another study by Doğan et al. (2012), it was found that the TDO fuel blends (with maximum 70 % TDO) can be used satisfactorily with minimal effect on the performance of the diesel engine.

2.4.2. Tyre pyrolysis char

Pyrolysis provides an option for organic matter conversion into a solid that is rich is carbon. This type of solid is commonly called char. In the tyres scenario, this carbonaceous solid fraction (also termed PCB) equates to the original CB and the inorganic substances (e.g. Ca, Zn and Si) used during the tyre manufacturing process (Chaala et al., 1996; Miguel et al., 1998; Roy et al., 2005). The composition of char is dependent upon the composition of the tyre and the conditions of pyrolysis. Moreover, the economic feasibility of WTP is considerably influenced by the char yield and quality (Pakdel et al., 2001; Zhang et al., 2008). At temperatures for achievement of good-grade tyre conversion (about 500 °C), the pyrolytic carbon black consists of roughly between 35 to 40 wt.% summation of ash and FC, and this value could even be lower depending upon the composition of the tyre.

Table 2-8 shows the properties of pyrolytic char as reported in literature. Additionally, depending upon the complexity and extremity of the process, it may comprise of carbon-containing material originating from repolymerisation reactions between the derivatives of polymer (Merchant and Petrich, 1993; Chaala et al., 1996; Roy et al., 1999; de Marco Rodriguez et al., 2001; Murillo et al., 2006b). Thus, part of the organic vapours generated in the pyrolysis process are transformed, via dehydrogenation and dealkylation reactions, into coke or get absorbed on the surface of the char (Helleur et al., 2001;

Berrueco et al., 2005; Zhang et al., 2008). The PCB, as highlighted by Senneca et al. (1999), is therefore expected to be coarser compared to the initial carbon black. The authors, based on these findings, propose that there is a likelihood of the particles of CB acting as seed nuclei in which there is growth, by crosslinking and/or cyclisation, of coherent structures of solid carbon. The char obtained when vacuum pyrolysis is used has a concentration similar to that of the original CB due to the fact that the adsorption of hydrocarbon on the surface of CB is hampered by the use of lower pressures.

Pyrolytic carbon black, as reported by several authors, is used to produce activated carbon (Merchant and Petrich, 1993; Teng et al., 1995; San Miguel et al., 2003; Murillo et al., 2005). In a detailed review by Mui et al. (2004) on activated carbons (ACs), it is pointed out that using CO_2 and steam, waste tyres have been used to produce activated carbons with BET-determined surface areas of not more than 1000 $m^2 g^{-1}$. The ACs can also be used as fillers in road pavements, for reinforcement of rubber goods with low value, as pigment for printing ink, or can be mixed with bitumen for enhancement of its rheological characteristics.

Ideally, PCB can be used for rubber manufacturing, but its ability to be reused is limited by high inorganic impurities concentration (Mastral et al., 1999a; Martínez et al., 2013) as well as the structure of the particle i.e. the degree of aggregation (González et al., 2001), although the PCB obtained in a study carried out by Faulkner and Weinecke (2001) portrayed properties similar to those of medium grade type based on iodine and dibutyl phthalate absorption, discoloration of toluene, mean particle size as well as BET surface area. Zhang et al. (2008) carried out a pyrolysis experiment at vacuum pressure using a FBR and obtained pyrolytic CB with a BET surface area value of about 68 $m^2 g^{-1}$. The authors pointed out that this BET surface area value lies in between the values of N550 series (about 45 $m^2 g^{-1}$) and N600 series (about 90 $m^2 g^{-1}$) of commercial CBs.

Table 2-8: Properties of pyrolytic char as reported in literature

Property	References				
	Conesa et al. (2004)	Cunliffe and Williams (1998a)	Galvagno et al. (2002)	Li et al. (2004)	Olazar et al. (2008a)
Proximate analysis (wt.%)					
Ash	8.27	11.6	15.33	12.32	-
Moisture	0.37	0.4	3.57	2.35	-
VM	7.78	2.8	12.78	16.14	-
Ultimate analysis (wt.%)					
S	1.9	2.3	2.13	2.32	2.7
N	0.1	0.7	0.34	0.61	0.3
H	0.6	0.9	1.77	2.28	1.3
Cl	-	0.08	-	-	-
C	88.19	90.6	85.31	82.17	80.3
CV (MJ kg-1)	30.8	30.5	30.7	31.5	29.3
Surface area (m^2/g)	93	64	-	-	83
Metals (wt.%)					
Zn	6.68	4.1	4.06	-	3.8
Si	1.69	0.42	-	-	-
Pb	0.01		Tr	-	-
Fe	0.04	0.2	0.54	-	-
Ca	0.13	1.2	-	-	-
Al	-	0.15	1.09	-	-

Several studies on investigation of char properties as CB substitute have been carried out by various researchers (Darmstadt et al., 1995; Sahouli et al., 1996; Roy et al., 1999; Kaminsky and Mennerich, 2001; Pantea et al., 2003; Tang and Huang, 2005; Mikulova et al., 2013). There is a difference in properties between the CB obtained from pyrolysis and the commercial CB. According to Williams and Besler (1995), the major carbonaceous char source is the initial CB filler. It has been reported that the CB obtained at vacuum pyrolysis conditions have lower pyrolytic CB content compared to those obtained at atmospheric pressure at the same temperature (Darmstadt et al., 1995).

Activity as well as the surface chemistry is key for tyre rubber manufacture using pyrolytic CB due to the fact that these characteristics influence the strength of interaction between the CB and rubber (Roy et al., 1999; Roy et al., 2005). Sahouli et al. (1996). Darmstadt et al. (1995) have shown that the

recovered CB surface chemistry has some similarity with low-grade commercial CB. Another important CB property is the surface roughness, which has an influence on CB active sites interaction with the elastomer (Darmstadt et al., 1995; Sahouli et al., 1996). The increase in pressure as well as pyrolysis temperature, according to the authors, during pyrolysis under vacuum conditions leads to reduction in the surface roughness.

The BET surface area of the pyrolytic CB obtained in a synthetic rubber pyrolysis study carried out by Kaminsky and Mennerich (2001) was 85 m^2 g^{-1}, which was lower than the value (115 m^2 g^{-1}) for the CB used during the formulation of the tyre rubber. In addition, the authors pointed out that the high content (about 10 wt. %) of ash would limit the application of char for commercial purposes. In a study by Tang and Huang (2005), the BET surface area of the char obtained was 64.8 m^2 g^{-1}, which was lower that the value (80 m^2 g^{-1}) for the N330 commercial CB series. The content of ash in this case was 15.4 wt.%, which was much higher than that (0.4 wt.%) of commercial CB. The content of ash in commercial CB, for appropriate use in the manufacture of tyres, must be less than 0.5 wt. % (Tang and Huang, 2005). In another study carried out by Cunliffe and Williams (1998a), the ash content in the recovered char was about 12 wt.%, which as well limits its use as an alternative CB.

The most important property, however, is seemingly the mineral concentration, and demineralisation, according to Chaala et al. (1996), is the appropriate process that can be used for the removal of these compounds. With the application of successive acid-base treatments, the content of ash can be reduced to less than 1 wt.% (Roy et al., 2005). The carbon black, with grades in the range of N100 and N700 series, obtained using the furnace process is the most popular brand for the manufacture of rubber (Liang, 2007). Some characteristics and properties of the CBs applied in the manufacture of tyres are presented in Table 2-9.

In conclusion, PCB recovery has some limitations which, to some extent, hinders the economic viability of waste tyre pyrolysis. Although PCB consist of more than 80 wt.% carbon-containing material, other limitations in terms of particle size, content of ash, structure, absorption characteristics, activity as well the surface chemistry add to its heterogeneity. This is a consequence of the use of various commercial CB grades during the manufacture of tyres, in addition to the complex nature of the pyrolysis process, which leads to the modification of the properties of original CB.

Table 2-9: Carbon black properties in tyre manufacture (Patnaik and Brown, 2010)

Name	Abbrev.	ASTM design	Tensile strength (MPa)	Particle size (nm)	Relative road wear abrasion	Relative laboratory abrasion
medium thermal	MT	N990	9.80	250-350	-	0.18
Fine thermal	FT	N880	12.60	180-200	-	0.22
Semi-reinforcing furnace	SRF	N770	14.70	70-96	0.60	0.48
High modulus furnace	HMF	N683	16.10	49-73	0.66	0.56
Fast extruding furnace	FEF	N550	18.20	39-55	0.72	0.64
High abrasion furnace	HAF	N330	22.40	28-36	1.00	1.00
Easy processing channel	EPC	N300	21.70	30-35	0.90	0.80
Intermediate SAF	ISAF	N220	23.10	24-33	1.15	1.25
Super abrasion furnace	SAF	N110	25.20	20-25	1.25	1.35

2.4.2.1. Tyre pyrolytic char upgrading

The upgrading of pyrolytic char has revolved around the improvement of char characteristics via post-pyrolysis with the goal of obtaining ACs. Studies on minimisation of deposition of carbon through tyre post-pyrolysis (at a temperature range of 670-860 °C) were carried out using vacuum pyrolysis (Pantea et al., 2003). This secondary treatment influenced the surface chemistry of the obtained CBs in the sense that their electrical conductivity was boosted and they became more aromatic compared with commercial CBs.

Activating agents like CO_2 or steam are needed to facilitate the production of ACs from carbon-containing chars. During the reaction between carbon and steam as activating agent, H_2, carbon monoxide (CO), carbon dioxide (CO_2) and CH_4 are mainly produced whereas CO is the primary gas product when CO_2 plays the role of the activating agent. The reaction involving carbon leads to production of gases, which open up the char pores, thereby increasing the surface areas to values (400-1500 m^2/g) close to those of ACs (Cunliffe and Williams, 1999). Consequently, carbon is lost or

'burned off', and this tends to be more intense with increase in the reaction time and/or gasification temperatures. The tyre pyrolytic chars ash content, as seen in Table 2-8 is in the range of 8-15 wt.%, and this content relatively increases when carbon is lost through 'burn-off'.

Cunliffe and Williams (1998a) and Cunliffe and Williams (1999) carried out an investigation on tyre pyrolysis char upgrading, where CO_2 or steam were used as activating agents. Four different temperatures (835, 865, 900 and 935 °C) were used during the activation. Using concentrated HCl for ash removal, the content of ash was lowered to between 2-5 wt.%. The maximum BET surface area (640 $m^2 g^{-1}$) of the produced AC was obtained when activation was carried out at 935 °C, where a carbon burn-off of 65 wt.% was achieved. From the observed characteristics of the carbon pore size, there was an indication that they were majorly mesoporous. The series of reactions leading to the burn-off included formation of micropores, widening of pores, destruction of the pore wall and surface area loss. The surface area of the activated carbons recorded using CO_2 as the activating agent was lower by 20 % compared to those produced using steam as the activating agent.

In a study carried out by Teng et al. (1995) on activation of chars (obtained from tyre pyrolysis via thermogravimetry) at 900 °C using CO_2/He as activating agents, the surface are of chars increased from 100 $m^2 g^{-1}$ to 813 $m^2 g^{-1}$ after activation, accompanied with a burn-off of 50 %. Another study on char activation was conducted by Zabaniotou and Stavropoulos (2003). The activation was carried out in a FBR at temperatures of between 850 and 1000 °C at different reaction times, where either steam or CO_2 played the role of activating agents. The authors reported maximum BET surface areas of approximately 600 $m^2 g^{-1}$ at prolonged activation times and higher temperatures (high burn-off degrees) for either of the activating agents.

Li et al. (2004) subjected pyrolytic char produced at 550 °C to activation for 4 hours in a FBR at a temperature range of 850-950 °C using CO_2 as the activating agent. The authors highlighted that the burn-off at 850 °C activation temperature was 21.3 %. This value increased to 51.3 % when the activation temperature was increased to 950 °C. The shift in these two activation temperatures also led to an increase in the surface area of the activated carbons from 125 $m^2 g^{-1}$ at 850 °C to 306 $m^2 g^{-1}$ (maximum value obtained) at 950 °C. In another study by Helleur et al. (2001), tyre pyrolysis chars produced at 550 °C were first carbonised for one hour at 900 °C in nitrogen environment before being activated at varied activation durations using either CO_2 or steam. The maximum AC surface area of 302 $m^2 g^{-1}$ was achieved at an activation duration of 3 hours, with steam as the activating agent.

2.4.3. Tyre pyrolysis gas

The primary products of thermal degradation of tyres are dienes (in particular butadiene) and alkenes. Light hydrocarbons are produced as a result of secondary reactions involving gaseous pyrolysis

products. The CV of tyre pyrolysis gas, as reported in literature, is in the range of 20-65 MJ/ m^3, and it is dependent on the composition of the gas, which by extension depends on pyrolysis temperature, reactor type, heating rate among other factors (Williams et al., 1990a; Leung et al., 2002; Kyari et al., 2005; Rada et al., 2012).

In a study by Kyari et al. (2005), pyrolysis gases obtained using different tyre brands and types were analysed to determine its composition. The gas composition significantly varied depending on the type of the tyre used. For instance, the yield of methane ranged from 14.1-27.9 vol.% while that of hydrogen was between 13.8-27.6 vol.%. The overall CV ranged from 29.9-42.1 MJ/m^3, and it was as well influenced by the type of the tyre used. In another study by Cypres and Bettens (1989), the gases obtained from pyrolysis of different tyre types had remarkable differences composition wise. The six various tyre types investigated, for example, revealed that ethene, ethane and hydrogen produced varied by more than 100 % in terms of concentration.

Waste tyre pyrolysis gas mainly contains hydrogen (H_2), carbon dioxide, methane, hydrogen sulphide (H_2S), carbon monoxide, ethane (C_2H_6), propane (C_3H_8), ethene (C_2H_4), propene (C_3H_6), butadiene (C_4H_6), butene (C_4H_8) and butane (C_4H_{10}). The composition the gas depends on the rubber composition used in the tyre manufacturing process. These components include; SBR, NR, chloroprene rubber, nitrile rubber, polybutadiene rubber. When tyre thermal decomposition occurs, free highly reactive radicals, which generally are sub-units of the initial molecule of the rubber, are produced (Dodds et al., 1983).

2.5. Desulphurisation of waste tyre pyrolysis oil

There are many reasons as to why fuels that contain sulphur should be desulphurised. Key among them is the emissions that accompany the combustion of sulphur-containing fuels, and this is extremely dangerous from the environment point of view. The sulphur content in TDO is high, and this contributes to sulphate particulate matter and SO_2 emission, thereby endangering welfare and public health (Ucar et al., 2005a; Palmer et al., 2007; Chen et al., 2013). In addition, the organic sulphur compounds present in fossil fuels contribute to the corrosion of sections of internal combustion engines, poisoning of catalytic converters and pollution of the air. In view of this, the air quality improvement and elongation of internal combustion engines lifespan can be realised by ensuring that the recovered oils have a low content of organic sulphur. Different techniques for removal of sulphur have been developed in the last few decades. They include biocatalytic desulphurisation, biodesulphurisation, hydrodesulphurisation, oxidative desulphurisation and selective adsorption (Song and Ma, 2003; Campos-Martin et al., 2004). Out of these methods, HDS is the technique currently used on the largest scale for sulphur removal in fuel oils in the refineries.

2.5.1. Hydrodesulphurisation

Hydrodesulphurisation, also commonly termed distillate hydrotreatment occurs at high pressures ranging from 30-130 atm and high temperatures of between 300-400 °C in presence of an active catalyst (Te et al., 2001; Ahmad and Ahmad, 2013). Tyre-derived oil contains DBT, and as such HDS may not be effective in their treatment due to the steric sulphur atom hindrance (Huang et al., 2004; Dharaskar et al., 2013). Owing to the high operating costs associated with HDS and the need for expensive catalysts, ODS has gained preference as the sulphur removal technique in TDOs (Al-Lal et al., 2015). From studies on hydrodesulphurisation of diesel fuels, there has been an indication that alkyl-Dibenzothiophene consisting of alkyl groups at 6- and/or 4-position are the organosulphur compounds that remain at levels below 0.1 wt.%. These compounds, which are categorised as extremely refractory, have a low reactivity during hydrodesulphurisation (Wan and Yen, 2007; Chen et al., 2010).

2.5.2. Oxidative desulphurisation

Over the last two decades, ODS technique of sulphur removal has been of great interest, and as such a number of ODS technologies have been developed. The operating conditions for ODS are milder than those of HDS. In ODS, the conversion of sulphur-containing compounds into their corresponding sulphoxides and sulphones takes place after which these sulphoxides and sulphones, which are polar, are removed via solvent extraction (Te et al., 2001; Song and Ma, 2003; Al-Lal et al., 2015). Figure 2-2 shows the mechanisms of oxidation of sulphur-containing compounds in oils into polar sulphoxides and sulphones. For the removal of aromatics, sulphur and soot in fuel oils, sulphuric acid can be used. In a study carried out by Eterigho and Olutoye (2008) using NaOH and sulphuric acid to enhance fuel oils quality, the content of sulphur and viscosity decreased whereas the flash point increased.

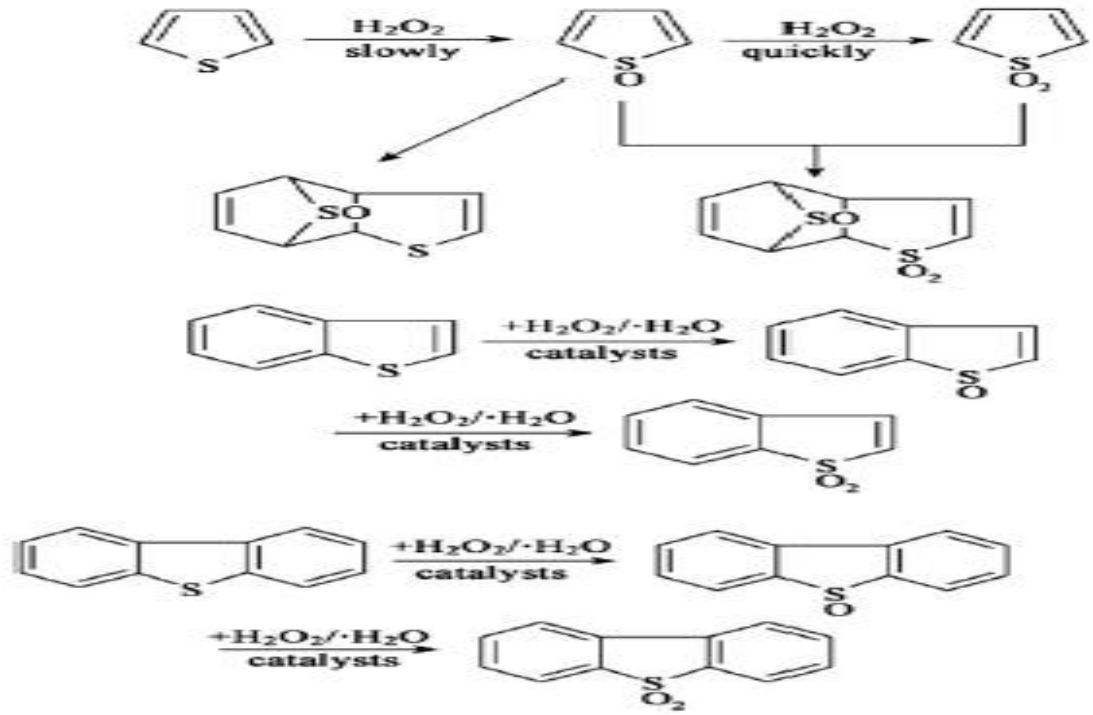

Figure 2-2: Mechanisms of oxidation of sulphur compounds (Lingyan et al., 2004; Chen et al., 2010)

Peroxyacids, as oxidants, are very effective (Aida and Yamamoto, 1994). In a study carried out by Zannikos et al. (1995) on desulphurisation of petroleum fractions at mild conditions using combined oxidation and liquid-liquid extraction, 90 % sulphur removal was achieved. A number of ODS studies involving the use of hydrogen peroxide and acetic acid, hydrogen peroxide and formic acid and sulphuric acid have been carried out by different researchers (Murugan et al., 2008a; Bunthid et al., 2010; Aydın and İlkılıç, 2012; Dehkordi et al., 2013; Al-Lal et al., 2015). The use of hydrogen peroxide during ODS has been widespread since its conversion leads to complete decomposition into H_2O and oxygen, and therefore no pollutants are produced in the process (Zhang et al., 2009). Moreover, the use of H_2O_2 with an acid during ODS can speed up the desulphurisation process.

In a study carried out by Ali et al. (2006) with incorporation of hydrogen peroxide and formic acid, a reduction in fuel sulphur content from 1044 mg/L to 100 mg/L was achieved. In another study by Ali et al. (2009), using hydrogen peroxide and acetic acid as part of the oxidation system in presence of sulphuric acid catalyst, a 90% petroleum products sulphur reduction was reported. Studies on combined oxidation and adsorption for sulphur reduction in TDO naphtha have previously been carried out. For instance, Bunthid et al. (2010) investigated the effect of lone oxidation, lone adsorption and combined oxidation and adsorption on sulphur removal. In the study, char served as the adsorbent whereas hydrogen peroxide and formic acid were used in the oxidation system. They found out that, with lone adsorption, a 47.6 % sulphur reduction was achieved while the sulphur content was reduced by 41.5 % through oxidation only. However, the reduction oil sulphur content was higher (57.8 %)

when both adsorption and oxidation were employed in the process. Recently the ability of sulphuric acid to act as a desulphurisation agent was investigated by Nabi et al. (2014). In the study, 8 % concentric hydrosulphuric acid together with TDO was subjected to stirring after which the mixture was left to settle for forty hours, forming two distinct layers. It was found that the raw oil was dark reddish in colour while the desulphurised oil was yellowish.

Although there has been development in the use of ODS method, low efficiency still remains a critical concern as the sulphur compounds tend to have a higher polarity compared to hydrocarbons. In addition, sulphoxides or sulphones, which are the oxidised sulphur compounds, have a higher polarity in comparison with sulphides.

Solvent extraction, also commonly termed liquid-liquid extraction is a compounds separation technique that utilises the differences in relative solubilities of two immiscible liquids, commonly an organic solvent and water. It refers to solute distribution between two immiscible liquid phases that are in contact with each other (Rydberg, 2004). The separation of extremely polar sulphoxides or sulphones from the non-polar compounds in the oxidised oil can be achieved through solvent extraction by making use of a polar solvent. Acetonitrile, owing to its relatively low BP of 355 K, is considered an optimal solvent for use during extraction. In addition, its separation from sulphone solutes via distillation at a boiling point range of 550-950 K is much easier (Chen et al., 2010). Sulphur compounds in the light fraction of oil, by virtue of being highly polar, are spread across the acetonitrile phase (Shiraishi et al., 1998, 2002). In a study carried out by Murata et al. (2004) using acetonitrile as the extraction solvent, the sulphur content in oil was reduced by 80 %. Similar results were obtained by Shiraishi et al. (2003).

Table 2-10 shows the comparison of properties of the original TDO and desulphurised oil obtained from a study in which one ultra-sound assisted oxidative desulphurisation unit was used.

Table 2-10: Properties of original and desulphurised tyre-derived oil (Chen et al., 2013)

Property	Original tyre oil	Desulphurised tyre oil
Water and sediment (vol. %)	0.30	2.80
Viscosity (mm^2/s)	4.08	1.42
Sulphur content (ppm)	8880	2800
Heating value (MJ/kg)	42.12	41.10
Density (kg/m^3)	970	910
Carbon residue, micro (wt.%)	3.17	1.61

2.6. Recent studies on thermogravimetry and kinetic models application

The study of waste tyre pyrolysis kinetics has drawn interest from many researchers as understanding the kinetics of this process is key in the design and optimisation of industrial scale scrap tyre recycling units. In order to determine the kinetics of mass loss linked to materials' valorisation during the thermal degradation in absence of oxygen, derivative thermogravimetry and thermogravimetric analysis are often used (Luyima et al., 2012; López et al., 2013). Kinetic parameters play a vital role in reactor designs with the best operating conditions (Zhao et al., 2012; Abdelouahed et al., 2017). Model-free and model-fitting methods are commonly used to determine the kinetic parameters during solids decomposition (Vyazovkin and Dollimore, 1996; Anca-Couce et al., 2014; de Godois Baroni et al., 2016).

Aboulkas et al. (2008) applied FR model to determine the activation energy (E_a) of co-pyrolysis polyethylene with olive residues, while Cai and Bi (2009) used FWO method to determine the same kinetic parameter for wheat straw pyrolysis. In another study conducted by Brems et al. (2011), FWO method was used in the determination of activation energy of polyethylene-terephthalate and polystyrene pyrolysis process. Previous studies on mass loss kinetics of scrap tyres and rubber have mainly focused on TGA (Castaldi et al., 2007; Kwon and Castaldi, 2009; Januszewicz et al., 2017), but studies on application of various models on thermogravimetric data are still scanty or unavailable. In this study, therefore, model-free and model-fitting methods were applied to thermogravimetric data to establish the model kinetics associated with the waste tyre pyrolysis process.

2.7. Techniques of designing experiments

2.7.1. Response surface methodology

2.7.1.1. Brief history of response surface methodology

Response surface methodology (RSM) is a compendium of techniques used to statistically design data and numerically optimise designs of processes and products (Myers et al., 2004). This design technique came into use in the 1950s after Box and Wilson (1951) published their work. Most of the underlying concepts, according to Mead and Pike (1975), had already been in use and had been discussed earlier in the 1930s. Nonetheless, there is no doubt that as a result of the work published by Box and Wilson (1951), there has been a rise and continuous evolution of the application of RSM in the research sphere (Myers et al., 2004). The ancient difficulty in planning and analysis of experiments in a bid to find conditions desirable for a group of design variables, according to Myers et al. (1989), was the motivation behind the work by Box and Wilson (1951).

2.7.1.2. Description of response surface methodology

Response surface methodology is among the best techniques used to empirically study the relationship between one or more estimated response functions. (Voznesensky, 1974). It makes use of statistical and mathematical methods to depict the domain of all practicable solutions for a process model, and once the model development is completed, process optimisation can be conducted devoid of a trial and error procedure (Box et al., 1978). RSM constitutes selected statistical and mathematical methods used for analysis of problems in which the input variables influence the responses (Montgomery, 2004). Regression analysis, with basis on polynomials, is used to define the relationship between the input variables and the responses.

RSM deals with surface estimation from a normally paltry lot of observations, with the primary goal of establishing the input variables levels that can have the response maximised (Balkin and Lin, 2000). RSM is premised on the assumption that the response Y has a relationship with a clique of design variables X_1, X_2,….,X_P in addition to the fact that the approximation of the relationship can be done (using a polynomial model) in a certain section of inputs (Myers et al., 1989). The first order and second order models are the most common polynomial functions for approximation (Montgomery, 2009). Equations (2-1) and (2-2) present the first order and second order polynomial functions respectively.

$$Y = \beta_0 + \beta_1 X_1 + \beta_2 X_2 + \cdots + \beta_p X_p + \epsilon \quad \textbf{(2-1)}$$

$$Y = \beta_0 + \sum_{i=1}^{p} \beta_i X_i + \sum_{i=1}^{p} \beta_{ii} X_i^2 + \sum_{i<j} \sum_{i<j} \beta_{ij} X_i X_j + \epsilon \quad \textbf{(2-2)}$$

In general, the common error variance, σ^2 assumption is made and the ordinary least squares aids in the estimation of coefficients (Myers et al., 1989). The effective estimation of model parameters, according to Montgomery (2009), is dependent on the correct use of experimental designs for data collection. Response surface designs is the terminology for designs used to fit response surfaces. The most common response surface designs are the CCD, Box-Behnken design, small CCD and orthogonal design, which incorporates the fractional and 2^k factorial design points (Box and Behnken, 1960). The small CCD was used during this research study. Polynomial models generally give a sensible true functional relationship approximation for a particular sub-area owing to its focus in a confined search space area. The premise is that if the true response function can adequately be approximated by the

fitted surface, then there is very little difference between the analysis of the fitted surface and that of the actual system (Montgomery, 2009).

2.7.1.3. The sequential nature of response surface methodology

Response surface methodology is a procedure that is sequential, and its aim is to quickly and efficiently guide the experimenter to the overall optimum domain. Ordinarily, at the elementary stages, a first-order model (Equation (2-1)) is fitted due to the fact that there is a likelihood that the domain being investigated could be far from the optimum, and consequently there is small curvature detection in the system. Subsequently, the approach of steepest ascent is applied so as to provide guidance in search of operability region's most favourable area. The steepest ascent is in the direction that is perpendicular to the response which is fitted, and matches with the direction which produces the most rapid increase in the fitted response. The stages along the course are proportionate to the approximated regression coefficients. The iteration of the procedure is carried out until the first order model lack of fit shows the optimum condition domain (Montgomery, 2009). After the location of the optimum domain, the fitting of the second order model (Equation (2-2)) is conducted before the analysis for location of the optima is carried out (Figure 2-3). In the course of the entire procedure, the subsequent stage is planned using the information from the previous stage. There may be need to conduct extra runs to get additional information about the response in some sections of the domain that the initial design may have inadequately covered (Myers et al., 1989). Sequential design together with extra experimental runs fall in the design augmentation concept (Myers et al., 1989).

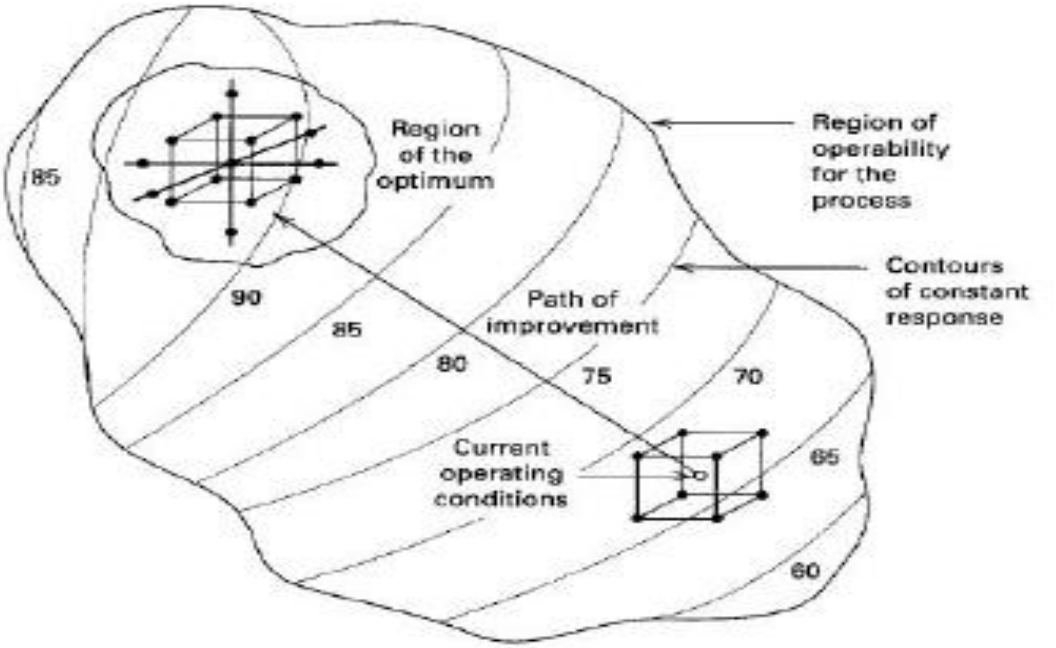

Figure 2-3: Sequential nature of the response surface methodology (Montgomery, 2009)

2.7.2. Design and analysis of computer experiments

Design and analysis of computer experiments (DACE) is a statistical technique that was established by Sacks et al. (1989), and has been extensively studied. DACE has found its extensive application in the field of engineering as solution to problems associated with expensive optimisation of designs. These fields of application include electronic circuits design, computational fluid dynamics and analysis of finite elements (Grierson and Pak, 1993; Bates et al., 1996; Lee and Hajela, 1996; Pierret and Van den Braembussche, 1997; Jin et al., 2001; Jin et al., 2002; Buche et al., 2005). In cases where processes involve a lot of complexity, such that physical experimentation becomes extremely expensive, time consuming, or even impossible to conduct, then simulation of the system through mathematical modelling comes in handy (Sacks et al., 1989). Although advances have been made in terms of computer capacity improvement, exorbitant computational cost renders complex engineering simulations impractical.

In DACE, data from an experimental design is used to build a surrogate or a metamodel (also known as model of model) before being optimised. Consequently, a larger simulator is used to model the physical process, and the computer code aids to directly conduct the experiments (Bates et al., 1996). The behaviour of the system can be approximated either by deterministic or stochastic model. When stochastic simulation model is used for experimentation, it presents a behaviour similar to that of a physical system (Myers et al., 2004). On the other hand, there is a difference between experimentation using a deterministic model and experimentation of the physical system due to the fact there is no random error linked with the output. Consequently, when the code is run with unchanged inputs, identical response values will be achieved (Sacks et al., 1989). Sacks et al. (1989) were behind the introduction and pursuit of deterministic models, and they put forth the idea of using a statistical model that views the response as if it were a stochastic process realisation.

Gaussian stochastic process model is the name given to the statistical model which Sacks et al. (1989) adopted. The advantage of the Gaussian stochastic process model is that it provides a statistical fundamental for computation of an efficient response predictor at untried inputs, and it thus permits the estimation of the uncertainty of the predictor. According to the proposal by Sacks et al. (1989), the concept is to select a design with high response predictability at untried inputs of the experimental domain and supplement it by use of extra design points. The aim of augmenting the design is to lay emphasis on sampling that has high uncertainty of the predictor so that scrutiny can be dedicated to the space parts that are not adequately explored (Jones, 2001). Computer experiments, in contrast with conventional RSM, aims at finding a model for approximation of true response surface in a much broader span (in some cases extending over the whole operability domain) of the design parameters. This, consequently requires models that have more complexity in comparison with the first and second order polynomial models.

2.7.3. Nonparametric and semiparametric response surface methodology

Nonparametric and semiparametric response surface methodology (NPRSM) suits situations in which the polynomial models in the domain of operability do not accommodate the response (Myers, 1999; Myers et al., 2004). This can happen in the event that there is need to fit a model that covers a section of the space of the factor, which happens to be bigger than the portion generally considered in conventional RSM techniques (Myers et al., 2004). The meaning of the terminology 'nonparametric response surface methodology' is that there is absence of a particular model, and that the analysis primarily focuses on prediction. This, therefore, leads to the application of kernel-based methods of regression. Semiparametric response surface methodology, on the other hand, implies that there is the use of a model, but not of a standard polynomial nature (Myers et al., 2004). According to Myers (1999), NPRSM may be used in the following cases:

(i) If there is need to achieve optimum conditions
(ii) If the interest in the response surface appearance is more than that in interpretative function
(iii) If the function exhibits nonlinearity, but not certainly well-behaved
(iv) If the designs must originate from a space-filling grid and do not have to honour the 'form of the model'

There is a huge difference in terms of various aspects (modelling, design and optimisation approaches) between RSM and NPRSM. However, the difference between NPRSM and DACE is not as clear. The reason behind the development of DACE as one of the modelling techniques was to help address the issue of high simulation costs of complex engineering processes (Sacks et al., 1989). NPRSM, on the other hand, has been mainly used in the fields of biotechnology and biopharmacy (Myers et al., 2004). Sequential sampling and deterministic stochastic Gaussian process were used in DACE at the onset, but over time, other models like thin plate splines and neural networks have been developed. Going forward, DACE may be perceived as being a component of NPRSM.

There have been developments, with links in NPRSM and DACE, in the field of optimisation of algorithm parameters. The major techniques that have been introduced in this field are sequential optimisation of parameters (Bartz-Beielstein et al., 2005) and effective global optimisation (Jones et al., 1998). The primary objective of these techniques is to aid in quantification of the significance of each variable and interactions between variables. In the case of multiple instances, these techniques provide a view of the interaction between instance properties and the parameters. In addition, these techniques also support the performance of interpolation within the variable settings as well as the extrapolation to parameter space domains that were hitherto undetected. These techniques can play an important role as far as algorithm interpretation and enhancement is concerned (Hutter et al., 2009; Hutter et al., 2010).

In NPRSM, conventional RSM designs like CCD and factorial designs are commonly used (Myers et al., 2004). It is important, however, to note that conventional RSM designs are suitable in cases where the design domain is regular of if the experimenter is interested in a polynomial model. A regular domain of design can be depicted as a space surrounded by the p-dimensional hypersphere or hypercube, where every point within or on the sphere or cube is considered a possible design point. Due to practical problems associated with the operability, availability and feasibility of the system under study, there may be need to create holes in the design domain, slice portions of the sphere, or cut up the cube corners (Kennard and Stone, 1969). Moreover, when the experiments are time-consuming or expensive, the number of runs that can be achieved is reduced. This number of trials is relatively smaller than the number of conceptually possible experiments.

In the cases where there is a fixed model as well as the number of achievable trials, most RSM designs result in an extremely huge number of required replicates (Kennard and Stone, 1969). If there is an occurrence of nonstandard conditions like unusual requirements of the sample size or an irregular experimental domain, then computer-generated designs are deemed preferable (Montgomery, 2009). Computer-generated designs are commonly referred to as optimal designs because of their optimality with respect to a particular criterion. G-optimality, A-optimality and D-optimality are the commonly used optimality criteria (Montgomery, 2009). D- and A-optimality focus on estimating the regression coefficients and encompass the minimisation of a function of the covariance matrix of the parameters least squares estimates (Santner et al., 2003; Montgomery, 2009). G-optimal designs, on the other hand, focuses on response prediction and its aim is to reduce the variance of the maximum scaled prediction in the design domain (Montgomery, 2009).

The common procedure in computer-generated designs is to define the model (usually a polynomial model), establish the interest region, choose the number of runs to conduct, define the criterion of optimality and finally select the points of design (that would interest the experimenter) from a group of preferred points. The preferred points are normally a network of points that are spaced over the practicable design domain (Montgomery, 2009). With the development of DACE, there has been introduction of other criteria-founded designs. They are more complex to achieve in comparison with the designs aforementioned. Typically, the Gaussian stochastic model is presumed and the design criteria has a functional relationship with its unknown variables (Santner et al., 2003). For a set number of trials and for a particular structure of correlation, these criteria of design targets to select a design that will give the best response prediction at untried inputs in the experimental domain.

CHAPTER THREE

3. Materials and methods

This chapter presents the materials and methods used for the kinetic study of the pyrolysis of the tyre crumb (section 3.1) as well as the materials and the methodology followed during the study of the oxidative desulphurisation of tyre-derived oil (section 3.2). The first part (section 3.1) describes the thermogravimetric analysis equipment and procedure as well as the steps followed to establish the kinetics of the tyre crumb pyrolysis by non-isothermal means. The software used for thermogravimetric data extraction is mentioned here. The background of kinetic modelling used to study the thermal decomposition of solid materials is also presented. In the second part of this chapter (section 3.2), the materials and the experimental set-up used to carry out the oxidative desulphurisation experiments is described. In addition, the procedure for the ODS process as well as the sample analysis methods are presented. The design of experiments criteria, technique and software is also outlined in this chapter.

3.1. Materials and methods: Kinetic modelling of scrap tyre pyrolysis

3.1.1. Samples and characterisation

The granulated tyre rubber used for the thermogravimetric and non-isothermal kinetics study was supplied by Mathe Group, Hammarsdale, KwaZulu Natal, South Africa. The tyre granule size ranged from 0.841 to 2.5 mm. The elemental analysis of the tyre crumb was carried out using vario EL cube elemental analyser, and the content of oxygen in the tyre crumb was calculated by difference.

3.1.2. Thermal decomposition

The thermogravimetric analysis was carried out in a Differential Scanning Calorimeter-Thermogravimetric analyser SDT Q6OO (Photograph A-1 in Appendix A). The number of balance beams in the analyser were two, where one of the beams was used for the sample while the other was used for reference. As per the procedure, the ceramic pans were first placed on each of the balance beams to tare. With the aid of a spatula, the sample of the tyre granule was placed in one of the pans. The pan was then placed on the beam balance using a tweezer. The initial weight of the tyre granules was in the range of 5.68-9.59 mg for the four heating rates used for TGA study. The initial mass of the sample does not affect the mass loss kinetics as this process is dependent on both the initial and final weight of the sample. During the TGA experiments, the samples of the tyre granules were heated from 20 to 600 °C in presence of nitrogen flowing at 100 mL/min to ensure non-oxidation (which is not desirable in pyrolysis) of the tyre granule samples. Four heating rates of 2, 5, 10 and 20 °C/min were

used during the thermogravimetric experiments in order to determine the tyre granule pyrolysis behaviour. The thermogravimetric and derivative thermogravimetric data were generated using the TA instruments software, whereas MATLAB R2015a (matrix laboratory) software was used to generate the plots.

3.1.3. Kinetic modelling

The TG and DTG data was used to establish the kinetics of the crumb tyre pyrolysis process. Three model-free methods i.e. the KAS, FWO and FR aided in the determination of the activation energies. The activation energies from the best performing model-free method (based on the coefficient of determination values) were loaded into the model-fitting method (CR model) to determine the reaction model and the pre-exponential factors.

The thermal degradation of solid state materials is commonly expressed according to Equation (3-1):

$$\frac{d\alpha}{dt} = k(T).f(\alpha) \quad \textbf{(3-1)}$$

where k(T) is the reaction rate constant, α is the conversion degree, while $\frac{d\alpha}{dt}$ is the rate of conversion over time. The degree of conversion, α can be determined by Equation (3-2) :

$$\alpha = \frac{m_0 - m_t}{m_0 - m_f} \quad \textbf{(3-2)}$$

where m_0 is the sample weight at the start, m_f the sample weight at the end, and m_t the sample weight at a given temperature. k(T) is expressed according to Arrhenius Equation (3-3) as :

$$k(T) = A \exp\left(-\frac{E_a}{RT}\right) \quad \textbf{(3-3)}$$

where R (8.314 J mol^{-1} K^{-1}) is the universal gas constant, E_a the activation energy and A the pre-exponential factor.

Combining Equations (3-1) and (3-3) gives Equation (3-4) :

$$\frac{d\alpha}{dt} = A \exp\left(-\frac{E_a}{RT}\right) f(\alpha) \quad \textbf{(3-4)}$$

If there is a temperature increase with a constant heating rate, $\left(\frac{K}{s}\right)$, then introduction of $\beta = \frac{dT}{dt} = \frac{dT}{d\alpha} \times \frac{d\alpha}{dt}$ into Equation (3-4) gives Equation (3-5).

$$\frac{d\alpha}{dT} = \frac{A}{\beta} \exp\left(-\frac{E_a}{RT}\right) f(\alpha) \quad \textbf{(3-5)}$$

Integration of Equation (3-5) gives Equation (3-6), which is the underlying equation that is used in the calculation of kinetic parameters during non-isothermal thermal degradation of solid state materials.

$$\int_0^{\alpha} \frac{d\alpha}{f(\alpha)} = g(\alpha) = \frac{A}{\beta} \int_{T_0}^{T} \exp^{\left(-\frac{E_a}{RT}\right)} dT \quad \textbf{(3-6)}$$

where T_0 is the temperature at the initial stage of the experiment and $g(\alpha)$ is the conversion integral function.

3.1.3.1. Kissinger-Akahira-Sunose method

The Kissinger-Akahira-Sunose (KAS) method (Kissinger, 1957; Akahira and Sunose, 1971) is expressed as Equation (3-7):

$$\ln\left(\frac{\beta}{T^2}\right) = \ln\left(\frac{AE_a}{R\, g(\alpha)}\right) - \frac{E_a}{RT} \quad \textbf{(3-7)}$$

where, the plot of $\ln\left(\frac{\beta}{T^2}\right)$ against $\frac{1}{T}$ gives a straight line. The slope of this plot can then be used to determine the E_a.

3.1.3.2. Iso-conversional Flynn-Wall-Ozawa model

The Flynn-Wall-Ozawa (FWO) model (Ozawa, 1965; Flynn and Wall, 1966) uses Doyle's approximation of the integral of temperature (Doyle, 1961) and it is an iso-conversional integral method which is expressed according to Equation (3-8):

$$\ln(\beta) = \ln\left(\frac{AE_a}{R\, g(\alpha)}\right) - 5.331 - 1.052\frac{E_a}{R}\frac{1}{T} \quad \textbf{(3-8)}$$

Therefore, for a constant α value, the plot $\ln(\beta)$ against $\frac{1}{T}$ for different heating rates gives a straight line. The slope of this plot can then be used to determine the value of E_a.

3.1.3.3. The Friedman method

The Friedman (FR) method (Friedman, 1964) is among the iso-conversional methods employed to determine the activation energy. This method relies upon the premise that the chemistry of the degradation is dependent solely on the weight loss rate and does not depend on the temperature. The expression for the FR method is as shown in Equation (3-9):

$$\ln\left(\frac{d\alpha}{dt}\right) = \mathrm{Ln}\left[\beta\left(\frac{d\alpha}{dT}\right)_{\alpha,i}\right] = \mathrm{Ln}(A_\alpha) + \mathrm{Ln}[\,f(\alpha)] - \frac{E_\alpha}{RT_{\alpha,i}} \qquad \textbf{(3-9)}$$

where E_α and A_α represent the activation energy and pre-exponential factor at a specific conversion degree respectively. The subscript i relates to the value at a specific heating rate. Assuming the process mechanism is independent of the heating rate, then the value of $f(\alpha)$ at constant α also is independent of it. The slope from the plot of $\mathrm{Ln}\left[\beta\left(\frac{d\alpha}{dT}\right)_{\alpha,i}\right]$ versus $\frac{1}{T_{,i}}$ gives the activation energy value which is independent of $f(\alpha)$.

3.1.3.4. Coats-Redfern (CR)

The mechanism of thermal degradation from mass loss can be described using CR method (Coats and Redfern, 1964). Using this method, the pre-exponential factor, E_a and reaction order can be determined. This method is based upon Equation (3-6), and an asymptotic approximation $\frac{2RT}{E_a} \to 0$ of the equation gives Equation (3-10):

$$\ln\left(\frac{g(\alpha)}{T^2}\right) = \ln\left(\frac{AR}{\beta E}\right) - \frac{E_a}{RT} \qquad \textbf{(3-10)}$$

where, the plot $\ln\left(\frac{g(\alpha)}{T^2}\right)$ versus $\frac{1}{T}$ gives a straight line where, E_a is calculated from the slope, while the pre-exponential factor is deduced using the intercept term. The CR integral method is commonly used in the description of the pyrolysis reaction process. Table 3-1 presents the expressions for $g(\alpha)$ values for various kinetic mechanisms, including the first, second, and third order reactions .The selection of the appropriate mechanism due to thermal decomposition of the solid state materials is based on high regression coefficient values.

Table 3-1: Theoretical expression of f (α) and g (α) for different reaction models (White et al., 2011; Islam et al., 2015; Islam et al., 2016).

Mechanism	f (α)	g (α)
Reaction order models		
First order (F1)	$(1-\alpha)$	$-\ln(1-\alpha)$
Second order (F2)	$(1-\alpha)^2$	$(1-\alpha)^{-1}-1$
Third order (F3)	$(1-\alpha)^3$	$\left[\frac{(1-\alpha)^{-2}-1}{2}\right]$
Diffusion models		
1-D diffusion (D1)	$0.5\,\alpha$	α^2
2-D diffusion (D2)	$[-\ln(1-\alpha)]^{-1}$	$[(1-\alpha).\ln(1-\alpha)]+\alpha$
3-D diffusion (D3)	$\frac{3(1-\alpha)^{\frac{2}{3}}}{2\left(1-(1-\alpha)^{\frac{1}{3}}\right)}$	$\left[1-(1-\alpha)^{\frac{1}{3}}\right]^2$
Geometrical contraction models		
Contracting area (R2)	$2(1-\alpha)^{\frac{1}{2}}$	$\left[1-(1-\alpha)^{\frac{1}{2}}\right]$
Contracting volume (R3)	$3(1-\alpha)^{\frac{2}{3}}$	$\left[1-(1-\alpha)^{\frac{1}{3}}\right]$

3.2. Materials and methods: Oxidative desulphurisation of tyre-derived oil

3.2.1. Materials and experimental set-up

The tyre-derived oil (with a sulphur content of 8689 mg/L) used for the oxidative desulphurisation experiments was obtained from FFS Refiners, Durban, South Africa. Hydrogen peroxide (50 wt.%) and formic acid with a concentration of 95 wt.% were purchased from Shalom Laboratory supplies, South Africa. The hydrogen peroxide was used as received whereas the formic acid was further subjected to dilution to a concentration of 85 wt.% using the procedure presented in Appendix B-1. The NN-Dimethylformamide, supplied by Sigma-Aldrich, was used without any modification. Acetonitrile with a concentration of 99.8 % was supplied by Macron Fine Chemicals™, and was also

used as received. The details of the chemicals used for the oxidative desulphurisation experiments are presented in Table 3-2.

Table 3-2: Details of the chemicals used for the ODS experiments

Material	Supplier	Concentration	Modified
TDO	FFS Refiners	8689 mg/L	No
H_2O_2	Shalom laboratory supplies	50 wt.%	No
Formic acid	Shalom laboratory supplies	95 wt.%	Yes
Dimethylformamide	Sigma-Aldrich	≥ 99.9 %	No
Acetonitrile	Macron Fine Chemicals™	99.8 %	No

The properties of the TDO and chemicals used in the ODS experiments are presented in Table B-1, Table B-2, Table B-3, Table B-4 and Table B-5 in Appendix B-2. The equipment utilised for the oxidation stage of the oxidative desulphurisation experiments consisted of a water bath (temperature-controlled), a 250 mL round-bottom flask, a reflux condenser and a mechanical stirrer with customised blades and shaft. The liquid-liquid extraction was carried out using a 60 mL separatory funnel. The experimental setup for the ODS process is presented in Figure 3-1 while Photograph B-1 shows the photograph of the actual setup.

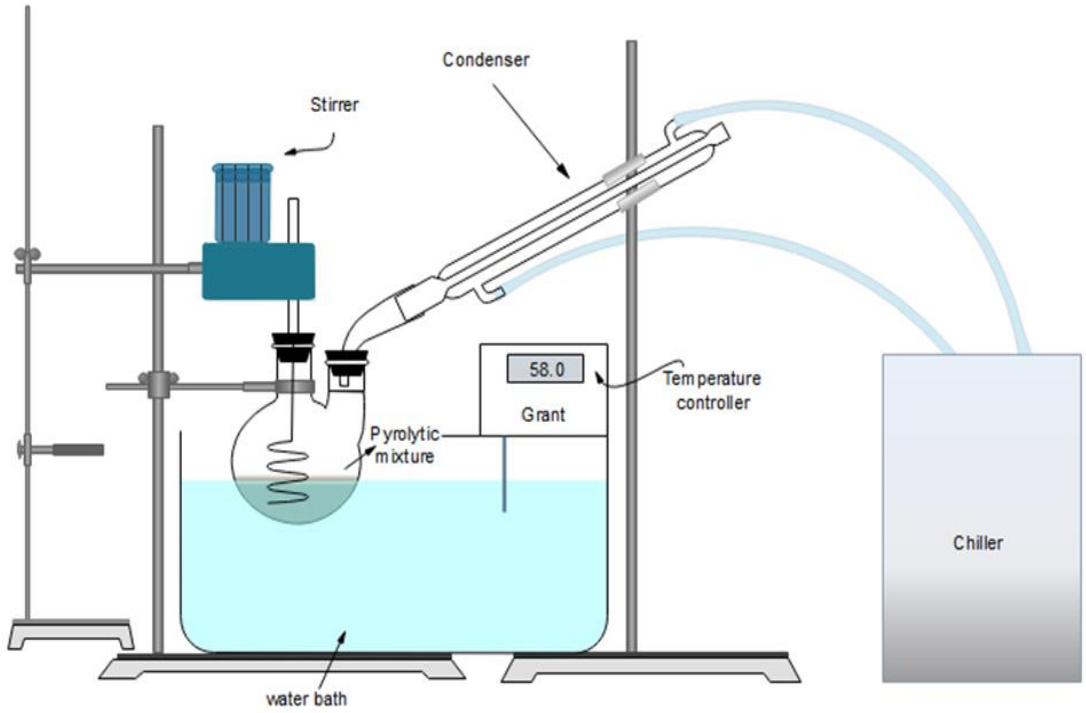

Figure 3-1: Experimental setup for the ODS

3.2.2. Procedure for the oxidative desulphurisation of TDO

The oxidative desulphurisation experiments were conducted using a water bath, placed in a fume cupboard. The stirring speed and the amount of TDO in all runs were kept constant at 300 rpm and 100 mL respectively. During the experiments, the temperature needed for a given run was first set on the water bath. This was followed by the transfer of the TDO amount (100 mL in all experiments) into the round-bottom flask. The required volumes of hydrogen peroxide and formic acid were then transferred into the round-bottom flask after which the reflux condenser was connected. The flask was then clamped and placed in the water bath, while setting and monitoring the reaction time simultaneously. The water bath was switched off at the end of the set reaction time. The round-bottom flask was then removed from the water bath, and the oxidised TDO was transferred to a beaker ready for solvent extraction.

Two different solvents i.e. acetonitrile (ACN) and dimethylformamide (DMF) were used for solvent extraction. The solvent to oil ratio used for each of the solvents was 1:1. In addition, acetonitrile to oil ratio of 1:2 was also used for comparison of the solvent to oil ratio effect on extraction. During the 1:1 solvent to oil ratio extraction process, 10 mL of the solvent and 10 mL of the oxidised TDO were transferred into a separatory funnel, whereas for the 1:2 solvent to oil ratio case, 5 mL of the solvent (acetonitrile) and 10 mL of the oxidised TDO were transferred into a separatory funnel. This was followed by vigorous manual shaking of the mixture (with repeated venting for pressure release) for approximately three minutes. The mixture was then charged with deionised water (10 mL) and left to

settle for five minutes, where the aqueous layer was formed at the bottom while the oil layer was formed at the top. In order to separate the two phases, the stopcock was opened to allow lower aqueous phase to be collected at the bottom, while the oil phase was collected from the top. The two layers were collected at different sections of the separatory funnel to ensure the two phases did not mix.

The experimental setup for the solvent extraction process is shown in Figure 3-2, while Photograph B-2 in Appendix B-3 shows the photograph of the actual setup. The first, second and third stages followed during the solvent extraction process, on the other hand, are presented in Photograph 3-1, Photograph 3-2 and Photograph 3-3 respectively. Photograph 3-1 shows the clamping of the separatory funnel containing the oxidised TDO and solvent mixture, whereas Photograph 3-2 shows the state of the mixture after vigorous shaking. Photograph 3-3 presents the appearance of the mixture after settling. The oil phase was then transferred to a sample bottle and labelled ready for analysis. A representation of the labelled samples is shown in Photograph B-3 (Appendix B-4). Inductively coupled plasma atomic emission spectroscopy (ICP-AES) was used to analyse the content of sulphur in both the original and the desulphurised tyre oils. The percentage reduction in sulphur content of the TDO was calculated using Equation (3-11).

$$\%\ \text{of sulphur removal} = \frac{S_0 - S_f}{S_0} \times 100 \qquad \textbf{(3-11)}$$

where S_0 (mg/L) is the content of sulphur in the TDO before desulphurisation while S_f (mg/L) is the content of sulphur in the oil after desulphurisation.

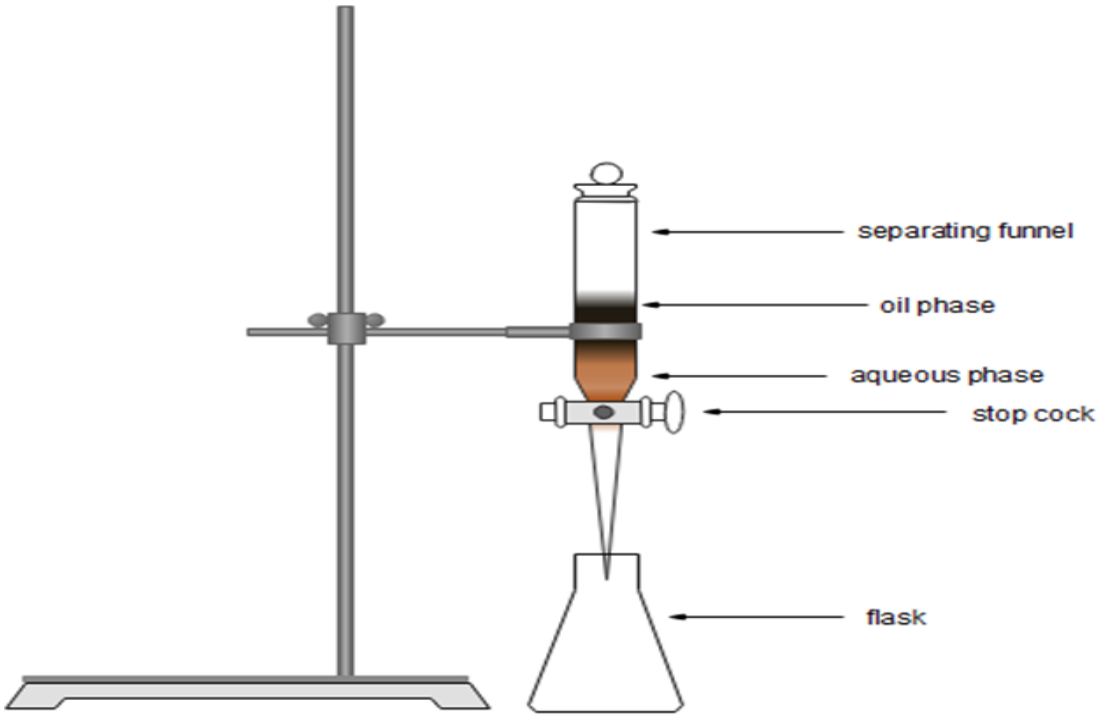

Figure 3-2: Experimental setup for the solvent extraction process

Photograph 3-1: First extraction stage (before mixing)

Photograph 3-2: Second extraction stage (after mixing)

Photograph 3-3: Third extraction stage (after settling)

3.2.3. The procedure of ICP-AES analysis

The ICP-AES analysis for sulphur content determination in the original and desulphurised tyre oils was conducted using Thermo Scientific iCAP 6000 ICP Spectrometer with a radio frequency (RF) power of 1.35 kW. Argon was used as both the carrier gas and auxiliary gas. The flow of the carrier and auxiliary gases was maintained at 0.65 and 1 L/min respectively. On the other hand, the rate of flow in the MicroMist nebuliser was kept at 2 mL/min. The standard used internally for sulphur was 1µg/mL Yttrium. MARS microwave digester (CEM Corporation) was used for microwave digestion of the oil samples before the ICP-AES analysis. One millilitre of hydrogen peroxide and 6 mL of 2 % HNO_3 were added to the TDO samples during the microwave digestion. In the process of microwave digestion, the level of power was set at 100 % of 1600 W. The hold time, pressure and ramp time for the digestion process were 10 min, 800 psi and 25 min respectively. The introduction of the digested oil samples into the spectrometer was done with the aid of a peristatic pump through an auto sampler. The samples were then passed through a nebuliser, producing fine aerosols. The large droplets were removed using a spray chamber whereas the smaller ones were passed to the plasma. In the plasma, the solvent vaporised while the residual sample got atomised and ionised. The ions (in the plasma) were excited, leading to emission of characteristic light. The light was measured by Echelle optical design with charge injection device solid-state detector. The accuracy (recovery) of the of the control standard was 100.1 %. In order to process the data from the spectrometer, the iTEVA software was used.

3.2.4. Design of experiments

The design and analysis of experiments was carried out with the aid of the Design-Expert® Software Version 10-Stat-Ease. The central composite design of the response surface methodology was applied in the investigation of the interaction of parameters during the ODS of the tyre-derived oil. Small central composite design, which is the minimal-point designs required for the estimation of the terms in a second order model, was applied to generate the experimental runs and analyse the sulphur removal in the tyre pyrolysis oil.

The design points for a central composite design are star points (also called axial points), centre points and two-level factorial/fractional factorial design points. All possible combinations of +1 and -1 are contained in the two-level factorial component of the design. For instance, in the two factors scenario, four design points exist i.e. (-1, -1), (+1, -1), (-1, +1) and (+1, +1). On the other hand, for axial points, all of the factors apart from a single factor (with the value of +/- α) are set to 0. The axial points for a two factor scenario are (-α, 0) (+α, 0) (0, - α) (0, + α). As the name suggests, centre points are points in which all levels are set to coded level 0 i.e. the middle point (0, 0) of the range of each factor. To obtain a good estimate of pure error (experimental error), the centre points are repeated between 4-6

times. Figure 3-3 presents the design points for a typical two-factor (α=1.41) central composite design where the shaded circle, unshaded circle and unshaded square represent the factorial, axial and central point respectively. Figure 3-4, on the other hand, shows a CCD with three factors where α=1.68. The total number of experiments (N) for a central composite design can be determined according to Equation (3-12).

$$N = 2k + 2^k + N_0 \quad \textbf{(3-12)}$$

where k is the number of factors, 2k the axial points, N_0 the centre points and 2^K the factorial points.

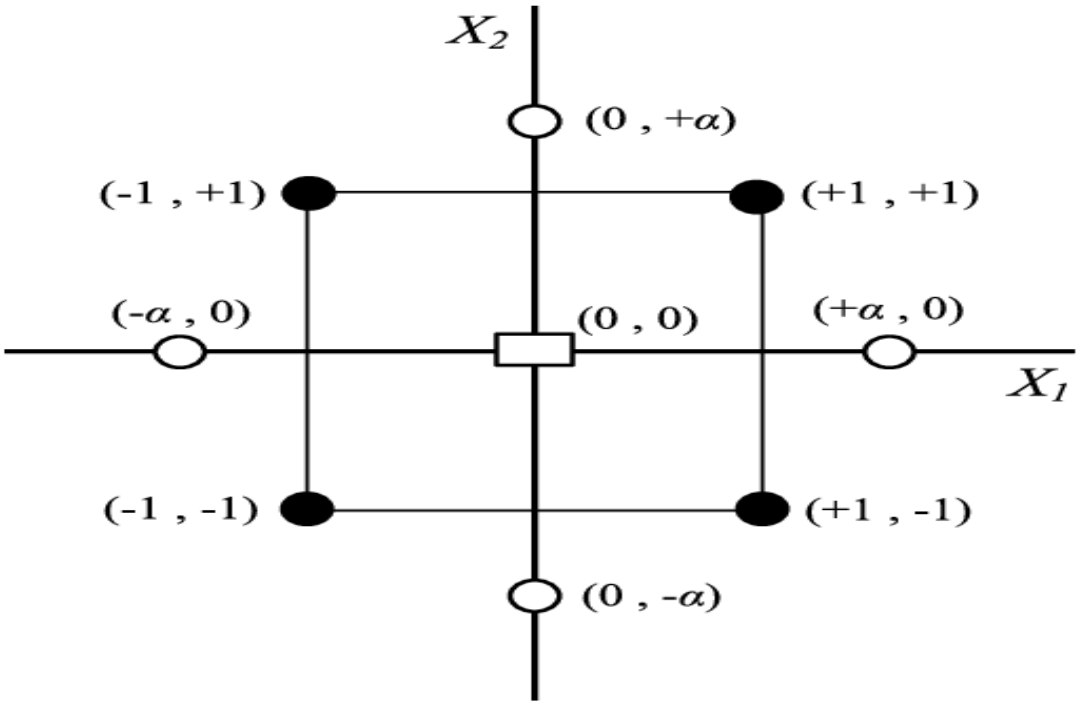

Figure 3-3: Typical design points for a two-factor central composite design (Sangsefidi et al., 2017)

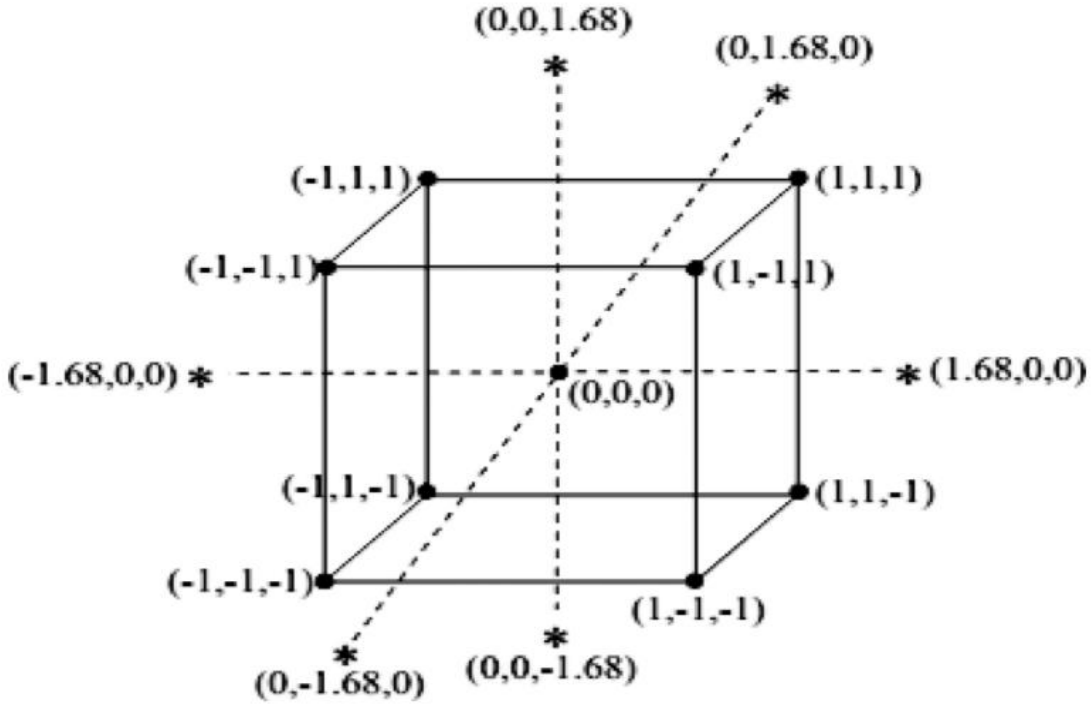

Figure 3-4: Three-factor central composite design (Kazemi-Beydokhti et al., 2015)

The centre point in the central composite design aids to determine the experimental error. The distance from the centre points to the axial points depends on the number of factors (Montgomery, 2001). In a central composite design, five levels of each factor are required. These levels are -α, -1, 0, 1, and α. One of the exceptional features of a CCD is the capability of its structure to lend itself to sequential experimentation.

Table 3-3 shows the design ranges for the 4 factors investigated during the oxidative desulphurisation of the TDO. These ranges were chosen, partly, based on the ODS studies carried out previously (Chen et al., 2010; Aydın and İlkılıç, 2012; Al-Lal et al., 2015). Based on the design criteria, the total number of runs obtained for each of the solvent extraction scenarios was 21. The runs consisted of eight, five and eight axial points, centre points and factorial points respectively. Since three different solvent extraction scenarios were used, the total number of ODS runs carried out was 84 i.e. 21 runs for the oxidation step of the TDO and 63 experiments for the solvent extraction.

Table 3-3: The levels of factors for the central composite design

Parameter	Levels				
	$-\alpha$	-1	0	$+1$	$+\alpha$
A:HCOOH (mL)	3.95	6	9	12	14.05
B:H_2O_2 (mL)	4.64	6	8	10	11.36
C:Temperature (°C)	47.27	50	54	58	60.73
D:Reaction time (min)	33.18	40	50	60	66.82

CHAPTER FOUR

4. Results and discussion: Kinetic modelling of scrap tyre pyrolysis

This chapter presents the results and discussion of the non-isothermal kinetic modelling of the pyrolysis of tyre crumb.

4.1. Characteristics of the tyre crumb

The results of the proximate and elemental analyses of the scrap tyre from the present study and those by other authors from previous studies are presented in Tables 4-1 and 4-2. It can be seen that there is a similarity in the results of elemental and proximate analyses obtained from this study and those from previous studies. The volatile matter content (average value from thermogravimetry) was approximately 64 wt.%.

Table 4-1: Proximate analyses of tyre crumb

Proximate analysis (wt. %)				Reference
VM	FC	MC	Ash	
63.6	-	-	-	This study
69.8	24.8	-	5.3	Irmak Aslan et al. (2017)
61.6	33.5	2.0	2.9	Miranda et al. (2013)
71.5	28.5	0.2	8.3	Singh et al. (2012)
66.0	29.1	0.4	4.9	López et al. (2013)

The results of the elemental analysis (Table 4-2) indicated that the carbon, hydrogen, nitrogen and sulphur contents were 83.54, 7.55, 0.35 and 1.84 wt.% respectively. The oxygen content (determined by difference), on the other hand was 6.73 wt.%.

Table 4-2: Elemental analyses of the tyre crumb

Elemental analysis (wt.%)					Reference
C	H	N	S	O	
83.54	7.55	0.35	1.84	6.73	This study
84.2	7.1	0.4	2.1	6.2	Irmak Aslan et al. (2017)
82.0	7.1	0.7	1.9	-	Januszewicz et al. (2017)
-	-		1.5	-	Miranda et al. (2013)
77.60	7.0	0.43	1.4	7.7	Singh et al. (2012)
86.00	8.4	0.5	1.9	3.2	López et al. (2013)

4.2. Pyrolysis of the tyre crumb

4.2.1. Thermogravimetric and derivative thermogravimetric thermograms

The TG and DTG thermograms of the tyre crumb pyrolysis for the temperature ramp rates of 2, 5, 10 and 20 °C min^{-1} are shown in Figures 4-1, 4-2, 4-3 and 4-4 respectively. The detailed data that shows the track of the tyre crumb thermal degradation and conversion are presented in Tables C-1, C-2, C-3 and C-4 (Appendix C) for the heating rates 2, 5, 10 and 20 °C min^{-1} respectively. The average weight loss for the four heating rates was found to be 63.64 wt.%. The thermal decomposition started at about 270 °C and 285 °C and was complete at about 460 °C and 475 °C for the rates of 2 °C min^{-1} and 5 °C min^{-1} respectively. At temperature ramp rates of 10 and 20 °C min^{-1}, the decomposition started at about 290 °C and 315 °C and was complete at about 480 °C and 500 °C respectively. For all the heating rates, there was no further weight loss above the temperature of 500 °C.

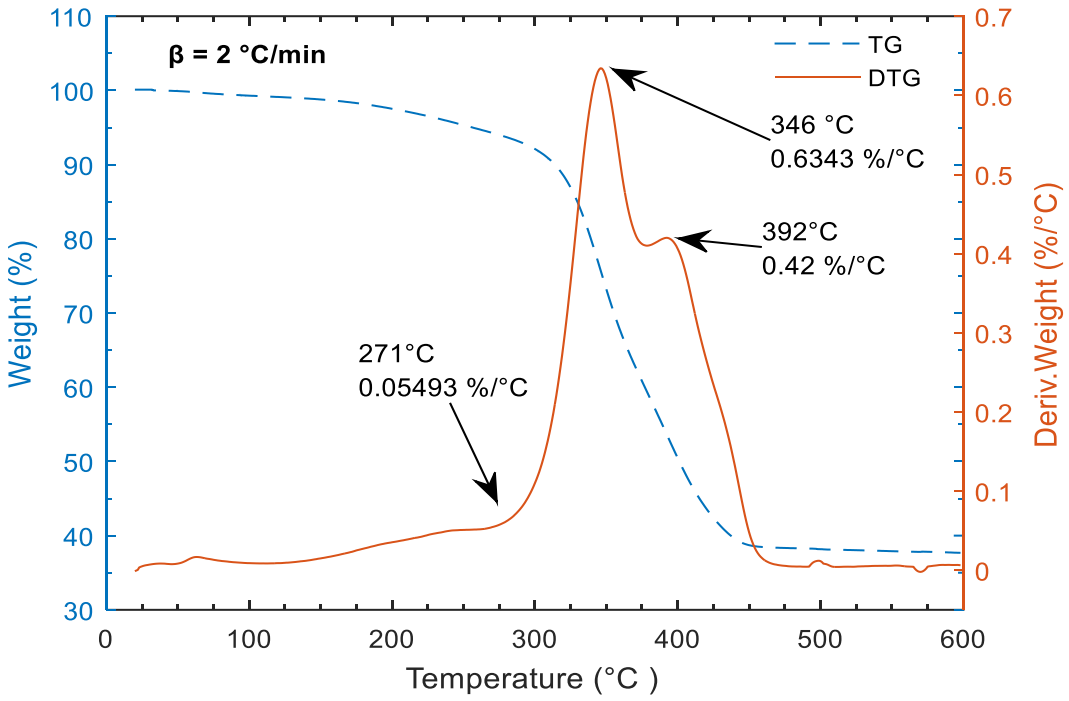

Figure 4-1: TG/DTG thermograms at 2 °C/min

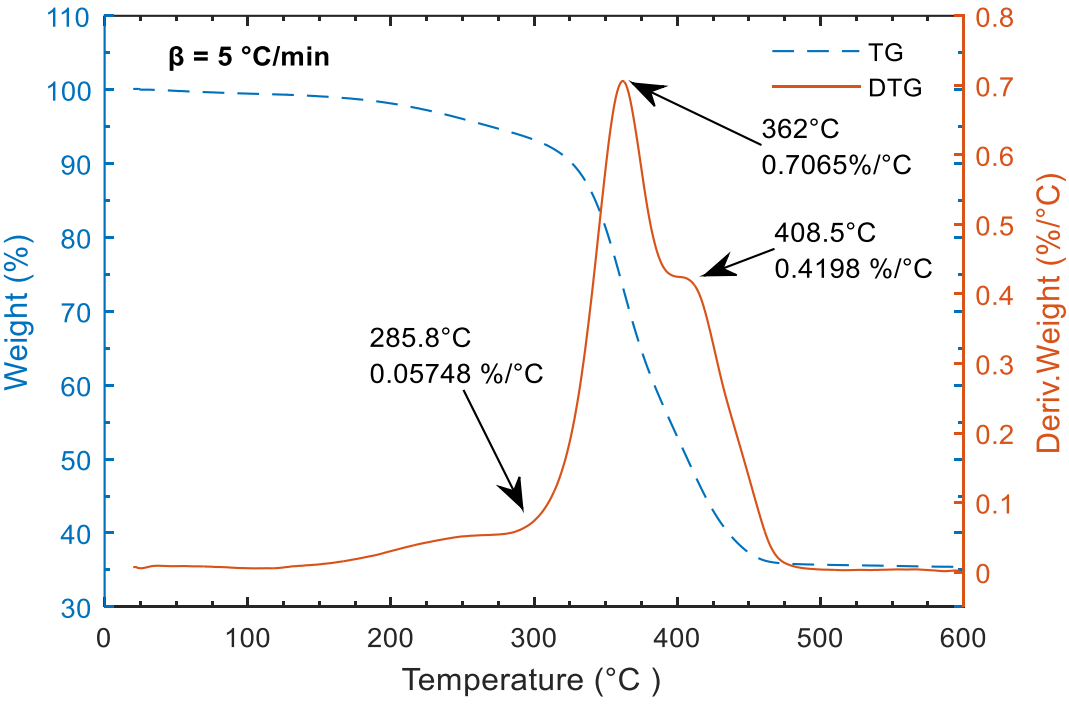

Figure 4-2: TG/DTG thermograms at 5 °C/min

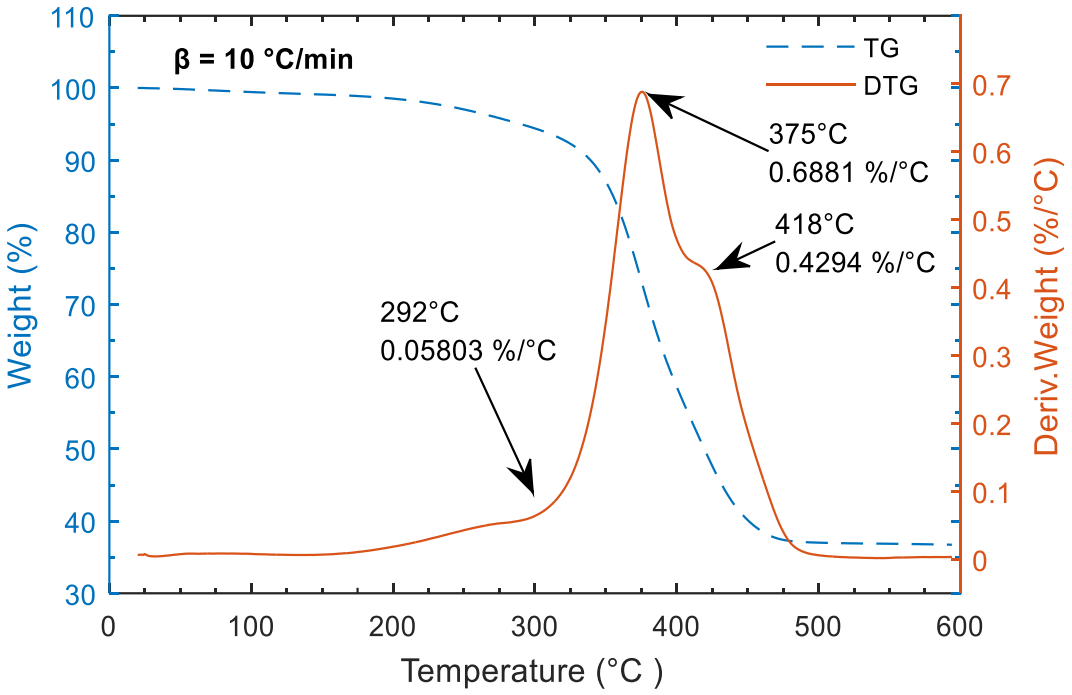

Figure 4-3: TG/DTG thermograms at 10 °C/min

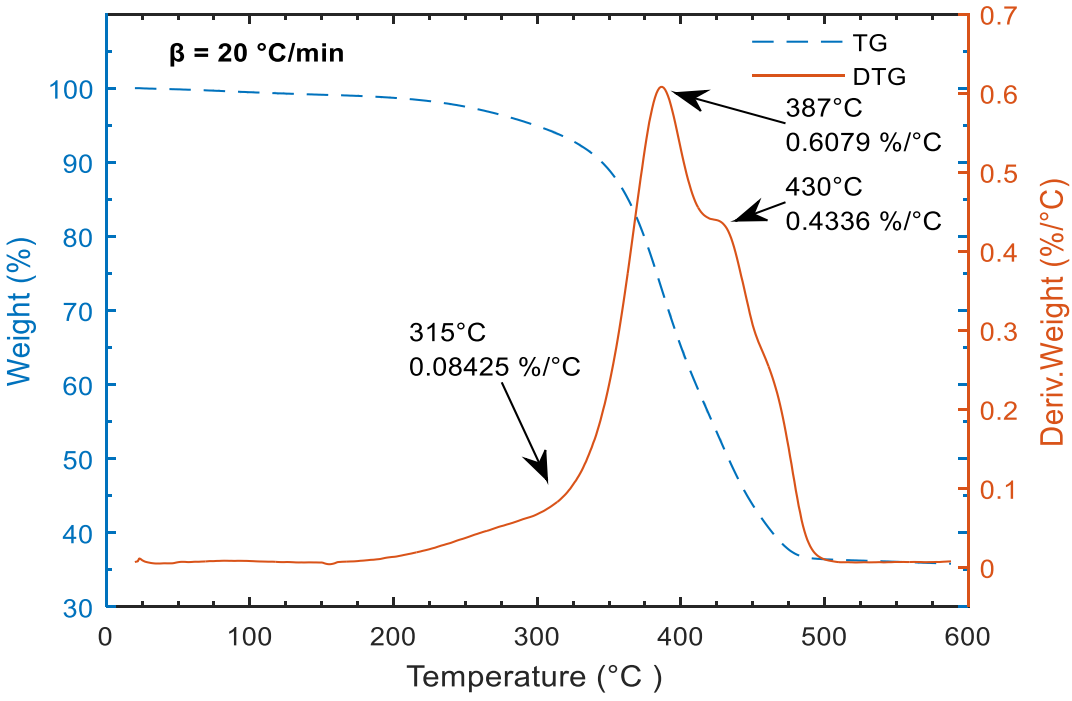

Figure 4-4: TG/DTG thermograms at 20 °C/min

As seen in the the DTG thermograms in Figures 4-1 to 4-4, three stages of decomposition are notable. The mean temperature (T_m) for each stage was determined by adding up the temperatures at that stage for each heating rate and then dividing the sum by four (number of heating rates). The first stage, which

is indicated by the arrows on the far left of each thermogram, involves the removal of lubricants and oil in the scrap tyre. Stage two, indicated by the second arrow from left on each thermogram, corresponds to the breakdown of NR. Stage two, as seen in Figures 4-1 to 4-4, also represents the peak temperature of the tyre crumb thermal degradation process. The third stage, indicated by arrows on the far right of each thermogram, represents the breakdown of butadiene rubber and styrene-butadiene rubber.

The mean temperature for the removal of lubricants and oil was found to be T_m = 291 °C, while the mean temperature for the breakdown of NR (also the mean peak temperature) was T_m = 368 °C. This value corresponds to that (T_m = 373.1 °C) reported by other authors (López et al., 2013). The breakdown of butadiene rubber and styrene-butadiene rubber occurred at a mean temperature of T_m = 412 °C. The TG/DTG thermograms show that the peak temperatures increase with increasing heating rates during the entire three-stage thermal decomposition process. This, however, occurs without the change in the profile of thermal degradation and could be as a result of reduced heat transfer efficiency at higher heating rates. Table 4-3 shows the temperatures for the three-stage thermal degradation of the tyre crumb at the four heating rates.

Table 4-3: Temperatures for the three-stage thermal degradation process

Heating rate	Process temperature (°C)		
	Stage one	Stage two	Stage three
2 °C min^{-1}	271	346	392
5 °C min^{-1}	285.8	362	408.5
10 °C min^{-1}	292	375	418
20 °C min^{-1}	315	387	430
Mean temperature	291	368	412

4.2.2. Temperature and mass loss variation with time

The plots of the temperature and mass loss versus time are presented in Figures 4-5, 4-6, 4-7 and 4-8 for the heating rates of 2, 5, 10 and 20 °C min^{-1} respectively. The temperature relates linearly with time (Figures 4-5 to 4-8) which implies that the mass loss during the pyrolysis process takes place with respect to temperature and time in the same significance. For the four heating rates, stage (I) represents the process of oil and lubricants removal in the tyre crumb. In stage (II), the process of the breakdown of natural rubber in tyre crumb takes place, while stage (III) represents butadiene rubber and styrene-butadiene rubber breakdown process.

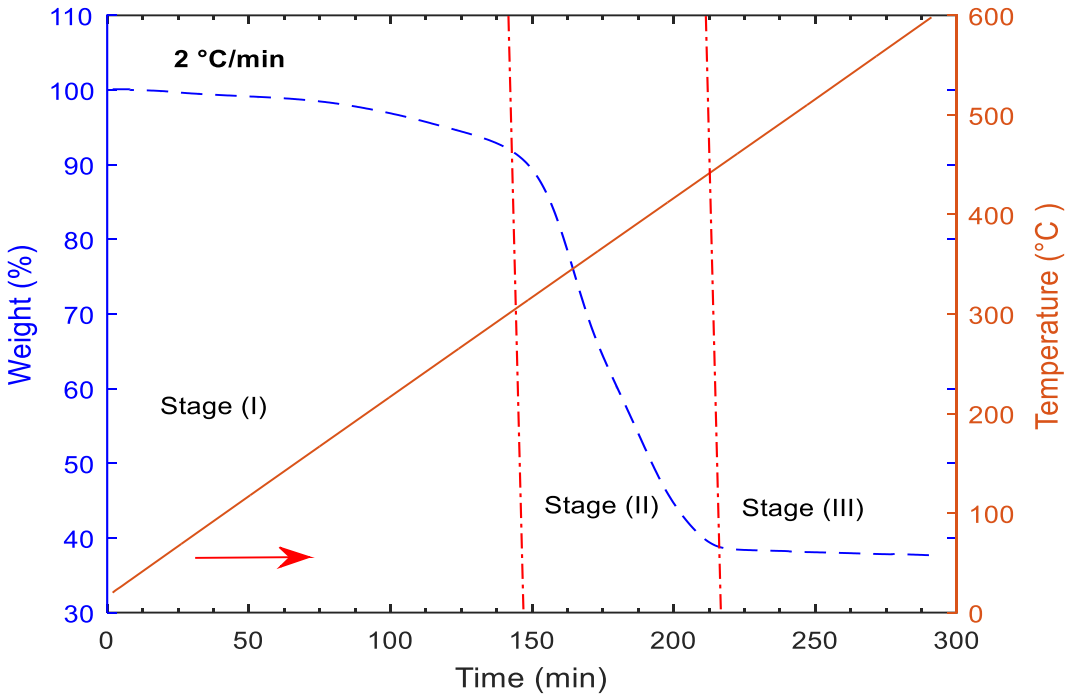

Figure 4-5: Mass loss and temperature against time (2 °C min^{-1})

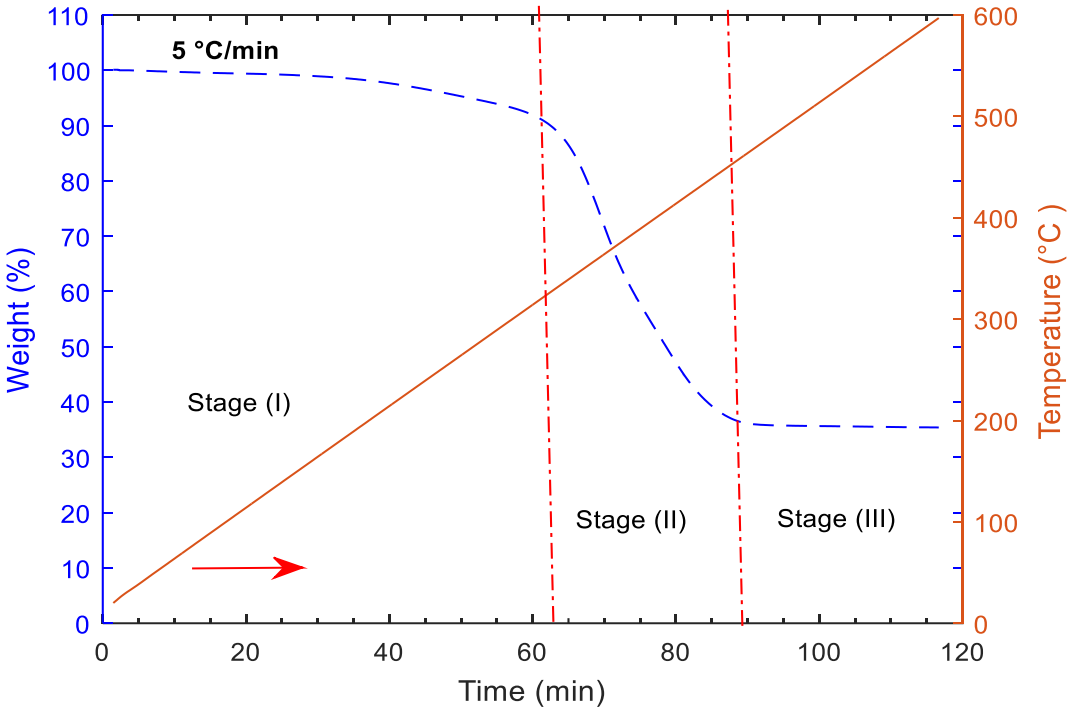

Figure 4-6: Mass loss and temperature against time (5 °C min^{-1})

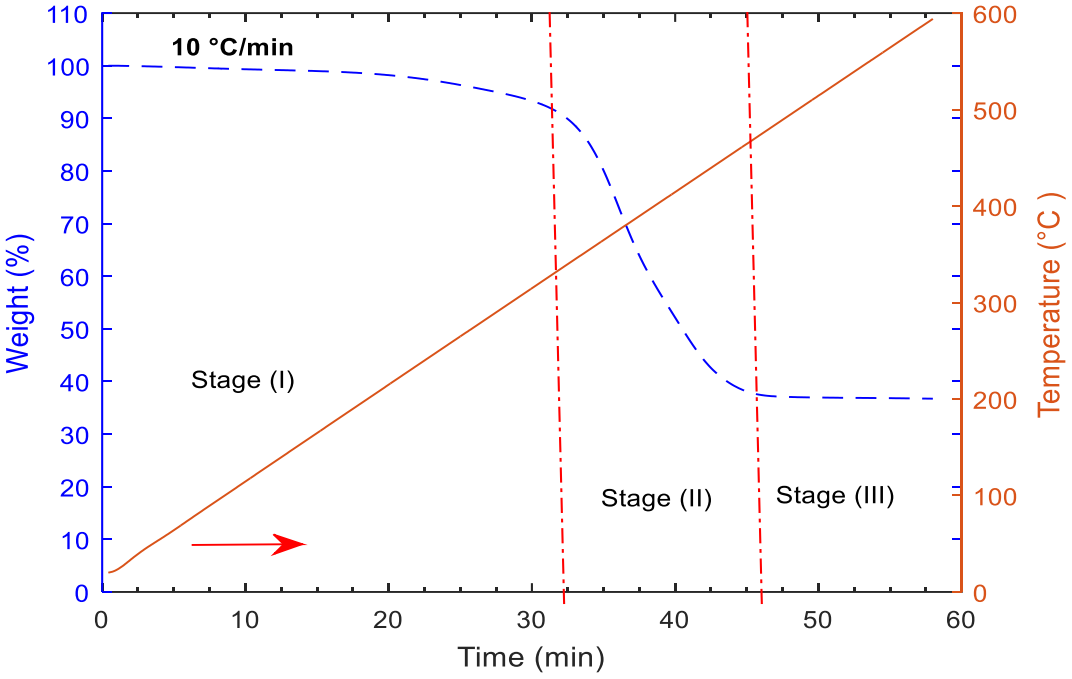

Figure 4-7: Mass loss and temperature against time (10 °C min^{-1})

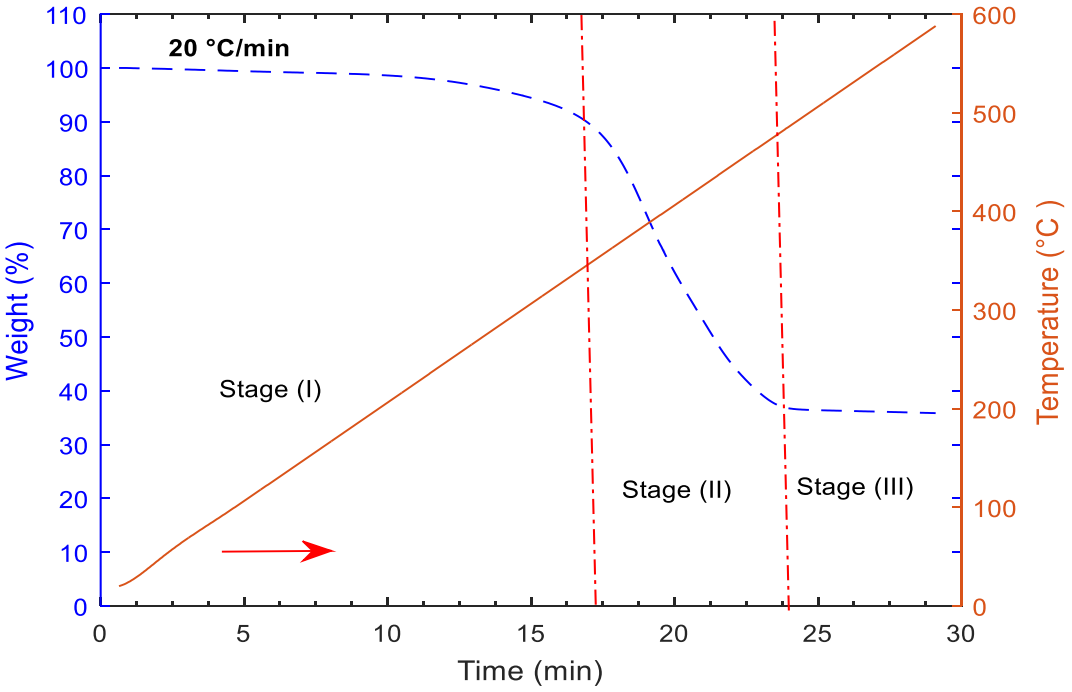

Figure 4-8: Mass loss and temperature against time (20 °C min^{-1})

4.2.3. The variation of conversion degree with temperature

Figure 4-9 shows the variation of conversion degree with temperature for the various heating rates. It can be seen that the degree of conversion increases with temperature for each of the heating rates. In

addition, the conversion degree is higher at lower heating rates at any chosen temperature. For example, at about 350 °C, the degree of conversion is about 0.4, 0.3, 0.2 and 0.17 for the heating rates of 2, 5, 10 and 20 °C min^{-1} respectively. This trend is constant throughout the thermal degradation process.

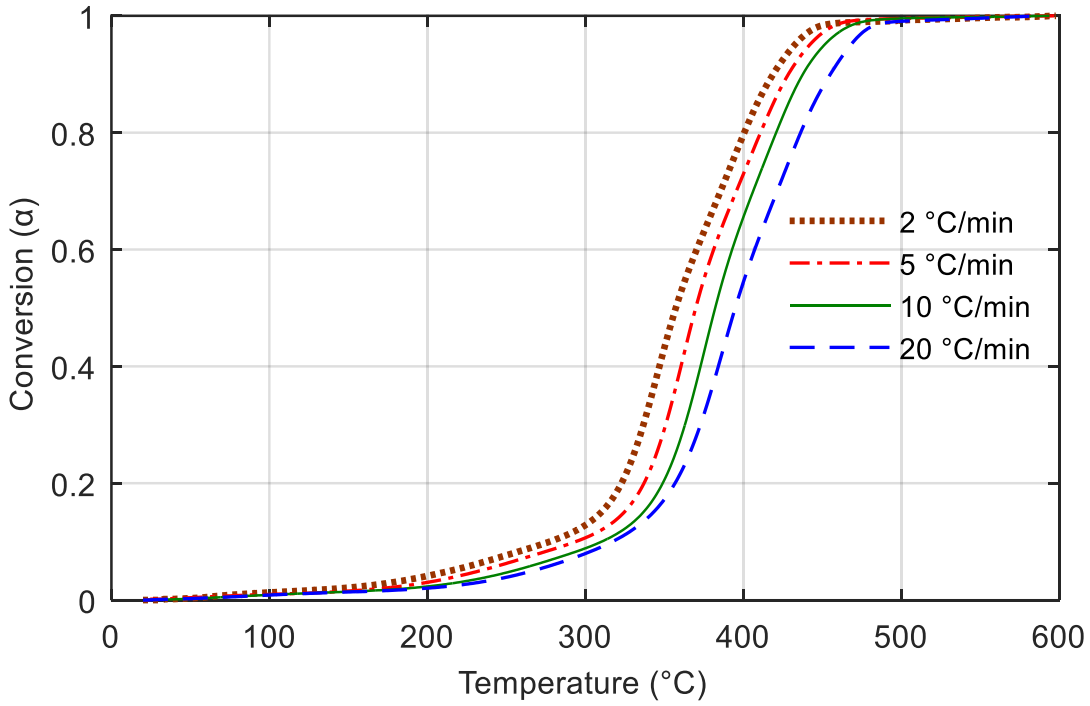

Figure 4-9: Variation of extent of conversion with temperature

4.3. Kinetic analysis of tyre pyrolysis

Three model-free methods (KAS and FWO and FR models) and model-fitting CR method were applied in the determination of kinetic parameters of the tyre pyrolysis process. The parameters determined were the activation energy and pre-exponential factor. The model-free methods were used to establish the relationship between the extent of conversion and the activation energies, while the CR model-fitting method was used to determine the pre-exponential factors using activation energies from the best performing model-free method. In addition, the CR model was used to determine the reaction mechanism (reaction order) associated with the process of pyrolysis of the tyre crumb.

4.3.1. Determination of activation energies using model-free methods

Using the KAS model, the plot $\ln\left(\frac{\beta}{T^2}\right)$ versus $\frac{1}{T}$ gave a slope of $-\frac{E_a}{R}$, from which E_a was determined while the plot of $\ln(\beta)$ versus $\frac{1}{T}$ using the FWO model gave a slope of $-1.052\frac{E_a}{R}$, from which E_a was determined. For the FR model, on the other hand, the slope from the plot of $\mathrm{Ln}\left[\beta\left(\frac{d\alpha}{dT}\right)_{\alpha,i}\right]$ versus

$\frac{1}{T_{,i}}$ aided in the calculation of activation energies. Figures 4-10 and 4-11 show the kinetic plot of the tyre crumb pyrolysis using the KAS and FWO models respectively while Figure 4-12 shows a similar plot obtained using the FR model.

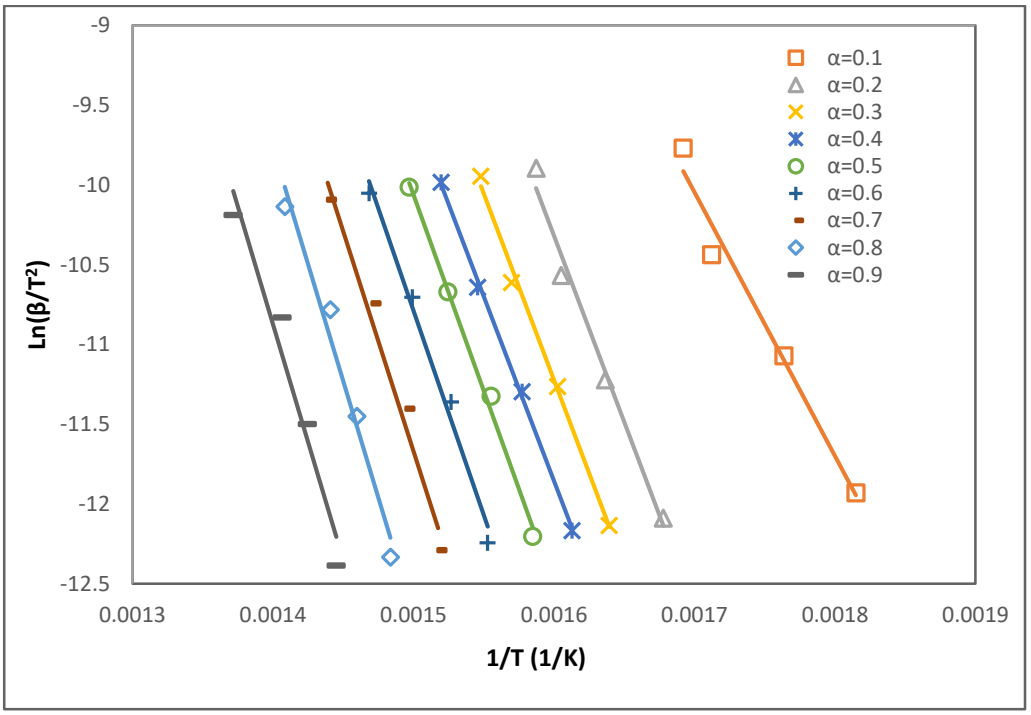

Figure 4-10: KAS plot at various conversion degrees.

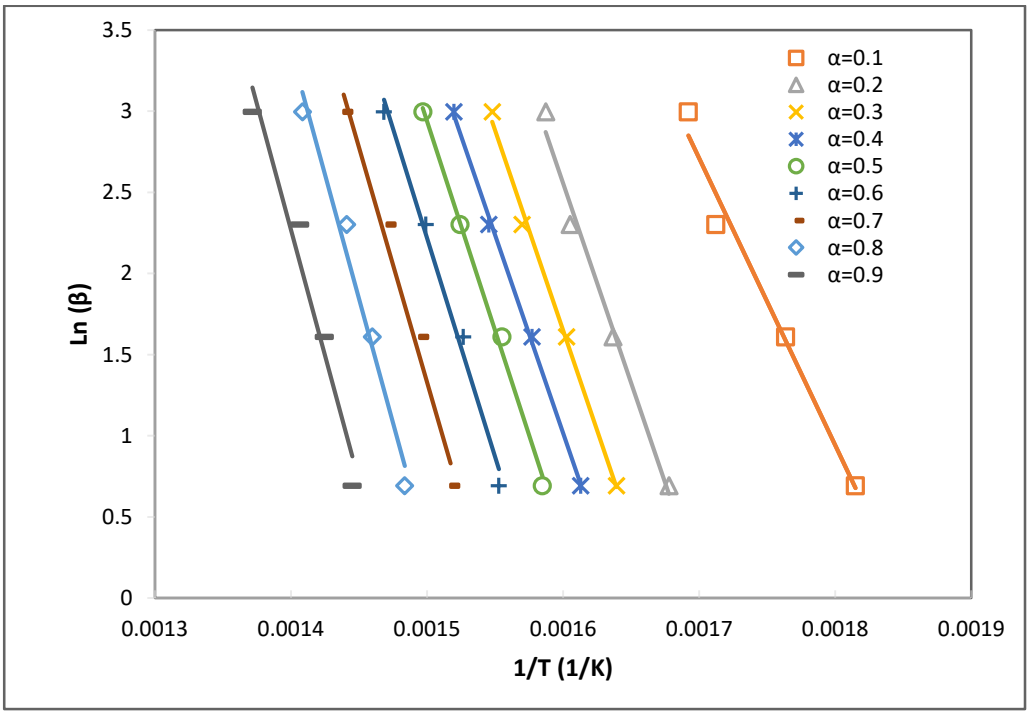

Figure 4-11: FWO plot at various conversion degrees.

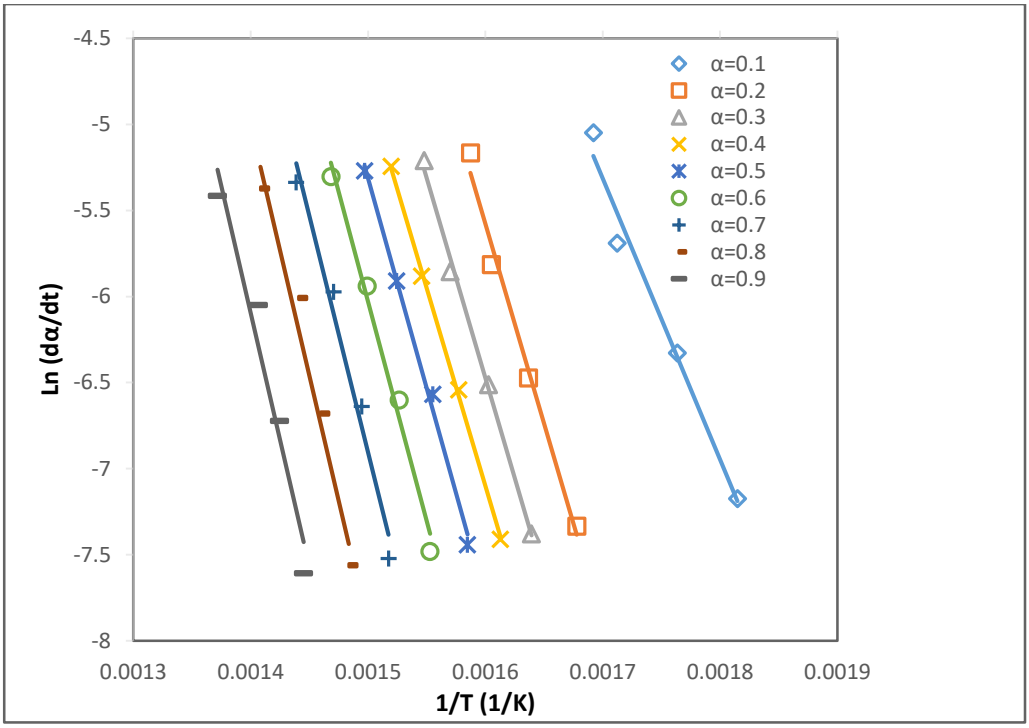

Figure 4-12: FR plot at various conversion degrees.

The conversion degrees considered ranged between α = 0.1-0.9 (Figures 4-10 to 4-12), while those below 0.1 and above 0.9 were not included owing to the low correlation coefficients (Damartzis et al., 2011). Table 4-4 shows the activation energy values calculated using KAS, FWO and FR models. The average values of the activation energies obtained were 206.01 kJ mol^{-1}, 206.08 kJ mol^{-1} and 204.82 kJ mol^{-1} using KAS, FWO and FR models respectively. The values of activation energy obtained indicate that the three methods were in agreement, with a deviation of below 1% between KAS and FWO models. This validates the reliability of the three model-free methods (which are all direct models) to fit the TGA data, in addition to having excellent predictive power (Lopez-Velazquez et al., 2013). The average E_a obtained using the FR model was slightly lower than the values obtained using the KAS and FWO models. The highest coefficient of determination values as seen in Table 4-4, for the three methods, were obtained at conversion degrees of between α = 0.3-0.5, while at α of between 0.7-0.9 lowest R^2 values were achieved.

The kinetic analysis indicates that the activation energy is highly dependent upon conversion extent, an indication that tyre crumb thermal decomposition is a complex process that encompasses various reactions that occur at different stages. As seen in Table 4-4, for the three models (KAS, FWO and FR), there is a sharp increase in the activation energies with change in the conversion degree from 0.1 to 0.2. The activation energies then almost remain unchanged in the conversion degree range of α = 0.2-0.3. The E_a values slightly drop as the conversion degree increases from 0.3 to 0.4, after which there is a continuous increase in activation energies up to α = 0.9. Based on the high coefficient of

determination values for each of the three models (0.9830 for KAS, 0.9847 for FWO and 0.9831 for FR), it can be concluded that the models fitted well the TGA data and can be used for reliable prediction of activation energies associated with the pyrolysis of waste tyres. Although, the three model-free methods performed well in fitting the TGA data and prediction of activation energies, the activation energy data from the FWO model was used in the determination of pre-exponential factors by applying the Coats-Redfern model. The choice to use the FWO model data was based on slightly higher R^2 for this model compared to the other two models, although the difference was not significant (Table 4-4). Subsequently, the curve fitting of the activation energy versus the conversion degrees and the determination of pre-exponential factors were performed by incorporating the values of activation energy obtained from the FWO model.

Table 4-4: Activation energies and coefficients of determination obtained using KAS, FWO and FR models

conversion (α)	E_a; KAS (kJ mol^{-1})	R^2	E_a; FWO ($kJ\ mol^{-1}$)	R^2	E_a; FR ($kJ\ mol^{-1}$)	R^2
0.1	137.53	0.9774	139.75	0.9801	135.63	0.9797
0.2	194.42	0.9860	194.49	0.9872	192.78	0.9875
0.3	194.38	0.9951	194.69	0.9956	192.99	0.9960
0.4	192.39	0.9986	192.97	0.9987	191.30	0.9990
0.5	204.06	0.9951	204.23	0.9956	202.92	0.9950
0.6	213.38	0.9876	213.30	0.9889	212.30	0.9869
0.7	229.14	0.9775	228.52	0.9796	228.14	0.9764
0.8	243.03	0.9750	241.95	0.9773	242.18	0.9737
0.9	245.72	0.9551	244.80	0.9591	245.15	0.9537
Average	206.01	0.9830	206.08	0.9847	204.82	0.9831

4.3.1.1. Establishment of the relationship between the activation energy and the degree of conversion via curve fitting

The goodness-of-fit tests were conducted in order to establish the relationship between the activation energy and the degree of conversion using the values from the FWO method. The summary of the parameters obtained from the goodness-of-fit tests is presented in Table 4-5, and this data is representative of the trend followed when the activation energies from KAS and FR models were used in goodness-of-fit tests. Results of the test indicate that the interdependence of activation energy and the degree of conversion for the tyre crumb pyrolysis process conforms to a sixth degree polynomial relationship. Figure 4-13 shows the plot for this relationship while Figure 4-14 shows the plot of its residuals. In the equation displayed in Figure 4-13, x and y represent the activation energy and the conversion degree respectively.

The difference between the R^2 and adjusted R^2 in the sixth degree polynomial case (robust off fitting criterion) was 0.0024, the lowest compared to the values obtained from the rest of the goodness-of-fit tests. The values of the root mean square error (RMSE) and norm of residuals (NOR) were almost the same for the sixth degree polynomial test, whereas the other fits showed a deviation in these values. The values of the sum of squared errors (SSE) and degrees of freedom error (DFE) were the lowest in the sixth degree polynomial case compared to the values obtained from other goodness-of-fit criteria. Only the seventh degree polynomial fitting criterion yielded comparable results, but the difference between R^2 and adjusted R^2 in this case was slightly larger. The eighth degree polynomial fitting test yielded the Not-a-Number (NaN) results for almost all the statistical parameters, and thus could not be quantified for assessment of the fit. The NaN result according to IEEE arithmetic representation implies that it is neither a number nor equal to anything, including itself (Pawlowicz et al., 2002; MathWorks, 2005).

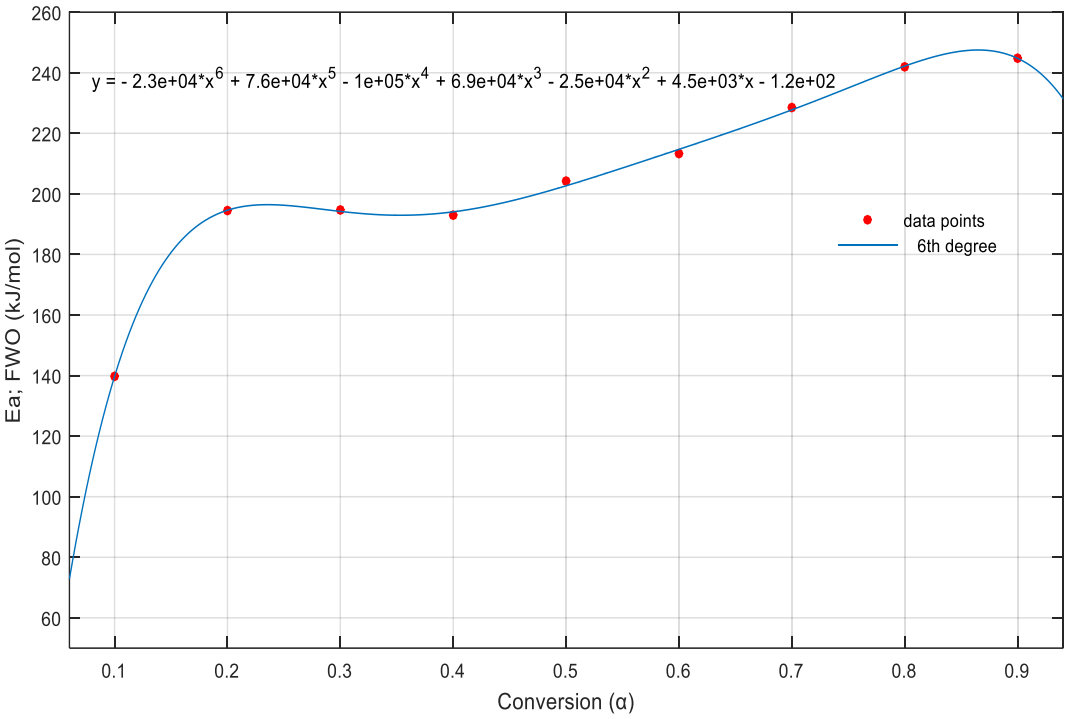

Figure 4-13: Polyfit of activation energy versus conversion (FWO).

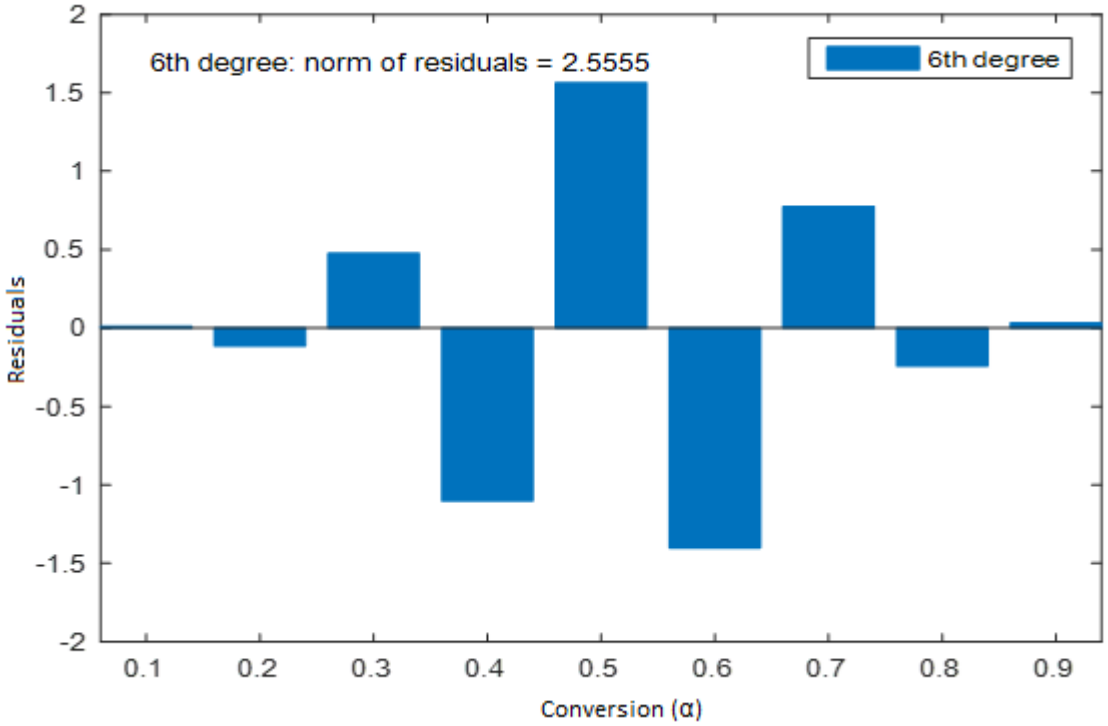

Figure 4-14: Residuals plot for the Polyfit of activation energy versus conversion (FWO)

Table 4-5: Summary of goodness-of-fit tests parameters for FWO method.

Fit	R^2	Adjusted R^2	DFE	SSE	RMSE	NOR
Interpolant	1.0000	NaN	0	0.00	NaN	NaN
Linear	0.8707	0.8269	6	1062.00	13.31	33.57
poly1 (robust off)	0.8623	0.8426	7	1127.00	12.69	33.57
poly1 (LAR robust)	0.8578	0.8375	7	1163.00	12.89	33.57
poly1 (Bisquare robust)	0.9175	0.9057	7	674.80	9.82	33.57
poly2 (robust off)	0.8758	0.8344	6	1016.00	13.01	31.87
poly2 (LAR robust)	0.9379	0.9172	6	508.00	9.20	31.87
poly2 (Bisquare robust)	0.9257	0.9010	6	607.60	10.06	31.87
poly3 (robust off)	0.9087	0.8539	5	747.10	12.22	27.33
poly3 (LAR robust)	0.8350	0.7360	5	1350.00	16.43	27.33
poly3 (Bisquare robust)	0.8849	0.8158	5	942.00	13.73	27.33
poly4 (robust off)	0.9831	0.9663	4	138.00	5.87	11.75
poly4 (LAR robust)	0.9876	0.9752	4	101.50	5.04	11.75
poly4 (Bisquare robust)	0.9771	0.9541	4	187.70	6.85	11.75
poly5 (robust off)	0.9954	0.9877	3	37.87	3.55	6.15
poly5 (LAR robust)	0.9932	0.9818	3	55.84	4.31	6.15
poly5 (Bisquare robust)	0.9943	0.9848	3	46.50	3.94	6.15
poly6 (robust off)	0.9992	0.9968	2	6.53	1.81	2.56
poly6 (LAR robust)	0.9984	0.9935	2	13.29	2.58	2.56
poly6 (Bisquare robust)	0.9991	0.9964	2	7.45	1.93	2.56
poly7 (robust off)	0.9992	0.9937	1	6.43	2.54	2.54
poly7 (LAR robust)	0.9979	0.9835	1	16.89	4.11	2.54
poly7 (Bisquare robust)	0.9988	0.9908	1	9.43	3.07	2.54
poly8 (robust off)	1.0000	NaN	0	0.00	NaN	0.00
poly8 (LAR robust)	NaN	NaN	0	NaN	NaN	NaN
poly8 (Bisquare robust)	NaN	NaN	0	NaN	NaN	NaN

4.3.2. Determination of pre-exponential factors using the CR model and the activation energy values from FWO model

The activation energies obtained from the FWO method were then fitted into the CR model in order to calculate the pre-exponential factors at different conversion degrees for the four heating rates.

4.3.2.1. Determination of the reaction order

The data was tested for three reaction models i.e. F1, F2 and F3. The CR plots yielded varied results for the three reaction orders at four heating rates. The CR plots for the F1, F2 and F3 reaction models are presented in Figures 4-15, 4-16 and 4-17 respectively while Table 4-6 shows the summary of the coefficients of determination based on which the reaction order was determined. It can be seen in Table 4-6 that the F2 model presented higher values of the coefficient of determination than the F1 and F3 models. Therefore, it can be concluded that the pyrolysis of the tyre crumb can best be described by the second order reaction mechanism, F2.

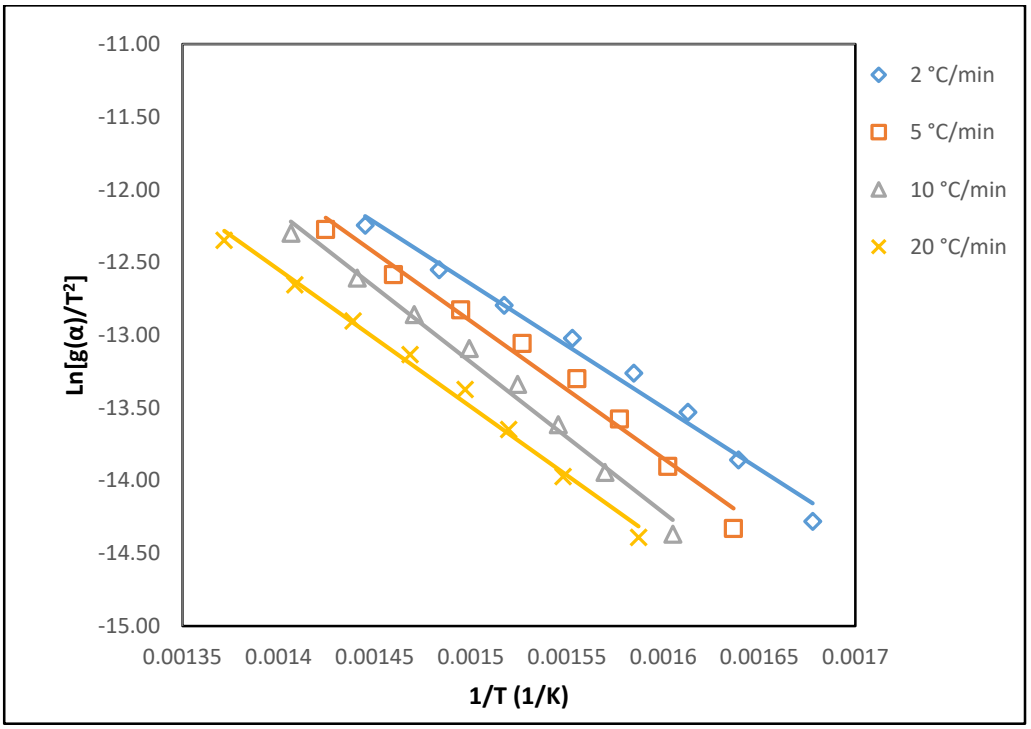

Figure 4-15: CR plot for the F1 reaction model

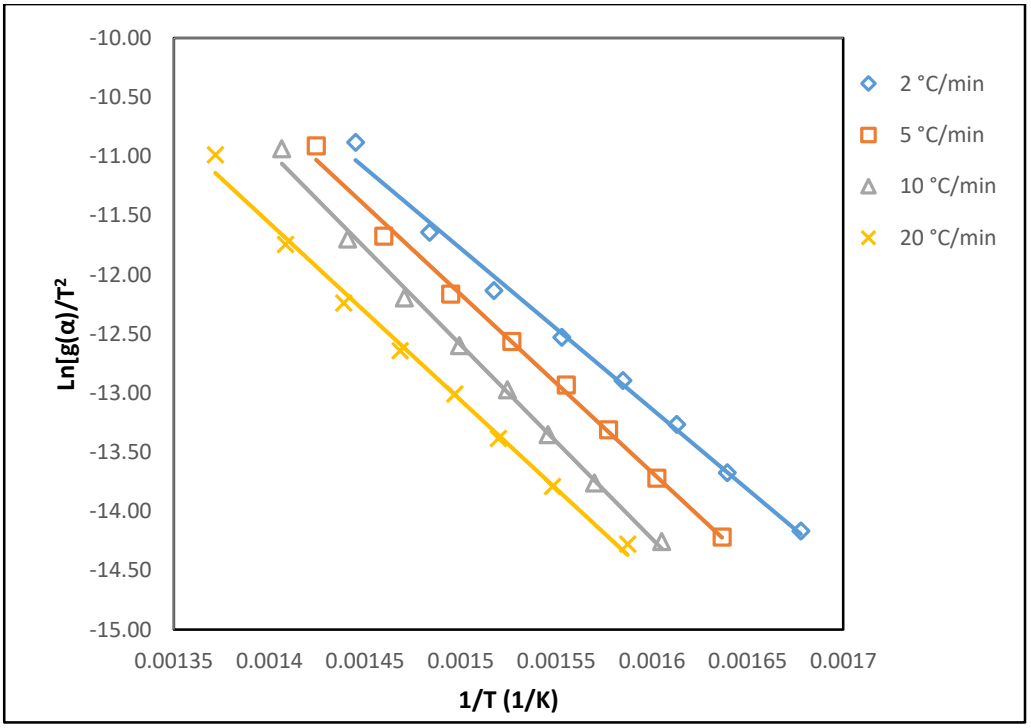

Figure 4-16: CR plot for the F2 reaction model

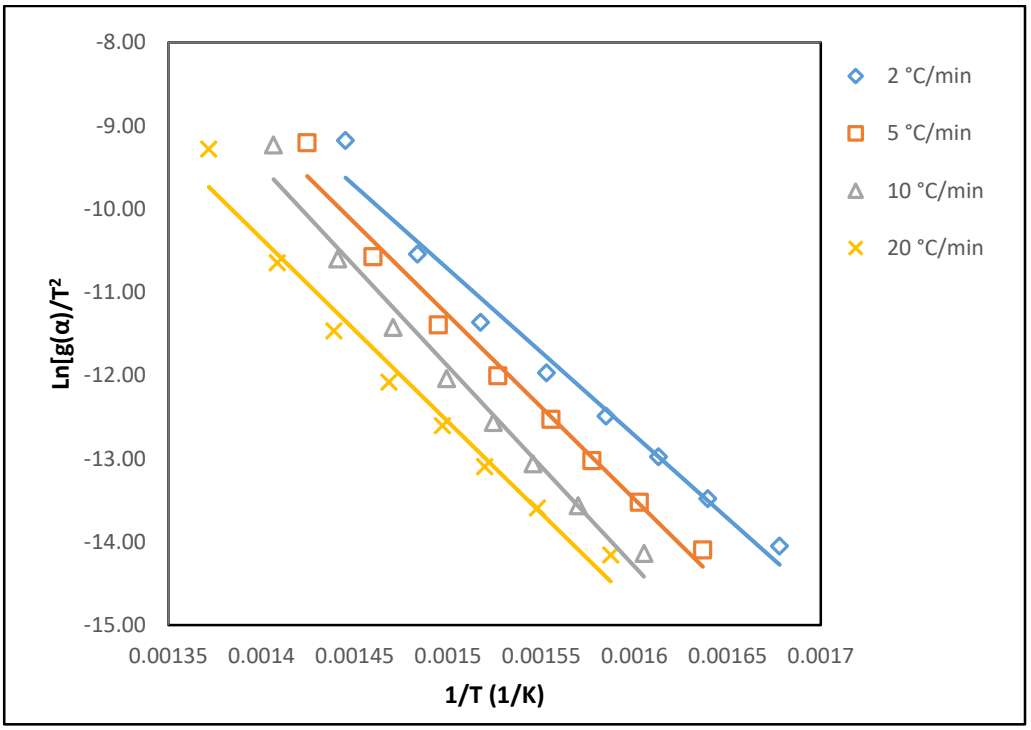

Figure 4-17: CR plot for the F3 reaction model

Table 4-6: Summary of coefficients of determination for reaction order selection

β (°C min^{-1})	F1 model	F2 model	F3 model
2	0.9865	0.9940	0.9779
5	0.9820	0.9955	0.9830
10	0.9889	0.9960	0.9802
20	0.9926	0.9942	0.9750

4.3.2.2. Pre-exponential factors obtained using selected F2 reaction model

The pre-exponential factors at different conversion degrees and heating rates determined using the CR model and the selected reaction model (F2 model) are presented in Table 4-7 while Table 4-8 shows the summary of comparison of kinetic parameters obtained in this research and those from previous related studies.

Table 4-7: Pre-exponential factors (min^{-1}) calculated with the CR model using E_a from FWO methods

Conversion (α)	β = 2 °C min^{-1}	β = 5 °C min^{-1}	β = 10 °C min^{-1}	β = 20 °C min^{-1}
0.1	1.78E+08	2.75E+09	2.68E+10	4.10E+09
0.2	2.48E+08	3.83E+09	3.74E+10	5.70E+09
0.3	2.48E+08	3.84E+09	3.74E+10	5.71E+09
0.4	2.46E+08	3.80E+09	3.71E+10	5.66E+09
0.5	2.61E+08	4.02E+09	3.92E+10	5.99E+09
0.6	2.72E+08	4.20E+09	4.10E+10	6.26E+09
0.7	2.92E+08	4.50E+09	4.39E+10	6.70E+09
0.8	3.09E+08	4.77E+09	4.65E+10	7.10E+09
0.9	3.12E+08	4.82E+09	4.70E+10	7.18E+09
Average	2.68E+08	4.14E+09	4.03E+10	6.16E+09

Table 4-8: Parameters of the kinetics of pyrolysis of waste tyres

E_a (kJ mol^{-1})	A (min^{-1})	Material	Reference
206.08	1.27 E+10	Tyre crumb	This research
128.9 - 192.9	-	Waste tyre	(Irmak Aslan et al., 2017)
80 - 95.3	-	Scrap tyre	(Singh et al., 2012)
160	2.49 E+10	Scrap tyre	(López et al., 2013)
78.72	3.05 E+05	Scrap tyre	(Uzun and Yaman, 2014)

The average pre-exponential factors obtained using the selected F2 model were 2.68E+08, 4.14E+09, 4.03E+10 and 6.16E+09 min^{-1} for the heating rates of 2, 5, 10 and 20 °C min^{-1} respectively, giving an overall mean pre-exponential factor of 1.27E+10 min^{-1}. As seen in Table 4-7, at a given conversion degree, the pre-exponential factors generally increase with heating rates. However, a drop in the pre-exponential factors is observed as the heating rate increases from 10 to 20 °C min^{-1} for all conversion degrees. On the other hand, for each of the heating rates, the pre-exponential factor increases as the conversion degree, α increases from 0.1 to 0.2. The pre-exponential factor then remains almost

unchanged as α shifts from 0.2 to 0.3. As the thermal degradation progresses from α = 0.3 to α = 0.4, the pre-exponential factor drops slightly. The pre-exponential factor then continuously increases in the α value range of 0.4-0.9.

The overall mean pre-exponential factor (1.27E+10 min^{-1}) compares well with the value obtained in a study carried out by López et al. (2013) where a mean pre-exponential factor value of 2.49×10^{10} min^{-1} was obtained. In another study conducted by Uzun and Yaman (2014), mean E_a and pre-exponential factors of 78.72 kJ mol^{-1} and 3.05×10^5 min^{-1} respectively were obtained. The discrepancy in the values of pre-exponential factors and activation energies obtained could be as a result of the differences in the scrap tyre composition, particularly the percentage compositions of NR, BR and SBR, which greatly influence the kinetics of the tyre pyrolysis process. Moreover, the difference in models used as well as the variation in the approach to kinetics study is also a contribution to the differences in kinetic parameters obtained.

4.3.2.3. Surface fitting

Surface fitting (with 95 % confidence bounds) of conversion degrees, pre-exponential factors and activation energies was done by applying the least squares method. The fit with the highest adjusted R^2 values, lowest SSE, lowest RMSE and highest DFE was chosen as best fit. In all goodness-of-fit tests, the values of R^2 and adjusted R^2 were equal to unity. For all the goodness-of-fit tests, the first degree polynomial for both x and y inputs (poly 11) was found to be the best fit for the data loaded, while the tests for polynomials above the second degree polynomial yielded poorly conditioned results. Table 4-9 shows the summary of parameters of the goodness-of-fit tests.

Table 4-9: Summary of the results of surface goodness-of-fit tests.

2 °C min^{-1}					
Fit type	SSE	RMSE	DFE	R^2	Adjusted R^2
Poly 11	5.68E-14	9.73E-08	6.00	1.00	1.00
Poly 12	7.37E-14	1.36E-07	4.00	1.00	1.00
Poly21	4.44E-14	1.05E-07	4.00	1.00	1.00
Poly22	4.00E-14	1.15E-07	3.00	1.00	1.00
Lowess (Linear)	6.57E-14	1.39E-07	3.40	1.00	1.00
Lowess (quadratic)	7.02E-14	1.22E-07	4.75	1.00	1.00
5 °C min^{-1}					
Fit type	SSE	RMSE	DFE	R^2	Adjusted R^2
Poly 11	9.55E-12	1.26E-06	6.00	1.00	1.00
Poly 12	8.41E-12	1.45E-06	4.00	1.00	1.00
Poly21	1.43E-11	1.89E-06	4.00	1.00	1.00
Poly22	7.73E-12	1.61E-06	3.00	1.00	1.00
Lowess (Linear)	2.87E-11	2.90E-06	3.40	1.00	1.00
Lowess (quadratic)	2.32E-11	2.21E-06	4.75	1.00	1.00
10 °C min^{-1}					
Fit type	SSE	RMSE	DFE	R^2	Adjusted R^2
Poly 11	7.57E-10	1.12E-05	6.00	1.00	1.00
Poly 12	1.41E-09	1.88E-05	4.00	1.00	1.00
Poly21	8.15E-10	1.43E-05	4.00	1.00	1.00
Poly22	7.71E-10	1.60E-05	3.00	1.00	1.00
Lowess (Linear)	1.28E-09	1.94E-05	3.40	1.00	1.00
Lowess (quadratic)	2.23E-09	2.17E-05	4.75	1.00	1.00
20 °C min^{-1}					
Fit type	SSE	RMSE	DFE	R^2	Adjusted R^2
Poly 11	2.66E-11	2.11E-06	6.00	1.00	1.00
Poly 12	2.64E-11	2.57E-06	4.00	1.00	1.00
Poly21	3.12E-11	2.79E-06	4.00	1.00	1.00
Poly22	2.55E-11	2.91E-06	3.00	1.00	1.00
Lowess (Linear)	5.82E-11	4.14E-06	3.40	1.00	1.00
Lowess (quadratic)	5.91E-11	3.53E-06	4.75	1.00	1.00

Figures 4-18, 4-19, 4-20 and 4-21 show the plots of the best fits with pre-exponential factor values determined at heating rates of 2, 5 ,10, and 20 °C min^{-1} respectively, for the various activation energy values.

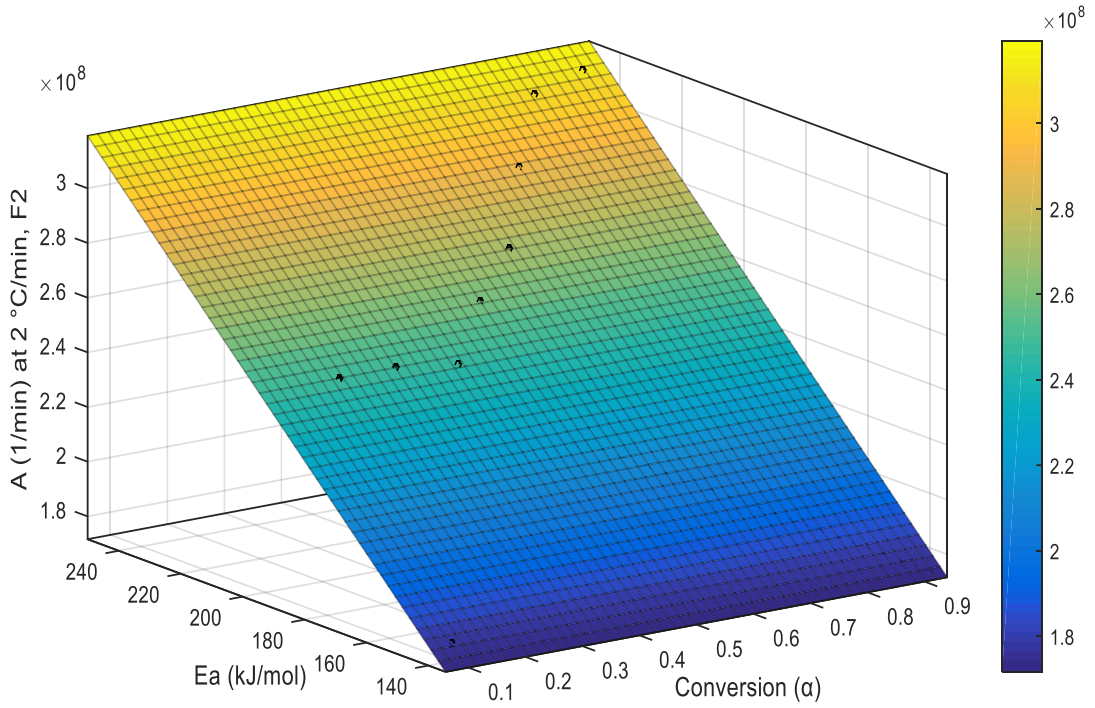

Figure 4-18: Surface fitting of conversion degree, E_a and pre-exponential factor (2 °C min^{-1})

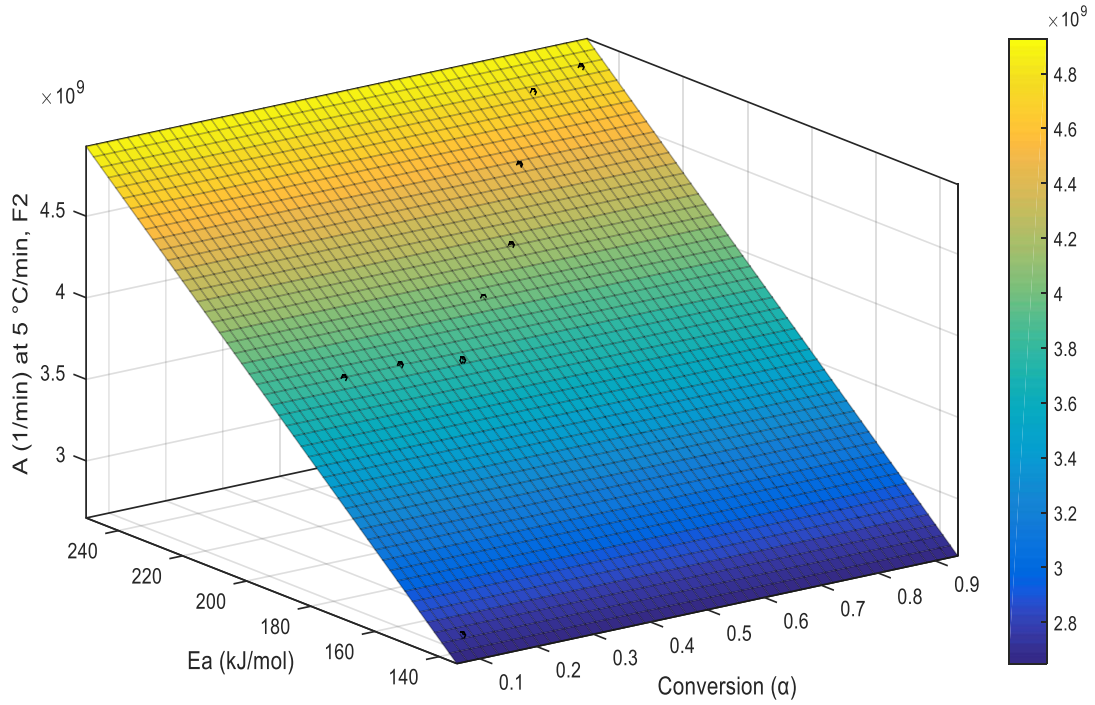

Figure 4-19: Surface fitting of conversion degree, E_a and pre-exponential factor (5 °C min^{-1})

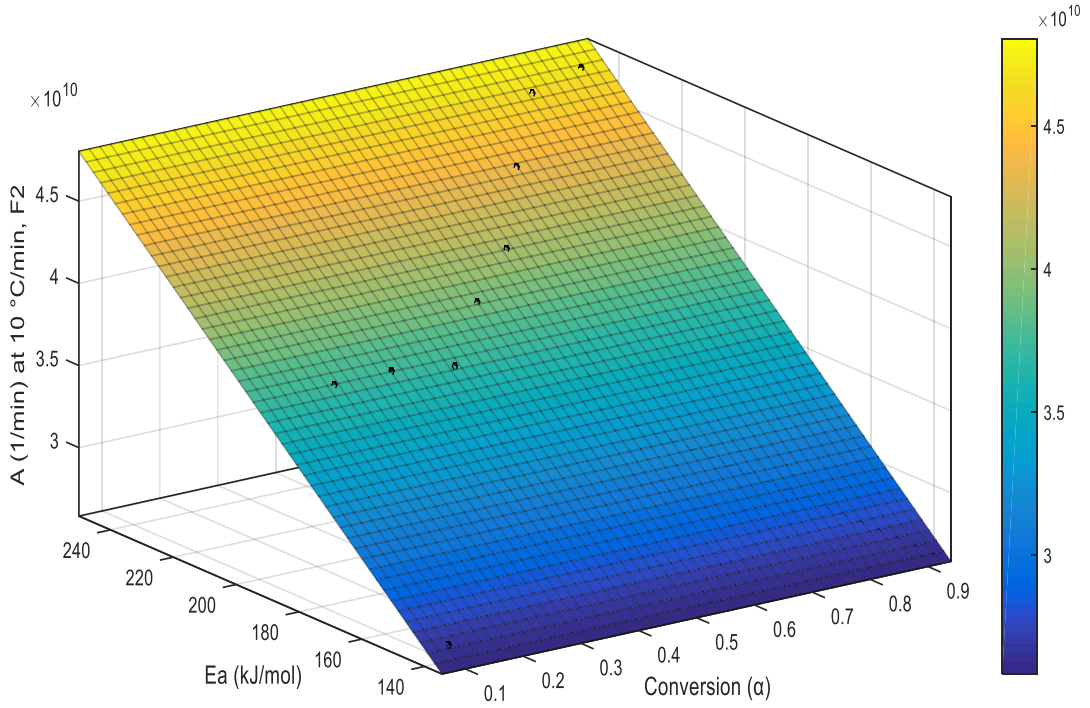

Figure 4-20: Surface fitting of conversion degree, E_a and pre-exponential factor (10 °C min^{-1})

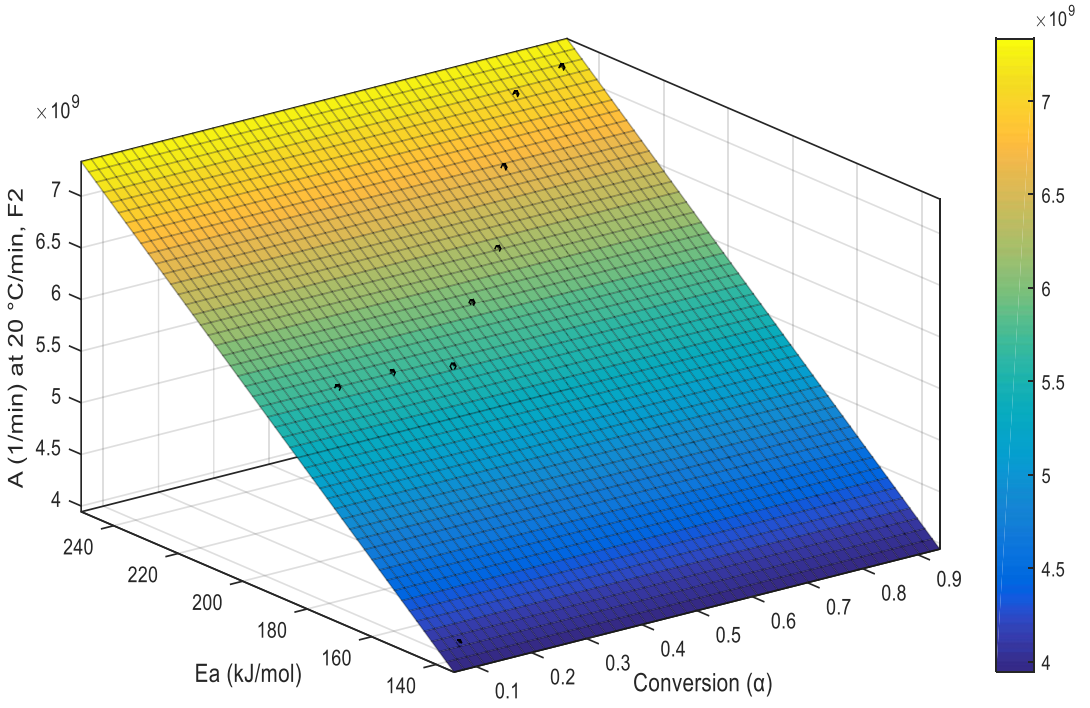

Figure 4-21: Surface fitting of conversion degree, E_a and pre-exponential factor (20 °C min^{-1})

The values of the activation energies and the pre-exponential factors used for surface fitting at different degrees of conversion were obtained from Tables 4-4 and 4-7. As seen in Figures 4-18, 4-19, 4-20 and 4-21, the relationship between the degree of conversion, the activation energy and the pre-exponential

factor conforms to a first order polynomial for both x and y inputs (poly 11). It can also be noted that, for each of the four heating rates, the activation energy and the pre-exponential factor increases continuously at the degree of conversion range of 0. 1 to 0.3. There is then a slight drop in the values of the activation energy and the pre-exponential factor at $\alpha = 0.4$. This is followed by a continuous increase in the two parameters (activation energy and pre-exponential factor) between the α of 0.5 and 0.9.

CHAPTER FIVE

5. Results and discussion: Oxidative desulphurisation of tyre-derived oil

The results of the oxidative desulphurisation of the tyre-derived oil are presented in this chapter. The results are presented with incorporation of the central composite design analysis.

5.1. Results of sulphur removal in the tyre-derived oil

Table 5-1 presents the sulphur removal percentages for various parameter interactions as obtained using the CCD. The sulphur removal percentages presented are for oils extracted using two acetonitrile (ACN) to oil ratios (1:1 and 1:2) and 1:1 dimethylformamide (DMF) to oil ratio. The sulphur removal was in the range of 34.02 to 86.05 % for the various factor interactions using 1:1 acetonitrile to oil ratio while sulphur removal values ranging from 27.91 to 52.77 % were achieved using 1:2 acetonitrile to oil ratio. On the other hand, using a 1:1 DMF to oil ratio during the extraction, the lowest and highest sulphur removal were 3.80 and 35.00 % respectively. It can be seen that the highest sulphur removal was achieved in the case when 1:1 acetonitrile to oil ratio was used during the solvent extraction of the oxidised oils. The results from this case, therefore were used further to model the ODS of tyre-derived oil. Table 5-1 also shows that the values of the sulphur removal vary for the five centre points (runs 10, 11, 13, 16 and 17) used in the experimental design. The variation in the values of sulphur removal despite the identical experimental conditions could be attributed to the errors resulting from the positioning of the stirrer within the round bottom flask, the slight difference in the time between the end of the oxidation stage and the start of the solvent extraction process. In addition, the errors originating from the equipment used to measure the solvents as well as the ICP-AES equipment could have also played a part in the variation of the sulphur removal.

Table 5-1: CCD of sulphur removal for various parameter interactions

Run order	A: HCOOH (mL)	B: H_2O_2 (mL)	C: Temperature (°C)	D: Reaction time (min)	Sulphur removal		
					S_1 (%)	S_2 (%)	S_3 (%)
1	6	10	58	60	66.08	33.78	25.85
2	12	10	58	40	69.86	34.23	30.05
3	3.95	8	54	50	55.04	27.91	24.46
4	12	10	50	40	84.41	42.03	33.51
5	14.05	8	54	50	72.78	34.95	35
6	9	8	60.73	50	84.49	45.87	3.8
7	6	6	50	40	52.39	47.74	15.79
8	12	6	50	60	70.22	39.98	18.4
9	6	6	58	40	34.02	32.05	11.58
10	9	8	54	50	82.94	43.54	20.18
11	9	8	54	50	86.05	36.82	16.87
12	9	8	54	33.18	79.85	45.61	22.49
13	9	8	54	50	74.61	43.55	18.08
14	9	4.64	54	50	60.05	32.12	6.79
15	9	11.36	54	50	64.97	52.77	25.14
16	9	8	54	50	81.42	43.15	27.69
17	9	8	54	66.82	66.21	41.74	20.11
18	9	8	54	50	83.57	42.2	21.07
19	9	8	47.27	50	68.05	45.15	16.18
20	12	6	58	60	82.15	44.04	31.39
21	6	10	50	60	59.97	32.48	10.65

S_1: Sulphur removal using 1:1 acetonitrile to TDO ratio

S_2: Sulphur removal using 1:2 acetonitrile to TDO ratio

S_3: Sulphur removal using 1:1 dimethylformamide to TDO ratio

5.2. Model fitting and diagnosis

The model results presented further are those for sulphur removal in which 1:1 acetonitrile to oil ratio was used during the solvent extraction. Preliminary results of model fitting suggested that the quadratic model is a better predictor of sulphur removal during ODS. However, a negative predicted R^2 value indicated that, in fact, the overall mean is better predictor of the sulphur removal than the suggested model. The summary of model statistics is presented in Table 5-2.

Table 5-2: Summary of model Statistics

Source	SD	R^2	Adjusted R^2	Predicted R^2	PRESS	
Linear	11.67	0.3802	0.2252	-0.0923	3838.3	
2FI	11.83	0.6015	0.2030	-4.8809	20664.7	
Quadratic	6.18	0.9348	0.7827	-1.5430	8935.6	Suggested
Cubic	4.31	0.9789	0.8943		+	Aliased

Due to the negative value of predicted R^2, model modification was performed in order to improve the model's sulphur removal predictability. In the model reduction procedures using p value criterion, Akaike information criterion (AICc) and Bayesian information criterion (BIC), the backward selection was used while 'all hierarchical' selection was applied when adjusted R^2 was used as the reduction criterion. The summary of model reduction tests based on various criteria is presented in Table 5-3. The reduced cubic model (RCM) obtained using BIC as the reduction criterion had the highest predictability compared to the suggested quadratic model and the other reduced cubic models (Table 5-3). This RCM was used in subsequent analysis and presentation of model results for sulphur removal in the tyre-derived oil.

Table 5-3: Model reduction tests

Model	Criterion	Model statistics					
		p	LOF	R^2	Adj. R^2	Pred. R^2	Adequate Precision
Quadratic	suggested	0.0154	0.1053	0.9348	0.7827	-1.5430	9.218
RCM	p value	0.0005	0.4250	0.9530	0.8825	0.7139	14.764
RCM	AICc	0.0010	0.1277	0.8362	0.7270	0.3694	9.192
RCM	BIC	0.0009	0.8926	0.9776	0.9254	0.8356	16.878
RCM	Adj. R^2	0.0007	0.5536	0.9661	0.9032	0.8548	16.132
RQM	p value	0.0008	0.1701	0.8760	0.7746	0.4114	10.528
RQM	AICc	0.0010	0.1277	0.8362	0.7270	0.3694	9.192
RQM	BIC	0.0011	0.2284	0.9199	0.8219	0.6811	10.813
RQM	Adj. R^2	0.0011	0.2284	0.9199	0.8219	0.6811	10.813

5.3. Model analysis

The obtained reduced cubic model (RCM) in terms of coded factors for the sulphur removal in the tyre-derived oil can be expressed according to Equation (5-1). This model shows the relationship between the dependent variable (sulphur removal) and the independent variables. In Equation (5-1), the synergetic and antagonistic effects are represented by the positive and negative signs that appear before the linear terms respectively. Equation (5-1) can predict the sulphur removal for particular levels of each factor, in which case the factors' low and high levels are coded as −1 and +1 respectively. Moreover, this equation can aid to identify the relative impact of the factors through the comparison of factor coefficients.

$$S_{removal} = 81.46 + 5.27A + 1.46B + 4.89C - 4.06D - 8.77AB + 1.21AC - 3.73AD - 6.50BD + 6.37CD - 6.01A^2 - 6.51B^2 - 1.64C^2 - 2.79D^2 - 6.75A^2C \quad \textbf{(5-1)}$$

Equation (5-2) shows the expression for the sulphur removal in terms of actual factors, and it can be used to make predictions about the sulphur removal for given levels of each factor. In this case, the specification of the levels should be in the original units for each factor. Equation (5-2) cannot be used

to determine the relative impact of each factor since the coefficients have been scaled to accommodate the units of each factor and the intercept is not at the central point of the design space.

$$S_{removal} = +493.69281 - 155.90802 * \mathrm{HCOOH} + 56.17528 * \mathrm{H_2O_2} - 11.72384 * \text{Temperature} - 2.49638 * \text{Reaction time} - 1.46212 * \mathrm{HCOOH} * \mathrm{H_2O_2} + 3.47424 * \mathrm{HCOOH} * \text{Temperature} - 0.12433 * \mathrm{HCOOH} * \text{Reaction time} - 0.32492 * \mathrm{H_2O_2} * \text{Reaction time} + 0.15925 * \text{Temperature} * \text{Reaction time} + 9.45315 * \mathrm{HCOOH}^2 - 1.62743 * {\mathrm{H_2O_2}}^2 - 0.10280 * \text{Temperature}^2 - 0.027904 * \text{Reaction time}^2 - 0.18743 * \mathrm{HCOOH}^2 * \text{Temperature} \quad \textbf{(5-2)}$$

The ANOVA results for the sulphur removal in the tyre-derived oil are presented in Table 5-4. These results are based on the reduced cubic model obtained after model reduction. The F-value of the model is 18.72 which means that the model is significant, in the sense that there is only a 0.09 % chance that an F-value of this magnitude could be due to noise. Table 5-4, shows that the significant model terms are A, C, D, AB, BD, CD, A^2, B^2, D^2 and A^2C since the p-values for each of these terms is less than 0.05. On the other hand, B, AC, AD and C^2 model terms are not significant since the p-values in these cases are greater than 0.1. It is important, however, to note that the hierarchical factor B (H_2O_2), which is among the insignificant model terms is involved in more than one significant interactions.

The number of significant model terms outweighs the non-hierarchical insignificant terms, which implies that the model fits well the experimental data. Moreover, the lack of fit (LOF) F-value of 0.12 shows its insignificance in comparison with pure error i.e. there is an 89.26 % possibility that such a large F-value for the LOF could be because of noise. The insignificant LOF implies that the model fits well. The coefficient of determination, R^2 value of 0.9776 implies that the empirical model could explain the over 97.76 % of the data deviation, an indication of statistical significance of the regression model. The obtained adjusted R^2 value of 0.9254 indicates that the correlation between the experimental and predicted responses is high. In addition, the difference of less than 0.2 between the adjusted R^2 = 0.9254 and predicted R^2 = 0.8356 indicates that the two coefficient of determination values were in reasonable agreement. The adequate precision, which is the measure of the signal to noise ratio was 16.878 (>4), a desirable value with an adequate signal. This, therefore, implies that the model can be applied for design space navigation.

Table 5-4: ANOVA for the CCD of the reduced cubic model for sulphur removal

Source	SS	DF	MS	F-value	p-value	Remarks
Model	3435.2	14	245.37	18.72	0.0009	significant
A-HCOOH	157.35	1	157.35	12	0.0134	
B-H_2O_2	12.1	1	12.1	0.92	0.3737	
C-Temperature	135.14	1	135.14	10.31	0.0183	
D-Reaction time	93.02	1	93.02	7.1	0.0373	
AB	255.02	1	255.02	19.46	0.0045	
AC	11.62	1	11.62	0.89	0.3828	
AD	46.1	1	46.1	3.52	0.1099	
BD	139.93	1	139.93	10.68	0.0171	
CD	324.62	1	324.62	24.77	0.0025	
A^2	540.64	1	540.64	41.25	0.0007	
B^2	633.28	1	633.28	48.31	0.0004	
C^2	40.43	1	40.43	3.08	0.1296	
D^2	116.36	1	116.36	8.88	0.0247	
A^2C	150.88	1	150.88	11.51	0.0146	
Residual	78.65	6	13.11			
Lack of Fit	4.34	2	2.17	0.12	0.8926	not significant
Pure Error	74.3	4	18.58			
Correction total	3513.85	20				

R^2 = 0.9776, adjusted R^2 = 0.9254, predicted R^2 = 0.8356, adequate precision = 16.878

5.4. Diagnostics plots

The plot of predicted sulphur removal versus experimental values is presented in Figure 5-1. It can be seen that there is a good agreement (R^2 = 0.9776) between the predicted and actual sulphur removal, an indication that the model is adequate and significant, and thus can perfectly be used to reproduce the experimental data in the range studied.

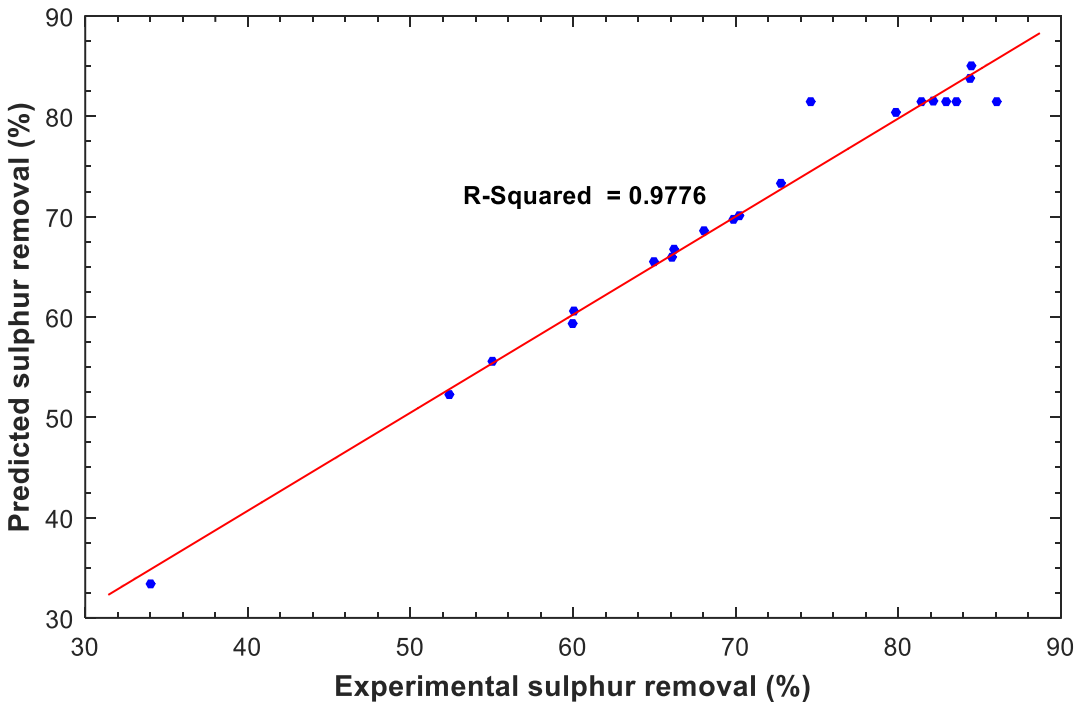

Figure 5-1: Plot of predicted versus experimental sulphur removal.

Figure 5-2 shows the plot of externally studentized residuals against the run number whereas Figure D-1 (Appendix D) shows the corresponding plot for internally studentized residuals. There is a random dispersal of residuals around the line, which is also an indication of the adequacy of the reduced cubic model (Figure 5-2).

Figure 5-3 presents the normal probability plot of the externally studentized residuals while its corresponding plot for internally studentized residuals is presented in Figure D-2 (Appendix D). There is a consistent appearance of the data points obtained on a linear trendline (Figure 5-3), which signifies the absence of obvious dispersal, and that the residuals are normally distributed.

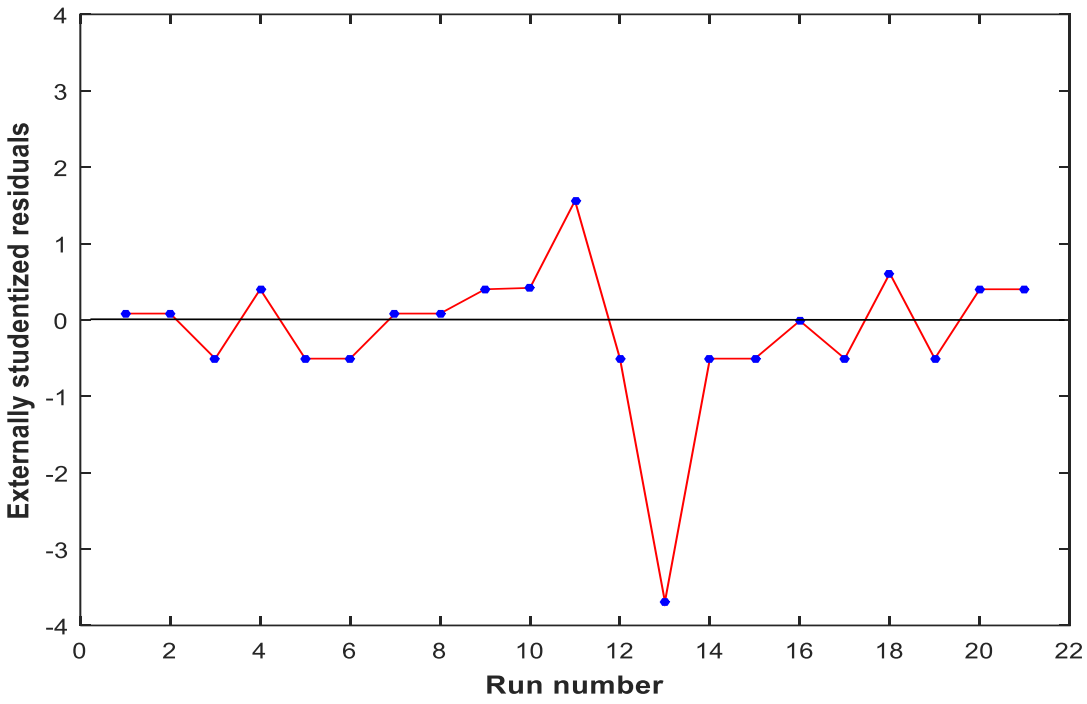

Figure 5-2: Plot of externally studentized residuals versus run number.

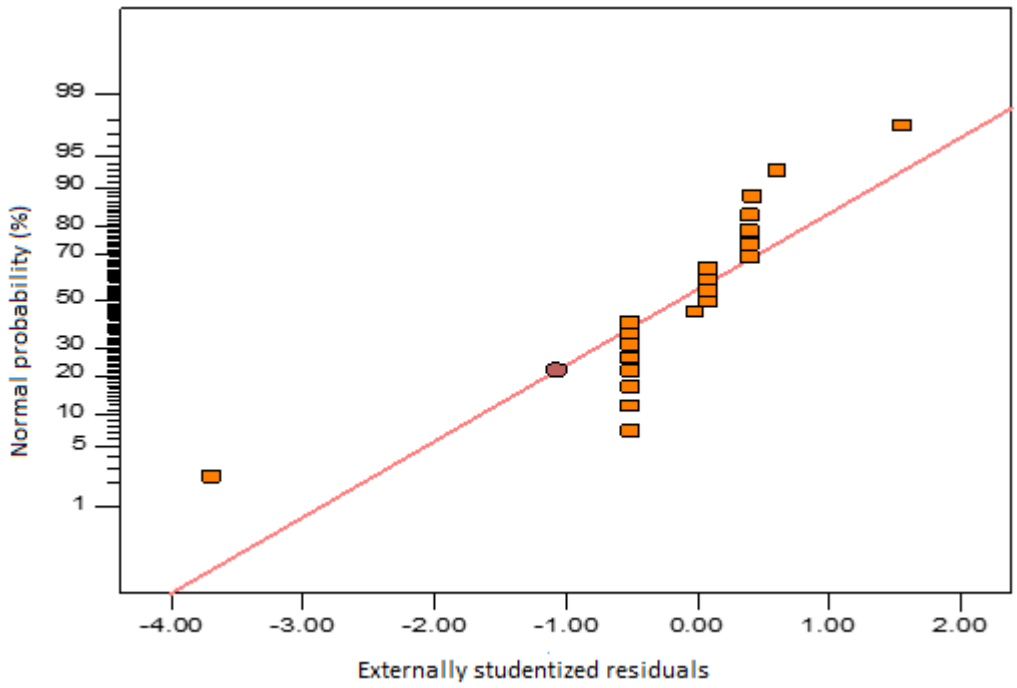

Figure 5-3: Normal probability plot of externally studentized residuals.

The plot of externally studentized residuals against the predicted sulphur removal is presented in Figure 5-4 while the plot of internally studentized residuals versus the predicted values is shown in Figure D-3 (Appendix D).

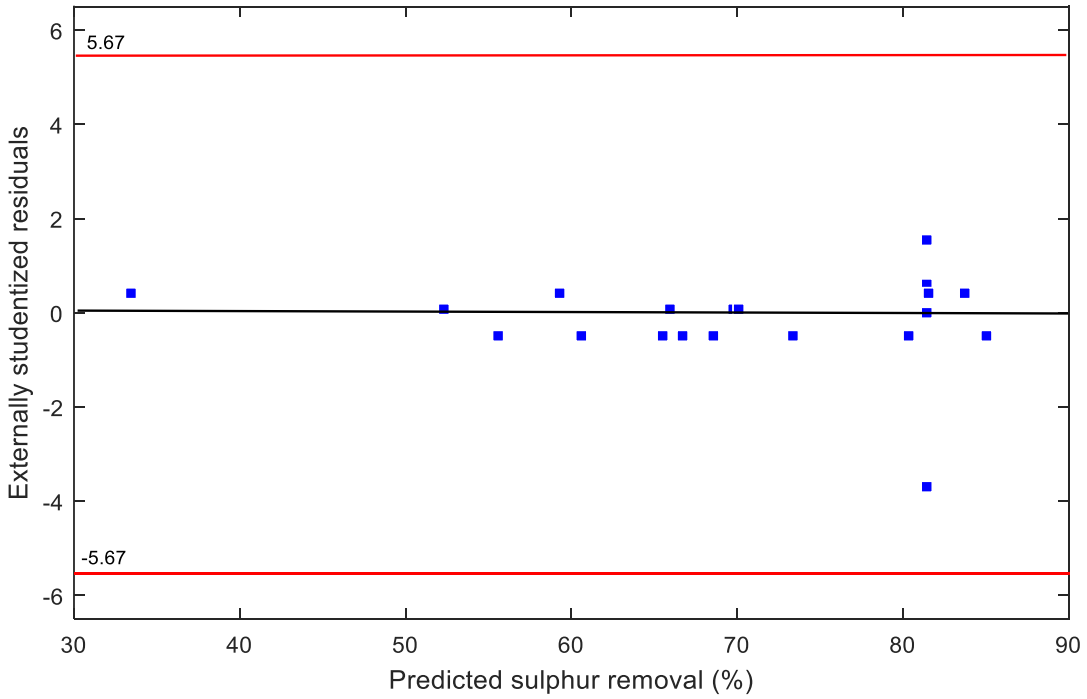

Figure 5-4: Plot of externally studentized residuals versus predicted values

5.5. Influence statistics

The influence statistics values provide potential or actual measures of the influence of individual runs. The plots give a clearer perspective of outliers. Cook's distance shows the magnitude of change of the overall regression function when the i^{th} point is excluded in model fitting. It is fundamentally the summation of prediction differences at each point occasioned by exclusion of a point in fitting the model. Leverage is a measure of the magnitude of influence of each point on the model fit. A leverage value of one at a given point indicates that the model precisely fits the observation at that particular point. If a run has a leverage that is more than twice the average value (ratio of sum total of terms in the model to runs number in the design), then it is commonly considered to have high leverage, and such a run hardly has other runs close to it within the factor space.

Difference in Fits (DFFITS), which has a relation and close similarity with externally studentized residuals (Montgomery et al., 2012), indicates the magnitude of the change in prediction at the i^{th} point in the event of its non-inclusion in model fitting (Belsley et al., 2005). Despite the differences in raw values resulting from DFFITS and Cook's distance, a closed-form formula for inter-conversion of

these values exists (Cohen et al., 2013). The larger the absolute value of DFFITS, the greater the influence it has on the fitted model. On the other hand, DFBETAS is a measure of the extent of change in a coefficient estimate if the i^{th} point is not included for fitting the model (Myers, 1990; Stat-Ease, 2005).

The plot for Cook's distance versus the run number is shown in Figure 5-5. It can be seen that there were no values outside of the red line limit value of one, an indication of absence of outliers and that none of the runs would create an influential change in the model if excluded.

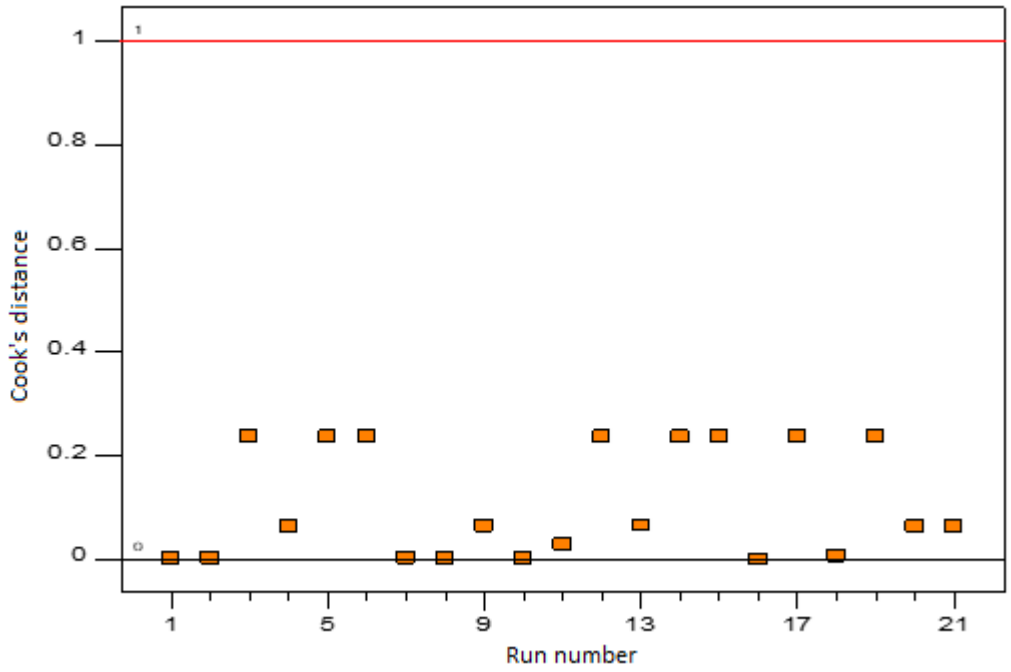

Figure 5-5: Plot of Cook's distance versus run number

The plot for DFFITS versus the run number is shown in Figure 5-6. None of the data points has an absolute DFFITS value above 2.53546 or below −2.53546, and thus it can be concluded that there is no influential point that would change the prediction if not included in fitting the model.

The plots for leverage and DFBETAS versus run are presented in Figure D-4 and Figure D-5 in Appendix D respectively. Table D-1 (Appendix D), on the other hand presents the overall model diagnostics as well as the values of the influence statistics.

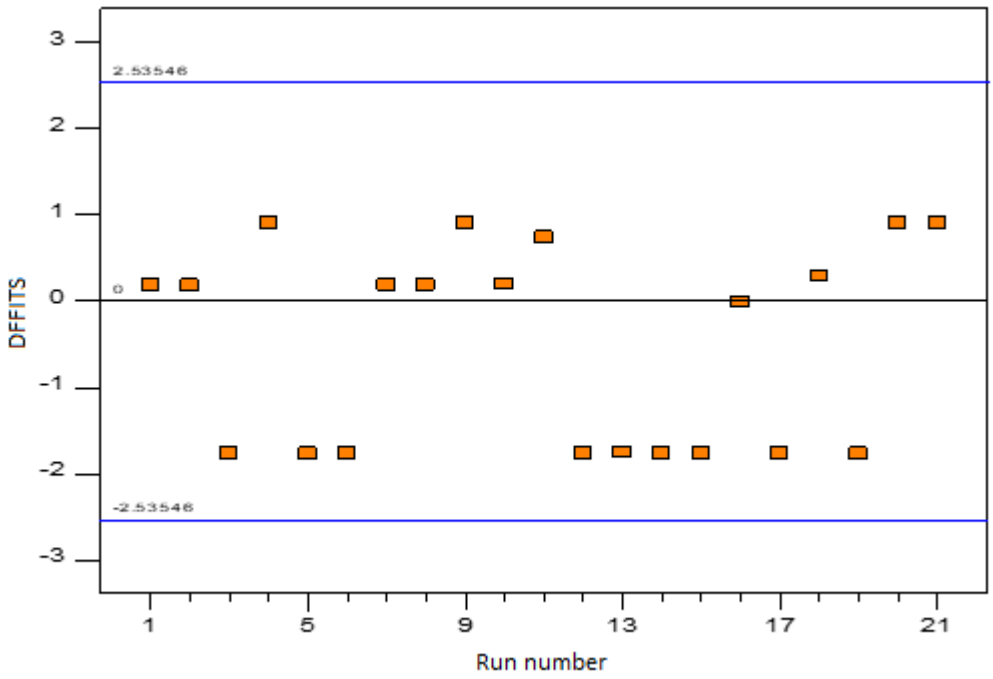

Figure 5-6: Plot of DFFITS versus run number

5.6. Perturbation plots and interaction graphs

The perturbation plot showing the sulphur removal as a function of all factors on one graph is presented in Figure 5-7. This plot indicates the behaviour of change of the response as each factor deviates from the selected point of reference, with the other remaining factors being constant at the reference value. The reference point in this case is set at the design space mid-point i.e. the coded zero level of each factor. The perturbation, therefore, shows how the factorial level deviates from the modified reference point of all the factors.

It can be seen that, formic acid amount (A), hydrogen peroxide amount (B), Temperature (C) and reaction time (D) are the parameters involved in the control of sulphur removal in the tyre-derived oil (Figure 5-7). The sharpness of the formic acid and temperature curvatures is an indication of high sensitivity of sulphur removal to these two factors. The reaction time showed a slightly sharper curvature than the hydrogen peroxide amount (flattest of all factors), which indicates that it had more influence on sulphur removal than hydrogen peroxide amount. However, the influence of the reaction time on sulphur removal was lower compared to that of either the amount of formic acid or temperature.

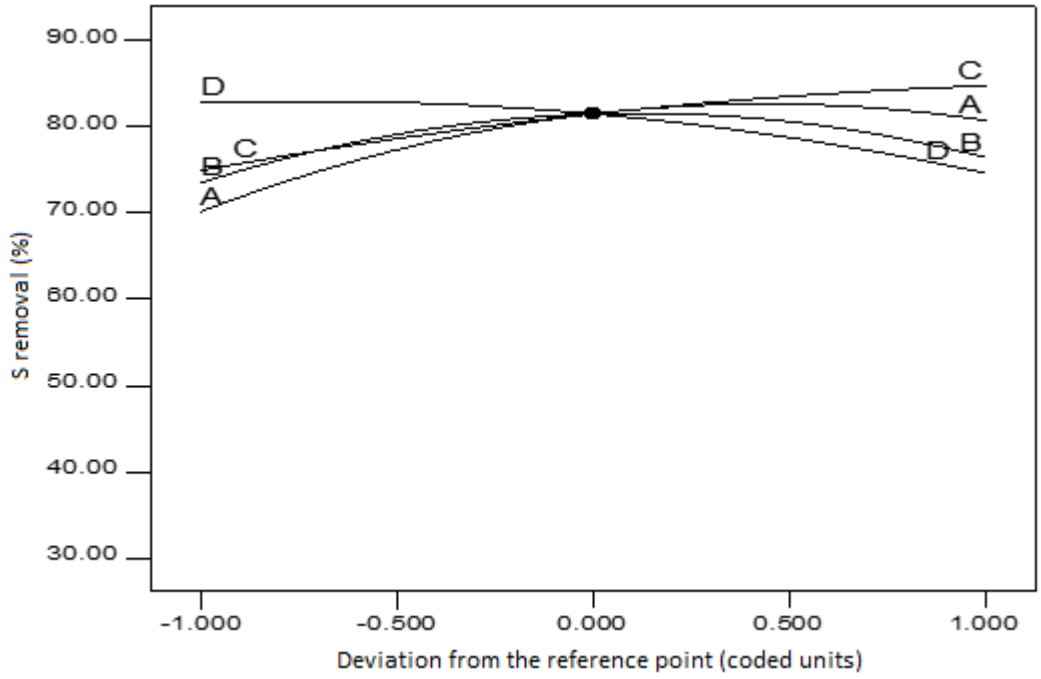

Figure 5-7: Plot of perturbation of the four parameters

The two-factor interaction plots for AB (formic acid and hydrogen peroxide), AC (formic acid and temperature) and CD (temperature and reaction time) at mid-level points of the other two factors are presented in Figures 5-8, 5-9 and 5-10 respectively.

Least-significant-difference (LSD) bars in the interaction graphs are used to determine if a difference between two means exists. The bar height is dependent on the design, confidence level and model. The LSD can aid in testing for a significant difference in predictions if a significant overall model result is obtained from ANOVA. The interaction plots indicate the average LSD I-beams around the predictions. There is a high likelihood of significant differences in predictions if there is no overlapping of the I-beams (Stat-Ease, 2005).

Figure 5-8 indicates that there is a significant difference between the two hydrogen peroxide amount levels when the formic acid amount is set at either low (6 mL) or high (12 mL) level. This is because the LSD bars do not overlap in this case.

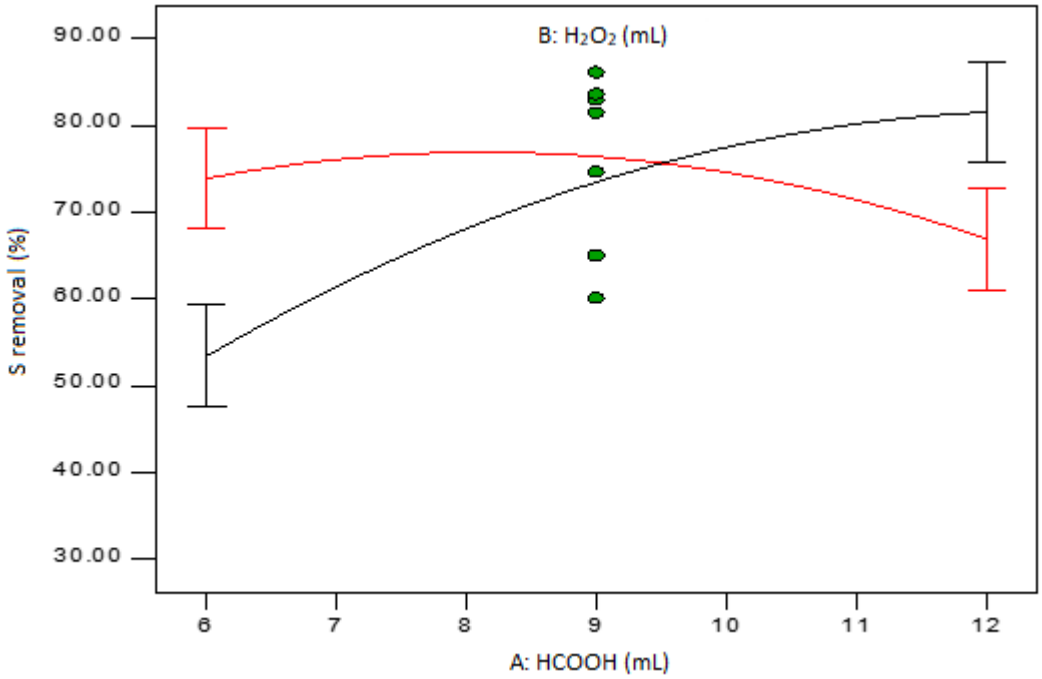

Figure 5-8: Interaction plot of formic acid and hydrogen peroxide amounts at mid-level temperature and reaction time

On the other hand, Figure 5-9, as evidenced by overlapping LSD bars at both ends, shows that there is not a significant difference in the two temperature levels when the formic acid amount is set at either low or high level.

The interaction between the temperature and reaction time (Figure 5-10) indicates that at low temperature (50 °C) level, the reaction time presents a significant difference in its low and high levels. The case is different when temperature is set at high (58 °C) level, where, as justified by the overlapping LSD bars, there is not a significant difference in reaction time levels.

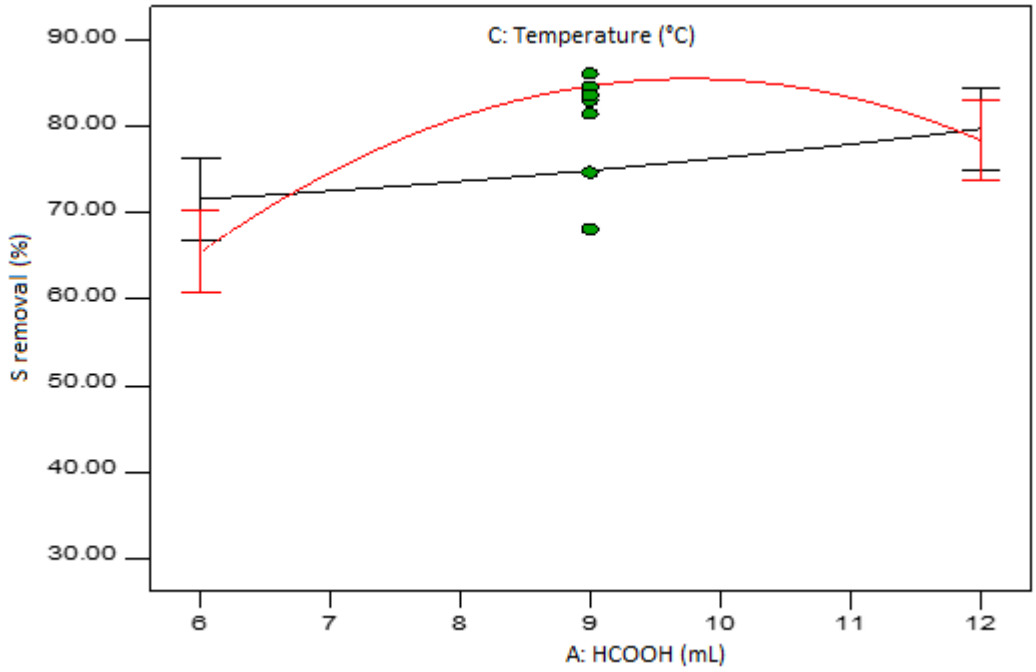

Figure 5-9: Interaction plot of formic acid and temperature at mid-level reaction time and hydrogen peroxide amount

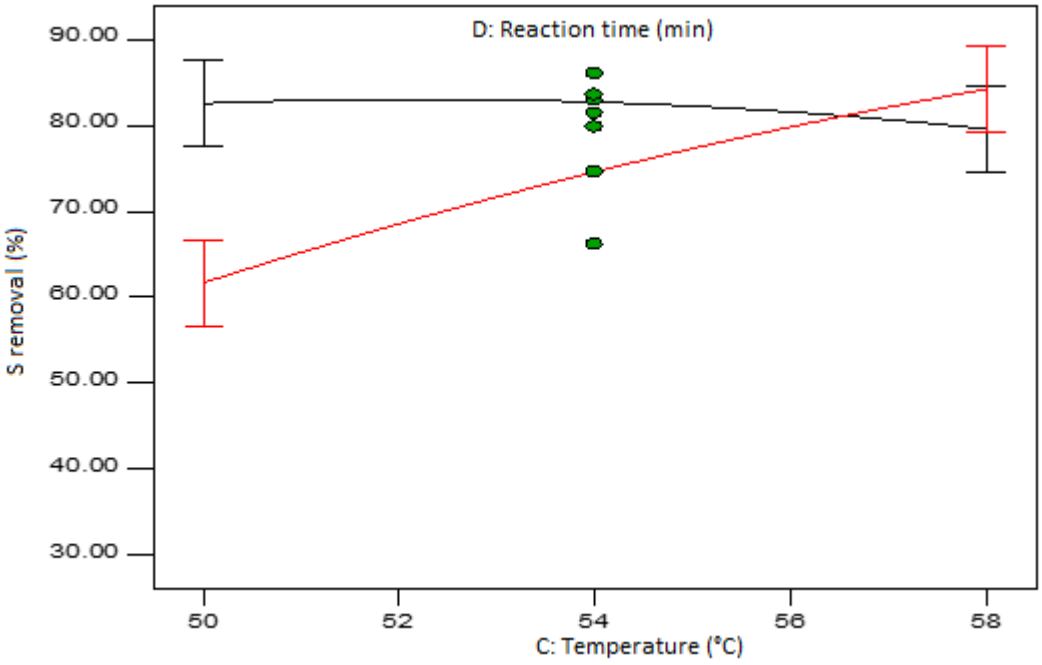

Figure 5-10: Interaction plot of temperature and reaction time at mid-level formic acid and hydrogen peroxide amounts

5.7. Response surface plots

Since there was interaction of parameters during the ODS process, sulphur reduction could not be analysed as a function of each individual factor. Contour and 3D response surface plots were used to show the effect two given factors on the response (sulphur reduction) at mid-level values of the other two factors. The mid-level slice points included the five centre points as denoted by the dot at the centre of the contour plots. Replication of the centre points improves the prediction power at the middle of the experimental range. The response surface plots of factor interactions presented are those of AB, AC, AD, BD and CD (Figures 5-11 to 5-20)

Figure 5-11 and 5-12 show the 3D and contour response surface plots of sulphur removal variation with formic acid and hydrogen peroxide at mid-level temperature of T = 54 °C and reaction time of 50 min. It is evident from Figures 5-11 and 5-12 that the interaction between the two factors (formic acid and hydrogen peroxide) significantly affects the sulphur removal. The highest values of sulphur removal were achieved at formic acid amount of between 9-12 mL and the corresponding hydrogen peroxide amount of between 6.0-9 mL. As the amount of formic acid increases from 6 to 12 mL, the sulphur removal is enhanced. On the other hand, the sulphur removal increases as the hydrogen peroxide amount increases from 6 to about 9 mL, beyond which the sulphur removal begins to decrease. Sulphur removal of 83.04 % was achieved at an approximate combination of 11 mL and 7.5 mL of formic acid and hydrogen peroxide respectively.

The results of sulphur removal as per parameters used in Figures 5-11 and 5-12 differ from that (53 %) obtained by Al-Lal et al. (2015) in which the oxidative desulphurisation experiment was performed using 14 mL of formic acid and 6 mL of hydrogen peroxide. This variation could be as result of different temperatures used as well as the use of different solvents during extraction. In another study conducted by Chen et al. (2010), sulphur removal of 27.5 % was achieved by applying ultrasound-assisted oxidative desulphurisation and using hydrogen peroxide as an oxidant and a transition metal catalyst before subsequent acetonitrile extraction. This sulphur removal value differs from the ones in the present study, probably due to the use of a different catalyst.

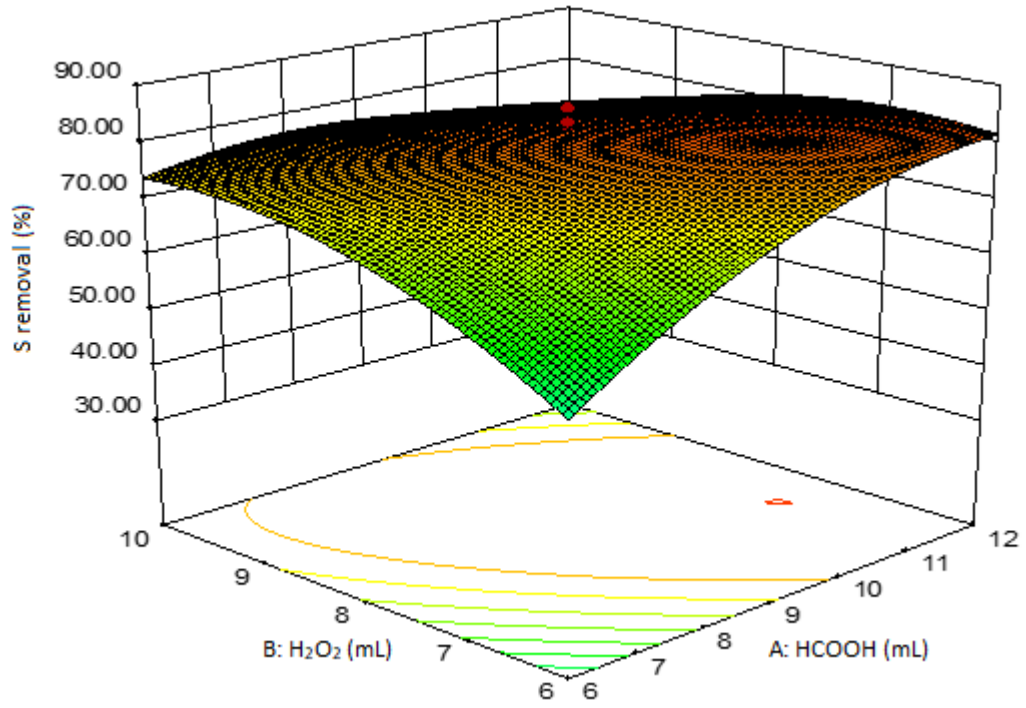

Figure 5-11: Response surface 3D plot of sulphur removal as a function of HCOOH and H_2O_2; T = 54 °C, reaction time = 50 min.

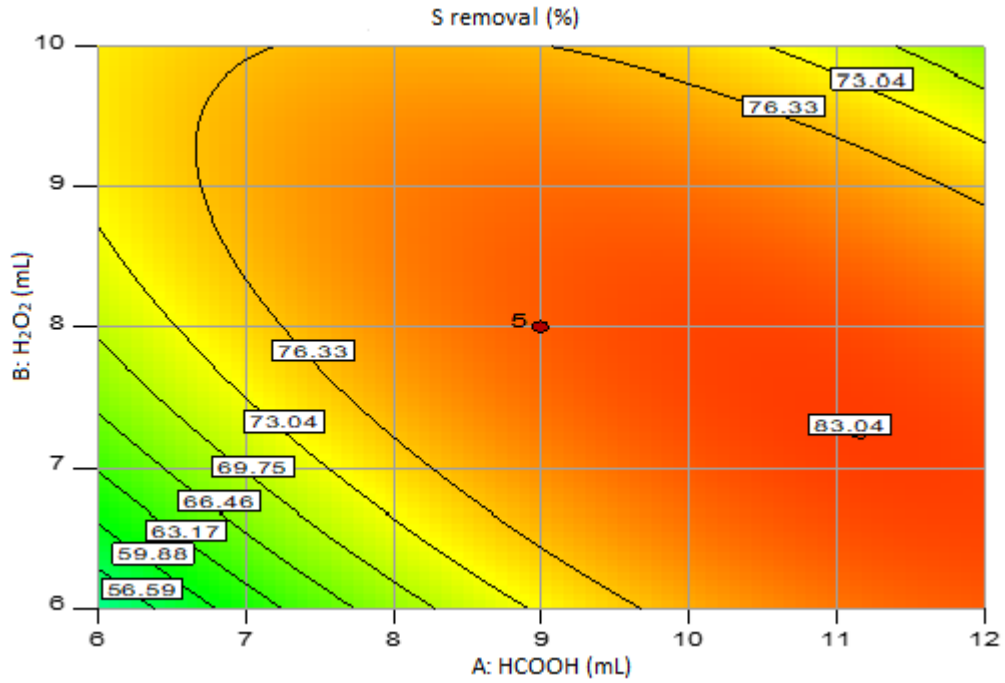

Figure 5-12: Response surface contour plot of sulphur removal as a function of HCOOH and H_2O_2; T = 54 °C, reaction time = 50 min.

The Response surface 3D and contour plots of sulphur removal as a function of formic acid and temperature at mid-level points of H_2O_2 = 8 mL and reaction time = 50 min are shown in Figures 5-13 and 5-14 while Figures 5-15 and 5-16 show the response surface plots of sulphur removal as a function of formic acid and reaction time at mid -level H_2O_2 = 8 mL and T = 54 °C. It can be seen in Figures 5-13 to 5-16, that there is a similar trend of the effect of formic acid amount on sulphur removal as that observed in Figures 5-11 and 5-12. The interaction of factors in the former, however, is not as significant as that observed in the later.

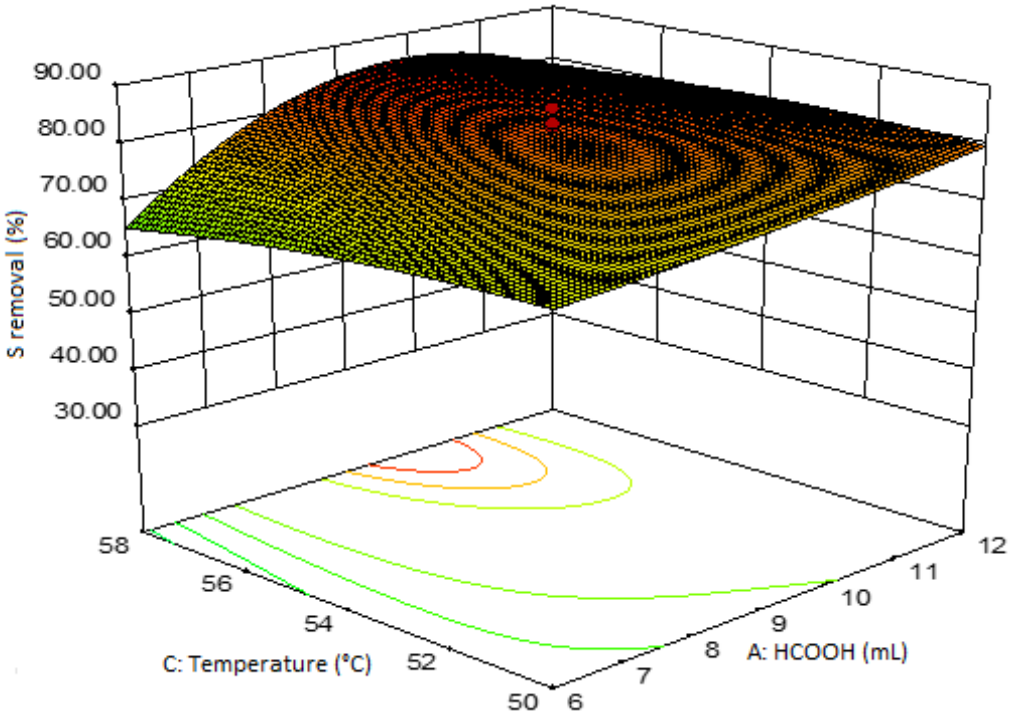

Figure 5-13: Response surface 3D plot of sulphur removal as a function of HCOOH and temperature; H_2O_2 = 8 mL, reaction time = 50 min.

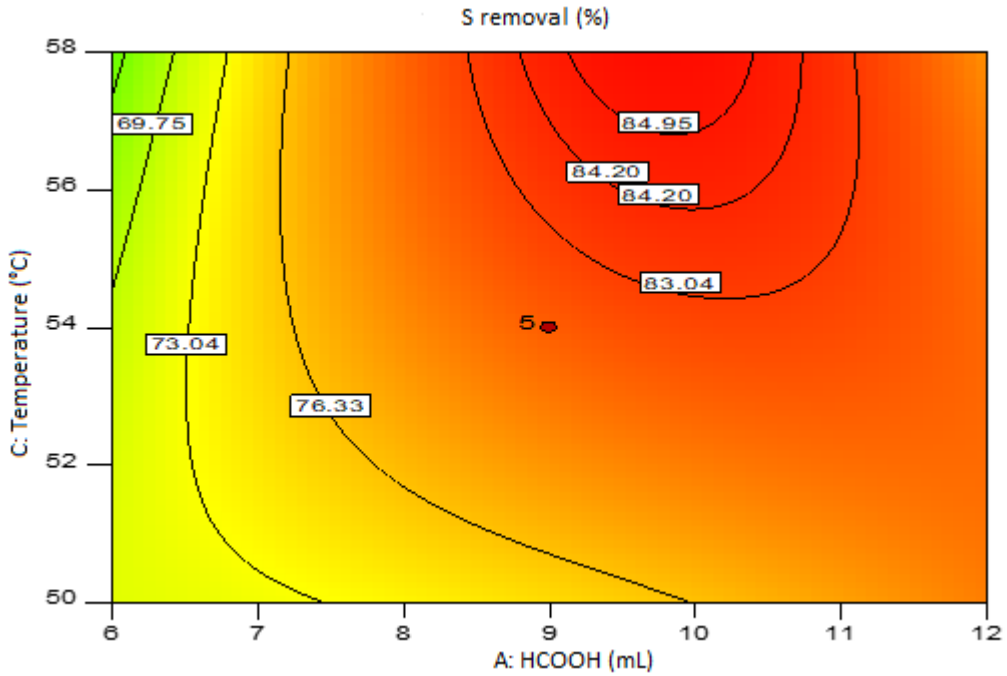

Figure 5-14: Response surface contour plot of sulphur removal as a function of HCOOH and temperature; H_2O_2 = 8 mL, reaction time = 50 min.

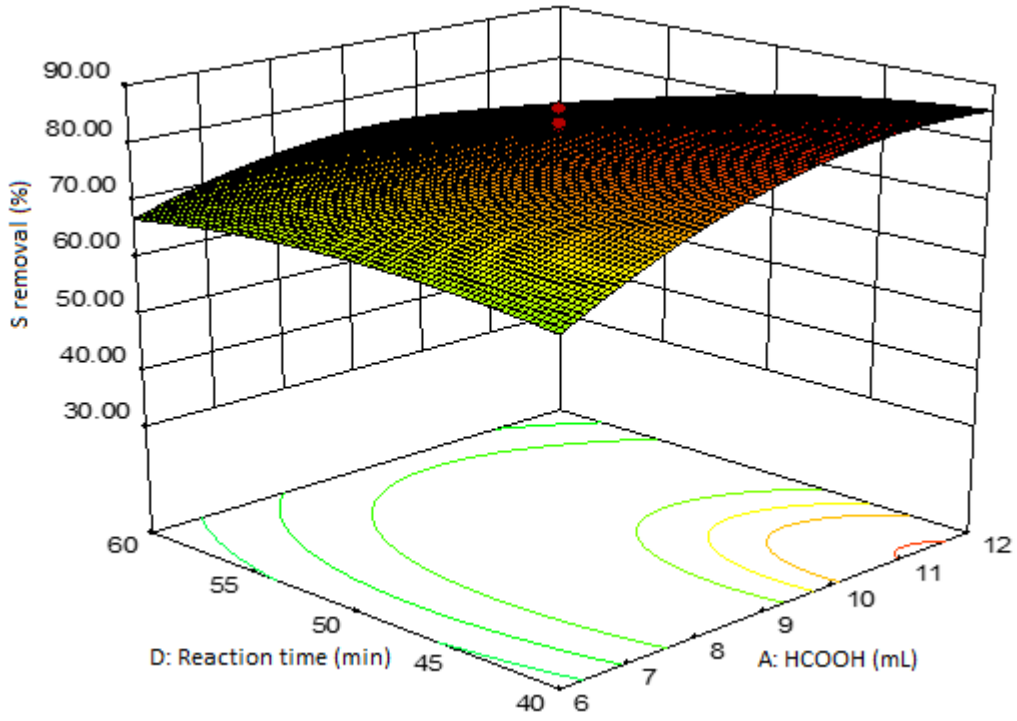

Figure 5-15: Response surface 3D plot of sulphur removal as a function of HCOOH and reaction time; H_2O_2 = 8 mL, T = 54 °C.

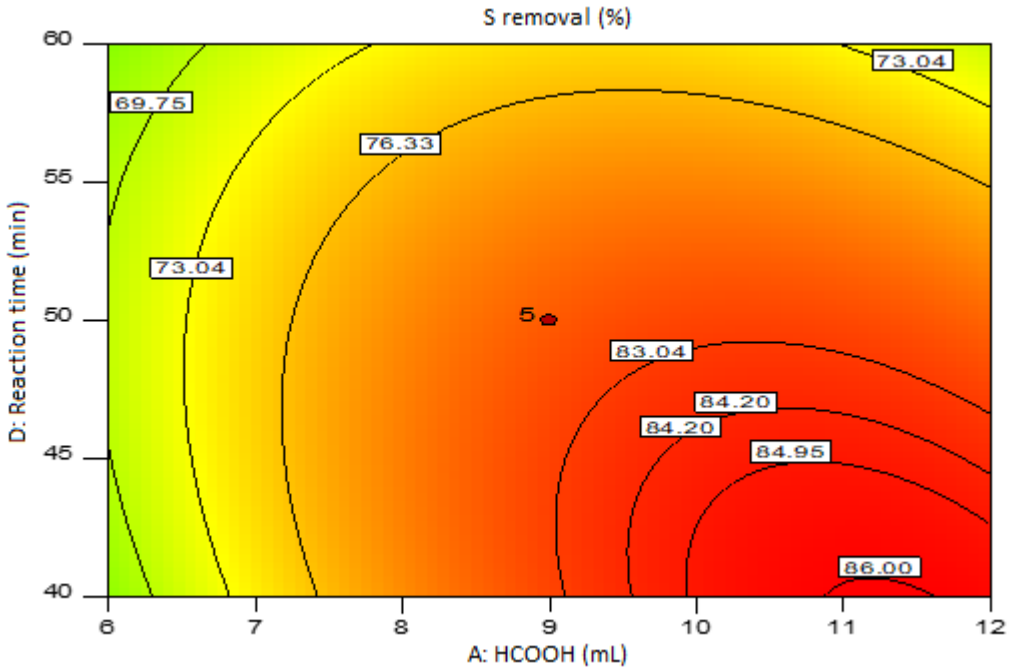

Figure 5-16: Response surface contour plot of sulphur removal as a function of HCOOH and reaction time; H_2O_2 = 8 mL, T = 54 °C.

Figures 5-17 and 5-18 present the response surface 3D and contour plots of sulphur removal as a function of hydrogen peroxide and reaction time at middle levels of HCOOH = 9 mL and T = 54 °C. It can be deduced from Figures 5-17 and 5-18 that there is a significant interaction between the amount of hydrogen peroxide and reaction time. The highest sulphur removal values were observed at reaction times of between 40-45 minutes and the corresponding hydrogen peroxide amount of between 7.5-9.5 mL. For example, at reaction time of 40 minutes and an approximate hydrogen peroxide amount of 9 mL, sulphur removal of 84.95 % could be achieved.

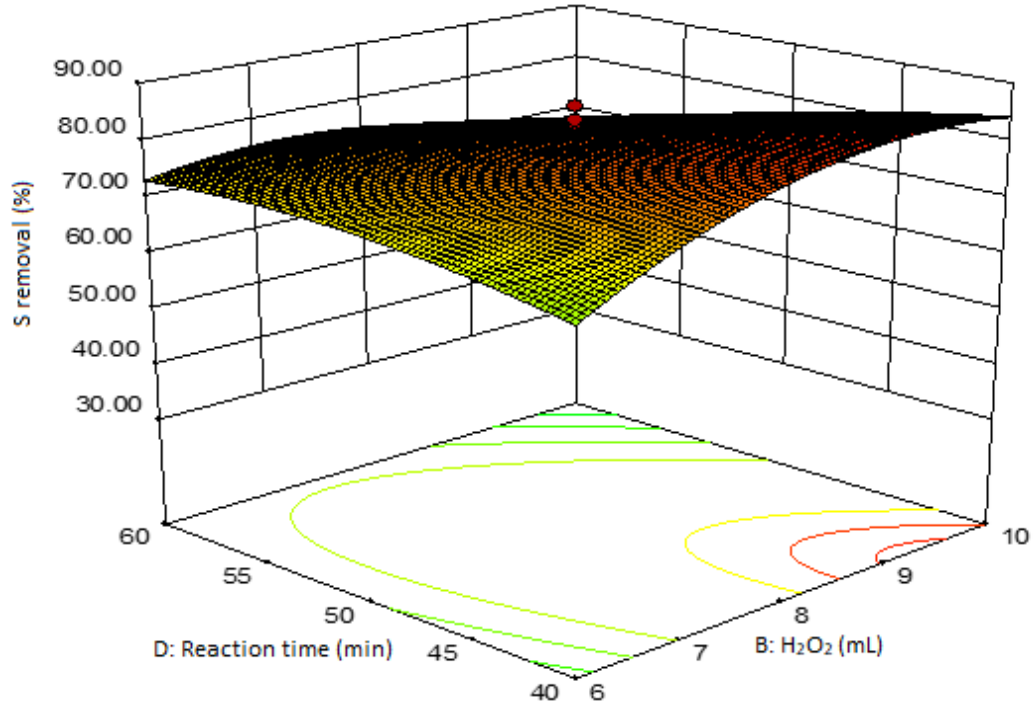

Figure 5-17: Response surface 3D plot of sulphur removal as a function of H_2O_2 and reaction time; HCOOH = 9 mL, T = 54 °C.

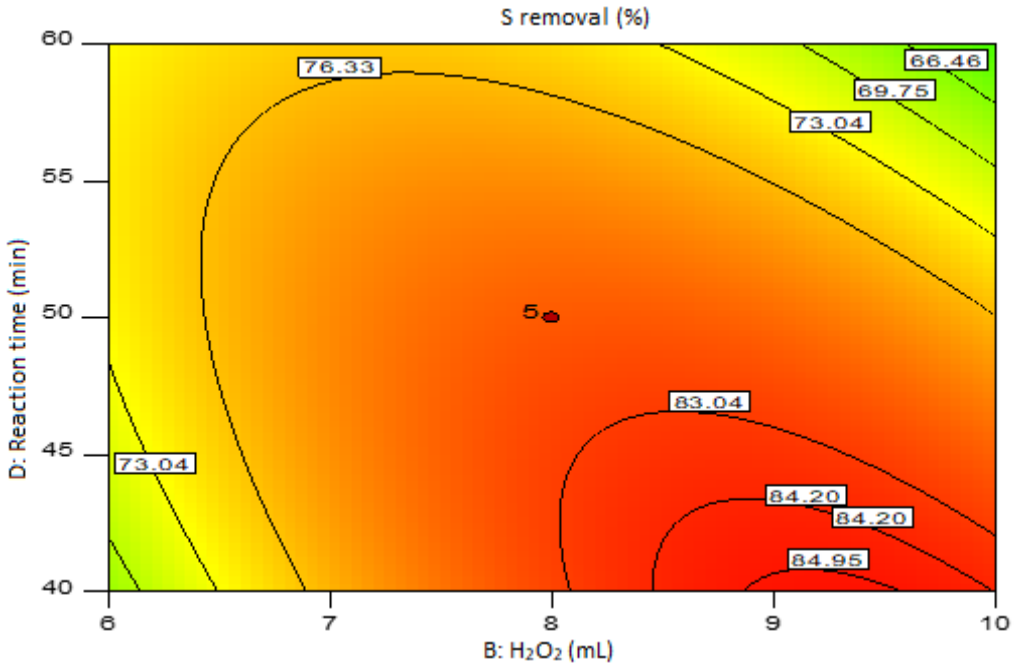

Figure 5-18: Response surface contour plot of sulphur removal as a function of H_2O_2 and reaction time; HCOOH = 9 mL, T = 54 °C

The response surface 3D and contour plots of sulphur removal as a function of temperature and reaction time at mid-level slice points of HCOOH = 9 mL and H_2O_2 = 8 mL are shown in Figures 5-19 and 5-20. There is, clearly, a significant interaction between the temperature and reaction time with regard to sulphur removal. The highest sulphur removal in this case was achieved at low to mid reaction times and low to high levels of temperature. With increasing temperature from low levels to high levels, the sulphur removal is enhanced, with the maximum sulphur removal (84.20 %) being achieved at about T = 57 °C and reaction time of between 45-60 minutes. At higher temperatures, the increase in reaction time appeared not to have an effect on the sulphur removal. This is because, at higher temperatures, the conversion of sulphur-containing compounds in the tyre-derived oil to sulphones and sulphoxides is achieved much faster. A similar trend was observed in a study carried out by Al-Lal et al. (2015), in which longer reaction times had little impact on the sulphur removal.

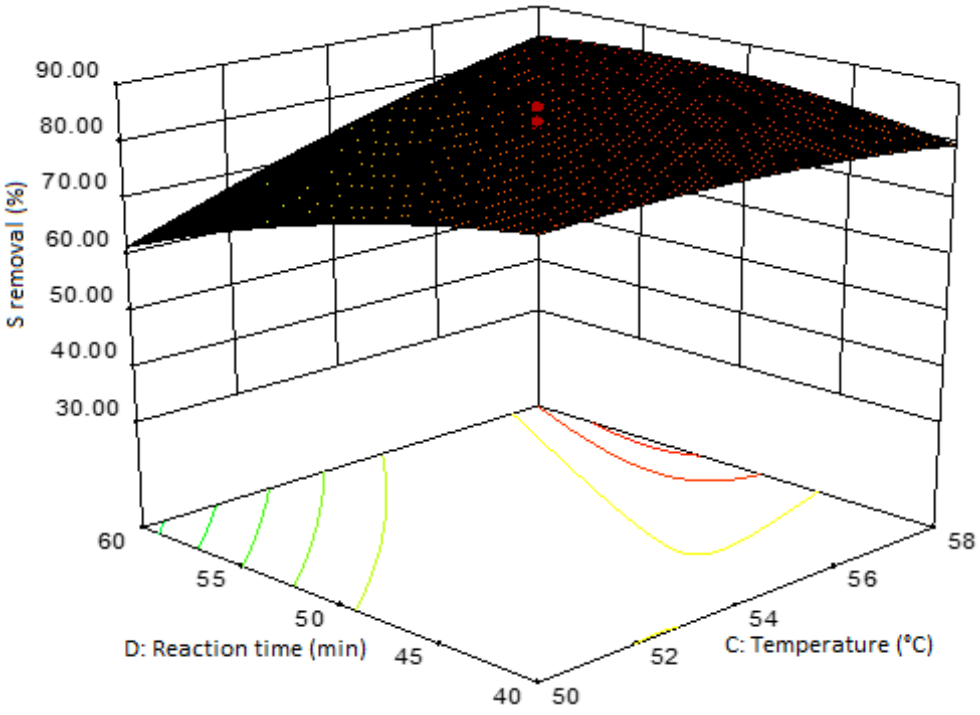

Figure 5-19: Response surface 3D plot of sulphur removal as a function of temperature and reaction time; HCOOH = 9 mL, H_2O_2 = 8 mL.

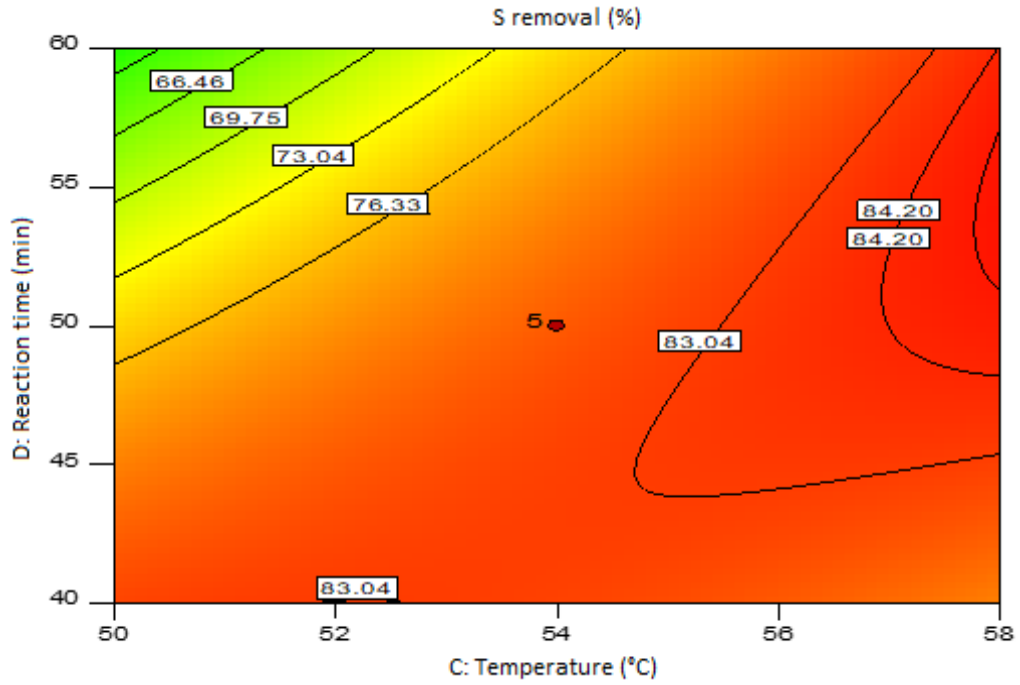

Figure 5-20: Response surface contour plot of sulphur removal as a function of temperature and reaction time; HCOOH = 9 mL, H_2O_2 = 8 mL.

5.8. Optimisation of the ODS process

Numerical optimisation was used to determine the optimal conditions for sulphur removal in the TDO. The optimisation method used by Design-Expert® Software is based on a technique developed by Derringer and Suich (1980), and its description can be found in (Myers et al., 2009). The parameters' goals were set to be within the range of the design space while the goal of the response was set to 'maximise', with lower and upper limits of 85 and 90 respectively. Under the aforementioned optimisation criteria, the ramps results (with a response desirability of one) shown in Figure 5-21 were obtained. Formic acid amount of 11.96 mL, hydrogen peroxide amount of 7.56 mL, reaction temperature of 50.1 °C and reaction time of 40.7 min could be used to achieve a 90.18 % sulphur removal in the waste tyre oil. In addition, a desirability value of one is an indication of an ideal case for the sulphur removal. Figure 5-22 shows the desirability bar graph of the input variables and the response (sulphur removal) while the optimisation criteria is presented in Table 5-5. The starting points for optimisation and solutions from optimisation are presented in Table D-2 and Table D-3 respectively.

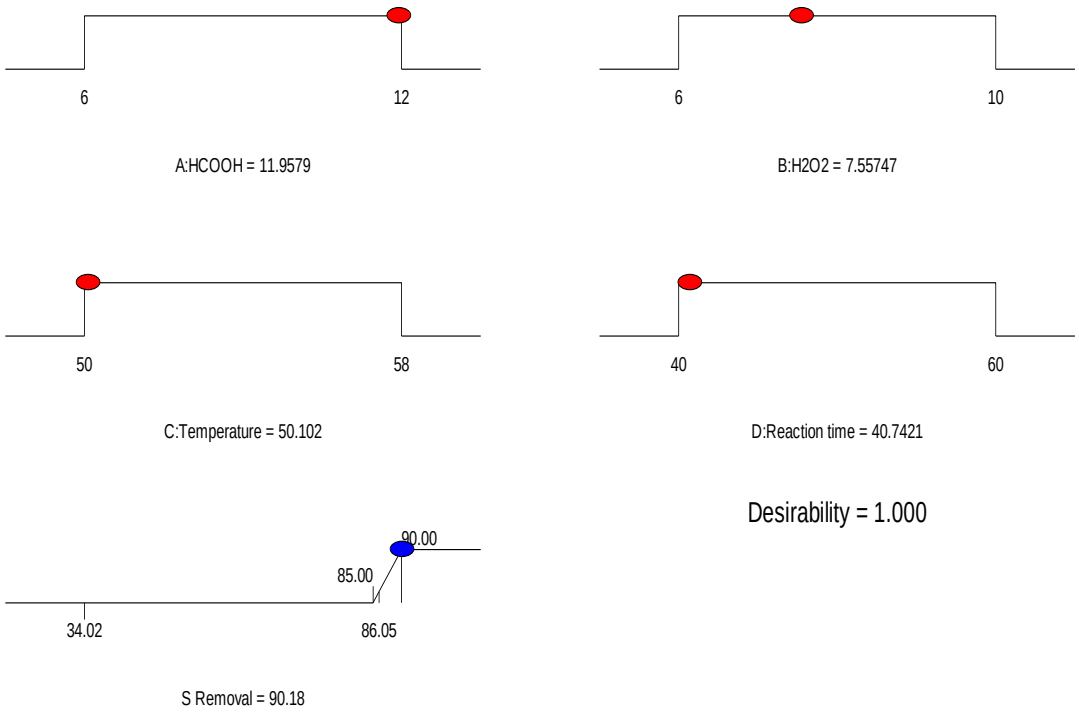

Figure 5-21: Predicted numerical optimisation ramps for targeted sulphur removal.

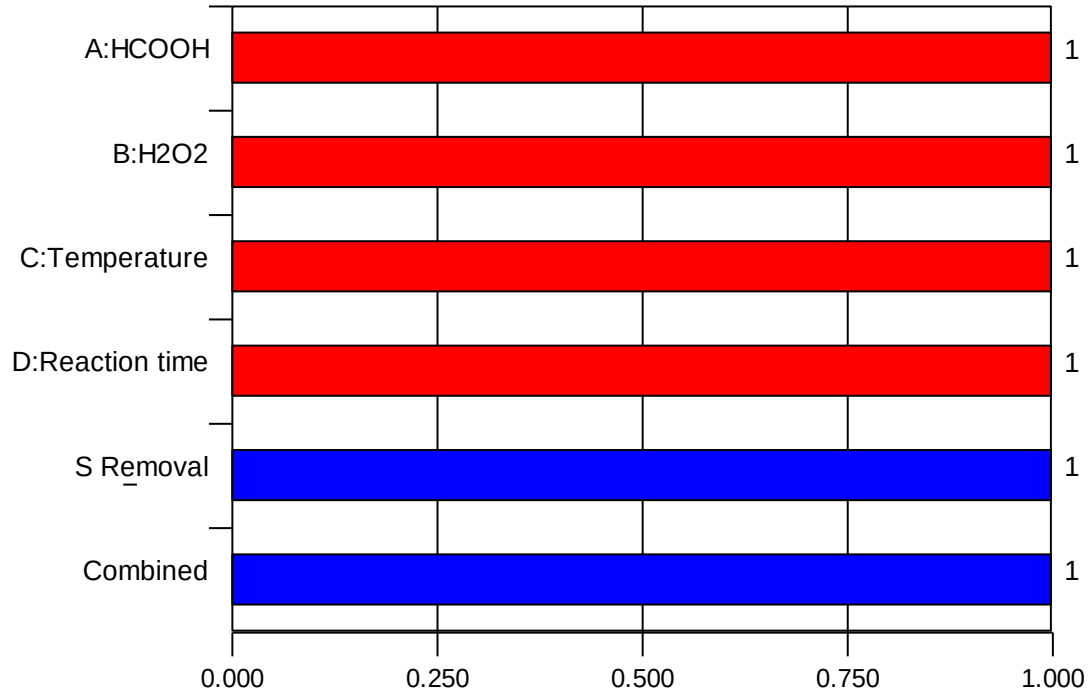

Figure 5-22: Desirability bar graph of parameters investigated

Table 5-5: Optimisation criteria

Name	Goal	Lower Limit	Upper Limit	Lower Weight	Upper Weight	Importance
A:HCOOH	in range	6	12	1	1	3
B:H_2O_2	in range	6	10	1	1	3
C:Temperature	in range	50	58	1	1	3
D:Reaction time	in range	40	60	1	1	3
S Removal	maximize	85	90	1	1	5

CHAPTER SIX

6. Conclusions and future work

Pyrolysis of waste tyres provides an avenue for obtaining products with high calorific value such as pyrolysis oil. Information on pyrolysis of waste tyres with investigation of the effects of different parameters and product yields exists in literature. In addition, some work on thermogravimetric analysis of waste tyres has also been carried out by different researchers. There is, however, no trace of data in literature on the application of non-isothermal models to kinetically model the waste tyre pyrolysis process. This research gap was the motivation behind one of the main objectives of the present research.

On the other hand, the sulphur content in oils obtained via the pyrolysis of waste tyres is high. This limits its application in real combustion processes owing to high levels of toxic emissions. Oxidative desulphurisation is considered a complementary technology for deep desulphurisation of fuels. Studies on sulphur removal in tyre-derived oils via oxidative desulphurisation have previously been conducted by various researchers. However, in most of these studies, the key parameters that could have huge influence on the oxidative desulphurisation process were kept constant during the experiments. This research, therefore, sought to investigate the interaction of parameters during the oxidative desulphurisation of tyre-derived oil. In addition, the optimisation of the ODS process was performed.

The conclusions and suggested future work for both the kinetic modelling of waste tyre pyrolysis and the oxidative desulphurisation of tyre-derived oil are subsequently presented in following subsections of this chapter.

6.1. Kinetic modelling of scrap tyre pyrolysis

In view of the objective to carry out the kinetic study of the waste tyre pyrolysis process, the thermogravimetric analysis was carried out at four heating rates of 2, 5, 10, and 20 °C min^{-1} in the presence of nitrogen. The ultimate analysis of the tyre crumb used for the thermogravimetric experiments revealed that the carbon, hydrogen, nitrogen and sulphur contents were 83.54, 7.55, 0.35 and 1.84 wt.% respectively. The oxygen content was 6.73 wt.%, while the proximate analysis indicated that the volatile matter content was approximately 64 wt.%. The thermogravimetric data obtained was loaded into three models (KAS, FWO and FR) to determine the activation energies associated with the tyre crumb pyrolysis. In addition, in order to determine the pre-exponential factors, model-fitting Coats-Redfern method was used.

The thermogravimetric analysis revealed that the thermal decomposition of the tyre crumb started at about 270 °C and 285 °C and was complete at about 460 °C and 475 °C for the rates of 2 °C min^{-1} and

5 °C min^{-1} respectively. At temperature ramp rates of 10 and 20 °C min^{-1}, the decomposition started at about 290 °C and 315 °C and was complete at about 480 °C and 500 °C respectively. For all the heating rates, there was no further weight loss above the temperature of 500 °C. From DTG thermograms, it was noted that the pyrolysis of the tyre crumb involved three stages i.e. the removal of lubricants and oil in the scrap tyre, breakdown of natural rubber, and breakdown of butadiene rubber and styrene-butadiene rubber. It was also observed that the peak temperatures increase with increasing heating rates during the entire three-stage thermal decomposition process.

Degrees of conversion ranging between $\alpha = 0.1$-0.9 were considered during the application the KAS, FWO and FR models. The degrees of conversion below 0.1 and above 0.9 were excluded due to low correlation coefficients. The average values of activation energies obtained were 206.01, 206.08 and 204.82 kJ mol^{-1} using KAS, FWO and FR models respectively. The values of E_a obtained indicate that results from the three models were in agreement, with a deviation of below 1% between values from KAS and FWO models. The average E_a obtained using the FR model was slightly lower than the values obtained using the KAS and FWO models. The kinetic analysis shows that the activation energy is highly dependent on the extent of conversion, which is an indication that the tyre crumb thermal degradation is a complex process that involves various reactions at different stages. For each of the three models (KAS, FWO and FR), it was observed that there is a sharp increase in activation energy with change in conversion degree from 0.1 to 0.2. The activation energies then almost remain unchanged in the conversion degree range of 0.2-0.3. The activation energies slightly drop as the conversion changes from 0.3 to 0.4, after which there is a continuous increase in E_a up to $\alpha = 0.9$. The high coefficient of determination values (0.9830 for KAS model, 0.9847 for FWO model and 0.9831 for FR model) is a confirmation that the models fitted well the TGA data and therefore can reliably be used for prediction of activation energies associated with the pyrolysis of scrap tyres.

The activation energies from the FWO model were used to conduct the goodness-of-fit tests in order to establish the relationship between the activation energy and the extent of conversion. Results of the test indicate that the interdependence of activation energy and the degree of conversion for the tyre crumb pyrolysis process conforms to a sixth degree polynomial relationship. The sixth degree polynomial presented the smallest difference between the R^2 and adjusted R^2 compared with the results of the rest of the goodness-of-fit tests. The trend followed by the FWO was representative of the trends followed when the activation energies from KAS and FR models were used for goodness-of-fit tests.

Using the activation energies obtained from the FWO model, the Coats-Redfern method was applied in order to determine the pre-exponential factors at various degrees of conversion for the four heating rates. The data was tested for three reaction models i.e. F1, F2 and F3. The F2 model presented higher regression coefficient values than the F1 and F3 models. From the analysis of the plots of the three reaction models, it was concluded that the pyrolysis of the tyre crumb can best be described by the

second order reaction, F2. The pre-exponential factors were, therefore, determined from the Coats-Redfern F2 reaction order plot. Results indicated that the average pre-exponential factors obtained were 2.68E+08, 4.14E+09, 4.03E+10 and 6.16E+09 min^{-1} for the heating rates of 2, 5, 10 and 20 °C min^{-1} respectively, giving an overall mean pre-exponential factor of 1.27E+10 min^{-1}. In addition, it was observed that at a given conversion degree, the pre-exponential factors generally increased with heating rates. However, there was a drop in the pre-exponential factors as the heating rate changed from 10 to 20 °C min^{-1} for all conversion degrees.

Surface fitting of the conversion degrees, pre-exponential factors and activation energies was done by applying the least squares method. In all the surface fitting tests, the values of R^2 and adjusted R^2 were equal to unity. The results showed that the first degree polynomial for both x and y inputs (poly 11) was the best fit for the data loaded, while the tests for polynomials above the second degree polynomial yielded poorly conditioned results.

The kinetic data obtained from this study could play an important role in the design and optimisation of industrial scale scrap tyre pyrolysis units. The kinetic parameters (E_a and A) can provide vital information for the design of reactors and achievement of the best operating conditions for scrap tyre pyrolysis plants. The findings from the present kinetic study could provide an insight for the improvement of the general operability of scrap tyre thermal conversion processes via pyrolysis.

6.2. Oxidative desulphurisation of tyre-derived oil

The oxidative desulphurisation of tyre-derived oil was studied by incorporating the central composite design of the response surface methodology. In order to achieve this objective, the interaction of the amount of formic acid, amount hydrogen peroxide, reaction time and temperature were investigated using the CCD small design. In addition, three different solvent extraction scenarios were used during the extraction of the oxidised tyre-derived oils. The three solvent extraction cases were 1:1 acetonitrile to TDO ratio, 1:2 acetonitrile to TDO ratio and 1:1 NN-dimethylformamide to TDO ratio.

The sulphur removal was in the range of 34.02 to 86.05 % for the various factor interactions using 1:1 acetonitrile to TDO ratio, while sulphur removal values ranging from 27.91 to 52.77 % were achieved using 1:2 acetonitrile to TDO ratio. On the other hand, using a 1:1 dimethylformamide to TDO ratio during the extraction, the lowest and highest sulphur removal percentages were 3.80 and 35.00 % respectively. The highest sulphur removal was achieved in the case when 1:1 acetonitrile to TDO ratio was used during the solvent extraction of the oxidised oils. The results from this case were, therefore, used further to model the oxidative desulphurisation process of the tyre-derived oil.

Preliminary results of model fitting suggested that the quadratic model is a better predictor of the sulphur removal during the oxidative desulphurisation. However, a negative predicted R^2 value meant that the overall mean was in fact a better predictor of the sulphur removal than the suggested model. In order to improve the performance of the model in terms of sulphur removal predictability, model reduction using various criteria was performed. The results of model reduction yielded a reduced cubic model, which was used for further analysis and modelling of the oxidative desulphurisation of the tyre-derived oil.

The ANOVA results of the reduced cubic model revealed that the p-value was 0.0009 (< 0.05), an indication that the model is significant with only a 0.09 % chance that the F-value associated with this p-value could be due to noise. The significance of the model was further justified by a high value of p (0.8926) for the model's lack-of-fit. The coefficient of determination value of 0.9776 implies that the empirical model could explain the over 97.76 % of the data deviation, an indication of statistical significance of the regression model. Moreover, an adjusted R^2 of 0.9254 indicates that the correlation between the experimental and predicted responses is high. The difference of less than 0.2 between the adjusted R^2 = 0.9254 and predicted R^2 = 0.8356 indicates that the two regression coefficient values were in reasonable agreement. Lastly, the adequate precision of 16.878 (> 4) was a desirable value with an adequate signal, implying that the model can be applied for design space navigation.

Since there was interaction of parameters during the oxidative desulphurisation, sulphur reduction could not be analysed as a function of each individual factor. Contour and 3D response surface plots were used to show the effect of two given factors on sulphur reduction at mid-level values of the other two factors. The 3D and contour response surface plots of the sulphur removal variation with formic acid and hydrogen peroxide at mid-level temperature of T = 54 °C and reaction time of 50 min indicated that the highest values of sulphur removal were achieved at formic acid amount of between 9-12 mL and the corresponding hydrogen peroxide amount of between 6.0-9 mL. As the amount of formic acid increased from 6 to 12 mL, the sulphur removal was enhanced. On the other hand, the sulphur removal increased as the hydrogen peroxide amount increased from 6 to about 9 mL, beyond which the sulphur removal started to decrease.

Numerical optimisation was performed in order to determine the optimal conditions for sulphur removal in the tyre-derived oil. The parameters' goals were set to be within the range of the design space while the goal of the response was set to 'maximise', with lower and upper limits of 85 and 90 respectively. The optimisation results showed that formic acid amount of 11.95 mL, hydrogen peroxide amount of 7.56 mL, reaction temperature of 50.1 °C and reaction time of 40.7 min could be used to achieve a 90.18 % sulphur removal in the tyre-derived oil.

In summary, the findings from the oxidative desulphurisation of tyre-derived oil obtained from this research can play a key role in minimising the levels of emission during the combustion of oils obtained from the pyrolysis of waste tyres. In addition, the knowledge from the present study could be useful in commercialisation of efficient sulphur removal technology in tyre-derived oils, which can then be blended with other fuels such as diesel for use in real combustion processes.

6.3. Recommendation for future work

This research was devoted toward the kinetic study of scrap tyre pyrolysis and the modelling approach of oxidative desulphurisation of tyre-derived oil.

The suggested future work on kinetic modelling of the scrap tyre pyrolysis process could involve carrying out the thermogravimetric experiments at higher heating rates. The thermogravimetric data can then be used for the kinetic study of the process using the non-isothermal approach. This investigation could provide an understanding of the behaviour of the kinetics at high heating rates. Narrower intervals of conversion degrees could be used in future work when applying the isoconversional models to investigate the effect of the change in intervals on the performance of the models.

The oxidative desulphurisation in the present research involved the use hydrogen peroxide and formic acid as part of the oxidation system. In future work, a different organic acid, such as acetic acid, could be used together with hydrogen peroxide as part of the oxidation system. This can be done by using the same design of experiments criteria as that used in the present study.

REFERENCES

Abdelouahed, L., Leveneur, S., Vernieres-Hassimi, L., Balland, L. and Taouk, B. (2017). Comparative investigation for the determination of kinetic parameters for biomass pyrolysis by thermogravimetric analysis. *Journal of Thermal Analysis and Calorimetry*: 1-13.

Aboulkas, A., El Harfi, K., Nadifiyine, M. and El Bouadili, A. (2008). Thermogravimetric characteristics and kinetic of co-pyrolysis of olive residue with high density polyethylene. *Journal of Thermal Analysis and Calorimetry*, 91 (3): 737-743.

Aguado, J., Serrano, D. and Escola, J. (2006). Catalytic upgrading of plastic wastes. *Feedstock Recycling and Pyrolysis of Waste Plastics: Converting Waste Plastics into Diesel and Other Fuels*: 73-110.

Aguado, R., Olazar, M., Vélez, D., Arabiourrutia, M. and Bilbao, J. (2005). Kinetics of scrap tyre pyrolysis under fast heating conditions. *Journal of Analytical and Applied Pyrolysis*, 73 (2): 290-298.

Ahmad, S. and Ahmad, M. I. (2013). Desulfurization of Oils; Produced from Pyrolysis of Scrap Tires. *NUST Journal of Engineering Sciences*, 6 (1): 27-32.

Aida, T. and Yamamoto, D. (1994). Annual Book of ASTM Standards, 2005. Standard test method for determination of sulfur compounds in natural gas and gaseous fuels by gas chromatography and chemilumi-nescence. *Prepr. Pap. Am. Chem. Soc., Div. Fuel Chem*, 39: 623.

Akahira, T. and Sunose, T. (1971). Joint convention of four electrical institutes. *Res Rep Chiba Inst Technol*, 16: 22-31.

Al-Lal, A.-M., Bolonio, D., Llamas, A., Lapuerta, M. and Canoira, L. (2015). Desulfurization of pyrolysis fuels obtained from waste: Lube oils, tires and plastics. *Fuel*, 150: 208-216.

Ali, M. F., Al-Malki, A. and Ahmed, S. (2009). Chemical desulfurization of petroleum fractions for ultra-low sulfur fuels. *Fuel Processing Technology*, 90 (4): 536-544.

Ali, M. F., Al-Malki, A., El-Ali, B., Martinie, G. and Siddiqui, M. N. (2006). Deep desulphurization of gasoline and diesel fuels using non-hydrogen consuming techniques. *Fuel*, 85 (10–11): 1354-1363.

Alvarez, R., Callén, M. S., Clemente, C., Díaz-Bautista, M. A., López, J. M., Mastral, A. M. and Murillo, R. (2004). Slagging in fluidized bed combustion of rubber tire. Inorganic component evolution. *Industrial & engineering chemistry research*, 43 (24): 7762-7767.

Anca-Couce, A., Berger, A. and Zobel, N. (2014). How to determine consistent biomass pyrolysis kinetics in a parallel reaction scheme. *Fuel*, 123: 230-240.

Arabani, M., Mirabdolazimi, S. and Sasani, A. (2010). The effect of waste tire thread mesh on the dynamic behaviour of asphalt mixtures. *Construction and Building Materials*, 24 (6): 1060-1068.

Arabiourrutia, M., Lopez, G., Elordi, G., Olazar, M., Aguado, R. and Bilbao, J. (2007). Product distribution obtained in the pyrolysis of tyres in a conical spouted bed reactor. *Chemical Engineering Science*, 62 (18-20): 5271-5275.

Aydın, H. and İlkılıç, C. (2012). Optimization of fuel production from waste vehicle tires by pyrolysis and resembling to diesel fuel by various desulfurization methods. *Fuel*, 102: 605-612.

Aylón, E., Callén, M. S., López, J. M., Mastral, A. M., Murillo, R., Navarro, M. V. and Stelmach, S. (2005). Assessment of tire devolatilization kinetics. *Journal of Analytical and Applied Pyrolysis*, 74 (1–2): 259-264.

Aylón, E., Fernández-Colino, A., Murillo, R., Navarro, M., García, T. and Mastral, A. (2010). Valorisation of waste tyre by pyrolysis in a moving bed reactor. *Waste Management*, 30 (7): 1220-1224.

Aylón, E., Fernández-Colino, A., Navarro, M., Murillo, R., García, T. and Mastral, A. (2008). Waste tire pyrolysis: comparison between fixed bed reactor and moving bed reactor. *Industrial & Engineering Chemistry Research*, 47 (12): 4029-4033.

Balkin, S. D. and Lin, D. K. (2000). A neural network approach to response surface methodology. *Communications in Statistics-Theory and Methods*, 29 (9-10): 2215-2227.

Banar, M., Akyıldız, V., Özkan, A., Çokaygil, Z. and Onay, Ö. (2012). Characterization of pyrolytic oil obtained from pyrolysis of TDF (Tire Derived Fuel). *Energy Conversion and Management*, 62: 22-30.

Barlaz, M. A., Eleazer, W. E. and Whittle, D. J. (1993). Potential to use waste tires as supplemental fuel in pulp and paper mill boilers, cement kilns and in road pavement. *Waste management & research*, 11 (6): 463-480.

Bartz-Beielstein, T., Lasarczyk, C. W. and Preuß, M. 2005. Sequential parameter optimization. In: Proceedings of *Evolutionary Computation, 2005. The 2005 IEEE Congress on*. IEEE, 773-780.

Bates, R., Buck, R., Riccomagno, E. and Wynn, H. (1996). Experimental design and observation for large systems. *Journal of the Royal Statistical Society. Series B (Methodological)*: 77-94.

Belsley, D. A., Kuh, E. and Welsch, R. E. (2005). *Regression diagnostics: Identifying influential data and sources of collinearity*. John Wiley & Sons.

Benallal, B., Roy, C., Pakdel, H., Chabot, S. and Poirier, M. A. (1995). Characterization of pyrolytic light naphtha from vacuum pyrolysis of used tyres comparison with petroleum naphtha. *Fuel*, 74 (11): 1589-1594.

Benazzouk, A., Douzane, O., Langlet, T., Mezreb, K., Roucoult, J. and Quéneudec, M. (2007). Physico-mechanical properties and water absorption of cement composite containing shredded rubber wastes. *Cement and Concrete Composites*, 29 (10): 732-740.

Berrueco, C., Esperanza, E., Mastral, F. J., Ceamanos, J. and García-Bacaicoa, P. (2005). Pyrolysis of waste tyres in an atmospheric static-bed batch reactor: Analysis of the gases obtained. *Journal of Analytical and Applied Pyrolysis*, 74 (1–2): 245-253.

Betancur, M., Martínez, J. D. and Murillo, R. (2009). Production of activated carbon by waste tire thermochemical degradation with CO 2. *Journal of Hazardous Materials*, 168 (2): 882-887.

Box, G. E. and Behnken, D. W. (1960). Some new three level designs for the study of quantitative variables. *Technometrics*, 2 (4): 455-475.

Box, G. E., Hunter, W. G. and Hunter, J. S. (1978). Statistics for experimenters.

Box, G. E. P. and Wilson, K. B. (1951). On the Experimental Attainment of Optimum Conditions. *Journal of the Royal Statistical Society*, 13 (1)

Brems, A., Baeyens, J., Beerlandt, J. and Dewil, R. (2011). Thermogravimetric pyrolysis of waste polyethylene-terephthalate and polystyrene: A critical assessment of kinetics modelling. *Resources, Conservation and Recycling*, 55 (8): 772-781.

Bridgwater, A. and Peacocke, G. (2000). Fast pyrolysis processes for biomass. *Renewable and Sustainable Energy Reviews*, 4 (1): 1-73.

Buche, D., Schraudolph, N. N. and Koumoutsakos, P. (2005). Accelerating evolutionary algorithms with Gaussian process fitness function models. *IEEE Transactions on Systems, Man, and Cybernetics, Part C (Applications and Reviews)*, 35 (2): 183-194.

Buekens, A. (1977). Some observations on the recycling of plastics and rubber. *Conservation & Recycling*, 1 (3-4): 247-271.

Buekens, A. (2006). Introduction to feedstock recycling of plastics. *Feedstock recycling and pyrolysis of waste plastics*, 6 (7): 1-41.

Buekens, A., White, R. L., Walendziewski, J., Lee, K.-H., Masuda, T., Tago, T., Manos, G., Yanik, J., Karayildirim, T. and Miskolczi, N. (2006). Feedstock recycling and pyrolysis of waste plastics: converting waste plastics into diesel and other fuels.

Bunthid, D., Prasassarakich, P. and Hinchiranan, N. (2010). Oxidative desulfurization of tire pyrolysis naphtha in formic acid/H2O2/pyrolysis char system. *Fuel*, 89 (9): 2617-2622.

Cai, J. and Bi, L. (2009). Kinetic analysis of wheat straw pyrolysis using isoconversional methods. *Journal of Thermal Analysis and Calorimetry*, 98 (1): 325.

Callén, M., Hall, S., Mastral, A., Garcia, T., Ross, A. and Bartle, K. (2000). PAH presence in oils and tars from coal–tyre coprocessing. *Fuel Processing Technology*, 62 (1): 53-63.

Campos-Martin, J., Capel-Sanchez, M. and Fierro, J. (2004). Highly efficient deep desulfurization of fuels by chemical oxidation. *Green Chemistry*, 6 (11): 557-562.

Castaldi, M. J., Kwon, E. and Weiss, B. (2007). Beneficial Use of Waste Tires: An Integrated Gasification and Combustion Process Design via Thermo-Gravimetric Analysis (TGA) of Styrene–Butadiene Rubber (SBR) and Poly-Isoprene (IR). *Environmental Engineering Science*, 24 (8): 1160-1178.

Chaala, A., Darmstadt, H. and Roy, C. (1996). Acid-base method for the demineralization of pyrolytic carbon black. *Fuel Processing Technology*, 46 (1): 1-15.

Chaala, A. and Roy, C. (1996). Production of coke from scrap tire vacuum pyrolysis oil. *Fuel Processing Technology*, 46 (3): 227-239.

Chang, Y.-M. (1996). On pyrolysis of waste tire: Degradation rate and product yields. *Resources, Conservation and Recycling*, 17 (2): 125-139.

Chen, F. and Qian, J. (2003). Studies of the thermal degradation of waste rubber. *Waste Management*, 23 (6): 463-467.

Chen, L., Guo, S. and Zhao, D. (2007). Oxidative Desulfurization of Simulated Gasoline over Metal Oxide-loaded Molecular Sieve1. *Chinese Journal of Chemical Engineering*, 15 (4): 520-523.

Chen, T.-C., Shen, Y.-H., Lee, W.-J., Lin, C.-C. and Wan, M.-W. (2010). The study of ultrasound-assisted oxidative desulfurization process applied to the utilization of pyrolysis oil from waste tires. *Journal of Cleaner Production*, 18 (18): 1850-1858.

Chen, T.-C., Shen, Y.-H., Lee, W.-J., Lin, C.-C. and Wan, M.-W. (2013). An economic analysis of the continuous ultrasound-assisted oxidative desulfurization process applied to oil recovered from waste tires. *Journal of Cleaner Production*, 39: 129-136.

Cheung, K.-Y., Lee, K.-L., Lam, K.-L., Chan, T.-Y., Lee, C.-W. and Hui, C.-W. (2011). Operation strategy for multi-stage pyrolysis. *Journal of Analytical and Applied Pyrolysis*, 91 (1): 165-182.

Clark, C., Meardon, K. and Russell, D. (1993). *Scrap tire technology and markets*. William Andrew Inc.

Coats, A. W. and Redfern, J. (1964). Kinetic parameters from thermogravimetric data. *Nature*, 201 (4914): 68-69.

Cohen, J., Cohen, P., West, S. G. and Aiken, L. S. (2013). *Applied multiple regression/correlation analysis for the behavioral sciences*. Routledge.

Collins, L., Downs, W., Gibson, E. and Moore, G. (1974). An evaluation of discarded tires as a potential source of fuel. *Thermochimica Acta*, 10 (2): 153-159.

Conesa, J. A., Font, R. and Marcilla, A. (1996). Gas from the pyrolysis of scrap tires in a fluidized bed reactor. *Energy & Fuels*, 10 (1): 134-140.

Conesa, J. A., Gálvez, A., Mateos, F., Martín-Gullón, I. and Font, R. (2008). Organic and inorganic pollutants from cement kiln stack feeding alternative fuels. *Journal of Hazardous Materials*, 158 (2): 585-592.

Conesa, J. A., Martin-Gullon, I., Font, R. and Jauhiainen, J. (2004). Complete study of the pyrolysis and gasification of scrap tires in a pilot plant reactor. *Environmental science & technology*, 38 (11): 3189-3194.

Cunliffe, A. and Williams, P. (1998a). Properties of chars and activated carbons derived from the pyrolysis of used tyres. *Environmental Technology*, 19 (12): 1177-1190.

Cunliffe, A. M. and Williams, P. T. (1998b). Composition of oils derived from the batch pyrolysis of tyres. *Journal of Analytical and Applied Pyrolysis*, 44 (2): 131-152.

Cunliffe, A. M. and Williams, P. T. (1999). Influence of process conditions on the rate of activation of chars derived from pyrolysis of used tires. *Energy & Fuels*, 13 (1): 166-175.

Cypres, R. and Bettens, B. (1989). Production of benzoles and active carbon from waste rubber and plastic materials by means of pyrolysis with simultaneous post-cracking. In: *Pyrolysis and gasification*. Elsevier Applied Science, London, 209-229.

Dai, X., Yin, X., Wu, C., Zhang, W. and Chen, Y. (2001). Pyrolysis of waste tires in a circulating fluidized-bed reactor. *Energy*, 26 (4): 385-399.

Damartzis, T., Vamvuka, D., Sfakiotakis, S. and Zabaniotou, A. (2011). Thermal degradation studies and kinetic modeling of cardoon (Cynara cardunculus) pyrolysis using thermogravimetric analysis (TGA). *Bioresource Technology*, 102 (10): 6230-6238.

Darmstadt, H., Roy, C. and Kaliaguine, S. (1995). Characterization of pyrolytic carbon blacks from commercial tire pyrolysis plants. *Carbon*, 33 (10): 1449-1455.

Daugaard, D. E. and Brown, R. C. (2003). Enthalpy for pyrolysis for several types of biomass. *Energy & Fuels*, 17 (4): 934-939.

de Godois Baroni, É., Tannous, K., Rueda-Ordóñez, Y. J. and Tinoco-Navarro, L. K. (2016). The applicability of isoconversional models in estimating the kinetic parameters of biomass pyrolysis. *Journal of Thermal Analysis and Calorimetry*, 123 (2): 909-917.

de Marco Rodriguez, I., Laresgoiti, M. F., Cabrero, M. A., Torres, A., Chomón, M. J. and Caballero, B. (2001). Pyrolysis of scrap tyres. *Fuel Processing Technology*, 72 (1): 9-22.

Dehkordi, A., Sobati, M. and Nazem, M. (2013). An experimental investigation on the oxidative desulfurization of kerosene feedstock. *Energy Sources, Part A: Recovery, Utilization, and Environmental Effects*, 35 (3): 226-234.

DeMarini, D. M., Lemieux, P. M., Ryan, J. V., Brooks, L. R. and Williams, R. W. (1994). Mutagenicity and chemical analysis of emissions from the open burning of scrap rubber tires. *Environmental science & technology*, 28 (1): 136-141.

Derringer, G. and Suich, R. (1980). Simultaneous optimization of several response variables. *Journal of quality technology*, 12 (4): 214-219.

Dharaskar, S. A., Varma, M. N., Shende, D. Z., Yoo, C. K. and Wasewar, K. L. (2013). Synthesis, characterization and application of 1-butyl-3 methylimidazolium chloride as green material for extractive desulfurization of liquid fuel. *The Scientific World Journal*, 2013

Dhir, S., Uppaluri, R. and Purkait, M. (2009). Oxidative desulfurization: Kinetic modelling. *Journal of Hazardous Materials*, 161 (2): 1360-1368.

Díez, C., Martínez, O., Calvo, L. F., Cara, J. and Morán, A. (2004). Pyrolysis of tyres. Influence of the final temperature of the process on emissions and the calorific value of the products recovered. *Waste Management*, 24 (5): 463-469.

Dodds, J., Domenico, W., Evans, D., Fish, L., Lassahn, P. and Toth, W. 1983. *Scrap tires: a resource and technology evaluation of tire pyrolysis and other selected alternate technologies*. EG and G Idaho, Inc., Idaho Falls (USA).

Doğan, O., Çelik, M. B. and Özdalyan, B. (2012). The effect of tire derived fuel/diesel fuel blends utilization on diesel engine performance and emissions. *Fuel*, 95: 340-346.

Doyle, C. (1961). Kinetic analysis of thermogravimetric data. *Journal of applied polymer science*, 5 (15): 285-292.

Dũng, N. A., Klaewkla, R., Wongkasemjit, S. and Jitkarnka, S. (2009). Light olefins and light oil production from catalytic pyrolysis of waste tire. *Journal of Analytical and Applied Pyrolysis*, 86 (2): 281-286.

Elbaba, I. F., Wu, C. and Williams, P. T. (2010). Catalytic pyrolysis-gasification of waste tire and tire elastomers for hydrogen production. *Energy & Fuels*, 24 (7): 3928-3935.

Eterigho, E. J. and Olutoye, M. A. (2008). Quality improvement of an acid treated fuel oil. *Leonardo Electronic Journal of Practices and Technologies*, 7 (12): 95-104.

European Tyre and Rubber Manufacturers' Association. *End-of-life tyres management report 2011*. Available: http://www.etrma.org/uploads/Modules/Documentsmanager/brochure-elt-2011-final.pdf (Accessed 23.08.2017).

Evans, A. and Evans, R. (2006). The composition of a tyre: typical components. *The Waste & Resources Action Programme*: 5.

Fabián-Mijangos, L. and Cedeño-Caero, L. (2010). V loading effect on V2O5/ZrO2 catalysts for oxidative desulfurization. *Industrial & Engineering Chemistry Research*, 50 (5): 2659-2664.

Fairburn, J. A., Behie, L. A. and Svrcek, W. Y. (1990). Ultrapyrolysis of n-hexadecane in a novel micro-reactor. *Fuel*, 69 (12): 1537-1545.

Faulkner, B. and Weinecke, M. (2001). Carbon black production from waste tires. *Minerals & metallurgical processing*, 18 (4): 215-220.

Fernández, A. M., Barriocanal, C. and Alvarez, R. (2012). Pyrolysis of a waste from the grinding of scrap tyres. *Journal of Hazardous Materials*, 203–204: 236-243.

Flynn, J. H. and Wall, L. A. (1966). A quick, direct method for the determination of activation energy from thermogravimetric data. *Journal of Polymer Science Part C: Polymer Letters*, 4 (5): 323-328.

Friedman, H. L. 1964. Kinetics of thermal degradation of char-forming plastics from thermogravimetry. Application to a phenolic plastic. In: Proceedings of *Journal of Polymer Science: Polymer Symposia*. Wiley Online Library, 183-195.

Galvagno, S., Casu, S., Casabianca, T., Calabrese, A. and Cornacchia, G. (2002). Pyrolysis process for the treatment of scrap tyres: preliminary experimental results. *Waste Management*, 22 (8): 917-923.

García-Gutiérrez, J. L., Fuentes, G. A., Hernández-Terán, M. E., García, P., Murrieta-Guevara, F. and Jiménez-Cruz, F. (2008). Ultra-deep oxidative desulfurization of diesel fuel by the Mo/Al2O3-H2O2 system: The effect of system parameters on catalytic activity. *Applied Catalysis A: General*, 334 (1–2): 366-373.

Gieré, R., Smith, K. and Blackford, M. (2006). Chemical composition of fuels and emissions from a coal+ tire combustion experiment in a power station. *Fuel*, 85 (16): 2278-2285.

Giugliano, M., Cernuschi, S., Ghezzi, U. and Grosso, M. (1999). Experimental evaluation of waste tires utilization in cement kilns. *Journal of the Air & Waste Management Association*, 49 (12): 1405-1414.

Gomez, C., Velo, E., Barontini, F. and Cozzani, V. (2009). Influence of secondary reactions on the heat of pyrolysis of biomass. *Industrial & Engineering Chemistry Research*, 48 (23): 10222-10233.

González, J. F., Encinar, J. M., Canito, J. L. and Rodríguez, J. J. (2001). Pyrolysis of automobile tyre waste. Influence of operating variables and kinetics study. *Journal of Analytical and Applied Pyrolysis*, 58–59: 667-683.

Grierson, D. and Pak, W. (1993). Optimal sizing, geometrical and topological design using a genetic algorithm. *Structural Optimization*, 6 (3): 151-159.

Groves, S. A., Lehrle, R. S., Blazsó, M. and Székely, T. (1991). Natural rubber pyrolysis: Study of temperature-and thickness-dependence indicates dimer formation mechanism. *Journal of Analytical and Applied Pyrolysis*, 19: 301-309.

Harker, J. H. and Backhurst, J. R. (1981). Fuel and energy. *London and New York, Academic Press, 1981. 373 p.*,

Haw, K.-G., Bakar, W. A. W. A., Ali, R., Chong, J.-F. and Kadir, A. A. A. (2010). Catalytic oxidative desulfurization of diesel utilizing hydrogen peroxide and functionalized-activated carbon in a biphasic diesel–acetonitrile system. *Fuel Processing Technology*, 91 (9): 1105-1112.

Helleur, R., Popovic, N., Ikura, M., Stanciulescu, M. and Liu, D. (2001). Characterization and potential applications of pyrolytic char from ablative pyrolysis of used tires. *Journal of Analytical and Applied Pyrolysis*, 58–59: 813-824.

Heywood, J. B. (1988). Internal combustion engine fundamentals.

Huang, C., Chen, B., Zhang, J., Liu, Z. and Li, Y. (2004). Desulfurization of gasoline by extraction with new ionic liquids. *Energy & Fuels*, 18 (6): 1862-1864.

Hutter, F., Hoos, H. H., Leyton-Brown, K. and Murphy, K. 2010. Time-bounded sequential parameter optimization. In: Proceedings of *International Conference on Learning and Intelligent Optimization*. Springer, 281-298.

Hutter, F., Hoos, H. H., Leyton-Brown, K. and Murphy, K. P. 2009. An experimental investigation of model-based parameter optimisation: SPO and beyond. In: Proceedings of *Proceedings of the 11th Annual conference on Genetic and evolutionary computation*. ACM, 271-278.

İlkılıç, C. and Aydın, H. (2011). Fuel production from waste vehicle tires by catalytic pyrolysis and its application in a diesel engine. *Fuel Processing Technology*, 92 (5): 1129-1135.

Irmak Aslan, D., Parthasarathy, P., Goldfarb, J. L. and Ceylan, S. (2017). Pyrolysis reaction models of waste tires: Application of Master-Plots method for energy conversion via devolatilization. *Waste Management*,

Isayev, A. (2005). Recycling of rubber.

Islam, M. A., Asif, M. and Hameed, B. H. (2015). Pyrolysis kinetics of raw and hydrothermally carbonized Karanj (Pongamia pinnata) fruit hulls via thermogravimetric analysis. *Bioresource Technology*, 179: 227-233.

Islam, M. A., Auta, M., Kabir, G. and Hameed, B. H. (2016). A thermogravimetric analysis of the combustion kinetics of karanja (Pongamia pinnata) fruit hulls char. *Bioresource Technology*, 200: 335-341.

Islam, M. R., Haniu, H. and Beg, M. R. A. (2008). Liquid fuels and chemicals from pyrolysis of motorcycle tire waste: product yields, compositions and related properties. *Fuel*, 87 (13): 3112-3122.

Islam, M. R., Haniu, H. and Fardoushi, J. (2009). Pyrolysis kinetics behavior of solid tire wastes available in Bangladesh. *Waste Management*, 29 (2): 668-677.

Januszewicz, K., Klein, M., Klugmann-Radziemska, E. and Kardas, D. (2017). Thermogravimetric analysis/pyrolysis of used tyres and waste rubber. *Physicochemical Problems of Mineral Processing*, 53 (2): 802-811.

Jin, R., Chen, W. and Sudjianto, A. 2002. On sequential sampling for global metamodeling in engineering design. In: Proceedings of *ASME 2002 International Design Engineering Technical Conferences and Computers and Information in Engineering Conference*. American Society of Mechanical Engineers, 539-548.

Jin, Y., Olhofer, M. and Sendhoff, B. 2001. Managing approximate models in evolutionary aerodynamic design optimization. In: Proceedings of *Evolutionary Computation, 2001. Proceedings of the 2001 Congress on*. IEEE, 592-599.

Jones, D. R. (2001). A taxonomy of global optimization methods based on response surfaces. *Journal of global optimization*, 21 (4): 345-383.

Jones, D. R., Schonlau, M. and Welch, W. J. (1998). Efficient global optimization of expensive black-box functions. *Journal of Global optimization*, 13 (4): 455-492.

Kaminsky, W. and Mennerich, C. (2001). Pyrolysis of synthetic tire rubber in a fluidised-bed reactor to yield 1,3-butadiene, styrene and carbon black. *Journal of Analytical and Applied Pyrolysis*, 58–59: 803-811.

Kaminsky, W., Mennerich, C. and Zhang, Z. (2009). Feedstock recycling of synthetic and natural rubber by pyrolysis in a fluidized bed. *Journal of Analytical and Applied Pyrolysis*, 85 (1–2): 334-337.

Kar, Y. (2011). Catalytic pyrolysis of car tire waste using expanded perlite. *Waste Management*, 31 (8): 1772-1782.

Kawakami, S., Inoue, K., Tanaka, H. and Sakai, T. (1980). Pyrolysis process for scrap tires. In. ACS Publications.

Kazemi-Beydokhti, A., Azizi Namaghi, H., Asgarkhani, H. and Zeinali Heris, S. (2015). Prediction of stability and thermal conductivity of sno2nanofluid via statistical method and an artificial neural network. *Brazilian Journal of Chemical Engineering*, 32 (4): 903-917.

Kennard, R. W. and Stone, L. A. (1969). Computer aided design of experiments. *Technometrics*, 11 (1): 137-148.

Kissinger, H. E. (1957). Reaction kinetics in differential thermal analysis. *Analytical chemistry*, 29 (11): 1702-1706.

Kwon, E. and Castaldi, M. J. (2008). Investigation of mechanisms of polycyclic aromatic hydrocarbons (PAHs) initiated from the thermal degradation of styrene butadiene rubber (SBR) in N2 atmosphere. *Environmental science & technology*, 42 (6): 2175-2180.

Kwon, E. and Castaldi, M. J. (2009). Fundamental understanding of the thermal degradation mechanisms of waste tires and their air pollutant generation in a N2 atmosphere. *Environmental science & technology*, 43 (15): 5996-6002.

Kyari, M., Cunliffe, A. and Williams, P. T. (2005). Characterization of oils, gases, and char in relation to the pyrolysis of different brands of scrap automotive tires. *Energy & Fuels*, 19 (3): 1165-1173.

Laird, D. A., Brown, R. C., Amonette, J. E. and Lehmann, J. (2009). Review of the pyrolysis platform for coproducing bio-oil and biochar. *Biofuels, Bioproducts and Biorefining*, 3 (5): 547-562.

Laresgoiti, M. F., Caballero, B. M., de Marco, I., Torres, A., Cabrero, M. A. and Chomón, M. J. (2004). Characterization of the liquid products obtained in tyre pyrolysis. *Journal of Analytical and Applied Pyrolysis*, 71 (2): 917-934.

Laresgoiti, M. F., de Marco, I., Torres, A., Caballero, B., Cabrero, M. A. and Chomón, M. J. (2000). Chromatographic analysis of the gases obtained in tyre pyrolysis. *Journal of Analytical and Applied Pyrolysis*, 55 (1): 43-54.

Larsen, M. B., Schultz, L., Glarborg, P., Skaarup-Jensen, L., Dam-Johansen, K., Frandsen, F. and Henriksen, U. (2006). Devolatilization characteristics of large particles of tyre rubber under combustion conditions. *Fuel*, 85 (10–11): 1335-1345.

Lee, J. and Hajela, P. (1996). Parallel genetic algorithm implementation in multidisciplinary rotor blade design. *Journal of Aircraft*, 33 (5): 962-969.

Lehmann, C. M., Rostam-Abadi, M., Rood, M. J. and Sun, J. (1998). Reprocessing and reuse of waste tire rubber to solve air-quality related problems. *Energy & Fuels*, 12 (6): 1095-1099.

Leung, D. and Wang, C. (1999). Kinetic modeling of scrap tire pyrolysis. *Energy & fuels*, 13 (2): 421-427.

Leung, D. Y. C. and Wang, C. L. (1998). Kinetic study of scrap tyre pyrolysis and combustion. *Journal of Analytical and Applied Pyrolysis*, 45 (2): 153-169.

Leung, D. Y. C., Yin, X. L., Zhao, Z. L., Xu, B. Y. and Chen, Y. (2002). Pyrolysis of tire powder: influence of operation variables on the composition and yields of gaseous product. *Fuel Processing Technology*, 79 (2): 141-155.

Levendis, Y. A., Atal, A., Carlson, J., Dunayevskiy, Y. and Vouros, P. (1996). Comparative study on the combustion and emissions of waste tire crumb and pulverized coal. *Environmental science & technology*, 30 (9): 2742-2754.

Li, S.-Q., Yao, Q., Chi, Y., Yan, J.-H. and Cen, K.-F. (2004). Pilot-scale pyrolysis of scrap tires in a continuous rotary kiln reactor. *Industrial & engineering chemistry research*, 43 (17): 5133-5145.

Liang, L. (2007). Recovery and evaluation of the solid products produced by thermocatalytic decomposition of tire rubber compounds. Texas A&M University.

Lin, J., Gaustad, G. and Trabold, T. A. (2013). Profit and policy implications of producing biodiesel–ethanol–diesel fuel blends to specification. *Applied Energy*, 104: 936-944.

Lingyan, K., Gang, L. and Xiangsheng, W. (2004). Catalytic oxidative desulphurization of liquid Fuels. *CHEMISTRY-PEKING-*, 67 (3): 178-184.

Lopez-Velazquez, M. A., Santes, V., Balmaseda, J. and Torres-Garcia, E. (2013). Pyrolysis of orange waste: A thermo-kinetic study. *Journal of Analytical and Applied Pyrolysis*, 99: 170-177.

López, F. A., Centeno, T. A., Alguacil, F. J. and Lobato, B. (2011a). Distillation of granulated scrap tires in a pilot plant. *Journal of Hazardous Materials*, 190 (1-3): 285-292.

López, F. A., Centeno, T. A., Alguacil, F. J. and Lobato, B. (2011b). Distillation of granulated scrap tires in a pilot plant. *Journal of Hazardous Materials*, 190 (1–3): 285-292.

López, F. A., El Hadad, A. A., Alguacil, F. J., Centeno, T. A. and Lobato, B. (2013). Kinetics of the Thermal Degradation of Granulated Scrap Tyres: a Model-free Analysis. *Materials Science*, 19 (4): 403-408.

Lopez, G., Aguado, R., Olazar, M., Arabiourrutia, M. and Bilbao, J. (2009). Kinetics of scrap tyre pyrolysis under vacuum conditions. *Waste Management*, 29 (10): 2649-2655.

López, G., Olazar, M., Aguado, R. and Bilbao, J. (2010). Continuous pyrolysis of waste tyres in a conical spouted bed reactor. *Fuel*, 89 (8): 1946-1952.

Lopez, G., Olazar, M., Aguado, R., Elordi, G., Amutio, M., Artetxe, M. and Bilbao, J. (2010). Vacuum pyrolysis of waste tires by continuously feeding into a conical spouted bed reactor. *Industrial & Engineering Chemistry Research*, 49 (19): 8990-8997.

Lucchesi, A. and Maschio, G. (1983). Semi-active carbon and aromatics produced by pyrolysis of scrap tires. *Conservation & recycling*, 6 (3): 85-90.

Luyima, A., Zhang, L., Kers, J. and Laurmaa, V. (2012). Recovery of Metallic Materials from Printed Wiring Boards by Green Pyrolysis Process. *Materials Science*, 18 (3): 238-242.

Martínez, J. D., Puy, N., Murillo, R., García, T., Navarro, M. V. and Mastral, A. M. (2013). Waste tyre pyrolysis – A review. *Renewable and Sustainable Energy Reviews*, 23: 179-213.

Mastral, A., Alvarez, R., Callén, M., Clemente, C. and Murillo, R. (1999a). Characterization of chars from coal− tire copyrolysis. *Industrial & engineering chemistry research*, 38 (7): 2856-2860.

Mastral, A., Callen, M. and Garcia, T. (2000a). Fluidized bed combustion (FBC) of fossil and nonfossil fuels. A comparative study. *Energy & fuels*, 14 (2): 275-281.

Mastral, A., Murillo, R., Callen, M. and Garcia, T. (2000b). Optimisation of scrap automotive tyres recycling into valuable liquid fuels. *Resources, Conservation and Recycling*, 29 (4): 263-272.

Mastral, A., Murillo, R., Callén, M. and Garcıa, T. (1999b). Application of coal conversion technology to tire processing. *Fuel Processing Technology*, 60 (3): 231-242.

Mastral, A., Murillo, R., Callen, M., Garcia, T. and Snape, C. (2000c). Influence of process variables on oils from tire pyrolysis and hydropyrolysis in a swept fixed bed reactor. *Energy & Fuels*, 14 (4): 739-744.

Mastral, A. M., Callén, M. S., Murillo, R. and GarcÍa, T. (1999c). Combustion of high calorific value waste material: Organic atmospheric pollution. *Environmental science & technology*, 33 (23): 4155-4158.

MathWorks, I. (2005). *MATLAB: the language of technical computing. Desktop tools and development environment, version 7*. MathWorks.

Mead, R. and Pike, D. (1975). A biometrics invited paper. A review of response surface methodology from a biometric viewpoint. *Biometrics*, 31 (4): 803-851.

Merchant, A. A. and Petrich, M. A. (1993). Pyrolysis of scrap tires and conversion of chars to activated carbon. *AIChE Journal*, 39 (8): 1370-1376.

Miguel, G. S., Fowler, G. D. and Sollars, C. J. (1998). Pyrolysis of tire rubber: porosity and adsorption characteristics of the pyrolytic chars. *Industrial & engineering chemistry research*, 37 (6): 2430-2435.

Mikulova, Z., Sedenkova, I., Matejova, L., Večeř, M. and Dombek, V. (2013). Study of carbon black obtained by pyrolysis of waste scrap tyres. *Journal of Thermal Analysis and Calorimetry*, 111 (2): 1475-1481.

Miranda, M., Pinto, F., Gulyurtlu, I. and Cabrita, I. (2013). Pyrolysis of rubber tyre wastes: A kinetic study. *Fuel*, 103: 542-552.

Mirmiran, S., Pakdel, H. and Roy, C. (1992). Characterization of used tire vacuum pyrolysis oil: nitrogenous compounds from the naphtha fraction. *Journal of Analytical and Applied Pyrolysis*, 22 (3): 205-215.

Mokhtar, W. N. A. W., Bakar, W. A. W. A., Ali, R. and Kadir, A. A. A. (2015). Optimization of oxidative desulfurization of Malaysian Euro II diesel fuel utilizing tert-butyl hydroperoxide–dimethylformamide system. *Fuel*, 161: 26-33.

Montgomery, D. C. (2001). Design and Analysis of Experiments, John Wiley & Sons. *New York*: 64-65.

Montgomery, D. C. (2004). *Design and Analysis of Experiments 6th Edition with Design Expert Software*. John Wiley & Sons.

Montgomery, D. C. (2009). Design and analysis of experiments. John Wiley & Sons, New York. *Design and analysis of experiments. 7th ed. John Wiley & Sons, New York.*: -.

Montgomery, D. C., Peck, E. A. and Vining, G. G. (2012). *Introduction to linear regression analysis*. John Wiley & Sons.

Mui, E. L. K., Ko, D. C. K. and McKay, G. (2004). Production of active carbons from waste tyres—a review. *Carbon*, 42 (14): 2789-2805.

Murata, S., Murata, K., Kidena, K. and Nomura, M. (2004). A novel oxidative desulfurization system for diesel fuels with molecular oxygen in the presence of cobalt catalysts and aldehydes. *Energy & Fuels*, 18 (1): 116-121.

Murillo, R., Aranda, A., Aylón, E., Callén, M. S. and Mastral, A. M. (2006a). Process for the separation of gas products from waste tire pyrolysis. *Industrial & engineering chemistry research*, 45 (5): 1734-1738.

Murillo, R., Aylón, E., Navarro, M. V., Callén, M. S., Aranda, A. and Mastral, A. M. (2006b). The application of thermal processes to valorise waste tyre. *Fuel Processing Technology*, 87 (2): 143-147.

Murillo, R., Navarro, M., García, T., López, J., Callén, M., Aylón, E. and Mastral, A. (2005). Production and application of activated carbons made from waste tire. *Industrial & engineering chemistry research*, 44 (18): 7228-7233.

Murti, S. D. S., Choi, K.-H., Sakanishi, K., Okuma, O., Korai, Y. and Mochida, I. (2005). Analysis and removal of heteroatom containing species in coal liquid distillate over NiMo catalysts. *Fuel*, 84 (2–3): 135-142.

Murugan, S., Ramaswamy, M. and Nagarajan, G. (2009). Assessment of pyrolysis oil as an energy source for diesel engines. *Fuel Processing Technology*, 90 (1): 67-74.

Murugan, S., Ramaswamy, M. C. and Nagarajan, G. (2008a). A comparative study on the performance, emission and combustion studies of a DI diesel engine using distilled tyre pyrolysis oil–diesel blends. *Fuel*, 87 (10–11): 2111-2121.

Murugan, S., Ramaswamy, M. C. and Nagarajan, G. (2008b). Performance, emission and combustion studies of a DI diesel engine using Distilled Tyre pyrolysis oil-diesel blends. *Fuel Processing Technology*, 89 (2): 152-159.

Murugan, S., Ramaswamy, M. C. and Nagarajan, G. (2008c). The use of tyre pyrolysis oil in diesel engines. *Waste Management*, 28 (12): 2743-2749.

Myers, R. H. 1990. *Classical and modern regression with applications*.

Myers, R. H. (1999). Response surface methodology--current status and future directions. *Journal of Quality Technology*, 31 (1): 30.

Myers, R. H., Khuri, A. I. and Carter, W. H. (1989). Response surface methodology: 1966–l988. *Technometrics*, 31 (2): 137-157.

Myers, R. H., Montgomery, D. C. and Anderson-Cook, C. (2009). Response surface methodology. *New Jersey: John Wiley & Sons, Inc*, 20: 38-44.

Myers, R. H., Montgomery, D. C., Vining, G. G., Borror, C. M. and Kowalski, S. M. (2004). Response surface methodology: a retrospective and literature survey. *Journal of quality technology*, 36 (1): 53.

Nabi, A. R., Masud, M. H. and Alam, Q. I. (2014). Purification of TPO (Tire Pyrolytic Oil) and its use in diesel engine. *IOSR Journal of Engineering*, 4 (3): 1.

Napoli, A., Soudais, Y., Lecomte, D. and Castillo, S. (1997). Scrap tyre pyrolysis: are the effluents valuable products? *Journal of Analytical and Applied Pyrolysis*, 40: 373-382.

Navarro, F. J., Partal, P., Martínez-Boza, F. J. and Gallegos, C. (2010). Novel recycled polyethylene/ground tire rubber/bitumen blends for use in roofing applications: Thermo-mechanical properties. *Polymer Testing*, 29 (5): 588-595.

Nieto-Márquez, A., Atanes, E., Morena, J., Fernández-Martínez, F. and Valverde, J. L. (2016). Upgrading waste tires by chemical activation for the capture of SO2. *Fuel Processing Technology*, 144: 274-281.

Ogasawara, S., Kuroda, M. and Wakao, N. (1987). Preparation of activated carbon by thermal decomposition of used automotive tires. *Industrial & engineering chemistry research*, 26 (12): 2552-2556.

Olazar, M., Aguado, R., Arabiourrutia, M., Lopez, G., Barona, A. and Bilbao, J. (2008a). Catalyst effect on the composition of tire pyrolysis products. *Energy & Fuels*, 22 (5): 2909-2916.

Olazar, M., Lopez, G., Arabiourrutia, M., Elordi, G., Aguado, R. and Bilbao, J. (2008b). Kinetic modelling of tyre pyrolysis in a conical spouted bed reactor. *Journal of Analytical and Applied Pyrolysis*, 81 (1): 127-132.

Ozawa, T. (1965). A new method of analyzing thermogravimetric data. *Bulletin of the chemical society of Japan*, 38 (11): 1881-1886.

Pakdel, H., Pantea, D. M. and Roy, C. (2001). Production of dl-limonene by vacuum pyrolysis of used tires. *Journal of Analytical and Applied Pyrolysis*, 57 (1): 91-107.

Pakdel, H. and Roy, C. (1994). Simultaneous gas chromatographic—Fourier transform infrared spectroscopic—mass spectrometric analysis of synthetic fuel derived from used tire vacuum pyrolysis oil, naphtha fraction. *Journal of Chromatography A*, 683 (1): 203-214.

Pakdel, H., Roy, C., Aubin, H., Jean, G. and Coulombe, S. (1991). Formation of dl-limonene in used tire vacuum pyrolysis oils. *Environmental science & technology*, 25 (9): 1646-1649.

Palmer, K., Burtraw, D. and Shih, J.-S. (2007). The benefits and costs of reducing emissions from the electricity sector. *Journal of environmental management*, 83 (1): 115-130.

Pantea, D., Darmstadt, H., Kaliaguine, S. and Roy, C. (2003). Heat-treatment of carbon blacks obtained by pyrolysis of used tires. Effect on the surface chemistry, porosity and electrical conductivity. *Journal of Analytical and Applied Pyrolysis*, 67 (1): 55-76.

Parthasarathy, P., Choi, H. S., Park, H. C., Hwang, J. G., Yoo, H. S., Lee, B.-K. and Upadhyay, M. (2016). Influence of process conditions on product yield of waste tyre pyrolysis-A review. *Korean Journal of Chemical Engineering*, 33 (8): 2268-2286.

Patnaik, T. and Brown, B. (2010). Carbon black: why quality matters. *Rubber & plastics news*, 40 (10): 16-18.

Pawlowicz, R., Beardsley, B. and Lentz, S. (2002). Classical tidal harmonic analysis including error estimates in MATLAB using T_TIDE. *Computers & Geosciences*, 28 (8): 929-937.

Pierret, S. and Van den Braembussche, R. (1997). Turbomachinery blade design using a Navier-Stokes solver and artificial neural network. *VKI Lecture Series*, 5: 21-25.

Pulkrabek, W. W. (1997). *Engineering fundamentals of the internal combustion engine*.

Rada, E. C., Ragazzi, M., Dal Maschio, R., Ischia, M. and Panaitescu, V. N. (2012). Energy recovery from tyres waste through thermal option. *Scientific Bulletin, Politehnica University of Bucharest, Series D, Mechanical Engineering*, 74: 201-210.

Rezaiyan, J. and Cheremisinoff, N. P. (2005). *Gasification technologies: a primer for engineers and scientists*. CRC press.

Rofiqul, I. M., Haniu, H., Alam, B. R. and Takai, K. (2008). Preliminary investigation for engine performance by using tire-derived pyrolysis oil-diesel blended fuels. *Journal of Power and Energy Systems*, 2 (6): 1359-1372.

Rofiqul Islam, M., Haniu, H. and Rafiqul Alam Beg, M. (2008). Liquid fuels and chemicals from pyrolysis of motorcycle tire waste: Product yields, compositions and related properties. *Fuel*, 87 (13–14): 3112-3122.

Roy, C., Chaala, A. and Darmstadt, H. (1999). The vacuum pyrolysis of used tires: End-uses for oil and carbon black products. *Journal of Analytical and Applied Pyrolysis*, 51 (1–2): 201-221.

Roy, C., Chaala, A., Darmstadt, H., de Caumia, B., Pakdel, H. and Yang, J. (2005). Conversion of Used Tires to Carbon Black and Oil by Pyrolysis. In: *Rubber Recycling*. CRC Press Taylor & Francis Group Florida, 458-499.

Roy, C., Darmstadt, H., Benallal, B. and Amen-Chen, C. (1997). Characterization of naphtha and carbon black obtained by vacuum pyrolysis of polyisoprene rubber. *Fuel Processing Technology*, 50 (1): 87-103.

Roy, C., Labrecque, B. and de Caumia, B. (1990). Recycling of scrap tires to oil and carbon black by vacuum pyrolysis. *Resources, Conservation and Recycling*, 4 (3): 203-213.

Rydberg, J. (2004). *Solvent extraction principles and practice, revised and expanded*. CRC Press.

Sacks, J., Welch, W. J., Mitchell, T. J. and Wynn, H. P. (1989). Design and analysis of computer experiments. *Statistical science*: 409-423.

Sahouli, B., Blacher, S., Brouers, F., Darmstadt, H., Roy, C. and Kaliaguine, S. (1996). Surface morphology and chemistry of commercial carbon black and carbon black from vacuum pyrolysis of used tyres. *Fuel*, 75 (10): 1244-1250.

San Miguel, G., Fowler, G. D. and Sollars, C. J. (2003). A study of the characteristics of activated carbons produced by steam and carbon dioxide activation of waste tyre rubber. *Carbon*, 41 (5): 1009-1016.

Sangsefidi, Y., Mehraein, M., Ghodsian, M. and Motalebizadeh, M. R. (2017). Evaluation and Analysis of Flow over Arced Weirs Using Traditional and Response Surface Methodologies. *Journal of Hydraulic Engineering*, 143 (11): 04017048.

Santner, T., Williams, B. and Notz, W. (2003). The Design and Analysis of Computer Experiments Springer-Verlag. *New York. 283pp*,

Scala, F., Chirone, R. and Salatino, P. (2003). Fluidized bed combustion of tyre derived fuel. *Experimental thermal and fluid science*, 27 (4): 465-471.

Scheirs, J. (2006). Overview of commercial pyrolysis processes for waste plastics. *Feedstock recycling and pyrolysis of waste plastics: converting waste plastics into diesel and other fuels*: 381-433.

Seidelt, S., Müller-Hagedorn, M. and Bockhorn, H. (2006). Description of tire pyrolysis by thermal degradation behaviour of main components. *Journal of Analytical and Applied Pyrolysis*, 75 (1): 11-18.

Senneca, O., Salatino, P. and Chirone, R. (1999). A fast heating-rate thermogravimetric study of the pyrolysis of scrap tyres. *Fuel*, 78 (13): 1575-1581.

Shiraishi, Y., Hirai, T. and Komasawa, I. (1998). A deep desulfurization process for light oil by photochemical reaction in an organic two-phase liquid− liquid extraction system. *Industrial & engineering chemistry research*, 37 (1): 203-211.

Shiraishi, Y., Hirai, T. and Komasawa, I. (2002). Oxidative desulfurization process for light oil using titanium silicate molecular sieve catalysts. *Journal of chemical engineering of Japan*, 35 (12): 1305-1311.

Shiraishi, Y., Naito, T. and Hirai, T. (2003). Vanadosilicate molecular sieve as a catalyst for oxidative desulfurization of light oil. *Industrial & engineering chemistry research*, 42 (24): 6034-6039.

Shulman, V. (2004). *Tyre recycling*. iSmithers Rapra Publishing.

Siddique, R. and Naik, T. R. (2004). Properties of concrete containing scrap-tire rubber–an overview. *Waste Management*, 24 (6): 563-569.

Singh, S., Nimmo, W., Gibbs, B. and Williams, P. (2009). Waste tyre rubber as a secondary fuel for power plants. *Fuel*, 88 (12): 2473-2480.

Singh, S., Wu, C. and Williams, P. T. (2012). Pyrolysis of waste materials using TGA-MS and TGA-FTIR as complementary characterisation techniques. *Journal of Analytical and Applied Pyrolysis*, 94: 99-107.

Song, C. and Ma, X. (2003). New design approaches to ultra-clean diesel fuels by deep desulfurization and deep dearomatization. *Applied Catalysis B: Environmental*, 41 (1-2): 207-238.

Stat-Ease. (2005). *Stat-Ease Design Expert Package, Version 7.0. 0*: Stat-Ease Minneapolis.

Su, Y. and Deng, W. 2010. A thermogravimetric study of waste tire powder. In: Proceedings of *E-Product E-Service and E-Entertainment (ICEEE), 2010 International Conference on*. IEEE, 1-4.

Su, Y. and Zhao, B. 2009. Pyrolysis of waste tire powder and its comparison with Shenhua coal. In: Proceedings of *Energy and Environment Technology, 2009. ICEET'09. International Conference on*. IEEE, 262-265.

Tang, L. and Huang, H. (2005). Thermal plasma pyrolysis of used tires for carbon black recovery. *Journal of materials science*, 40 (14): 3817-3819.

Taylor, D. T. and Bottrill, R. P. (1995). The pyrolysis of automotive tyre waste. *Journal of the Institute of Energy*, 68 (474): 11-21.

Te, M., Fairbridge, C. and Ring, Z. (2001). Oxidation reactivities of dibenzothiophenes in polyoxometalate/H2O2 and formic acid/H2O2 systems. *Applied Catalysis A: General*, 219 (1–2): 267-280.

Teng, H., Serio, M. A., Wojtowicz, M. A., Bassilakis, R. and Solomon, P. R. (1995). Reprocessing of used tires into activated carbon and other products. *Industrial & engineering chemistry research*, 34 (9): 3102-3111.

Uçar, S. and Karagöz, S. (2014). Co-pyrolysis of pine nut shells with scrap tires. *Fuel*, 137: 85-93.

Ucar, S., Karagoz, S., Ozkan, A. R. and Yanik, J. (2005a). Evaluation of two different scrap tires as hydrocarbon source by pyrolysis. *Fuel*, 84 (14-15): 1884-1892.

Ucar, S., Karagoz, S., Ozkan, A. R. and Yanik, J. (2005b). Evaluation of two different scrap tires as hydrocarbon source by pyrolysis. *Fuel*, 84 (14–15): 1884-1892.

Unapumnuk, K., Lu, M. and Keener, T. C. (2006). Carbon distribution from the pyrolysis of tire-derived fuels. *Industrial & engineering chemistry research*, 45 (26): 8757-8764.

Uzun, B. and Yaman, E. (2014). Thermogravimetric characteristics and kinetics of scrap tyre and Juglans regia shell co-pyrolysis. *Waste Management & Research*: 0734242X14539722.

Voznesensky, V. (1974). Experiment Planning Statistical Methods for Technical and Economical Investigations. *Statistics, Moscow,(Russian)*,

Vyazovkin, S. and Dollimore, D. (1996). Linear and nonlinear procedures in isoconversional computations of the activation energy of nonisothermal reactions in solids. *Journal of chemical information and computer sciences*, 36 (1): 42-45.

Wampler, T. P. (2006). *Applied pyrolysis handbook*. CRC press.

Wan, M.-W. and Yen, T.-F. (2007). Enhance efficiency of tetraoctylammonium fluoride applied to ultrasound-assisted oxidative desulfurization (UAOD) process. *Applied Catalysis A: General*, 319: 237-245.

White, J. E., Catallo, W. J. and Legendre, B. L. (2011). Biomass pyrolysis kinetics: a comparative critical review with relevant agricultural residue case studies. *Journal of Analytical and Applied Pyrolysis*, 91 (1): 1-33.

Williams, P. and Brindle, A. (2003). Fluidised bed pyrolysis and catalytic pyrolysis of scrap tyres. *Environmental technology*, 24 (7): 921-929.

Williams, P. T. (2013). Pyrolysis of waste tyres: A review. *Waste Management*, 33 (8): 1714-1728.

Williams, P. T. and Besler, S. (1995). Pyrolysis-thermogravimetric analysis of tyres and tyre components. *Fuel*, 74 (9): 1277-1283.

Williams, P. T., Besler, S. and Taylor, D. T. (1990a). The pyrolysis of scrap automotive tyres. *Fuel*, 69 (12): 1474-1482.

Williams, P. T., Besler, S. and Taylor, D. T. (1990b). The pyrolysis of scrap automotive tyres: The influence of temperature and heating rate on product composition. *Fuel*, 69 (12): 1474-1482.

Williams, P. T. and Bottrill, R. P. (1995). Sulfur-polycyclic aromatic hydrocarbons in tyre pyrolysis oil. *Fuel*, 74 (5): 736-742.

Williams, P. T., Bottrill, R. P. and Cunliffe, A. M. (1998). Combustion of Tyre Pyrolysis Oil. *Process Safety and Environmental Protection*, 76 (4): 291-301.

Williams, P. T. and Taylor, D. T. (1993). Aromatization of tyre pyrolysis oil to yield polycyclic aromatic hydrocarbons. *Fuel*, 72 (11): 1469-1474.

World Business Council for Sustainable Development. (2008). *Managing End-of-Life Tires*. Available: http://www.bir.org/assets/Documents/industry/ManagingEndOfLifeTyres.pdf (Accessed 29.08.2017).

Xiao, G., Ni, M.-J., Chi, Y. and Cen, K.-F. (2008). Low-temperature gasification of waste tire in a fluidized bed. *Energy Conversion and Management*, 49 (8): 2078-2082.

Yang, J. and Roy, C. (1996). A new method for DTA measurement of enthalpy change during the pyrolysis of rubbers. *Thermochimica Acta*, 288 (1-2): 155-168.

Yu, G., Lu, S., Chen, H. and Zhu, Z. (2005). Diesel fuel desulfurization with hydrogen peroxide promoted by formic acid and catalyzed by activated carbon. *Carbon*, 43 (11): 2285-2294.

Zabaniotou, A. A. and Stavropoulos, G. (2003). Pyrolysis of used automobile tires and residual char utilization. *Journal of Analytical and Applied Pyrolysis*, 70 (2): 711-722.

Zadgaonkar, A. (2006). Process and equipment for conversions of waste plastics into fuels. *Feedstock Recycling and Pyrolysis of Waste Plastics: Converting Waste Plastics into Diesel and Other Fuels*: 709-728.

Zannikos, F., Lois, E. and Stournas, S. (1995). Desulfurization of petroleum fractions by oxidation and solvent extraction. *Fuel Processing Technology*, 42 (1): 35-45.

Zhang, G., Yu, F. and Wang, R. (2009). Research advances in oxidative desulfurization technologies for the production of low sulfur fuel oils. *Petroleum & Coal*, 51 (3): 196-207.

Zhang, X., Wang, T., Ma, L. and Chang, J. (2008). Vacuum pyrolysis of waste tires with basic additives. *Waste Management*, 28 (11): 2301-2310.

Zhao, H., Yan, H., Zhang, C., Sun, B., Zhang, Y., Dong, S., Xue, Y. and Qin, S. (2012). Thermogravimetry study of pyrolytic characteristics and kinetics of the giant wetland plant Phragmites australis. *Journal of thermal analysis and calorimetry*, 110 (2): 611-617.

APPENDICES

Appendix A: Equipment used for the TG experiments

A-1 Differential Scanning Calorimeter-Thermogravimetric analyser

Photograph A-1: Differential Scanning Calorimeter-Thermogravimetric Analyser

Appendix B: Materials and chemicals for oxidative desulphurisation

B-1 Calculations for dilution of formic acid

Dilution of formic acid from 95 wt. % to 85 wt.%

Molar mass of formic acid = 46.03 g/mol

Density of formic acid = 1.22 g/mL

Stock solution = 95 wt.%

Task: dilute to 85 wt. %

Procedure

Molarity of the stock (95 %):

$$1.22\ g/ml = 1220\ g/L\ of\ 95\ wt\%$$

$$0.95 \times 1220\ g/L = 1159\ \ g/L$$

$$Molarity = \frac{m}{M} = \frac{1159\ g/L}{46.03\ g/mol} = 25.18\ M = 25.18M$$

Molarity of the 85 wt. %:

$$0.85 \times 1220\ \ g/L = 1037\ g/L$$

$$Molarity = \frac{1037\ \ g/L}{46.03\ \ g/mol} = 22.53\ \ mol/L = 22.53\ M$$

Volume of stock solution and water required:

$$M_1V_1 = M_2V_2$$

Where,

$M_1 = 25.18M$

$M_2 = 22.53\ M$

To prepare 2.5 L of dilute acid i.e. $V_2 = 2.5\ L$:

$$V_1 = \frac{M_2V_2}{M_1} = \frac{22.53 \times 2.5L}{25.18} = 2.24\ L\ of\ stock\ solution$$

$$V_{H2O} = 2.5\ L - 2.24\ L = 0.26\ L\ = 260\ mL$$

Therefore 2.24 L of the stock solution (95wt.%) was added to 0.26 litres of water to make 2.5 litres of 85 wt.% formic acid.

B-2 Properties of tyre-derived oil and chemicals used

Table B-1: Physical and chemical properties of tyre-derived oil

Appearance	Dark brown
Physical state	liquid
Odor	Aromatic, unguent
Ph	4.7
Specific gravity(H20=1)	0.958
Density (kg/m^3)	958
Viscosity	45.8 SSU@100°F / 37.8°*C*
Volatiles by vol.%	60%
Boiling point	185°F / 85°*C*
Flash point	95°F / 35 °*C*
Auto ignition Temperature	800°F /427 °*C*

45.8 SSU = 6.06 cP @ 100°F/ 37.8°C

Table B-2: Properties of formic acid

Molar mass	46.03 g/mol
ASSAY	Min. 95 %
Water miscibility	complete
Residue on evaporation	0.002 %
Acetic acid (CH_3COOH)	0.1 %
Chloride (Cl)	0.001 %
Oxalate (C_2O_4)	0.005 %
Sulphate (SO_4)	0.005 %
Colour (APHA)	10
Sulphite (SO_3)	0.005 %

Supplier: Shalom laboratory supplies

Table B-3: Properties of hydrogen peroxide

Molar mass	34.01 g/mol
ASSAY	Min. 50 %
Acidity (H_2SO_4)	0.002 %
Chloride (Cl)	0.0005 %
Phosphate (PO_4)	0.0005 %
Sulphate (SO_4)	0.0003 %
Arsenic (As)	0.00005 %
Heavy metals (Pb)	0.0001 %
Iron (Fe)	0.000025 %
Nitrate (NO_3)	0.002 %
Ammonium (NH_3)	0.001 %

Supplier: Shalom laboratory supplies

Table B-4: Properties of acetonitrile

Appearance	Clear colourless liquid
Molar mass	41.05 g/mol
Assay	> = 99.8 %
Colour (APHA)	\< = 10
Formula	H3CCN
Boiling point	81.6 °C (1013 hPa)
Melting point	− 45.7 °C
Density	0.782 g/cm^3 (20 °C)
Flash point	2 °C (closed cup)

Supplier: Macron Fine Chemicals

Table B-5: Properties of NN-Dimethylformamide

Assay	≥ 99.9 %
Formula	C_3H_7NO
Molar mass	73.09 g/mol
Melting point	− 61 °C (lit.)
Boiling point	153 °C (lit.)
Flash point	58 °C (closed cup)
Density	0.944 g/mL (lit.)
Vapour pressure	2.7 mmHg (20 °C)
Refractive index	n20/D 1.430(lit.)
Vapour density	2.5 (vs air)
Autoignition temp.	833 °F
Residue on evaporation	<0.0005 %
impurities	≤0.030 % water
Explosive limit	15.2 %

Supplier: Sigma-Aldrich

B-3 Experimental setup for oxidation and extraction of tyre-derived oil

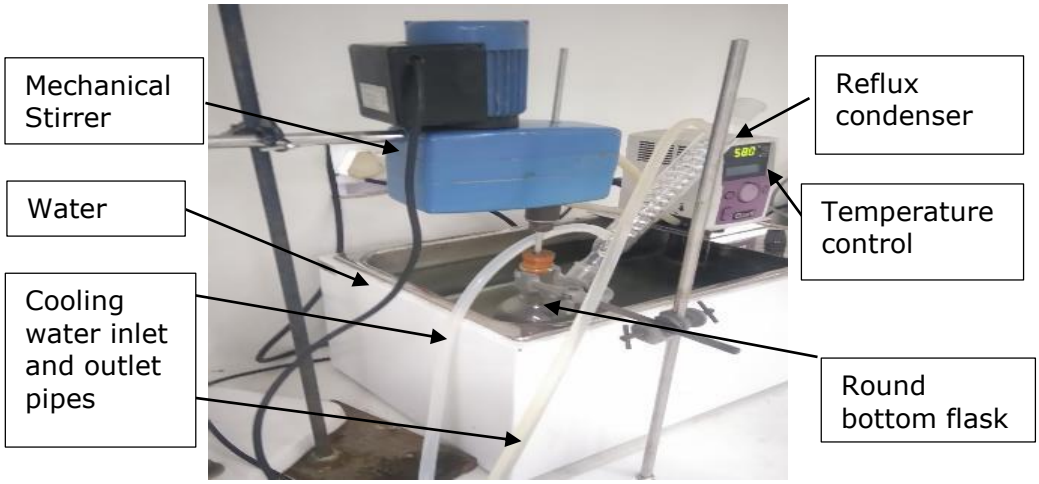

Photograph B-1: Photograph of experimental setup for oxidation of TDO

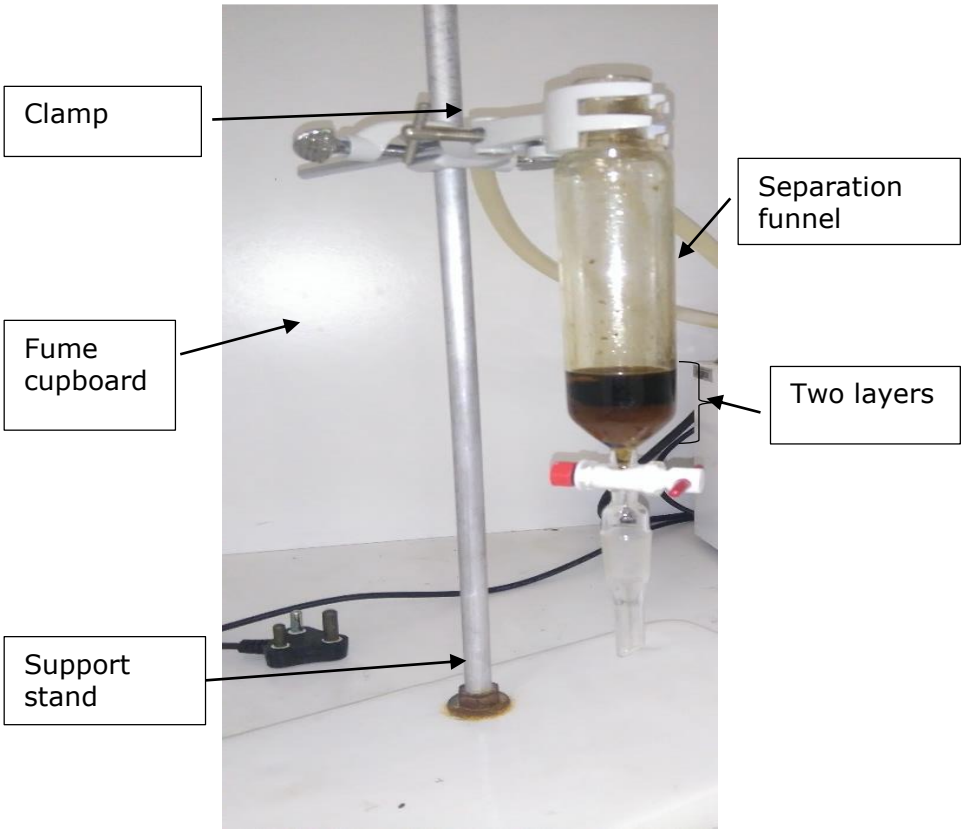

Photograph B-2: Photograph of experimental setup for solvent extraction

B-4 Samples ready for ICP-AES analysis

Photograph B-3: Representation of samples ready for ICP-AES analysis

Appendix C: Detailed TG/DTG and conversion data

Table C-1: Detailed TG/DTG and conversion data at 2 °C/min

Time (min)	Temp (°C)	Weight loss (%)	Derivative weight loss (% / °C)	Derivative weight loss (% / min)	Conversion
1.94	20	100.10	-0.001236	0.010430	0.000000
3.28	23	100.10	0.003545	0.012850	0.000000
4.86	26	100.10	0.005606	0.024010	0.000000
6.34	29	100.10	0.006718	0.013660	0.000000
7.81	32	100.10	0.007656	0.007303	0.000000
9.31	35	100.00	0.008257	0.012060	0.001602
10.79	38	100.00	0.008480	0.010690	0.001602
12.28	41	99.98	0.008309	0.021370	0.001923
13.77	44	99.95	0.007854	0.011910	0.002403
15.26	47	99.93	0.007766	0.022110	0.002724
16.74	50	99.91	0.008415	0.021310	0.003044
18.23	53	99.88	0.009824	0.022950	0.003525
19.72	56	99.85	0.012230	0.023520	0.004006
21.21	59	99.81	0.014980	0.028800	0.004647
22.70	62	99.76	0.016640	0.037050	0.005448
24.19	65	99.70	0.016560	0.034420	0.006409
25.68	68	99.66	0.015570	0.028020	0.007050
27.17	71	99.61	0.014490	0.024190	0.007851
28.66	74	99.57	0.013620	0.016900	0.008492
30.15	77	99.53	0.012660	0.013300	0.009133
31.64	80	99.50	0.011890	0.030780	0.009614
33.13	83	99.46	0.011310	0.030840	0.010255
34.62	86	99.43	0.010680	0.026180	0.010735

Table C-1 (Continued)

36.11	89	99.40	0.010160	0.017020	0.011216
37.61	92	99.37	0.009786	0.024150	0.011697
39.10	95	99.34	0.009435	0.021820	0.012178
40.59	98	99.31	0.009099	0.012340	0.012658
42.08	101	99.28	0.008949	0.015280	0.013139
43.58	104	99.26	0.008783	0.026910	0.013459
45.07	107	99.23	0.008653	0.026900	0.013940
46.56	110	99.20	0.008683	0.009206	0.014421
48.05	113	99.18	0.008618	0.011720	0.014741
49.55	116	99.15	0.008750	0.016670	0.015222
51.04	119	99.12	0.008949	0.008401	0.015703
52.53	122	99.10	0.009031	0.030850	0.016023
54.03	125	99.07	0.009397	0.013150	0.016504
55.52	128	99.04	0.009722	0.026300	0.016984
57.02	131	99.01	0.010240	0.011660	0.017465
58.52	134	98.98	0.010820	0.021820	0.017946
60.02	137	98.95	0.011440	0.016190	0.018427
61.52	140	98.91	0.012040	0.028240	0.019067
63.01	143	98.87	0.012840	0.002978	0.019708
64.51	146	98.84	0.013790	0.025390	0.020189
66.01	149	98.79	0.014730	0.037420	0.020990
67.51	152	98.75	0.015620	0.031480	0.021631
69.01	155	98.70	0.016640	0.038460	0.022432
70.51	158	98.65	0.017640	0.040380	0.023233
72.01	161	98.59	0.018780	0.043560	0.024195
73.51	164	98.54	0.019990	0.037160	0.024996
75.01	167	98.47	0.021220	0.053370	0.026118

Table C-1 (Continued)

76.51	170	98.41	0.022460	0.047980	0.027079
78.00	173	98.34	0.023870	0.046180	0.028201
79.50	176	98.27	0.025510	0.050410	0.029322
81.01	179	98.19	0.026850	0.063900	0.030604
82.50	182	98.10	0.028160	0.057860	0.032046
84.01	185	98.02	0.029630	0.049530	0.033328
85.51	188	97.93	0.030890	0.058560	0.034770
87.01	191	97.83	0.032250	0.072070	0.036372
88.50	194	97.73	0.033350	0.062530	0.037975
90.01	197	97.63	0.034430	0.071700	0.039577
91.51	200	97.52	0.035360	0.061760	0.041340
93.01	203	97.42	0.036230	0.067330	0.042942
94.51	206	97.31	0.037280	0.068140	0.044704
96.01	209	97.19	0.038270	0.075210	0.046627
97.51	212	97.08	0.039350	0.076280	0.048390
99.01	215	96.96	0.040510	0.082280	0.050312
100.51	218	96.84	0.041400	0.078180	0.052235
102.01	221	96.71	0.042560	0.081200	0.054318
103.51	224	96.58	0.043940	0.076120	0.056401
105.01	227	96.45	0.045410	0.094200	0.058484
106.52	230	96.31	0.046450	0.099130	0.060727
108.02	233	96.17	0.047440	0.097430	0.062971
109.52	236	96.02	0.048430	0.089750	0.065374
111.02	239	95.88	0.049510	0.097820	0.067617
112.53	242	95.73	0.050260	0.096700	0.070021
114.02	245	95.58	0.050540	0.098780	0.072424
115.53	248	95.42	0.050880	0.102800	0.074988

Table C-1 (Continued)

117.03	251	95.27	0.050990	0.106600	0.077391
118.54	254	95.12	0.051140	0.113000	0.079795
120.04	257	94.96	0.051380	0.101400	0.082359
121.54	260	94.81	0.051600	0.103800	0.084762
123.04	263	94.65	0.051950	0.102800	0.087326
124.55	266	94.50	0.052700	0.100500	0.089729
126.05	269	94.34	0.053880	0.101600	0.092293
127.55	272	94.18	0.055450	0.104300	0.094857
129.06	275	94.00	0.057380	0.102100	0.097741
130.56	278	93.83	0.059820	0.124500	0.100465
132.06	281	93.65	0.062930	0.120700	0.103349
133.57	284	93.45	0.066860	0.135400	0.106553
135.07	287	93.25	0.071930	0.136900	0.109758
136.57	290	93.02	0.077980	0.164700	0.113443
138.08	293	92.78	0.085360	0.174400	0.117289
139.58	296	92.51	0.094610	0.190500	0.121615
141.09	299	92.21	0.105700	0.204400	0.126422
142.59	302	91.88	0.119000	0.231000	0.131710
144.10	305	91.50	0.135400	0.268100	0.137798
145.60	308	91.07	0.155800	0.296500	0.144688
147.10	311	90.57	0.180300	0.351600	0.152700
148.61	314	89.99	0.209800	0.427700	0.161993
150.11	317	89.32	0.244700	0.491200	0.172729
151.62	320	88.53	0.284800	0.569800	0.185387
153.12	323	87.61	0.330300	0.665200	0.200128
154.62	326	86.55	0.380700	0.749500	0.217113
156.13	329	85.33	0.434100	0.861900	0.236661

Table C-1 (Continued)

157.63	332	83.95	0.487500	0.978300	0.258773
159.14	335	82.40	0.537800	1.085000	0.283608
160.65	338	80.71	0.579400	1.166000	0.310687
162.15	341	78.92	0.610500	1.214000	0.339369
163.66	344	77.04	0.629300	1.266000	0.369492
165.17	347	75.13	0.633800	1.272000	0.400096
166.67	350	73.23	0.621500	1.248000	0.430540
168.18	353	71.39	0.596100	1.208000	0.460022
169.69	356	69.65	0.562400	1.125000	0.487903
171.19	359	68.01	0.524100	1.045000	0.514180
172.70	362	66.50	0.487900	0.970800	0.538375
174.21	365	65.09	0.458400	0.902900	0.560968
175.72	368	63.76	0.436700	0.862700	0.582278
177.22	371	62.47	0.421700	0.848800	0.602948
178.73	374	61.23	0.413700	0.822200	0.622817
180.24	377	60.00	0.410500	0.811800	0.642525
181.74	380	58.77	0.410400	0.809700	0.662234
183.25	383	57.54	0.412500	0.811800	0.681942
184.76	386	56.29	0.415400	0.833300	0.701971
186.26	389	55.05	0.418400	0.845400	0.721839
187.77	392	53.78	0.420000	0.846700	0.742189
189.28	395	52.52	0.418300	0.845900	0.762378
190.79	398	51.27	0.412600	0.827500	0.782407
192.29	401	50.04	0.402200	0.787700	0.802115
193.80	404	48.86	0.386400	0.779700	0.821022
195.31	407	47.72	0.365400	0.734100	0.839289
196.82	410	46.66	0.340800	0.668500	0.856273

Table C-1 (Continued)

198.32	413	45.68	0.316200	0.624200	0.871976
199.83	416	44.76	0.293600	0.583900	0.886717
201.34	419	43.92	0.272600	0.554200	0.900176
202.85	422	43.13	0.253000	0.487600	0.912834
204.36	425	42.40	0.234500	0.459800	0.924531
205.87	428	41.72	0.217100	0.439500	0.935427
207.38	431	41.10	0.199000	0.400500	0.945361
208.88	434	40.53	0.179200	0.360000	0.954494
210.39	437	40.02	0.157100	0.325200	0.962666
211.9	440	39.58	0.132200	0.259900	0.969716
213.41	443	39.23	0.105000	0.202200	0.975324
214.92	446	38.95	0.078070	0.157100	0.979811
216.43	449	38.76	0.054420	0.098770	0.982855
217.94	452	38.63	0.036680	0.076490	0.984938
219.45	455	38.55	0.024630	0.054230	0.986220
220.95	458	38.49	0.017160	0.040030	0.987182
222.46	461	38.44	0.012480	0.021950	0.987983
223.97	464	38.41	0.009646	0.007509	0.988463
225.48	467	38.39	0.007773	0.011280	0.988784
226.99	470	38.37	0.006691	0.012110	0.989104
228.50	473	38.35	0.005892	0.020170	0.989425
230.01	476	38.33	0.005428	0.013170	0.989745
231.52	479	38.31	0.004909	0.019280	0.990066
233.03	482	38.30	0.004729	0.009092	0.990226
234.54	485	38.29	0.004705	0.022440	0.990386
236.05	488	38.27	0.004483	0.012280	0.990707
237.56	491	38.26	0.004476	0.003244	0.990867

Table C-1 (Continued)

239.07	494	38.25	0.008704	0.009640	0.991027
240.58	497	38.22	0.011580	0.258300	0.991508
242.09	500	38.17	0.011530	0.010490	0.992309
243.60	503	38.14	0.008039	0.023600	0.992790
245.11	506	38.12	0.006186	0.005772	0.993110
246.62	509	38.11	0.004340	0.009263	0.993270
248.13	512	38.10	0.004218	0.012300	0.993431
249.62	515	38.08	0.004350	0.015360	0.993751
251.12	518	38.07	0.004479	0.011230	0.993911
252.61	521	38.06	0.004494	0.002543	0.994071
254.11	524	38.04	0.004501	0.008682	0.994392
255.61	527	38.03	0.004853	0.008413	0.994552
257.10	530	38.01	0.004983	0.006763	0.994873
258.60	533	38.00	0.005152	0.012280	0.995033
260.09	536	37.98	0.005438	0.013120	0.995353
261.59	539	37.97	0.005527	0.010220	0.995514
263.09	542	37.95	0.005570	0.015170	0.995834
264.58	545	37.93	0.005648	0.004800	0.996154
266.07	548	37.91	0.005603	0.005916	0.996475
267.57	551	37.90	0.005845	0.004114	0.996635
269.07	554	37.88	0.005957	0.019330	0.996956
270.56	557	37.86	0.005426	0.000138	0.997276
272.06	560	37.85	0.004827	0.009840	0.997436
273.55	563	37.83	0.004562	-0.001948	0.997757
275.05	566	37.82	0.002081	0.003238	0.997917
276.54	569	37.81	-0.001875	0.025120	0.998077
278.04	572	37.84	-0.000917	0.004600	0.997597

Table C-1 (Continued)

279.53	575	37.82	0.004629	0.008083	0.997917
281.03	578	37.81	0.005421	-0.002304	0.998077
282.53	581	37.79	0.006074	0.014760	0.998398
284.02	584	37.77	0.006670	0.007431	0.998718
285.52	587	37.75	0.006673	0.023180	0.999039
287.02	590	37.73	0.006804	0.019190	0.999359
288.51	593	37.71	0.006643	0.009321	0.999680
290.01	596	37.69	0.006724	0.013910	1.000000

Table C-2: Detailed TG/DTG and conversion data at 5 °C/min

Time (min)	Temp (°C)	Weight loss (%)	Derivative weight loss (% / °C)	Derivative weight loss (% / min)	Conversion
1.47	20	100.10	0.007279	0.040410	0.000000
1.98	23	100.10	0.006105	0.033570	0.000000
2.48	26	100.00	0.005588	0.028950	0.001546
3.04	29	100.00	0.006701	0.026610	0.001546
3.66	32	100.00	0.008163	0.032960	0.001546
4.29	35	99.97	0.008968	0.039390	0.002010
4.91	38	99.95	0.009073	0.048930	0.002319
5.51	41	99.92	0.008784	0.061400	0.002783
6.09	44	99.89	0.008661	0.045090	0.003246
6.68	47	99.87	0.008481	0.035050	0.003555
7.27	50	99.84	0.008521	0.045340	0.004019
7.87	53	99.82	0.008621	0.043700	0.004328
8.47	56	99.79	0.008658	0.051950	0.004792
9.07	59	99.76	0.008443	0.062990	0.005256
9.66	62	99.74	0.008248	0.043530	0.005565
10.25	65	99.71	0.008269	0.053790	0.006029
10.85	68	99.69	0.008177	0.029230	0.006338
11.45	71	99.67	0.007945	0.042250	0.006647
12.04	74	99.64	0.007796	0.024500	0.007111
12.64	77	99.62	0.007383	0.037820	0.007420
13.23	80	99.60	0.007371	0.036130	0.007729
13.83	83	99.58	0.007096	0.049170	0.008038
14.42	86	99.55	0.006823	0.031590	0.008502
15.02	89	99.53	0.006319	0.032250	0.008811
15.62	92	99.52	0.006006	0.021200	0.008966

Table C-2 (Continued)

16.22	95	99.50	0.005778	0.020560	0.009275
16.81	98	99.48	0.005691	0.024620	0.009584
17.41	101	99.46	0.005505	0.029420	0.009893
18.01	104	99.45	0.005421	0.032410	0.010048
18.60	107	99.43	0.005448	0.021060	0.010357
19.20	110	99.42	0.005439	0.032900	0.010512
19.80	113	99.40	0.005544	0.035030	0.010821
20.40	116	99.38	0.005431	0.029600	0.011130
20.99	119	99.37	0.005559	0.029390	0.011285
21.59	122	99.35	0.005999	0.030470	0.011594
22.19	125	99.33	0.006720	0.034890	0.011903
22.78	128	99.31	0.007408	0.041820	0.012212
23.38	131	99.29	0.008256	0.035830	0.012521
23.98	134	99.26	0.008579	0.049940	0.012985
24.58	137	99.24	0.009007	0.040930	0.013294
25.17	140	99.21	0.009562	0.041980	0.013758
25.77	143	99.18	0.009998	0.049990	0.014222
26.37	146	99.15	0.010450	0.048320	0.014685
26.97	149	99.11	0.010860	0.065960	0.015304
27.57	152	99.08	0.011620	0.058170	0.015768
28.17	155	99.05	0.012250	0.048720	0.016231
28.77	158	99.01	0.012910	0.061400	0.016850
29.37	161	98.97	0.013800	0.054310	0.017468
29.96	164	98.92	0.014750	0.069760	0.018241
30.56	167	98.88	0.015640	0.072140	0.018859
31.16	170	98.83	0.016630	0.082990	0.019632
31.76	173	98.78	0.017820	0.084340	0.020405

Table C-2 (Continued)

32.36	176	98.72	0.018870	0.093100	0.021333
32.96	179	98.67	0.020130	0.094950	0.022105
33.56	182	98.60	0.021370	0.102900	0.023188
34.16	185	98.54	0.022690	0.116600	0.024115
34.76	188	98.47	0.023810	0.118600	0.025197
35.36	191	98.40	0.025230	0.121500	0.026279
35.95	194	98.32	0.026800	0.133000	0.027516
36.56	197	98.23	0.028580	0.141100	0.028907
37.15	200	98.14	0.030200	0.151900	0.030298
37.75	203	98.05	0.031770	0.155700	0.031690
38.35	206	97.96	0.033380	0.165500	0.033081
38.95	209	97.85	0.035040	0.170100	0.034781
39.55	212	97.74	0.036620	0.182100	0.036482
40.15	215	97.63	0.038110	0.185800	0.038182
40.75	218	97.52	0.039540	0.197400	0.039883
41.35	221	97.39	0.040840	0.212400	0.041892
41.95	224	97.27	0.042170	0.205400	0.043747
42.55	227	97.14	0.043320	0.222100	0.045757
43.15	230	97.01	0.044630	0.225400	0.047766
43.75	233	96.87	0.045850	0.239900	0.049930
44.35	236	96.74	0.046920	0.232200	0.051940
44.95	239	96.59	0.048030	0.240100	0.054259
45.55	242	96.45	0.049010	0.252800	0.056423
46.15	245	96.30	0.050010	0.256000	0.058742
46.76	248	96.15	0.050880	0.257400	0.061060
47.36	251	95.99	0.051500	0.252700	0.063534
47.95	254	95.84	0.051930	0.248800	0.065853

Table C-2 (Continued)

48.56	257	95.68	0.052360	0.258100	0.068326
49.16	260	95.52	0.052700	0.263200	0.070799
49.76	263	95.36	0.053000	0.270400	0.073273
50.36	266	95.21	0.053270	0.261000	0.075591
50.96	269	95.05	0.053390	0.257000	0.078065
51.56	272	94.89	0.053730	0.269000	0.080538
52.16	275	94.72	0.054070	0.266600	0.083166
52.76	278	94.56	0.054610	0.261200	0.085639
53.36	281	94.40	0.055350	0.270500	0.088113
53.96	284	94.23	0.056490	0.274200	0.090740
54.56	287	94.06	0.058240	0.280800	0.093368
55.16	290	93.88	0.060620	0.304400	0.096151
55.76	293	93.69	0.063640	0.304100	0.099088
56.36	296	93.50	0.067320	0.321700	0.102025
56.97	299	93.29	0.071970	0.356900	0.105271
57.57	302	93.07	0.077850	0.394700	0.108672
58.17	305	92.82	0.084860	0.417600	0.112537
58.77	308	92.56	0.093450	0.461700	0.116556
59.37	311	92.26	0.103800	0.528600	0.121193
59.97	314	91.94	0.116300	0.578000	0.126140
60.57	317	91.57	0.131400	0.677200	0.131860
61.17	320	91.15	0.149800	0.747000	0.138352
61.77	323	90.67	0.171700	0.855600	0.145772
62.37	326	90.12	0.198300	0.981400	0.154274
62.97	329	89.49	0.230100	1.138000	0.164013
63.57	332	88.75	0.267300	1.329000	0.175452
64.17	335	87.89	0.310500	1.544000	0.188746

Table C-2 (Continued)

64.78	338	86.89	0.359100	1.792000	0.204205
65.38	341	85.74	0.412300	2.058000	0.221982
65.98	344	84.42	0.469200	2.335000	0.242387
66.58	347	82.92	0.527000	2.639000	0.265574
67.18	350	81.25	0.582400	2.927000	0.291390
67.78	353	79.42	0.632500	3.159000	0.319678
68.38	356	77.45	0.672400	3.367000	0.350131
68.99	359	75.38	0.697600	3.527000	0.382130
69.59	362	73.25	0.706500	3.535000	0.415056
70.19	365	71.13	0.696000	3.490000	0.447828
70.79	368	69.06	0.669700	3.352000	0.479827
71.39	371	67.10	0.633300	3.171000	0.510125
71.99	374	65.26	0.592600	2.949000	0.538569
72.60	377	63.55	0.550800	2.751000	0.565002
73.20	380	61.96	0.513200	2.539000	0.589581
73.80	383	60.47	0.482800	2.403000	0.612614
74.40	386	59.07	0.459600	2.282000	0.634256
75.01	389	57.72	0.443400	2.203000	0.655124
75.61	392	56.41	0.433500	2.155000	0.675375
76.21	395	55.12	0.428100	2.141000	0.695316
76.81	398	53.84	0.425500	2.128000	0.715103
77.41	401	52.57	0.424500	2.112000	0.734735
78.02	404	51.30	0.423900	2.106000	0.754367
78.62	407	50.03	0.421800	2.108000	0.773999
79.22	410	48.77	0.417400	2.097000	0.793477
79.82	413	47.52	0.409400	2.063000	0.812800
80.42	416	46.30	0.396400	1.987000	0.831659

Table C-2 (Continued)

81.02	419	45.14	0.377300	1.894000	0.849590
81.62	422	44.04	0.353800	1.767000	0.866595
82.23	425	43.01	0.327800	1.624000	0.882517
82.83	428	42.07	0.300800	1.490000	0.897047
83.43	431	41.21	0.274700	1.371000	0.910342
84.03	434	40.42	0.250900	1.253000	0.922554
84.63	437	39.70	0.228900	1.153000	0.933684
85.23	440	39.05	0.207600	1.020000	0.943732
85.83	443	38.46	0.186400	0.930600	0.952852
86.44	446	37.93	0.165100	0.831500	0.961045
87.04	449	37.47	0.143500	0.716100	0.968156
87.64	452	37.07	0.121600	0.612000	0.974339
88.24	455	36.74	0.099810	0.507100	0.979440
88.84	458	36.47	0.078470	0.387800	0.983614
89.44	461	36.27	0.058730	0.286200	0.986706
90.05	464	36.12	0.042170	0.198200	0.989025
90.65	467	36.02	0.029720	0.138400	0.990570
91.25	470	35.95	0.021230	0.105300	0.991652
91.85	473	35.89	0.015650	0.079950	0.992580
92.45	476	35.85	0.012170	0.066650	0.993198
93.05	479	35.82	0.009706	0.063620	0.993662
93.65	482	35.79	0.007916	0.052220	0.994126
94.26	485	35.78	0.006623	0.044490	0.994280
94.86	488	35.76	0.005641	0.033910	0.994590
95.46	491	35.74	0.004975	0.034470	0.994899
96.06	494	35.73	0.004463	0.016910	0.995053
96.66	497	35.71	0.004042	0.010190	0.995362

Table C-2 (Continued)

97.27	500	35.70	0.003683	0.016030	0.995517
97.87	503	35.69	0.003476	0.019540	0.995672
98.47	506	35.68	0.003355	0.015690	0.995826
99.07	509	35.67	0.003181	0.017680	0.995981
99.67	512	35.66	0.002910	0.020160	0.996135
100.27	515	35.65	0.002756	0.012900	0.996290
100.87	518	35.65	0.002755	0.006289	0.996290
101.47	521	35.64	0.002852	0.021730	0.996445
102.07	524	35.63	0.002979	0.013300	0.996599
102.67	527	35.62	0.003193	0.017100	0.996754
103.27	530	35.61	0.003107	0.031970	0.996908
103.87	533	35.60	0.003004	0.012040	0.997063
104.47	536	35.59	0.002969	0.019320	0.997217
105.07	539	35.58	0.003042	0.026100	0.997372
105.67	542	35.57	0.003293	0.032030	0.997527
106.27	545	35.56	0.003373	0.009526	0.997681
106.87	548	35.55	0.003578	0.026240	0.997836
107.47	551	35.54	0.003693	0.026120	0.997990
108.07	554	35.53	0.003856	0.023430	0.998145
108.67	557	35.52	0.003819	0.008717	0.998300
109.28	560	35.51	0.003680	0.010150	0.998454
109.88	563	35.50	0.003784	0.012400	0.998609
110.47	566	35.49	0.003866	0.025230	0.998763
111.07	569	35.48	0.003677	0.007048	0.998918
111.68	572	35.46	0.003278	0.009571	0.999227
112.28	575	35.46	0.002903	0.016450	0.999227
112.88	578	35.45	0.002528	0.028170	0.999382

Table C-2 (Continued)

113.48	581	35.44	0.002049	0.020870	0.999536
114.08	584	35.43	0.001578	0.010980	0.999691
114.68	587	35.43	0.001342	0.001621	0.999691
115.28	590	35.43	0.001666	0.016040	0.999691
115.88	593	35.42	0.002111	0.009742	0.999845
116.48	596	35.41	0.002170	0.008532	1.000000

Table C-3: Detailed TG/DTG and conversion data at 10 °C/min

Time (min)	Temp (°C)	Weight loss (%)	Derivative weight loss (% / °C)	Derivative weight loss (% / min)	Conversion
0.43	20	100.00	0.006341	-0.035540	0.000000
1.02	23	100.00	0.006703	0.074610	0.000000
1.34	26	99.98	0.006470	0.061980	0.000316
1.61	29	99.97	0.004649	0.060570	0.000474
1.87	32	99.96	0.004283	0.051130	0.000632
2.12	35	99.94	0.004458	0.042640	0.000948
2.38	38	99.93	0.004874	0.042360	0.001106
2.65	41	99.91	0.005576	0.051510	0.001422
2.93	44	99.90	0.006275	0.063410	0.001581
3.23	47	99.88	0.006938	0.073660	0.001897
3.55	50	99.85	0.007559	0.074230	0.002371
3.86	53	99.83	0.008104	0.075270	0.002687
4.18	56	99.81	0.008394	0.082440	0.003003
4.49	59	99.78	0.008398	0.080100	0.003477
4.80	62	99.76	0.008204	0.081210	0.003793
5.10	65	99.73	0.008325	0.074710	0.004267
5.40	68	99.71	0.008379	0.091130	0.004584
5.69	71	99.68	0.008487	0.080870	0.005058
5.98	74	99.66	0.008422	0.082920	0.005374
6.28	77	99.63	0.008561	0.090430	0.005848
6.57	80	99.60	0.008565	0.090270	0.006322
6.87	83	99.58	0.008456	0.086220	0.006638
7.16	86	99.55	0.008528	0.079990	0.007112
7.46	89	99.53	0.008431	0.092000	0.007428
7.76	92	99.50	0.008305	0.077670	0.007903

Table C-3 (Continued)

8.06	95	99.48	0.008225	0.080050	0.008219
8.36	98	99.45	0.008127	0.086550	0.008693
8.66	101	99.43	0.007851	0.073560	0.009009
8.96	104	99.40	0.007538	0.078780	0.009483
9.26	107	99.38	0.007432	0.077820	0.009799
9.55	110	99.36	0.007338	0.068990	0.010115
9.85	113	99.34	0.007044	0.078750	0.010431
10.15	116	99.32	0.006866	0.066740	0.010748
10.45	119	99.30	0.006768	0.077710	0.011064
10.74	122	99.28	0.006741	0.068010	0.011380
11.04	125	99.26	0.006561	0.070810	0.011696
11.34	128	99.24	0.006460	0.060980	0.012012
11.64	131	99.22	0.006384	0.065910	0.012328
11.94	134	99.20	0.006406	0.060150	0.012644
12.24	137	99.18	0.006391	0.059920	0.012960
12.54	140	99.16	0.006440	0.064960	0.013276
12.84	143	99.14	0.006466	0.066030	0.013593
13.13	146	99.12	0.006597	0.066640	0.013909
13.43	149	99.10	0.006830	0.077010	0.014225
13.73	152	99.08	0.007058	0.067320	0.014541
14.03	155	99.06	0.007278	0.073050	0.014857
14.33	158	99.04	0.007635	0.078420	0.015173
14.63	161	99.02	0.008189	0.083070	0.015489
14.93	164	98.99	0.008609	0.088100	0.015963
15.23	167	98.96	0.008967	0.090010	0.016437
15.53	170	98.94	0.009468	0.091330	0.016754
15.82	173	98.91	0.010140	0.106400	0.017228

Table C-3 (Continued)

16.12	176	98.87	0.011060	0.104800	0.017860
16.42	179	98.84	0.011670	0.119000	0.018334
16.72	182	98.81	0.012490	0.126200	0.018808
17.02	185	98.77	0.013370	0.133400	0.019440
17.32	188	98.72	0.014350	0.135000	0.020231
17.62	191	98.68	0.015310	0.148900	0.020863
17.92	194	98.63	0.016330	0.158200	0.021653
18.22	197	98.58	0.017410	0.177300	0.022443
18.52	200	98.53	0.018560	0.188800	0.023234
18.82	203	98.47	0.019620	0.199400	0.024182
19.12	206	98.41	0.020830	0.213000	0.025130
19.42	209	98.35	0.022080	0.217300	0.026079
19.72	212	98.28	0.023350	0.232500	0.027185
20.01	215	98.21	0.024690	0.249400	0.028291
20.31	218	98.13	0.026120	0.264300	0.029556
20.61	221	98.05	0.027510	0.275300	0.030820
20.91	224	97.96	0.029170	0.299100	0.032243
21.21	227	97.87	0.030750	0.314000	0.033665
21.51	230	97.78	0.032230	0.321000	0.035088
21.81	233	97.68	0.033770	0.337000	0.036668
22.11	236	97.58	0.035460	0.353600	0.038249
22.41	239	97.47	0.037060	0.368000	0.039987
22.71	242	97.36	0.038640	0.386400	0.041726
23.01	245	97.24	0.040230	0.401400	0.043623
23.31	248	97.11	0.041720	0.425300	0.045677
23.61	251	96.99	0.043370	0.430000	0.047574
23.91	254	96.85	0.044810	0.439700	0.049787

Table C-3 (Continued)

24.21	257	96.72	0.046220	0.451900	0.051841
24.51	260	96.58	0.047580	0.480800	0.054054
24.81	263	96.43	0.048830	0.482100	0.056425
25.11	266	96.28	0.050010	0.501800	0.058796
25.41	269	96.13	0.051210	0.510900	0.061166
25.72	272	95.98	0.052100	0.518900	0.063537
26.02	275	95.82	0.052950	0.523900	0.066066
26.32	278	95.66	0.053470	0.526500	0.068595
26.62	281	95.50	0.054020	0.536600	0.071124
26.92	284	95.33	0.054880	0.554600	0.073811
27.22	287	95.17	0.055970	0.554200	0.076339
27.52	290	95.00	0.057070	0.571000	0.079026
27.82	293	94.83	0.058540	0.584900	0.081713
28.12	296	94.65	0.060450	0.606700	0.084558
28.42	299	94.46	0.062860	0.628400	0.087561
28.72	302	94.27	0.065910	0.649000	0.090564
29.02	305	94.07	0.069500	0.697800	0.093725
29.32	308	93.85	0.073850	0.737300	0.097202
29.62	311	93.63	0.079150	0.793700	0.100680
29.92	314	93.38	0.085280	0.839900	0.104631
30.22	317	93.12	0.092590	0.927400	0.108740
30.52	320	92.83	0.101300	1.013000	0.113324
30.82	323	92.51	0.111900	1.103000	0.118382
31.12	326	92.16	0.124100	1.239000	0.123913
31.42	329	91.77	0.139200	1.385000	0.130077
31.72	332	91.32	0.157300	1.565000	0.137190
32.02	335	90.83	0.178600	1.780000	0.144934

Table C-3 (Continued)

32.32	338	90.25	0.203800	2.025000	0.154101
32.62	341	89.61	0.233100	2.308000	0.164217
32.92	344	88.86	0.266800	2.647000	0.176071
33.22	347	88.01	0.305400	3.026000	0.189505
33.53	350	87.03	0.348400	3.465000	0.204994
33.83	353	85.92	0.395400	3.946000	0.222538
34.13	356	84.66	0.447700	4.464000	0.242453
34.43	359	83.24	0.499600	4.997000	0.264896
34.73	362	81.66	0.551900	5.532000	0.289869
35.03	365	79.92	0.600300	6.012000	0.317370
35.33	368	78.05	0.640900	6.426000	0.346926
35.63	371	76.07	0.670800	6.707000	0.378220
35.93	374	74.02	0.686300	6.868000	0.410621
36.23	377	71.94	0.686200	6.869000	0.443496
36.53	380	69.89	0.671000	6.711000	0.475897
36.84	383	67.91	0.643700	6.423000	0.507191
37.14	386	66.02	0.609100	6.069000	0.537063
37.44	389	64.25	0.572700	5.694000	0.565039
37.74	392	62.59	0.537500	5.345000	0.591275
38.04	395	61.03	0.506500	5.032000	0.615932
38.34	398	59.55	0.482800	4.804000	0.639324
38.64	401	58.14	0.465700	4.631000	0.661609
38.94	404	56.76	0.453100	4.505000	0.683420
39.24	407	55.42	0.444400	4.415000	0.704599
39.55	410	54.10	0.439400	4.372000	0.725462
39.85	413	52.79	0.435800	4.341000	0.746167
40.15	416	51.48	0.432400	4.311000	0.766872

Table C-3 (Continued)

40.45	419	50.19	0.427500	4.263000	0.787261
40.75	422	48.92	0.419500	4.207000	0.807334
41.05	425	47.67	0.407300	4.089000	0.827090
41.35	428	46.47	0.389400	3.910000	0.846057
41.65	431	45.33	0.365600	3.669000	0.864075
41.95	434	44.27	0.337300	3.369000	0.880828
42.25	437	43.31	0.306200	3.052000	0.896001
42.55	440	42.43	0.274900	2.737000	0.909910
42.85	443	41.66	0.245700	2.445000	0.922080
43.15	446	40.96	0.220000	2.189000	0.933144
43.45	449	40.34	0.197100	1.960000	0.942943
43.75	452	39.78	0.175900	1.759000	0.951794
44.05	455	39.28	0.155900	1.553000	0.959697
44.35	458	38.85	0.136400	1.359000	0.966493
44.65	461	38.47	0.117400	1.167000	0.972499
44.95	464	38.14	0.098840	0.980500	0.977715
45.26	467	37.87	0.080780	0.801700	0.981982
45.56	470	37.66	0.063970	0.628600	0.985301
45.86	473	37.49	0.049130	0.484400	0.987988
46.16	476	37.37	0.037040	0.358800	0.989885
46.46	479	37.27	0.027200	0.267300	0.991465
46.76	482	37.20	0.020180	0.189400	0.992572
47.06	485	37.15	0.015470	0.138800	0.993362
47.36	488	37.11	0.012150	0.120300	0.993994
47.66	491	37.08	0.009807	0.093290	0.994468
47.96	494	37.05	0.008043	0.079790	0.994942
48.26	497	37.03	0.006913	0.066960	0.995258

Table C-3 (Continued)

48.56	500	37.01	0.006030	0.061660	0.995575
48.86	503	37.00	0.005329	0.052480	0.995733
49.16	506	36.98	0.004676	0.050620	0.996049
49.46	509	36.97	0.004290	0.038170	0.996207
49.76	512	36.96	0.003751	0.034610	0.996365
50.06	515	36.95	0.003428	0.030060	0.996523
50.37	518	36.94	0.003146	0.031470	0.996681
50.67	521	36.93	0.002876	0.033920	0.996839
50.97	524	36.92	0.002697	0.020600	0.996997
51.27	527	36.91	0.002543	0.030570	0.997155
51.57	530	36.90	0.002318	0.024810	0.997313
51.87	533	36.90	0.002112	0.020880	0.997313
52.17	536	36.89	0.002022	0.018160	0.997471
52.47	539	36.88	0.001859	0.013750	0.997629
52.77	542	36.88	0.001847	0.014410	0.997629
53.07	545	36.87	0.001742	0.021110	0.997787
53.37	548	36.87	0.001893	0.010020	0.997787
53.67	551	36.86	0.002164	0.023330	0.997945
53.98	554	36.85	0.002551	0.025100	0.998103
54.28	557	36.85	0.002619	0.026140	0.998103
54.58	560	36.84	0.002669	0.028740	0.998261
54.88	563	36.83	0.002840	0.030470	0.998419
55.18	566	36.82	0.002913	0.031140	0.998578
55.48	569	36.81	0.003132	0.025780	0.998736
55.78	572	36.80	0.003259	0.036690	0.998894
56.08	575	36.79	0.003310	0.031900	0.999052
56.38	578	36.78	0.003204	0.033570	0.999210

Table C-3 (Continued)

56.68	581	36.77	0.003292	0.030960	0.999368
56.98	584	36.76	0.003322	0.032490	0.999526
57.29	587	36.75	0.003289	0.029040	0.999684
57.59	590	36.74	0.003269	0.027120	0.999842
57.89	593	36.73	0.003443	0.035470	1.000000

Table C-4: Detailed TG/DTG and conversion data at 20 °C/min

Time (min)	Temp (°C)	Weight loss (%)	Derivative weight loss (% / °C)	Derivative weight loss (% / min)	Conversion
0.64	20	100.00	0.006708	0.167200	0.000000
0.90	23	100.00	0.011480	0.148000	0.000000
1.08	26	99.97	0.008128	0.132800	0.000468
1.24	29	99.95	0.006359	0.124700	0.000779
1.39	32	99.94	0.005371	0.116000	0.000935
1.52	35	99.92	0.004917	0.100300	0.001247
1.65	38	99.91	0.004957	0.116100	0.001403
1.78	41	99.89	0.005198	0.128100	0.001714
1.91	44	99.87	0.005142	0.114900	0.002026
2.04	47	99.86	0.005419	0.122900	0.002182
2.17	50	99.84	0.006570	0.149500	0.002494
2.3	53	99.82	0.007045	0.171700	0.002805
2.44	56	99.80	0.006824	0.143500	0.003117
2.58	59	99.78	0.006833	0.147100	0.003429
2.72	62	99.76	0.007172	0.148700	0.003741
2.86	65	99.74	0.007188	0.151300	0.004052
3.01	68	99.72	0.007465	0.148700	0.004364
3.16	71	99.69	0.007800	0.149800	0.004832
3.32	74	99.67	0.007918	0.157400	0.005143
3.47	77	99.64	0.008184	0.151100	0.005611
3.63	80	99.62	0.008339	0.164000	0.005923
3.79	83	99.59	0.008418	0.161300	0.006390
3.95	86	99.57	0.008304	0.152600	0.006702
4.11	89	99.54	0.008220	0.157200	0.007170

Table C-4 (Continued)

4.26	92	99.52	0.008341	0.157600	0.007481
4.42	95	99.49	0.008290	0.166200	0.007949
4.57	98	99.47	0.008211	0.155100	0.008261
4.73	101	99.45	0.007978	0.161100	0.008572
4.88	104	99.42	0.007710	0.149100	0.009040
5.03	107	99.40	0.007489	0.147000	0.009352
5.18	110	99.38	0.007373	0.148300	0.009663
5.33	113	99.35	0.007222	0.141200	0.010131
5.48	116	99.33	0.007223	0.144800	0.010443
5.63	119	99.31	0.006915	0.144700	0.010754
5.78	122	99.29	0.006693	0.119400	0.011066
5.94	125	99.27	0.006761	0.143200	0.011378
6.09	128	99.25	0.006716	0.138500	0.011690
6.24	131	99.23	0.006439	0.122700	0.012001
6.39	134	99.21	0.006248	0.126400	0.012313
6.54	137	99.19	0.006247	0.122500	0.012625
6.69	140	99.17	0.006324	0.124700	0.012936
6.84	143	99.16	0.006343	0.129400	0.013092
6.99	146	99.14	0.006291	0.122400	0.013404
7.14	149	99.12	0.006164	0.124800	0.013716
7.29	152	99.10	0.005115	0.120000	0.014027
7.44	155	99.08	0.004016	0.031410	0.014339
7.59	158	99.08	0.004689	0.112700	0.014339
7.74	161	99.06	0.006653	0.142300	0.014651
7.89	164	99.04	0.007100	0.136800	0.014963
8.04	167	99.02	0.007306	0.152000	0.015274

Table C-4 (Continued)

8.19	170	98.99	0.007522	0.142500	0.015742
8.34	173	98.97	0.007697	0.157800	0.016054
8.49	176	98.95	0.008179	0.163300	0.016365
8.64	179	98.92	0.008609	0.170100	0.016833
8.79	182	98.89	0.009119	0.180100	0.017300
8.94	185	98.87	0.009625	0.200500	0.017612
9.09	188	98.84	0.010120	0.195200	0.018080
9.24	191	98.81	0.010730	0.219600	0.018547
9.39	194	98.77	0.011930	0.235200	0.019171
9.54	197	98.73	0.012770	0.261700	0.019794
9.69	200	98.70	0.013330	0.266100	0.020262
9.84	203	98.65	0.014130	0.277700	0.021041
9.99	206	98.61	0.015210	0.314600	0.021665
10.14	209	98.56	0.016340	0.319500	0.022444
10.29	212	98.51	0.017420	0.350400	0.023223
10.44	215	98.46	0.018650	0.376200	0.024002
10.59	218	98.40	0.019880	0.397300	0.024938
10.74	221	98.34	0.021240	0.424200	0.025873
10.89	224	98.27	0.022530	0.450600	0.026964
11.04	227	98.20	0.024070	0.483000	0.028055
11.19	230	98.13	0.025650	0.518500	0.029146
11.34	233	98.05	0.027460	0.542500	0.030393
11.48	236	97.96	0.029020	0.590900	0.031796
11.63	239	97.88	0.030540	0.606800	0.033042
11.78	242	97.78	0.032430	0.648600	0.034601
11.93	245	97.68	0.034430	0.690900	0.036160

Table C-4 (Continued)

12.08	248	97.58	0.036040	0.731500	0.037718
12.23	251	97.47	0.037850	0.747300	0.039433
12.38	254	97.35	0.039790	0.804800	0.041303
12.53	257	97.23	0.041720	0.835400	0.043173
12.68	260	97.10	0.043480	0.873000	0.045200
12.83	263	96.97	0.045240	0.907500	0.047226
12.98	266	96.83	0.046710	0.933900	0.049408
13.13	269	96.69	0.048600	0.967400	0.051590
13.28	272	96.54	0.050480	1.023000	0.053928
13.43	275	96.38	0.052180	1.032000	0.056421
13.58	278	96.22	0.053740	1.079000	0.058915
13.73	281	96.06	0.055330	1.104000	0.061409
13.88	284	95.89	0.057080	1.136000	0.064059
14.03	287	95.72	0.058930	1.179000	0.066708
14.18	290	95.54	0.060940	1.215000	0.069514
14.33	293	95.35	0.062600	1.259000	0.072475
14.48	296	95.16	0.064270	1.284000	0.075436
14.63	299	94.97	0.066440	1.327000	0.078398
14.78	302	94.76	0.069140	1.388000	0.081671
14.93	305	94.55	0.071860	1.437000	0.084944
15.08	308	94.33	0.075240	1.505000	0.088373
15.23	311	94.10	0.078910	1.578000	0.091958
15.38	314	93.86	0.082830	1.666000	0.095698
15.53	317	93.60	0.087630	1.748000	0.099751
15.68	320	93.33	0.093060	1.866000	0.103959
15.83	323	93.05	0.099630	1.985000	0.108323

Table C-4 (Continued)

15.98	326	92.74	0.107600	2.141000	0.113155
16.13	329	92.40	0.116000	2.322000	0.118454
16.28	332	92.04	0.126300	2.517000	0.124065
16.43	335	91.65	0.138600	2.750000	0.130143
16.58	338	91.21	0.152000	3.035000	0.137001
16.73	341	90.74	0.167400	3.344000	0.144327
16.88	344	90.21	0.185800	3.697000	0.152587
17.03	347	89.62	0.206900	4.116000	0.161783
17.18	350	88.97	0.231100	4.595000	0.171914
17.33	353	88.24	0.258100	5.147000	0.183292
17.48	356	87.42	0.288600	5.740000	0.196072
17.63	359	86.51	0.322600	6.419000	0.210256
17.78	362	85.49	0.359500	7.169000	0.226153
17.93	365	84.36	0.398800	7.940000	0.243766
18.08	368	83.10	0.439100	8.799000	0.263404
18.23	371	81.72	0.479400	9.571000	0.284913
18.38	374	80.22	0.517900	10.370000	0.308292
18.53	377	78.61	0.552600	11.070000	0.333385
18.68	380	76.90	0.580500	11.620000	0.360037
18.83	383	75.12	0.599700	12.010000	0.387781
18.98	386	73.29	0.607800	12.150000	0.416303
19.13	389	71.46	0.604500	12.090000	0.444825
19.28	392	69.66	0.591400	11.820000	0.472880
19.43	395	67.91	0.570600	11.390000	0.500156
19.59	398	66.23	0.545900	10.860000	0.526340
19.74	401	64.63	0.520600	10.360000	0.551278

Table C-4 (Continued)

19.89	404	63.11	0.497300	9.903000	0.574969
20.04	407	61.65	0.478000	9.524000	0.597724
20.19	410	60.25	0.462800	9.240000	0.619545
20.34	413	58.88	0.452300	9.002000	0.640898
20.49	416	57.53	0.445800	8.904000	0.661939
20.64	419	56.21	0.442200	8.852000	0.682512
20.79	422	54.88	0.440400	8.833000	0.703242
20.94	425	53.57	0.439300	8.825000	0.723660
21.09	428	52.25	0.436900	8.773000	0.744233
21.24	431	50.94	0.431400	8.653000	0.764651
21.39	434	49.66	0.421200	8.480000	0.784601
21.53	437	48.41	0.405200	8.127000	0.804084
21.68	440	47.22	0.384200	7.718000	0.822631
21.83	443	46.10	0.361200	7.219000	0.840087
21.98	446	45.05	0.337100	6.740000	0.856453
22.13	449	44.08	0.313900	6.248000	0.871571
22.28	452	43.18	0.294900	5.882000	0.885599
22.43	455	42.31	0.280900	5.620000	0.899158
22.58	458	41.49	0.268100	5.351000	0.911939
22.73	461	40.70	0.254400	5.095000	0.924252
22.89	464	39.96	0.238900	4.781000	0.935786
23.04	467	39.27	0.220600	4.423000	0.946540
23.19	470	38.64	0.198100	4.000000	0.956359
23.34	473	38.08	0.171100	3.419000	0.965087
23.49	476	37.60	0.140300	2.812000	0.972569
23.64	479	37.23	0.108900	2.159000	0.978335

Table C-4 (Continued)

23.79	482	36.96	0.077730	1.527000	0.982544
23.94	485	36.77	0.052570	1.032000	0.985505
24.09	488	36.65	0.034920	0.668600	0.987375
24.24	491	36.56	0.023610	0.446100	0.988778
24.39	494	36.51	0.016670	0.322300	0.989557
24.54	497	36.47	0.012630	0.244200	0.990181
24.69	500	36.43	0.010090	0.194500	0.990804
24.84	503	36.41	0.008658	0.173000	0.991116
24.99	506	36.38	0.007680	0.151100	0.991584
25.14	509	36.36	0.006815	0.134800	0.991895
25.29	512	36.34	0.006497	0.125800	0.992207
25.44	515	36.32	0.006544	0.134200	0.992519
25.59	518	36.30	0.006436	0.126400	0.992830
25.74	521	36.28	0.006238	0.119900	0.993142
25.89	524	36.26	0.006333	0.126700	0.993454
26.04	527	36.25	0.006528	0.136600	0.993610
26.19	530	36.23	0.006416	0.127900	0.993921
26.34	533	36.21	0.006419	0.115300	0.994233
26.49	536	36.19	0.006507	0.145000	0.994545
26.64	539	36.17	0.006580	0.124900	0.994857
26.79	542	36.15	0.006375	0.125200	0.995168
26.94	545	36.13	0.006605	0.131600	0.995480
27.09	548	36.11	0.006762	0.136900	0.995792
27.24	551	36.09	0.006840	0.134900	0.996103
27.40	554	36.07	0.006867	0.136300	0.996415
27.55	557	36.05	0.006799	0.135100	0.996727

Table C-4 (Continued)

27.70	560	36.03	0.006845	0.137800	0.997039
27.85	563	36.01	0.006925	0.137400	0.997350
280	566	35.98	0.006842	0.137600	0.997818
28.15	569	35.96	0.006608	0.136100	0.998130
28.30	572	35.94	0.006649	0.120700	0.998441
28.45	575	35.92	0.006732	0.143100	0.998753
28.60	578	35.90	0.006877	0.135600	0.999065
28.75	581	35.88	0.006952	0.136300	0.999377
28.90	584	35.86	0.007288	0.149000	0.999688
29.05	587	35.84	0.007578	0.150300	1.000000

Appendix D: Model analysis data for oxidative desulphurisation

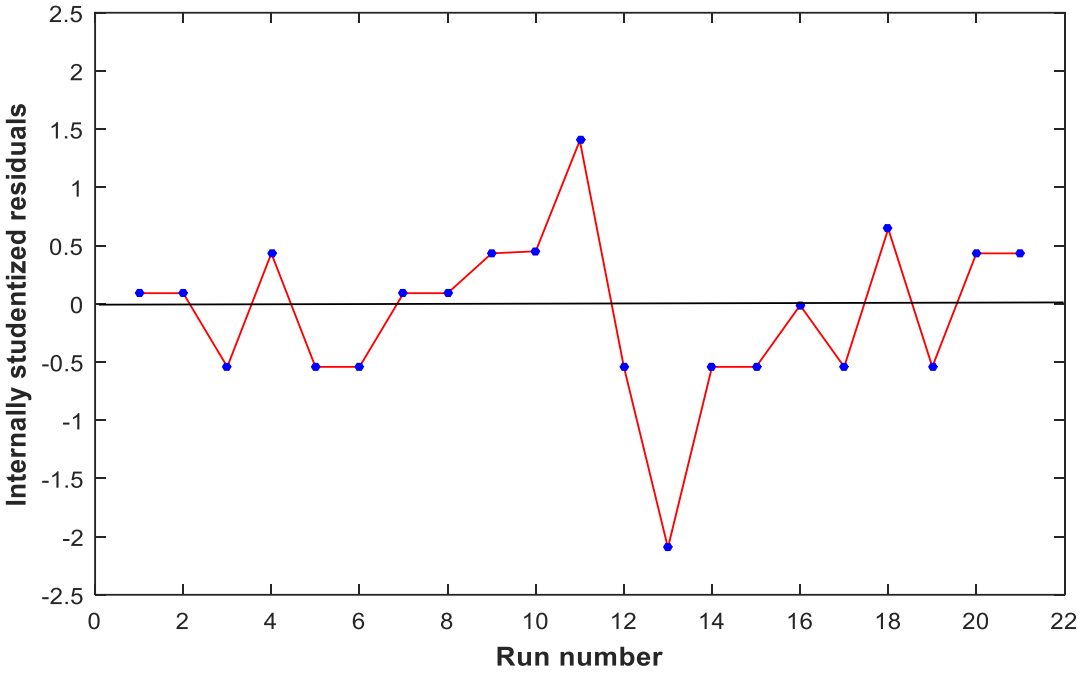

Figure D-1: Plot of internally studentized residuals versus run number.

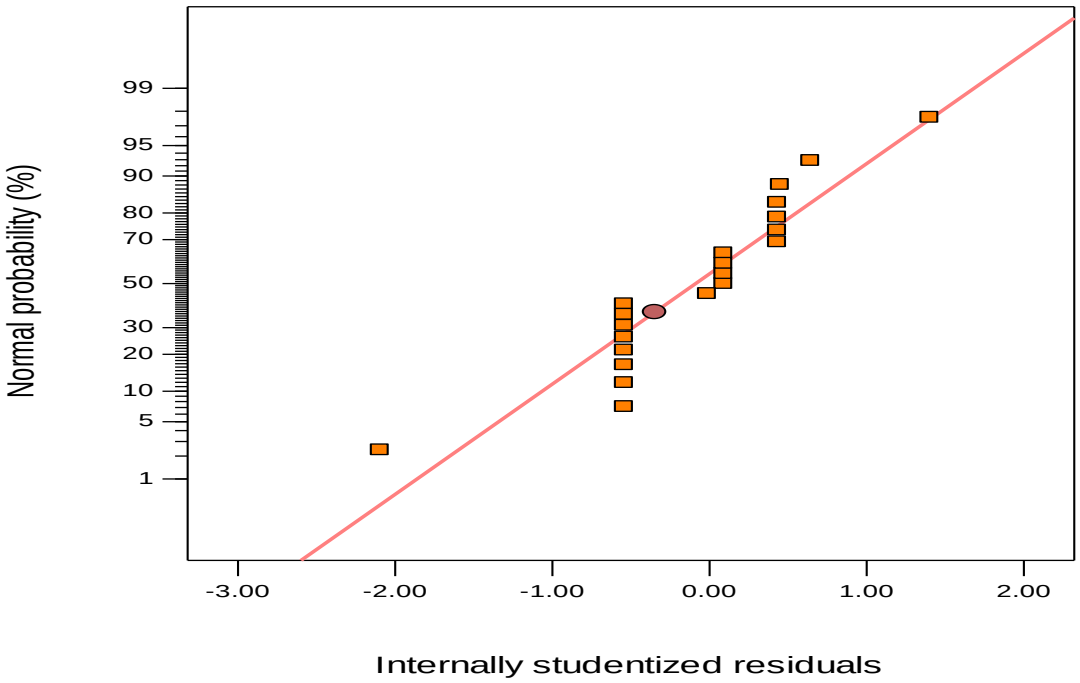

Figure D-2: Normal probability plot of internally studentized residuals.

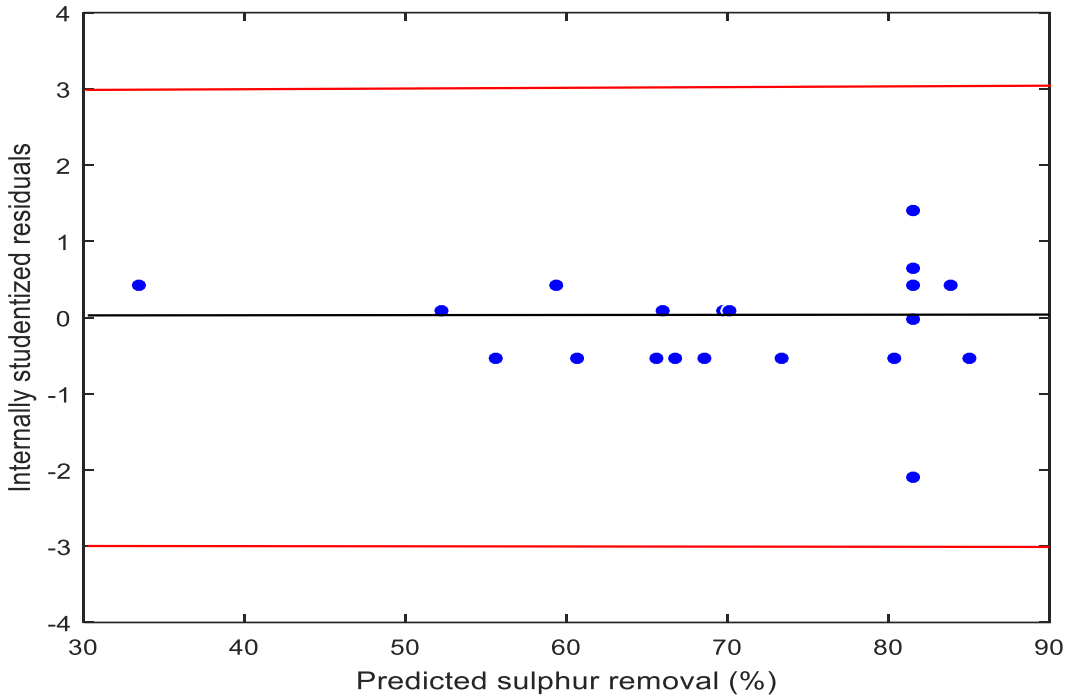

Figure D-3: Plot of internally studentized residuals versus predicted sulphur removal

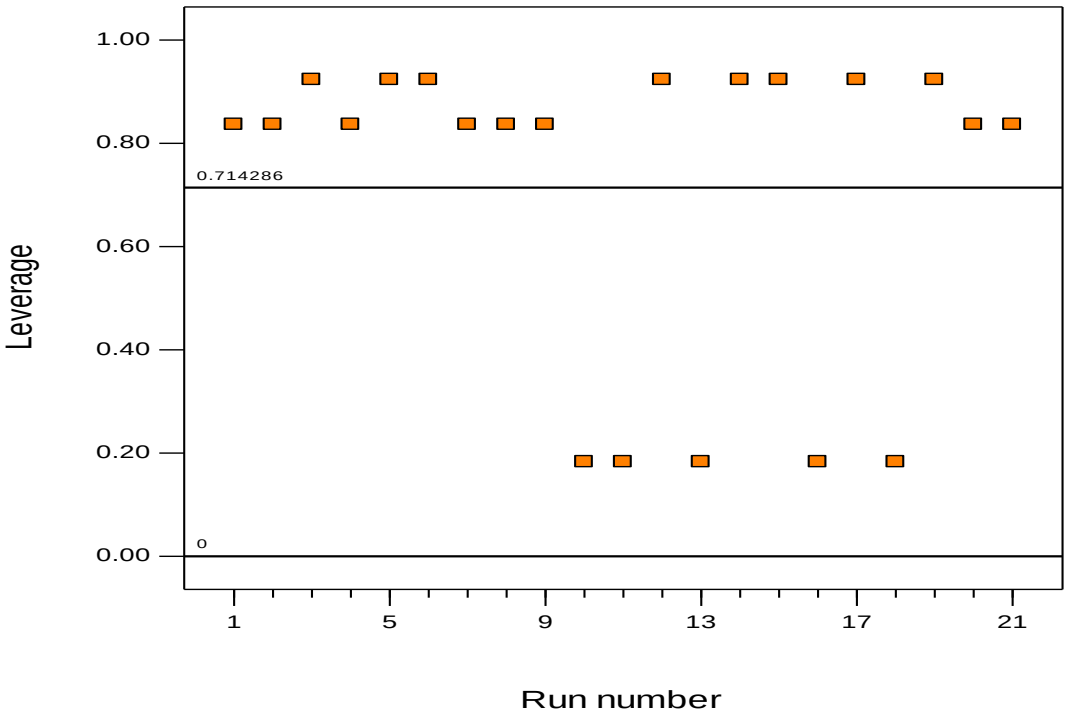

Figure D-4: Plot of leverage versus run number

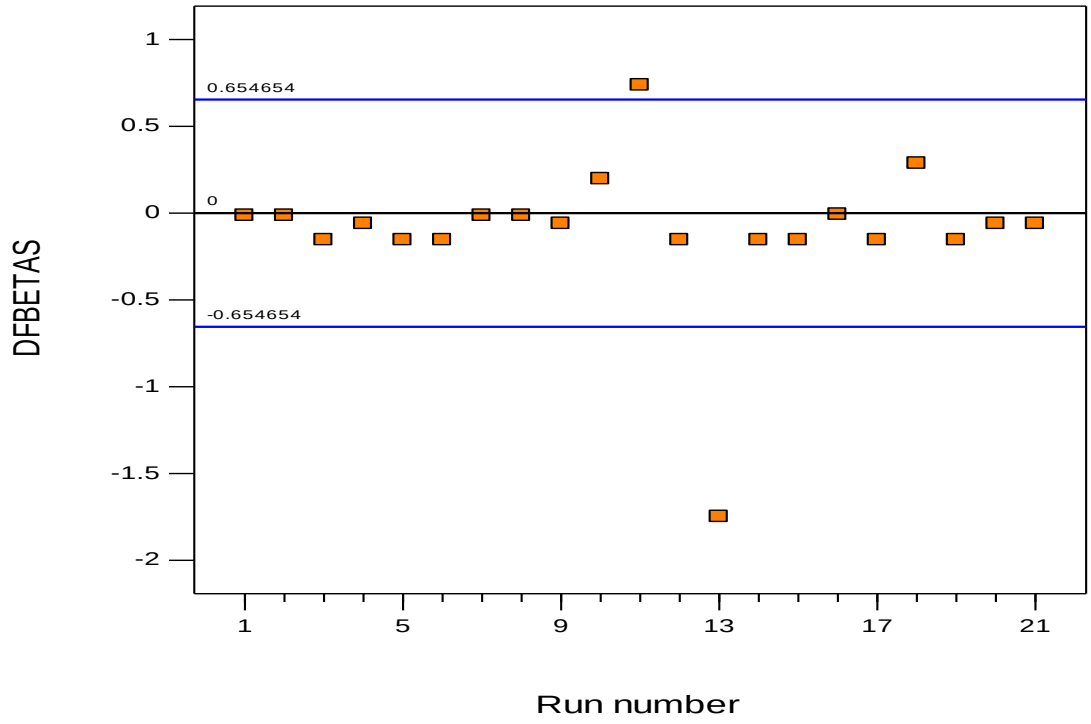

Figure D-5: Plot of DFBETAS versus run number

Table D-1: Model diagnostics and influence statistics

Run Order	Actual Value	Predicted Value	Leverage	Internally Studentized Residual	Externally Studentized Residual	Cook's Distance	DFFITS
1	66.08	65.95	0.837	0.091	0.083	0.003	0.188
2	69.86	69.73	0.837	0.091	0.083	0.003	0.188
3	55.04	55.58	0.924	-0.542	-0.507	0.237	-1.763
4	84.41	83.78	0.837	0.433	0.401	0.064	0.909
5	72.78	73.32	0.924	-0.542	-0.507	0.237	-1.763
6	84.49	85.03	0.924	-0.542	-0.507	0.237	-1.763
7	52.39	52.26	0.837	0.091	0.083	0.003	0.188
8	70.22	70.09	0.837	0.091	0.083	0.003	0.188
9	34.02	33.39	0.837	0.433	0.401	0.064	0.909
10	82.94	81.46	0.183	0.451	0.419	0.003	0.198
11	86.05	81.46	0.183	1.402	1.56	0.029	0.739
12	79.85	80.39	0.924	-0.542	-0.507	0.237	-1.763
13	74.61	81.46	0.183	-2.095	-3.689	0.066	-1.747
14	60.05	60.59	0.924	-0.542	-0.507	0.237	-1.763
15	64.97	65.51	0.924	-0.542	-0.507	0.237	-1.763
16	81.42	81.46	0.183	-0.013	-0.012	0	-0.006
17	66.21	66.75	0.924	-0.542	-0.507	0.237	-1.763
18	83.57	81.46	0.183	0.644	0.609	0.006	0.288
19	68.05	68.59	0.924	-0.542	-0.507	0.237	-1.763
20	82.15	81.52	0.837	0.433	0.401	0.064	0.909
21	59.97	59.34	0.837	0.433	0.401	0.064	0.909

Table D-2: Optimisation starting points

HCOOH	H_2O_2	Temperature	Reaction time
6.0000000	10.0000000	58.0000000	60.000000000
12.0000000	6.0000000	50.0000000	60.000000000
12.0000000	10.0000000	58.0000000	40.000000000
9.0000000	8.0000000	54.0000000	50.000000000
6.0000000	10.0000000	50.0000000	60.000000000
12.0000000	10.0000000	50.0000000	40.000000000
12.0000000	6.0000000	58.0000000	60.000000000
6.0000000	6.0000000	58.0000000	40.000000000
6.0000000	6.0000000	50.0000000	40.000000000
9.5754048	8.4798827	54.3465378	47.320621344
9.2812785	6.9933565	57.2719705	51.815682868
9.2596593	6.3798002	51.9936630	52.188162524
9.6817190	7.6365241	50.7577658	52.020713771
11.8990832	9.7666553	55.8177030	46.014673165
8.2866946	9.1717873	56.4062521	46.933391858
9.1321431	7.9552365	50.3462031	50.325756012
7.2162391	6.7453821	56.9970555	52.236840418
9.3521153	8.8180601	51.0111033	53.049341706
8.1604233	6.5855864	51.6510256	41.231153789
7.1158145	7.6604431	50.4294458	40.696389251
10.7643899	6.4368018	54.4440755	44.295850648
8.7267394	7.5657267	57.9764107	44.360713656
6.8731496	6.8818254	54.9649177	56.076260312
11.7548485	7.7728785	52.7741698	57.364232931
9.3958296	7.7957803	53.7449177	56.172761982

Table D-2 (Continued)

11.8380739	6.5730145	57.4345796	40.803441787
11.1287986	6.9864244	54.9793745	47.600765168
7.7180906	7.9641659	52.3951439	45.161006725
9.4297782	9.6799843	51.5230382	45.847378704
9.2971295	9.7156829	57.1524609	48.388640173
6.3755672	6.1137133	50.5940441	42.629291811
6.0890994	8.8936449	53.4786746	55.419097799
8.4470292	7.7652880	50.3489209	53.202339113
9.8053153	7.7032325	54.4940043	41.527041853
11.5578642	8.2710709	55.4995513	59.245665292
11.0656495	9.9867448	56.2991022	45.226203278
8.1119355	8.9646140	51.5559315	51.111413585
9.7291444	7.3425719	50.2571553	46.870954963
9.8425926	9.8537130	53.8925484	54.182523680
10.4142312	6.2632096	57.9594342	58.654955290
11.5681250	7.9592062	54.7440533	49.295253889
11.4227463	7.4472240	57.1874782	51.672110045
9.9565884	9.0202831	57.2714352	52.714778860
9.5929388	9.4297615	56.4589252	48.187014335
11.4706922	6.6629645	55.6386169	59.648807114
8.3720572	8.5395934	55.6363092	57.986281645
9.8796023	8.5878470	54.7175499	46.744910781
11.4466653	6.1390720	54.0960038	57.334442749
6.3589733	7.4671138	50.1613666	59.652742958
6.4727727	8.1417531	51.2027575	59.658447802
11.4852283	7.0029862	55.5843628	49.761440391

Table D-2 (Continued)

7.6163110	7.7278728	50.3171376	50.174774099
10.5190436	8.1237491	53.5052180	59.628204461
10.2084246	6.8845836	50.1581666	57.743759346
10.2295954	8.2267433	54.4293000	56.482127993
7.6499322	6.3971140	51.3562157	50.126961004
10.3195636	6.9027484	57.7140822	54.511149856
8.6271086	8.2207012	54.8068224	40.823840220
7.6384465	8.8658942	56.8549319	40.691717472
9.5121812	6.2778430	57.2274016	45.600750451
6.7353826	6.5067159	51.3857234	41.883408804
6.6163327	6.9126596	54.8734846	51.405847040
9.5362825	8.1502526	55.3109628	41.327667623
8.4936821	9.7959847	56.7498865	54.428061866
9.0093818	8.6132441	51.1210712	56.084803818
9.6018998	8.1602178	57.1101941	52.703597881
6.2646272	6.1331206	51.9335532	47.349450313
10.1124893	6.9097622	57.1369379	51.411739574
7.9855608	6.7413812	52.7938421	58.863206860
10.9672022	9.3787701	56.3115160	49.432681939
7.1008157	8.0730833	52.9184764	58.905205675
10.9934643	7.6430314	53.0857634	59.911160786
9.0550934	7.7568350	50.9158750	56.755446647
6.6748023	9.1616037	51.6178726	46.236353349
11.0408200	8.7721621	57.2849144	55.684289495
9.2427841	9.3006125	57.2358621	59.959997847
10.2680668	8.4568911	54.6431546	47.451197887

Table D-2 (Continued)

11.9534729	7.8870970	56.8732025	46.536861635
10.8036506	9.6940093	56.1967603	57.789354343
10.4866720	9.2095050	57.6231184	51.831415729
11.2278281	9.7661296	55.0860688	43.128917604
8.4063918	9.2483811	52.9196540	49.343020613
8.5305075	9.9202292	57.8281210	42.489515552
8.9035677	6.5389583	56.9612194	56.309884535
6.6734143	6.6257145	51.8142707	51.486800294
10.3764355	7.4407354	52.8126184	42.653884818
6.5475608	9.9800788	56.3308477	52.761473441
7.5534785	6.8339382	57.1908575	45.664458522
9.5203238	6.8487210	52.1064828	41.812953316
6.9545217	6.8553473	56.5475321	48.052644548
11.8480673	9.3860769	56.7952214	44.160216027
11.1309983	7.5632772	51.8899358	46.559207821
10.8248129	9.0711208	54.7449036	43.768485012
7.6602108	7.1436558	50.6379964	46.196620935
7.7734218	7.1047059	52.3056777	51.607130170
9.0363207	9.8371949	57.8657962	56.979444744
10.6436390	6.1236811	54.9388974	43.581766249
7.6222147	9.8199426	50.8555928	56.788418838
6.3769695	9.2283175	57.7549591	41.365993535
6.5219338	9.7596766	53.5997449	40.876245261
9.0726400	9.6363529	52.1416537	56.401344915
11.6133057	7.4618921	53.1431475	57.799212146
11.8921607	6.2404135	51.9986061	53.460709159

Table D-2 (Continued)

8.8828793	6.7731985	54.3126210	43.916733903
10.3959623	7.4977010	55.9946003	41.744722542
9.2852071	8.9796664	50.2609228	41.335973209
8.9360665	7.2391150	56.3027438	41.240109159
8.2743301	8.7801875	55.3953659	53.171425969
7.2806533	9.7119962	57.4802000	47.575264871

Table D-3: Solutions from optimisation

Number	HCOOH	H_2O_2	Temperature	Reaction time	S removal	Desirability
1	11.958	7.557	50.102	40.742	90.181	1.000
2	11.952	7.455	50.178	40.688	90.032	1.000
3	11.997	8.091	50.008	41.069	90.054	1.000
4	11.946	8.584	50.168	40.024	90.012	1.000
5	11.929	8.494	50.317	40.044	90.008	1.000
6	11.891	8.464	50.055	40.111	90.144	1.000
7	11.942	8.097	50.777	40.155	90.012	1.000
8	11.808	8.131	50.335	40.126	90.098	1.000
9	11.747	8.205	50.152	40.002	90.137	1.000
10	11.840	8.095	50.267	40.184	90.208	1.000
11	11.879	8.443	50.099	40.094	90.132	1.000
12	11.971	8.537	50.202	40.023	90.134	1.000
13	11.825	7.714	50.377	40.064	90.124	1.000
14	11.980	7.749	50.014	41.147	90.096	1.000
15	11.959	8.302	50.464	40.070	90.221	1.000
16	11.968	7.896	50.428	40.601	90.152	1.000
17	11.982	7.564	50.566	40.087	90.292	1.000
18	11.682	7.851	50.039	40.004	90.053	1.000
19	11.992	8.605	50.185	40.004	90.061	1.000
20	11.977	7.966	50.463	40.571	90.146	1.000
21	11.992	8.217	50.522	40.038	90.367	1.000
22	11.893	8.475	50.038	40.018	90.234	1.000
23	11.970	7.866	50.783	40.313	90.038	1.000
24	11.992	8.072	50.346	40.666	90.143	1.000
25	11.933	7.737	50.103	40.950	90.034	1.000

Table D-3 (Continued)

26	11.999	7.522	50.251	40.173	90.561	1.000
27	11.998	8.391	50.243	40.013	90.441	1.000
28	11.937	7.341	50.288	40.173	90.039	1.000
29	11.984	8.337	50.126	40.317	90.315	1.000
30	11.984	8.546	50.271	40.065	90.033	1.000
31	11.963	7.665	50.192	40.665	90.257	1.000
32	11.909	8.030	50.192	40.697	90.055	1.000
33	11.784	7.892	50.159	40.212	90.144	1.000
34	11.973	7.649	50.155	40.940	90.103	1.000
35	11.933	8.087	50.001	40.608	90.309	1.000
36	11.985	8.491	50.440	40.005	90.042	1.000
37	11.757	7.886	50.016	40.319	90.071	1.000
38	11.887	7.970	50.346	40.313	90.214	1.000
39	11.996	7.088	50.019	40.034	90.062	1.000
40	11.840	8.350	50.218	40.119	90.064	1.000
41	11.963	8.167	50.265	40.213	90.449	1.000
42	11.994	7.459	50.202	40.178	90.509	1.000
43	11.986	8.206	50.322	40.567	90.096	1.000
44	11.998	8.101	50.581	40.181	90.313	1.000
45	11.983	7.958	50.594	40.005	90.476	1.000
46	11.892	8.336	50.125	40.044	90.352	1.000
47	11.852	7.704	50.553	40.099	90.027	1.000
48	11.994	7.959	50.826	40.112	90.176	1.000
49	11.796	7.873	50.058	40.113	90.327	1.000
50	11.993	7.626	50.214	40.960	90.097	1.000
51	11.971	8.204	50.330	40.428	90.181	1.000

Table D-3 (Continued)

52	12.000	7.747	50.441	40.191	90.529	1.000
53	11.984	8.120	50.242	40.328	90.468	1.000
54	11.825	7.562	50.223	40.081	90.087	1.000
55	12.000	7.885	50.000	41.345	89.970	0.994
56	12.000	6.895	50.000	40.000	89.559	0.912
57	12.000	7.605	51.406	40.000	89.488	0.898
58	12.000	8.842	50.192	40.000	89.421	0.884
59	12.000	7.178	50.000	41.514	89.374	0.875
60	12.000	7.042	50.777	40.001	89.204	0.841
61	11.377	8.612	50.000	40.000	88.906	0.781
62	12.000	9.064	50.000	40.005	88.818	0.764
63	12.000	8.877	50.678	40.000	88.811	0.762
64	12.000	7.397	52.172	40.000	88.238	0.648
65	12.000	7.729	52.685	40.000	87.840	0.568
66	11.041	8.173	52.881	40.000	87.124	0.425
67	10.426	8.551	53.413	40.000	86.522	0.304
68	9.916	7.053	58.000	57.623	86.232	0.246
69	9.915	7.056	58.000	57.486	86.232	0.246
70	9.928	7.029	58.000	57.793	86.232	0.246
71	9.915	7.019	58.000	57.831	86.231	0.246
72	9.928	7.085	58.000	57.423	86.231	0.246
73	9.899	7.157	58.000	57.085	86.225	0.245
74	9.920	7.118	58.000	56.695	86.221	0.244
75	9.904	7.200	58.000	56.472	86.215	0.243
76	9.899	7.099	57.986	57.333	86.209	0.242
77	10.124	7.222	58.000	56.596	86.126	0.225

Table D-3 (Continued)

78	9.725	7.763	58.000	52.459	85.882	0.176
79	9.817	7.763	58.000	51.865	85.832	0.166
80	10.001	7.571	58.000	51.709	85.802	0.160
81	6.352	10.000	50.000	40.038	85.418	0.084
82	9.208	7.557	58.000	53.196	85.417	0.083
83	9.217	9.251	50.000	40.000	85.170	0.034
84	8.668	9.602	51.626	40.000	85.065	0.013
85	8.668	9.592	51.187	40.000	85.025	0.005